

SOLVING THE DILEMMA: TO WAVE OR TO OSCILLATE?  
OPPOSING FORMULATIONS OF THE SHALLOW  
WATER EQUATIONS IN RIVER MODELING

Volume II

A Dissertation

by

GARY EUGENE FREEMAN

Submitted to the Office for Graduate Studies of  
Texas A&M University  
in partial fulfillment of the requirements for the degree of  
DOCTOR OF PHILOSOPHY

December 1992

Major Subject: Civil Engineering

SOLVING THE DILEMMA: TO WAVE OR TO OSCILLATE?  
OPPOSING FORMULATIONS OF THE SHALLOW  
WATER EQUATIONS IN RIVER MODELING


Volume II


A Dissertation

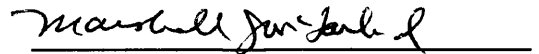
by

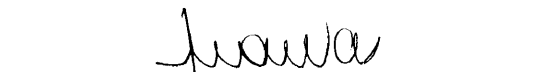
GARY EUGENE FREEMAN


Approved as to style and content by:

  
Ralph Wurbs  
(Chair of Committee)

  
Wesley P. James  
(Member)

  
Marshall J. McFarland  
(Member)

  
Juan B. Valdes  
(Member)

  
James T. P. Yao  
(Head of Department)

December 1992

## TABLE OF CONTENTS

## Volume I

	Page
INTRODUCTION . . . . .	1
RESEARCH OBJECTIVES . . . . .	3
THEORETICAL REVIEW AND DISCUSSION OF TEST MODELS . . . . .	4
PRIMITIVE EQUATION MODELS AND RMA-2V . . . . .	4
WAVE EQUATION MODELS AND ADCIRC-2DDI . . . . .	23
THE ADCIRC-2DDI MODEL . . . . .	30
FINITE ELEMENT FORMULATION OF TEST MODELS . . . . .	38
RMA-2V . . . . .	38
ADCIRC-2DDI . . . . .	40
SIMULATION OF TIME VARYING PROBLEMS . . . . .	47
TIME SIMULATION IN RMA-2V . . . . .	50
TIME SIMULATION IN ADCIRC-2DDI . . . . .	52
TESTING APPROACH AND METHODOLOGY . . . . .	58
SIMPLE TEST CASES . . . . .	58
RIPRAP TEST FACILITY MODEL . . . . .	67
REDEYE CROSSING . . . . .	69
SIMPLE TEST CASE RESULTS WITH RMA-2V . . . . .	74
SUDDEN DEPTH REDUCTIONS WITH RMA-2V . . . . .	74
SUDDEN DEPTH INCREASES AND RMA-2V . . . . .	117
SUBMERGED BUMPS WITH RMA-2V . . . . .	147
SUDDEN REDUCTIONS IN WIDTH WITH RMA-2V . . . . .	164
SUDDEN WIDTH EXPANSIONS WITH RMA-2V . . . . .	186
EXPOSED DIKES OR BRIDGE ABUTMENTS WITH RMA-2V . . . . .	203

## Volume II

	Page
SIMPLE TEST CASES WITH ADCIRC-2DDI . . . . .	215
THE FULLY NON-LINEAR MODEL . . . . .	218
THE LINEAR 2DDI MODEL . . . . .	231
SUDDEN DEPTH REDUCTIONS WITH 2DDI . . . . .	237
SUDDEN DEPTH INCREASES WITH 2DDI . . . . .	267
SUBMERGED BUMPS WITH 2DDI . . . . .	282
SUDDEN WIDTH REDUCTIONS WITH 2DDI . . . . .	294
SUDDEN WIDTH EXPANSIONS WITH 2DDI . . . . .	311
ABUTMENT REDUCTIONS WITH 2DDI . . . . .	329
JOHN L. GRACE, JR. RIPRAP TEST FACILITY . . . . .	344
RMA-2V RIPRAP TEST FACILITY MODEL RESULTS . . . . .	349
2DDI RIPRAP TEST FACILITY MODEL RESULTS . . . . .	361
THE MISSISSIPPI RIVER REDEYE CROSSING MODEL . . . . .	375
RMA-2V REDEYE CROSSING MODEL RESULTS . . . . .	380
2DDI REDEYE CROSSING MODEL RESULTS . . . . .	389
CONCLUSIONS . . . . .	396
CONCLUSIONS REGARDING RMA-2V . . . . .	397
CONCLUSIONS REGARDING ADCIRC-2DDI . . . . .	403
REFERENCES . . . . .	407
VITA . . . . .	413

## LIST OF FIGURES

## Volume I

	Page
Fig. 1. (a) Straight-Sided and (b) Curve-Sided Element Basins Used by Walters and Cheng (1980).	20
Fig. 2. Notation Used in Defining Water Depth in (a) River Modeling and (b) Ocean Modeling. . . . .	25
Fig. 3. Simple Test Case Bottom Profiles for (a) Sudden Depth Reduction and (b) for Sudden Depth Increase. . . . .	60
Fig. 4. Simple Test Case Bottom Profiles for (a) Bump Test and (b) for Sudden Width Change. . . . .	61
Fig. 5. Simple Test Grids Used in Model Testing - (a) Regular Grid, (b) Quadrilateral Grid, (c) Alternating Grid, and (d) "C" Grid. . . . .	63
Fig. 6. Test Grids used for (a) 40% Width Reduction, (b) 67% Width Expansion, and (c) 40% Abutment Reduction. . . . .	65
Fig. 7. Simple Test Case Grids Used to Test (a) 20% Abutment Reduction and (b) 60% Abutment Reduction. . . . .	66
Fig. 8. Partial Sections of Grid for Abrupt Change in Depth Showing Gradation of Resolution. . . . .	68
Fig. 9. Regular Test Grid for John L. Grace, Jr. Riprap Test Facility. . . . .	70
Fig. 10. Alternating Test Grid of the John L. Grace, Jr. Riprap Test Facility. . . . .	71
Fig. 11. Redeye Crossing Grid Used for Both Models Consisting of Entirely Triangular Elements. . .	72
Fig. 12. Regular Grid 3-D Water Surface Elevation and Velocity Plots for 50% Depth Reduction with EV = 5 and Resolution = 1. . . . .	76
Fig. 13. Velocity Vectors for Lower Section of Test Channel Showing Oscillations in Velocity and	

Direction of Flow. . . . . 77

Fig. 14. Water Surface Profiles for Regular Grid - Profiles 1 (Right Descending Side), and 6 (Left Descending Side) for EV = 5. . . . . 78

Fig. 15. Flow Continuity Versus Distance Down the Channel for Regular Grid with Eddy Viscosity Equal to 5 and Resolution = 1. . . . . 79

Fig. 16. Regular Grid Maximum and Minimum Transverse Water Surface Elevation and Velocity Values with Transverse Standard Deviation at EV = 5 and Resolution = 1 for Sudden Depth Reduction. . . . 80

Fig. 17. Alternating Grid 3-D Water Surface Elevation and Velocity Plots for 50% Depth Reduction with EV = 5 and Resolution = 1. . . . . 82

Fig. 18. Alternating Grid Maximum and Minimum Transverse Water Surface Elevation and Velocity Values with Transverse Standard Deviation at EV = 5 and Resolution = 1 for Sudden Depth Reduction. 83

Fig. 19. "C" Grid 3-D Water Surface Elevation and Velocity Plots for 50% Depth Reduction with EV = 5 and Resolution = 1. . . . . 85

Fig. 20. "C" Grid Maximum and Minimum Transverse Water Surface Elevation and Velocity Values with Transverse Standard Deviation at EV = 5 and Resolution = 1 for Sudden Depth Reduction. . . . 86

Fig. 21. Quadrilateral Grid 3-D Water Surface Elevation and Velocity Plots for 50% Depth Reduction with EV = 5 and Resolution = 1. . . . 87

Fig. 22. Quadrilateral Grid Maximum and Minimum Transverse Water Surface Elevation and Velocity Values with Transverse Standard Deviation with EV = 5 and Resolution = 1 for Sudden Depth Reduction. . . . . 88

Fig. 23. Flow Continuity vs Distance Down Channel for Four Test Grids for Sudden Reduction in Depth with EV = 5 and Resolution = 1. . . . .	90
Fig. 24. Combined Water Surface Elevation and Velocity Plots Showing Error Phase and Midside Node Values for Regular and "C" Grids with EV = 5 and Resolution = 1 for Depth Reduction. . . . .	91
Fig. 25. Combined Water Surface Elevation and Velocity Plot Showing Error Phase and Midside Values for Alternating and Quadrilateral Grids with EV = 5 and Resolution = 1. . . . .	92
Fig. 26. Continuity vs Distance Down Channel for Four Test Grids for Sudden Depth Reduction with Eddy Viscosity = 25 and Resolution = 1. . . . .	95
Fig. 27. Continuity vs Distance Down Channel for Four Test Grids for Sudden Reduction in Depth with EV = 125 and Resolution = 1. . . . .	96
Fig. 28. Flow Continuity vs Distance Down Channel for Four Test Grids for Sudden Depth Reduction with EV = 250 and Resolution = 1. . . . .	98
Fig. 29. Three Dimensional Water Surface Elevation Plots for Four Test Grids with Eddy Viscosity = 250 and Resolution = 1. . . . .	99
Fig. 30. Three Dimensional Velocity Plots for Four Test Grids for Sudden Depth Reduction with Eddy Viscosity = 250 and Resolution = 1. . . . .	100
Fig. 31. Continuity Versus Distance Down Channel for Four Test Grids with EV = 500 and Resolution = 1. . . . .	101
Fig. 32. Continuity vs Distance Down Channel for Four Test Grids with Resolution = 2 and EV = 5. . . . .	103
Fig. 33. Water Surface Elevations for Four Test Grids for 50% Depth Reduction with Resolution = 2 and	

	Page
EV = 5. . . . .	104
Fig. 34. Three Dimensional Velocity Plots for Four Test Grids for 50% Depth Reduction with Resolution = 2 and EV = 5. . . . .	105
Fig. 35. Continuity vs Distance Down Channel for Four Test Grids for 50% Depth Reduction with Resolution = 4 and EV = 5. . . . .	107
Fig. 36. Continuity vs Distance Down Channel for Four Test Grids for 50% Depth Reduction with Resolution = 8 and EV = 5. . . . .	108
Fig. 37. Maximum Continuity Deviation vs Eddy Viscosity with Regular and "C" Grids for Tested Resolutions for a 50% Reduction in Depth. . . . .	109
Fig. 38. Maximum Continuity Deviation vs Eddy Viscosity for Alternating and Quadrilateral Grids for Tested Resolutions with a 50% Reduction in Depth. . . . .	110
Fig. 39. Maximum Continuity Deviation Versus Eddy Viscosity for Alternating Grid for Test Resolutions with 25% and 75% Reductions in Depth. . . . . .	112
Fig. 40. Maximum Continuity Deviation Versus Percent Change in Depth per Element and Eddy Viscosity for Alternating Grid Using Data from 25%, 50%, and 75% Depth Reduction Tests. . . . .	113
Fig. 41. RMA-2V Continuity vs Channel Distance for Alternating Grid with 25% and 75% Depth Reductions for EV = 5 and Resolutions of 1 and 8 Elements on Step Face. . . . .	116
Fig. 42. Continuity vs Distance Down Channel for Test Grids with 93% Depth Increase for EV = 5 and Resolution = 1. . . . .	119
Fig. 43. Three Dimensional Water Surface Plots for	



Test Grids with 93% Depth Increase with EV = 5  
and Resolution = 1. . . . . 120

Fig. 44. Three Dimensional Velocity Surface Plots for  
93% Depth Increase for Regular and Alternating  
Grids with EV = 5 and Resolution = 1. . . . . 121

Fig. 45. Three Dimensional Velocity Surface Plots for  
93% Depth Increase for "C" and Quadrilateral  
Grids with EV = 5 and Resolution = 1. . . . . 122

Fig. 46. Maximum and Minimum Values for Water Surface  
Elevation and Velocity for Regular Grid for 93%  
Increase in Depth with EV = 5 and Resolution =  
1. . . . . 124

Fig. 47. Maximum and Minimum Values of Water Surface  
Elevation and Velocity for Alternating Grid for  
93% Depth Increase with EV = 5 and Resolution =  
1. . . . . 125

Fig. 48. Maximum and Minimum Values for Water Surface  
Elevation and Velocity for "C" Grid for 93% Depth  
Increase with EV = 5 and Resolution = 1. . . . . 126

Fig. 49. Maximum and Minimum Values for Water Surface  
Elevation and Velocity for Quadrilateral Grid for  
93% Depth Increase with EV = 5 and Resolution =  
1. . . . . 127

Fig. 50. Standard Deviation of Velocity along  
Transverse Cross Sections for Four Test Grids  
with 93% Depth Increase for EV = 5 and Resolution  
= 1. . . . . 128

Fig. 51. Continuity vs Distance Down Channel for 93%  
Depth Increase with EV = 25 and Resolution = 1. 130

Fig. 52. Continuity vs Distance Down Channel for 93%  
Depth Increase with EV = 125 and Resolution = 1. 131

Fig. 53. Continuity vs Distance Down Channel for 93%  
Depth Increase with EV = 250 and Resolution = 1. 132

Fig. 54. Continuity vs Distance Down Channel for 93% Depth Increase with EV = 500 and Resolution = 1. 133

Fig. 55. Three Dimensional Water Surface Elevation Plots for Four Test Grids with 93% Depth Increase with EV = 250 and Resolution = 2. . . . . 135

Fig. 56. Three Dimensional Velocity Surface Plots for 93% Depth Increase for Regular and Alternating Grids with EV = 250 and Resolution = 2. . . . . 136

Fig. 57. Three Dimensional Velocity Surface Plot for 93% Depth Increase for "C" and Quadrilateral Grids with EV = 250 and Resolution = 2. . . . . 137

Fig. 58. Continuity vs Distance Down Channel for Four Test Grids with 93% Depth Increase with EV = 5 and Resolution = 2. . . . . 138

Fig. 59. Continuity vs Distance Down Channel for Four Test Grids with 93% Depth Increase for EV = 5 and Resolution = 4. . . . . 139

Fig. 60. Continuity vs Distance Down Channel for Test Grids with 93% Depth Increase for EV = 5 and Resolution = 8. . . . . 140

Fig. 61. Maximum Continuity Deviation vs Eddy Viscosity for Regular and "C" Grids for Tested Resolution with a 93% Depth Increase. . . . . 142

Fig. 62. Maximum Continuity Deviation Versus Eddy Viscosity for Alternating and Quadrilateral Grids for Tested Resolutions with 93% Depth Increase. 143

Fig. 63. Maximum Continuity Deviation Versus Eddy Viscosity for Alternating Grid with 30% and 238% Increases in Depth. . . . . 145

Fig. 64. Maximum Continuity Deviation vs Percent Depth Change per Element for Alternating Grid Tests with 30%, 92%, and 238% Depth Increases. . 146

Fig. 65. RMA-2V Channel Continuity for 30% and 238%

Depth Increase with Resolution Equal to 1 and 8 Elements on Step. . . . .	148
Fig. 66. RMA-2V Continuity vs Distance Down Channel for Regular and Alternating Grids for Flow Over a Submerged Bump with EV = 5 and Resolution = 1. . . . .	150
Fig. 67. RMA-2V Water Surface Elevation and Velocity Surface Plots for Regular and Alternating Grids for Flow Over a Bump with Resolution = 1 and EV = 5. . . . .	151
Fig. 68. RMA-2V Continuity vs Distance Down Channel for Regular and Alternating Grids for Flow Over a Bump with EV = 25 and Resolution = 1. . . . .	152
Fig. 69. RMA-2V Continuity vs Distance Down Channel for Regular and Alternating Grids for Flow Over a Bump with EV = 125 and Resolution = 1. . . . .	153
Fig. 70. RMA-2V Continuity vs Distance Down Channel for Regular and Alternating Grids for Flow Over Bump for EV = 250 and Resolution = 1. . . . .	154
Fig. 71. RMA-2V Continuity vs Distance Down Channel for Regular and Alternating Grids for Flow Over a Bump with EV = 500 and Resolution = 1. . . . .	155
Fig. 72. RMA-2V Continuity vs Distance Down Channel for Regular and Alternating Grids for Flow Over a Bump with EV = 5 and Resolution = 2. . . . .	157
Fig. 73. RMA-2V Continuity vs Distance Down Channel for Regular and Alternating Grids for Flow Over a Bump with EV = 5 and Resolution = 4. . . . .	158
Fig. 74. RMA-2V Continuity vs Distance Down Channel for Regular and Alternating Grids for Flow Over a Bump for EV = 5 and Resolution = 8. . . . .	159
Fig. 75. RMA-2V Continuity vs Distance Down Channel for Alternating Grid for Flow Over a Submerged Bump with Resolution = 8. . . . .	161

Fig. 76. RMA-2V Maximum Continuity Deviation vs Eddy Viscosity for Alternating and Regular Grids for Tested Resolutions with 50% Depth Reduction Over Submerged Bump. . . . .	162
Fig. 77. RMA-2V Maximum Continuity Deviation vs Eddy Viscosity for Alternating Grid with 25 and 75% Depth Reduction on Submerged Bump. . . . .	163
Fig. 78. RMA-2V Maximum Continuity Deviation vs Percent Change in Depth per Element for Tests with 25, 50, and 75% Reduction in Depth on a Submerged Bump. . . . .	165
Fig. 79. RMA-2V Three Dimensional Water Surface and Velocity Plots for a 40% Reduction in Width with Resolution = 1 and EV = 125. . . . .	167
Fig. 80. RMA-2V Continuity vs Distance Down Channel a) for Hot Started Runs vs Cold Started Runs for EV = 125 and b) for Run with Node 450 Stagnated (Converged) vs Unstagnated (Near Converged). . .	169
Fig. 81. Central Section of Alternating Grid for Sudden Width Reduction Showing Node Numbers at Width Reduction and Location of Node 450. . . .	170
Fig. 82. RMA-2V Continuity vs Distance Down Channel for Regular and Alternating Grids for 40% Width Reduction with Resolution = 1. . . . .	171
Fig. 83. Section of Alternating Grid Showing a) X Resolution = 2 and Y Resolution = 1, b) X Resolution = 1 and Y Resolution = 2, and c) X and Y Resolution = 2. . . . .	173
Fig. 84. RMA-2V Continuity vs Distance Down Channel for Regular and Alternating Grids with 40% Width Reduction for Resolution = 2 in X and 1 in Y (Cross Channel). . . . .	174
Fig. 85. RMA-2V Continuity vs Distance Down Channel	

	for Regular and Alternating Grids for 40% Width Reduction with X Resolution = 1 and Y Resolution = 2. . . . .	175
Fig. 86.	RMA-2V Continuity vs Distance down Channel for Regular and Alternating Grids for 40% Width Reduction with X and Y Resolution = 2. . . . .	176
Fig. 87.	RMA-2V Continuity vs Distance Down Channel for Regular and Alternating Grids for 40% Width Reduction with X Resolution = 4 and Y Resolution = 1. . . . .	178
Fig. 88.	RMA-2V Continuity vs Distance Down Channel for Regular and Alternating Grids for 40% Width Reduction with Resolution = 1 in X and 4 in Y..	179
Fig. 89.	RMA-2V Continuity vs Distance Down Channel for Regular and Alternating Grids for 40% Width Reduction with X and Y Resolution = 4. . . . .	180
Fig. 90.	RMA-2V Continuity vs Distance Down Channel for Regular and Alternating Grids with 40% Width Reduction for X Resolution = 8 and Y Resolution = 1. . . . .	181
Fig. 91.	RMA-2V Continuity vs Distance Down Channel for Regular and Alternating Grids for 40% Width Reduction with X and Y Resolution = 8. . . . .	183
Fig. 92.	RMA-2V Maximum Continuity Deviation vs Eddy Viscosity (EV) for Regular and Alternating Grids for 40% Width Reduction for Individually Increased X and Y Resolutions. . . . .	184
Fig. 93.	RMA-2V Maximum Continuity Deviation vs Eddy Viscosity for Alternating and Regular Grids for 40% Width Reduction with X and Y Resolution Varied Equally. . . . .	185
Fig. 94.	RMA-2V Continuity Deviations vs Change in Width over Resolution for 20%, 40%, and 60%	

Reductions in Width for the Alternating Grid with X and Y Resolutions Varied Equally. . . . .	187
Fig. 95. RMA-2V Three Dimensional Water Surface and Velocity Plots for a 67% Width Expansion Alternating Grid with Resolution = 1 and EV = 125. . . . .	188
Fig. 96. RMA-2V Continuity vs Distance Down Channel for Regular and Alternating Grids for a 67% Width Expansion with Resolution = 1. . . . .	190
Fig. 97. RMA-2V Continuity vs Distance Down Channel for Regular and Alternating Grids for a 67% Width Expansion with Resolution = 2. . . . .	191
Fig. 98. RMA-2V Continuity vs Distance Down Channel for Regular and Alternating Grids for 67% Width Expansion with Resolution = 4. . . . .	192
Fig. 99. RMA-2V Continuity vs Distance Down Channel for Regular and Alternating Grids for 67% Width Expansion with Resolution = 8. . . . .	193
Fig. 100. Velocity Vector Plot for RMA-2V for 67% Width Expansion with Res = 1 and EV = 125. . . . .	195
Fig. 101. Velocity Vector Plot for RMA-2V for 67% Width Expansion with Res = 2 and EV = 125. . . . .	196
Fig. 102. Velocity Vector Plot for RMA-2V for 67% Width Expansion with Res = 4 and EV = 125. . . . .	197
Fig. 103. Velocity Vector Plot for RMA-2V for 67% Width Expansion with Res = 8 and EV = 125. . . . .	198
Fig. 104. RMA-2V Maximum Continuity Deviation vs Eddy Viscosity for Alternating and Regular Grids for Tested Resolutions with 67% Width Expansion. . . . .	199
Fig. 105. RMA-2V Maximum Continuity Deviation vs Eddy Viscosity for Alternating Grid with 25% and 150% Width Expansion. . . . .	201
Fig. 106. RMA-2V Continuity Deviations vs Change in	

Width per Element for 25%, 67%, and 150% Width Expansions for the Alternating Grid. . . . .	202
Fig. 107. RMA-2V Three Dimensional Water Surface and Velocity Surface Plots for 40% Abutment Reduction with Resolution = 1 and EV = 125. . . . .	204
Fig. 108. RMA-2V Continuity vs Distance Down Channel for Regular and Alternating Grids for a 40% Abutment Reduction with Resolution = 1. . . . .	206
Fig. 109. RMA-2V Continuity vs Distance Down Channel for Regular and Alternating Grids for a 40% Abutment Reduction with Resolution = 2. . . . .	207
Fig. 110. RMA-2V Continuity vs Distance Down Channel for Regular and Alternating Grids for 40% Abutment Reduction with Resolution = 4. . . . .	208
Fig. 111. RMA-2V Continuity vs Distance Down Channel for Regular and Alternating Grids for 40% Abutment Reduction with Resolution = 8. . . . .	209
Fig. 112. RMA-2V Maximum Continuity Deviation vs Eddy Viscosity for Alternating and Regular Grids for Tested Resolutions with 40% Abutment Reduction. . . . .	211
Fig. 113. RMA-2V Maximum Continuity Deviation vs Eddy Viscosity for Alternating Grid with 20% and 60% Abutment Reduction. . . . .	212
Fig. 114. RMA-2V Continuity Deviations vs Percent Abutment Reduction Divided by Resolution for 20%, 40%, and 60% Abutment Reductions for Alternating Grid. . . . .	213

## Volume II

Fig. 115. Time Series Plots of Water Surface Elevation and Velocity for 2DDI Model (Version 11.01) with Head of 0.01 Feet and with 12 Second
--

	Time Step. . . . .	222
Fig. 116.	Time Series Plots of Water Surface Elevation and Velocity for 2DDI Model (Version 19.11) with Head of 0.01 Feet with 12 Second Time Step. . . . .	223
Fig. 117.	Time Series Plots of Water Surface Elevation and Velocity for the 2DDI Model (Version 19.11) with a Head of 0.01 Feet for a Time Step of 90 Seconds. . . . .	224
Fig. 118.	Time Series Plots of Water Surface Elevation and Velocity for 2DDI Model (Version 19.11) with Head of 0.01 Feet with 1440 Second Time Step. . . . .	225
Fig. 119.	Time Series Plot for Water Surface Elevation and Velocity for 2DDI Model (V. 19) with 0.01 Ft. Head, 12 Second Time Step, and Ramp Length of 2 Days. . . . .	227
Fig. 120.	Time Series Plots of Water Surface Elevation and Velocity for 2DDI Model (V. 19) with Head of 0.01 Ft., with 12 Second Time Step, and Ramp Length of 0.05 Days. . . . .	228
Fig. 121.	Time Series Plots of Water Surface Elevation and Velocity for 2DDI Model (Version 19.11) with a Head of 1.0 Feet with 12 Second Time Step. . . . .	229
Fig. 122.	Continuity in Smooth Bottom Channel for Linear 2DDI Model with Flow Equal to Approximately 500,000 cfs for $\Delta t$ Equal to 12, 90, and 1440 Seconds. . . . .	234
Fig. 123.	Effects of Varying Lateral Diffusion (Eddy Viscosity) for Constant Head of 0.167 Ft with Time Step of 12 Seconds and Simulation Length of 2.0 Days for Linear 2DDI Model and Smooth Bottom	



Flume. . . . .	235
Fig. 124. Time History Plots of Water Surface Elevation and Velocity for Sudden Reduction in Depth with Fully Non-linear 2DDI Model for Head = 0.01 Ft and a 12 Second Time Step. . . . .	239
Fig. 125. Continuity in Channel vs Distance and Time for Fully Non-linear 2DDI Model for a Head of 0.01 Feet for a Sudden Reduction in Depth with Resolution = 1. . . . .	240
Fig. 126. Water Surface Elevations for 2DDI Model as Compared with HEC-2 and RMA-2V Models for Alternating Grid with Head = 1.59 Feet. . . . .	243
Fig. 127. Continuity for Linear 2DDI Model and Flow Rate vs Lateral Diffusion for Alternating Grid with Resolution = 1 and Head = 1.59 Feet. . . . .	246
Fig. 128. Continuity vs Distance Down Channel for Linear 2DDI Model for Regular and "C" Grids for Single Resolution Test with Head = 1.59 Feet and EV = 0.000195. . . . .	247
Fig. 129. Three Dimensional Water Surface Elevation Plots for Linear 2DDI Model for Test Grids with a Head of 1.59 Feet and EV = 0.000195. . . . .	248
Fig. 130. Three Dimensional Velocity Surface Plot for Linear 2DDI Model for Test Grids with Head = 1.59 Feet, EV = 0.000195, and Resolution = 1. . . . .	250
Fig. 131. Three Dimensional Velocity Surface Plots for Linear 2DDI Model for Alternating Grid for Increasing Lateral Diffusion with Head = 1.59 Feet and 12 Second Time Step. . . . .	252
Fig. 132. 2DDI Continuity vs Distance Down Channel for Test Grids with Sudden Reduction in Depth for Resolution = 1, EV = 0.0 and Head = 0.76 Ft. . . . .	253
Fig. 133. Three Dimensional Velocity Surface Plots	

	for Test Grids with EV = 0.0, Head = 0.76 Ft, and Time Step = 12 Seconds. . . . .	254
Fig. 134.	2DDI Channel Continuity for Sudden Depth Reduction Test Grids for Resolution = 2 with 12 Second Time Step. . . . .	256
Fig. 135.	2DDI Channel Continuity for Sudden Depth Reduction Test Grids for Resolution = 4 with a 12 Second Time Step. . . . .	257
Fig. 136.	2DDI Continuity for Sudden Depth Reduction Test Grids with a 12 Second Time Step for Resolution = 8. . . . .	258
Fig. 137.	Linear 2DDI Model Maximum Continuity Deviation vs Percent Change in Depth per Element for 50% and 25% Reduction in Depth for 500,000 cfs Flowrate for EV = 0.0 and 0.000195. . . . .	260
Fig. 138.	2DDI Water Surface Elevation and Velocity for Selected Nodes for Alternating Grid with 75% Depth Reduction with 0.4 Day Ramp. . . . .	262
Fig. 139.	2DDI Water Surface Elevation and Velocity for Selected Nodes for Alternating Grid with 75% Depth Reduction with 0.8 Day Ramp. . . . .	263
Fig. 140.	2DDI Maximum Deviation vs Percent Reduction in Depth for 25% to 75% Depth Reductions Compared to RMA-2V Results. . . . .	264
Fig. 141.	2DDI Water Surface Elevation vs HEC-2 Model Predictions for 25% and 75% Depth Reductions with Alternating Grid for 500,000 cfs. . . . .	266
Fig. 142.	Non-linear 2DDI Model Water Surface Elevation and Velocity for Sudden Depth Increase, Alternating Grid with 0.01 Ft Head, 0.4 Day Ramp, and EV = 0.0. . . . .	269
Fig. 143.	Non-linear 2DDI Model Continuity Results for Sudden Depth Increase, Alternating Grid with	

	EV = 0.0, Ramp = 0.4 Days, and Head at 0.01 Ft.	270
Fig. 144.	Linear 2DDI Model Water Surface Elevation and Velocity for Selected Nodes for Sudden Depth Increase, Alternating Grid with Resolution = 1, Head = 0.75 Ft, EV = 0.0, and 12 Second Time Step. . . . .	271
Fig. 145.	Linear 2DDI Continuity vs Distance Down Channel and 2DDI Water Surface Elevation with EV = 0.0 and 0.75 Ft. Head vs HEC-2 and RMA-2V. . .	273
Fig. 146.	Linear 2DDI Three Dimensional Water Surface Elevation Plots for Sudden Depth Increase Test Grids with EV = 0, Head = 0.75 Ft, Resolution = 1, and Time Step = 12 Seconds. . . . .	274
Fig. 147.	Linear 2DDI Three Dimensional Velocity Surface Plots for Sudden Depth Increase Test Grids with EV = 0.0, Head = 0.75, Resolution = 1, and Time Step = 12 Seconds. . . . .	275
Fig. 148.	Linear 2DDI Continuity vs Distance Down Channel for Sudden Depth Increase Test Grids, Resolution = 2 and 4, EV = 0.0, Head = 0.75 Ft, and a 12 Second Time Step. . . . .	276
Fig. 149.	2DDI Continuity for Resolution = 8 and Maximum Continuity Deviation vs % Depth Increase for 93% Depth Increase. . . . .	278
Fig. 150.	2DDI Channel Continuity for 30%, 93%, and 238% Depth Increase, Alternating Grid, Resolution = 1 and 8, Ev = 0.0, 12 Second Time Step. . . .	280
Fig. 151.	2DDI Maximum Deviation Data for 30%, and 238% Depth Increase Alternating Grid with EV = 0.0, and 12 Second Time Step Compared with RMA-2V Data. . . . .	281
Fig. 152.	Non-linear 2DDI Model Water Surface Elevation and Velocity for Submerged Bump	

	Alternating Grid with 0.01 Ft Head, 0.4 Day Ramp, and EV = 0.0. . . . .	283
Fig. 153.	Non-linear 2DDI Model Continuity Results for Submerged Bump, Alternating Grid with EV = 0.0, Ramp = 0.4 Days, Head at 0.01 Ft, and 12 Second Time Step. . . . .	284
Fig. 154.	Linear 2DDI Model Water Surface Elevation and Velocity for Selected Nodes for Submerged Bump Alternating Grid with Resolution = 1, Head = 0.178 Ft, EV = 0.0, and 12 Second Time Step. . .	285
Fig. 155.	Linear 2DDI Continuity vs Channel Distance with EV = 0.0, Ramp = 0.1 Day, Head = 0.178 Ft, 12 Second Time Step, and Water Surface Elevation Compared with HEC-2 and RMA-2V. . . . .	287
Fig. 156.	Linear 2DDI Three Dimensional Water Surface Elevation Plots for Submerged Bump Test Grids with EV = 0.0, Head = 0.178 Ft, Resolution = 1, and Time Step = 12 Seconds. . . . .	288
Fig. 157.	Linear 2DDI Three Dimensional Velocity Surface Plots for Submerged Bump Test Grids with EV = 0.0, Head = 0.178, Resolution = 1, and Time Step = 12 Seconds. . . . .	289
Fig. 158.	Linear 2DDI Continuity vs Distance Down Channel for Submerged Bump Test Grids, Resolution = 2 and 4, EV = 0.0, Head = 0.178 Ft, and a 12 Second Time Step. . . . .	290
Fig. 159.	2DDI Continuity for Resolution = 8, and Maximum Continuity Deviation for 25% and 50% Submerged Bump with EV = 0.0 and 12 Second Time Step. . . . .	292
Fig. 160.	2DDI Maximum Continuity Deviations for 75% Submerged Bump and Channel Flow Rate vs Resolution of Submerged Bump with EV = 0.0 and 12	

	Second Time Steps. . . . .	293
Fig. 161.	Linear 2DDI Continuity vs Channel Distance for 25%, 50% and 75% Submerged Bump, Alternating Grid, Resolution = 1 and 8, EV = 0.0, 12 Second Time Steps. . . . .	295
Fig. 162.	Non-linear 2DDI Model Water Surface Elevation and Velocity for 40% Width Reduction with Alternating Grid, 0.01 Ft Head, 0.4 Day Ramp, and EV = 0.0. . . . .	296
Fig. 163.	Non-linear 2DDI Model Continuity vs Channel Distance for Alternating 40% Width Reduction Grid at $t = 15,000, 25,500, 28,500, 33,000,$ and $36,000$ Seconds with 0.01 Ft Head, 0.4 Day Ramp and EV = 0.0. . . . .	297
Fig. 164.	Non-linear 2DDI Model Water Surface Elevation and Velocity for 40% Width Reduction with Alternating Grid, 0.01 Ft Head, 0.4 Day Ramp, EV = 0.0, and 1.5 Second Time Step. . . . .	299
Fig. 165.	Non-linear 2DDI Model Channel Continuity for 40% Width Reduction Alternating Grid at Simulation Times of 18,000, 22,500, 25,875, and 26,437 Seconds. . . . .	300
Fig. 166.	Linear 2DDI Water Surface Elevation and Velocity for 40% Width Reduction Alternating Grid with Resolution = 1, Head = 0.32 Ft, EV = 0.0 and 12 Second Time Step. . . . .	301
Fig. 167.	Linear 2DDI Continuity vs Channel Distance and Water Surface Elevation Compared to HEC-2 and RMA-2V for EV = 0.0 and 0.32 Ft Head. . . . .	303
Fig. 168.	Linear 2DDI Model Three Dimensional Water Surface Elevations for 40% Width Reduction Test Grids with EV = 0.0, Head = 0.32 Ft, Resolution = 1, and a 12 Second Time Step. . . . .	304

- Fig. 169. Linear 2DDI Model Three Dimensional Velocity Surface Plot for 40% Width Reduction Grids with EV = 0.0, Head = 0.32 Ft, Resolution = 1, and Time Step = 12 Seconds. . . . . 305
- Fig. 170. Linear 2DDI Continuity vs Channel Distance for 40% Width Reduction with Resolution Equal to 2 in X and 1 in Y, 1 in X and 2 in Y, and 2 in Both X and Y for Head = 0.32 Ft. . . . . 306
- Fig. 171. Linear 2DDI Channel Continuity for 40% Width Reduction with Resolution Equal a) 4 in X and 1 in Y, b) 1 in X and 4 in Y, and 4 in Both X and Y for Head = 0.32 Ft. . . . . 308
- Fig. 172. Linear 2DDI Channel Continuity for 40% Width Reduction with Resolution Equal to a) 8 in X, 1 in Y and b) 8 in Both X and Y for Head = 0.32 Ft with EV = 0.0. . . . . 309
- Fig. 173. 2DDI Continuity Deviations vs Percent Reduction in Width per Element for Test Grids with Head = 0.32 Ft, EV = 0.0, Ramp = 0.1 Day, and 12 Second Time Steps. . . . . 310
- Fig. 174. 2DDI Maximum Continuity Deviations vs Percent Width Reduction per Element for 20%, 40%, and 60% With Reductions with RMA-2V Data Plotted for Comparison. . . . . 312
- Fig. 175. Linear 2DDI Channel Continuity for 20%, 40%, and 60% Width Reduction Alternating Grid for Resolutions of 1 and 8, EV = 0.0, 12 Second Time Steps, and 0.1 Day Ramp. . . . . 313
- Fig. 176. Non-linear 2DDI Model Water Surface Elevation and Velocity for 67% Width Expansion with Alternating Grid, 0.01 Ft Head, 0.4 Day Ramp, and EV = 0.0. . . . . 315
- Fig. 177. Non-linear 2DDI Model Channel Continuity

	for Alternating Grid 67% Width Expansion at $t = 30,000, 41,500, 51,000,$ and $57,000$ Seconds with $0.01$ Ft Head, $0.4$ Day Ramp, and $EV = 0.0$ . . . .	316
Fig. 178.	Linear 2DDI Model Water Surface Elevation and Velocity for Selected Nodes for 67% Width Expansion Alternating Grid with $Res = 1,$ Head = $0.32$ Ft, and $EV = 0.0$ . . . . .	317
Fig. 179.	Linear 2DDI Continuity vs Channel Distance with $EV = 0.0,$ Ramp = $0.1$ Day, Head = $0.32$ Ft, $12$ Second Time Step, and Water Surface Elevation Compared with HEC-2 and RMA-2V. . . . .	318
Fig. 180.	Linear 2DDI Model Three Dimensional Water Surface Elevations for 67% Width Expansion Test Grids with $EV = 0.0,$ Head = $0.32$ Ft, Resolution = $1,$ and a $12$ Second Time Step. . . . .	319
Fig. 181.	Linear 2DDI Model Three Dimensional Velocity Surface Plot for 67% Width Expansion with $EV = 0.0,$ Head = $0.32$ Ft, Resolution = $1,$ and Time Step = $12$ Seconds. . . . .	320
Fig. 182.	Linear 2DDI Continuity vs Distance Down Channel for 67% Width Expansion Test Grids, Resolution = $2$ and $4,$ $EV = 0.0,$ Head = $0.32$ Ft, and a $12$ Second Time Step. . . . .	321
Fig. 183.	2DDI Continuity for Resolution = $8$ and Maximum Continuity Deviation for 67% Width Expansion with $EV = 0.0,$ Head = $0.32$ Ft, and a $12$ Second Time Step. . . . .	323
Fig. 184.	Linear 2DDI Velocity Vector Plot for 67% Width Expansion with Resolution = $1$ and $EV = 0.0$ . . . . .	324
Fig. 185.	Linear 2DDI Model Velocity Vector Plot for 67% Width Expansion with Resolution = $2$ and $EV = 0.0$ . . . . .	325

Fig. 186. Linear 2DDI Velocity Vector Plot for 67% Width Expansion with Resolution = 4 and EV = 0.0. . . . .	326
Fig. 187. Linear 2DDI Velocity Vector Plot for 67% Width Expansion with Resolution = 8 and EV = 0.0. . . . .	327
Fig. 188. Linear 2DDI Maximum Continuity Deviation vs Percent Expansion per Element for 25% and 150% Width Expansion Alternating Grid Tests with EV = 0.0 and Flow = 500,000 cfs. . . . .	328
Fig. 189. Linear 2DDI Channel Continuity for 25%, 67%, and 150% Width Expansion, Alternating Grid, Resolution = 1 and 8, EV = 0.0, 12 Second Time Steps. . . . .	330
Fig. 190. Non-linear 2DDI Model Water Surface Elevation and Velocity for 40% Abutment Reduction with Alternating Grid, 0.01 Ft Head, 0.4 Day Ramp, and EV = 0.0. . . . .	331
Fig. 191. Non-linear 2DDI Model Channel Continuity for Alternating Grid 40% Abutment Reduction Test at T = 21,000, 25,500, and 30,000 Seconds with 0.01 Ft Head, 0.4 Day Ramp, and EV = 0.0. . . . .	332
Fig. 192. Linear 2DDI Model Water Surface Elevation and Velocity for Standard Nodes for 40% Abutment Reduction Alternating Grid with Res = 1, Head = 0.18 Ft, and EV = 0.0. . . . .	333
Fig. 193. Linear 2DDI Continuity vs Channel Distance for Res = 1 and Water Surface Elevations for Standard Nodes with EV = 0.0, 0.18 Ft Head, and Ramp = 0.1 Day. . . . .	334
Fig. 194. Linear 2DDI Model Three Dimensional Water Surface Elevations for 40% Abutment Reduction with EV = 0.0, Head = 0.18 Ft, Resolution = 1,	



	and a 12 Second Time Step. . . . .	336
Fig. 195.	Linear 2DDI Model Three Dimensional Velocity Surface Plots for 40% Abutment Reduction with EV = 0.0, Head = 0.18 Ft, Resolution = 1, and a 12 Second Time Step. . . . .	337
Fig. 196.	Linear 2DDI Continuity vs Channel Distance for 40% Abutment Reduction with Resolution = 2 and 4, EV = 0.0, Head = 0.18 Ft, and a 12 Second Time Step. . . . .	338
Fig. 197.	2DDI Continuity for Resolution = 8 and Maximum Continuity Deviation for 40% Abutment Reduction with EV = 0.0, Head = 0.32 Ft, and a 12 Second Time Step. . . . .	340
Fig. 198.	Linear 2DDI Maximum Continuity Deviation vs Percent Reduction per Element for 20%, 40%, and 60% Abutment Reduction Alternating Grids with EV = 0.0 and a Flow of 500,000 cfs. . . . .	341
Fig. 199.	Linear 2DDI Channel Continuity for 20%, 40%, and 60% Abutment Reduction Alternating Grids, Resolution = 1 and 8, EV = 0.0, and 12 Second Time Steps. . . . .	342
Fig. 200.	Riprap Test Facility Inlet and Outlet Elevation Contours (a) as Modeled by Abraham (1991) Without Headbay or Tailbay, (b) Inlet with Headbay, and (c) Outlet with Tailbay. . . . .	345
Fig. 201.	John L. Grace, Jr. Riprap Test Facility Layout with Location of Cross Sections Where Prototype Data Was Collected. . . . .	347
Fig. 202.	John L. Grace, Jr. Riprap Test Facility Streamwise Velocity Data Collected by Maynord (1990) for Cross Section 3+71 at a Flow of 150 cfs. . . . .	348
Fig. 203.	Method Used by Maynord to Calculate Depth	

	Page
Averaged Velocity from Observed Data Points. . .	349
Fig. 204. RMA-2V Riprap Test Facility Lateral Velocity Distribution at Station 1+78 for Flow of 50 cfs with Observed and Calculated Data for Variable EV. . . . .	350
Fig. 205. RMA-2V Riprap Test Facility Water Surface and Bed Elevations for Variable EV and Manning's n Value for Regular Grid vs Observed Data. . . .	352
Fig. 206. RMA-2V Calculated Velocity vs Observed Data for Riprap Test Facility at Stations 2+03 and 2+42 with Flow of 50 cfs, $n = 0.032$ , and $EV =$ 0.03. . . . .	354
Fig. 207. RMA-2V Calculated Velocity vs Observed Data for Riprap Test Facility at Stations 2+81 and 3+06 with Flow of 50 cfs, $n = 0.032$ , and $EV =$ 0.03. . . . .	355
Fig. 208. RMA-2V Calculated Velocity vs Observed Data for Riprap Test Facility at Stations 3+31 and 3+71 with Flow of 50 cfs, $n = 0.032$ , and $EV =$ 0.03. . . . .	356
Fig. 209. RMA-2V Calculated Velocity vs Observed Data for Riprap Test Facility at Stations 4+10 and 4+50 with Flow of 50 cfs, $n = 0.032$ , and $EV =$ 0.03. . . . .	357
Fig. 210. RMA-2V Calculated Velocity vs Observed Data for Riprap Test Facility at Stations 4+97 and 5+38 with Flow of 50 cfs, $n = 0.032$ , and $EV =$ 0.03. . . . .	358
Fig. 211. RMA-2V Calculated Velocity vs Observed Data for Riprap Test Facility at Stations 5+78 and 6+25 with Flow of 50 cfs, $n = 0.032$ , and $EV =$ 0.03. . . . .	359
Fig. 212. RMA-2V Riprap Test Facility Model	

	Continuity at Each Corner Node Row for Regular and Alternating Grids with $EV = 0.03$ , Manning's $n = 0.032$ , and Flow = 50 cfs. . . . .	360
Fig. 213.	Linear 2DDI Riprap Test Facility Model Vector Plot Results with Head = 1.6 Ft, $EV = 0.001$ , Ramp = 0.1 Day, Time Step = 1.0 Second, and Time = 2.5 Hours. . . . .	363
Fig. 214.	Fully Non-linear 2DDI Velocity Vector Plot for Riprap Test Facility Model with Head = 1.79 Ft, $EV = 0.0$ , 0.1 Day Ramp and a 0.4 Second Time Step at Time = 250 Seconds. . . . .	364
Fig. 215.	Fully Non-linear 2DDI Riprap Test Facility Model Nodal Velocity Values for Inflow Boundary vs Time for Head = 1.79 Ft, $EV = 0.001$ , Ramp = 0.1, and Time Step = 0.4 Seconds. . . . .	365
Fig. 216.	Non-linear 2DDI Riprap Test Facility Dimensionless Lateral Velocity Distribution at Station 1+78 for (a) Varying $EV$ and (b) for $EV = 0.001$ Compared with RMA-2V and Observed Data . . . . .	367
Fig. 217.	Non-linear 2DDI Dimensionless Velocity vs Observed Data for Riprap Test Facility at Stations 2+03 and 2+42 with Flow of 2.2 cfs, $EV = 0.001$ , 0.4 Second Time Step, and 0.1 Day Ramp. . . . .	368
Fig. 218.	Non-linear 2DDI Dimensionless Lateral Velocity vs Observed and RMA-2V Data for Riprap Test Facility at Stations 2+81 and 3+06 with Flow of 2.2 cfs, $EV = 0.001$ , 0.4 Second Time Step, and 0.1 Day Ramp. . . . .	369
Fig. 219.	Non-linear 2DDI Dimensionless Lateral Velocity vs Observed and RMA-2V Data for Riprap Test Facility at Stations 3+31 and 3+71 with Flow of 2.2 cfs, $EV = 0.001$ , 0.4 Second Time Step, and 0.1 Day Ramp. . . . .	370

Fig. 220. Non-linear 2DDI Dimensionless Lateral Velocity vs Observed and RMA-2V Data for Riprap Test Facility at Stations 4+10 and 4+50 with Flow of 2.2 cfs, EV = 0.001, 0.4 Second Time Step, and 0.1 Day Ramp. . . . .	371
Fig. 221. Non-linear 2DDI Dimensionless Lateral Velocity vs Observed and RMA-2V Data for Riprap Test Facility at Stations 4+97 and 5+38 with Flow of 2.2 cfs, EV = 0.001, 0.4 Second Time Step, and 0.1 Day Ramp. . . . .	372
Fig. 222. Non-linear 2DDI Dimensionless Lateral Velocity vs Observed and RMA-2V Data for Riprap Test Facility at Stations 5+78 and 6+25 with Flow of 2.2 cfs, EV = 0.001, 0.4 Second Time Step, and 0.1 Day Ramp. . . . .	373
Fig. 223. Non-linear 2DDI Riprap Test Facility Model Continuity vs Location Down Channel for Flow of 2.2 cfs with Head = 0.02 ft, EV = 0.001, Ramp = 0.1 and Time Step = 0.4 Seconds. . . . .	374
Fig. 224. Continuity Lines used in Redeye Crossing Test Model Showing Corner Nodes not Included on Continuity Lines. . . . .	376
Fig. 225. Observed Hydrograph of Mississippi River at Baton Rouge, Louisiana for Jan 1 through Nov 10, 1990 and Stage Discharge Curves for Redeye Crossing Model Inlet and Outlet. . . . .	378
Fig. 226. Element Types and Locations Used in Redeye Crossing Mississippi River Model. . . . .	379
Fig. 227. Redeye Crossing Bed Elevations as Adjusted for RMA-2V Model. . . . .	381
Fig. 228. RMA-2V Velocity Vector Plot for Redeye Crossing with EV = 80 in Main Channel and 100 in All Other Areas for Flow Rate of 1,200,000 cfs. . . . .	383

Fig. 229. RMA-2V Velocity Vector Plot for Redeye Crossing Model with EV = 100 at All Locations in Model for Flow of 1,200,000 cfs. . . . .	384
Fig. 230. RMA-2V Calculated Depth of Flow for Redeye Crossing Model with EV = 100 at All Locations for Flow of 1,200,000 cfs. . . . .	385
Fig. 231. RMA-2V Total Velocity for Redeye Crossing Model with EV = 80 in River Channel and 100 on Remainder of Model. . . . .	386
Fig. 232. RMA-2V Redeye Crossing Model Continuity for Q = 1,200,000 cfs with EV = 100 at All Locations. Flow Over Point Accounts for About 3.15% of Total Flow. . . . .	387
Fig. 233. Fully Non-linear 2DDI Velocity Vector Results for Redeye Crossing Model. . . . .	391
Fig. 234. Non-linear 2DDI Redeye Crossing Model Velocity Plot Showing Low Velocities in Solution Just Prior to Terminal Instability (Velocity > 100 ft/sec). . . . .	392
Fig. 235. Linear 2DDI Velocity Vector Results for Redeye Crossing Model After 2 Day Simulation with 3 Second Time Steps. . . . .	393

## LIST OF TABLES

## Volume II

	Page
Table 1. Time Step Limits for 2DDI Model with Simple Test Grids for Maximum Expected Depths and Tested Grid Resolutions. . . . .	238
Table 2. Manning's n Values for Various Element Material Types and EV Values Used in Early RMA-2V Redeye Crossing Mississippi Model to Match Observed Conditions. . . . .	380

## SIMPLE TEST CASES WITH ADCIRC-2DDI

The ADCIRC-2DDI model input is based on terms and conditions usually associated with ocean modeling. Bottom elevations are assumed to be negative (below mean sea level) and are input in terms of bathymetry. This required the conversion of elevations from the RMA-2V geometry files such that elevations of 99.0 feet with a water surface elevation of 205.33 became bathymetric values of 106.33 with the water surface at an elevation of 0.0 feet (the equivalent of mean sea level). This conversion was accomplished at the same time the grid input file was reformatted to be acceptable to the 2DDI model.

The initial version of the model used for testing was 7.03 and additional preliminary tests were made using version 11.01, but prior to extensive testing version 19.11 was made available. Stability appeared to be about the same for all three models but only a few actual comparisons were documented. The 11.01 version included a reformulation of the convective terms in the generalized wave continuity equation and added options for modeling. The convective terms were modified to be non-conservative in version 11.01 to improve model stability and continuity (Westerink 1992). Version 19.11 included more input/output options and different methods for specifying which terms would be included in the calculations. Version 19.11 has also been modified to improve vectorization on multiple processor computers such as the Waterways Experiment Station's Cray Y-MP.

The 2DDI model was developed to model time dependant problems exclusively and the solution of steady state problems involves time stepping to a steady state solution. The time used in the initial tests varied from 0.75 to 3 days. For these particular problems, it appeared that if the model would not converge to a solution in 0.75 days it

would not converge at all. Thus the 0.75 day simulation length was used for initial testing for the fully non-linear model.

The 2DDI model allows the bottom friction factor  $C_f$  to be specified either globally or by element. Since the friction factor varies not only with the Manning's  $n$  value but also with depth, the friction factor had to be calculated for each node. A routine was added to the grid conversion program that used the bathymetric depth to calculate the friction factor based on a horizontal water surface at elevation 0.0 feet. In some instances this calculated friction factor could be in error by a few percent due to differences between the horizontal water surface used in calculations and the sloped water surface calculated by the model. This water surface elevation difference should be less than 1 to 2 feet and friction factor errors should be less than 3% for a 1.0 foot head difference across the model. This error was not expected to be significant in the results. The value of the friction factor was calculated as follows:

$$C_f = \frac{n^2 g}{h^{1/3}} \quad \text{Metric Units} \quad (105)$$

$$C_f = \frac{n^2 g}{(1.486 h^{1/6})^2} \quad \text{English Units} \quad (106)$$

In the RMA-2V model tests an  $n$  value of 0.02 was used for all simple test cases. The water depth was approximately 106.33 feet in the areas where the bottom was not raised (i.e. the deep portions of the grid - upstream from the sudden reduction in depth). Using these values the friction coefficient ( $C_f$ ) was calculated to be 0.00123. For tests where the depth was reduced significantly - the shallow areas downstream from the sudden reduction in depth for example - the friction coefficient was 0.00153.



The coriolis terms were set to zero in both models to avoid additional terms which would complicate model comparisons. This was also true of the tidal potential terms, wind stress terms, and atmospheric pressure terms in the 2DDI model. Numerical integration in the 2DDI model was performed initially in the preliminary testing (for versions 7.03 and 11.01) using 3 Gaussian quadrature points per element and using 4 for tests with version 19.11. Four quadrature points were used for all final testing and for all tests other than the early preliminary testing.

Time integration was done using time weighting factors of 0.35, 0.3, and 0.35 for the  $k+1$ ,  $k$ , and  $k-1$  time steps, respectively for the wave equation calculations for water surface at the  $k+1$  time step. Time weighting factors for the lateral diffusion terms in the momentum equation (which are variable in the 2DDI model) used a Crank-Nicolson (0.5 for the  $k$  and  $k+1$  time levels) approximation.

Lateral momentum diffusion (comparable to the eddy viscosity term or turbulent exchange coefficients in RMA-2V) was set to 0.0 for the initial testing of the 2DDI model. This value was increased when problems were noted with stability in the fully non-linear form of the model, but the increase in lateral viscosity or diffusion only added to the instability problem and slowed model operation dramatically. The dramatic reduction in model operating speed was due to the large number of iterations required to arrive at an acceptable solution with the lateral viscosity turned on. Varying the convergence accuracy value for this calculation showed no noticeable effect on convergence (or lack thereof). In the following discussion the lateral diffusion terms will also be called the eddy viscosity terms for continuity in discussions and ease in abbreviation of terms for plots. While the terms are not exactly the same in the two models they are both a mechanism for reducing flow momentum and serve the same theoretical purpose.

The model as provided did not allow the specification of flux boundary conditions. The flux boundary conditions were planned for a later release but testing could not wait for the planned release during the summer of 1992. The only boundary conditions that could be specified in the model were tidal (elevation) boundary conditions. Because of this it was necessary to simulate steady state conditions by using a very long tidal constituent wave. The constituent used was a Ssa - Solar semi-annual - with a period of 2191.43 hours. This wave had a long enough period that water surface elevations did not vary significantly during the 0.75 day simulations.

As a result the model was operated with head boundaries (tidal specifications) at each end of the test channel. The head boundary conditions were set initially using values from the RMA-2V model tests and adjusted to give the correct flow rate at the inflow boundary.

No provision is made in the model for the internal calculation of continuity check lines and continuity was calculated by an external program upon the completion of each 2DDI model run. The separate program used the depths and velocities at each time step to calculate continuity at each row of nodes along the channel as had previously been done for the RMA-2V model.

#### THE FULLY NON-LINEAR MODEL

Initial tests with the ADCIRC-2DDI model were attempted using the fully non-linear form of the model. It was found that the model would not converge with a head difference of 1.0 foot across the model and very small aberrations in velocity would grow until the model would blow up. At this time the FORTRAN code was modified such that when the maximum velocity in the model exceeded 100 feet per second

(or 100 meters per second if using metric units), the model would stop calculation and print a warning message.

Westerink, Luettich, and Scheffner (1992) indicate that the value of  $\tau_0$  - the primitive equation weighting factor - should be approximately equal ("same order of magnitude") to the maximum value of  $\tau$  as given in Equation 48. The value for  $C_f$  obtained from equation 150 is 0.00123 for the deep portions of the channel and 0.00153 for the portion of the channel with a 50% reduction in depth (as previously shown). Using these values  $\tau$  was calculated to be 0.0000521 and 0.000245 respectively.  $\tau_0$  was then set to 0.0003 - slightly higher than  $\tau$  maximum - in accordance with guidance in the above referenced User's Manual. The fully non-linear version of the model was unstable with  $\tau_0$  set to these values.

Since the model would not converge for the above values the primitive equation weighting factor ( $\tau_0$ ) was varied from a value of 0.00001 to 0.01. The values below 0.0001 produced no differences in continuity values in the channel and continuity values at the end of the simulations were identical with all runs producing very poor results. For values higher than 0.0001 the model became unstable earlier in the simulation and maximum velocity values were significantly higher. For example, when the weighting factor was changed from 0.0004 to 0.0008 the model exceeded the maximum allowable velocity of 100 feet per second and was stopped at time step 94 and 89 respectively with maximum velocities of 135 and 200 feet per second. Since the model was unstable at all values of  $\tau_0$  its value was reset to the estimated value for  $\tau_0$  of 0.0003.

The value of  $\Delta t$  was next varied from 5 seconds to 1440 seconds. This yielded Courant numbers ( $\Phi = (gh)^{1/2} \Delta t / \Delta x$ ) from 0.58 to 167.7. The fully non-linear form of the model would not converge at any Courant number but was represented

as being stable at Courant numbers less than 1.5.

(Westerink, Luettich, and Scheffner 1992)

Since the model would not converge in the fully non-linear form for the simple test cases, a smooth bottomed channel model was constructed. The channel was the same as that used for the simple test cases but without any bump or change in channel geometry or bottom slope as shown in Fig. 4(b). The channel had a constant slope which was identical to that used in the other simple test cases and a single resolution grid. The smooth bottomed channel was modeled in an attempt to find the velocity range in the simple test problems that could be modeled with the 2DDI model. The time step was set to 12 seconds ( $\Delta t = 1.5$ ),  $\tau_0$  was set to 0.0001 - the most stable value, and all other values were set to the value used in the sudden depth increase case for the RMA-2V model. The fully non-linear model was not stable for any tests with the smooth bottom channel.

After these numerous attempts to run the model in the fully non-linear form (NOLI=3 in Version 11.01) by varying the lateral momentum diffusion (eddy viscosity) terms, the time step, and the primitive momentum equation weighting term it became apparent that the fully non-linear model would not converge at all for this problem with a head of 1.0 foot. The head difference across the model was then reduced to 0.01 feet and  $\tau_0$  was set to 0.000002. Even at this low value for head and with estimated velocities of about one foot per second, the fully non-linear model would still not converge.

Velocity and water surface elevations were plotted for nodes laying one row to the left of the channel center-line (facing down channel or at  $Y = 700$  feet) and at:

- 1) the channel inlet ( $X = 0$ ),
- 2) midway from the inlet to the change in depth ( $X = 5000$ ),
- 3) at the beginning of the change in depth ( $X = 10000$ ),

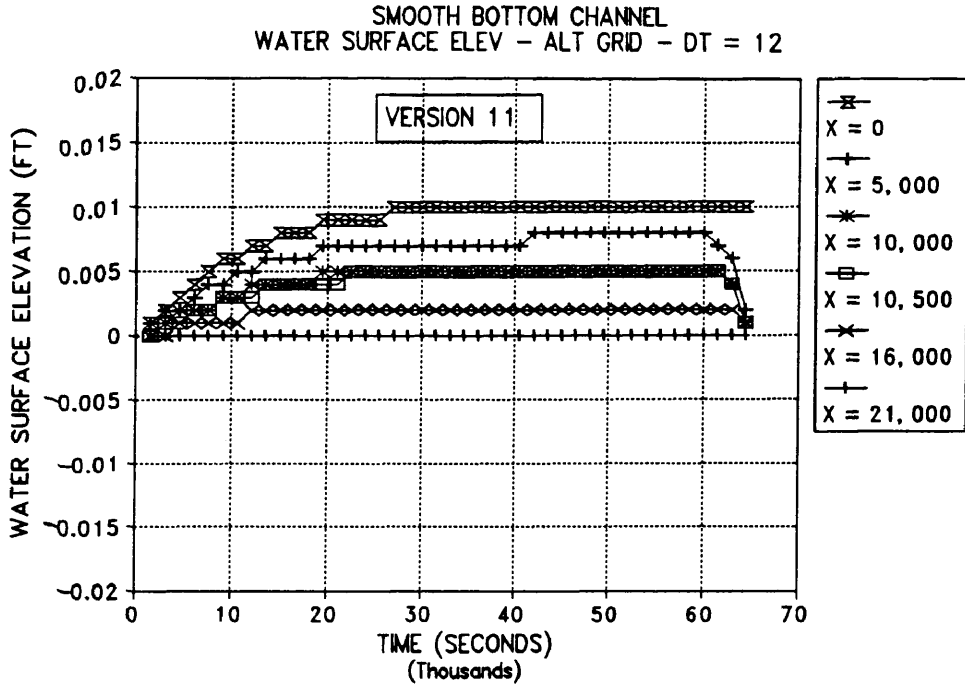
- 4) at the end of the change in depth ( $X = 10500$ ),
- 5) at midway from the end of the change in depth and the outlet ( $X = 16000$ ), and
- 6) and at the channel outlet ( $x = 21000$ ).

Some plots in the following sections will include a value at the end of the bump ( $X = 11,000$ ) or 500 feet downstream from the end of the sudden increase and decrease in depth - rather than the value at the end of the channel ( $X=21,000$  feet) since the water surface value is set by a boundary condition at the downstream end of the model.

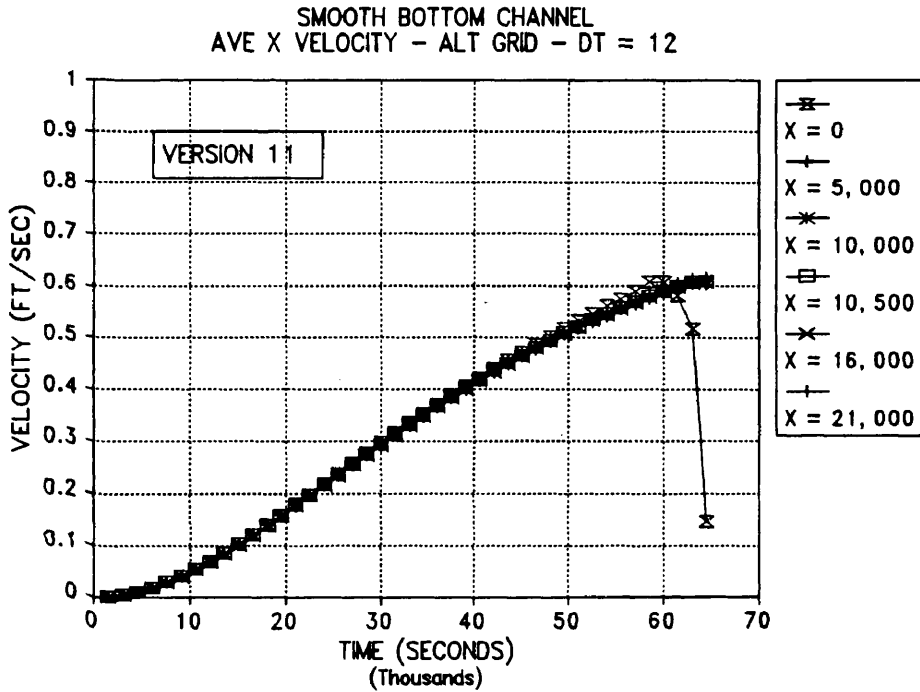
Fig. 115 shows water surface elevations and velocities for the six nodes listed above with a 12 second time step for version 11.01 while Fig. 116 shows the same values for version 19.11. Both plots are for a head of 0.01 feet across the model. Figs. 117 and 118 show water surface elevations and velocities for time steps of 90 and 1440 seconds for version 19.11. It can be noted that the water surface stabilizes and remains constant after the initial start up period for all 3 time steps.

There are some differences between results for versions 11.01 and 19.11 as shown in Figs. 115 and 116. This may be due to the length of the ramp which was specified at 0.2 days for version 19.11 but was calculated at the default value (slightly shorter) for version 11.01. Initial boundary condition water surface elevations are "ramped" up from zero slowly in an attempt to eliminate sudden shocks as a result of model start up. While the ramp time was set to 0.2 days (17,280 seconds) the ramp value is 0.96403 at 0.3 days and does not reach 0.99933 until 0.6 days. (Westerink, Luettich, Blain and Scheffner 1992) This value for version 19.11 is slightly higher (i.e. water surface ramps up faster) than for version 11.01 as can be seen by comparing  $X = 0$  values in Figs. 115 and 116.

All of the tests shown in Figs. 115 to 118 show a similar wave form at the end of the simulation just prior to

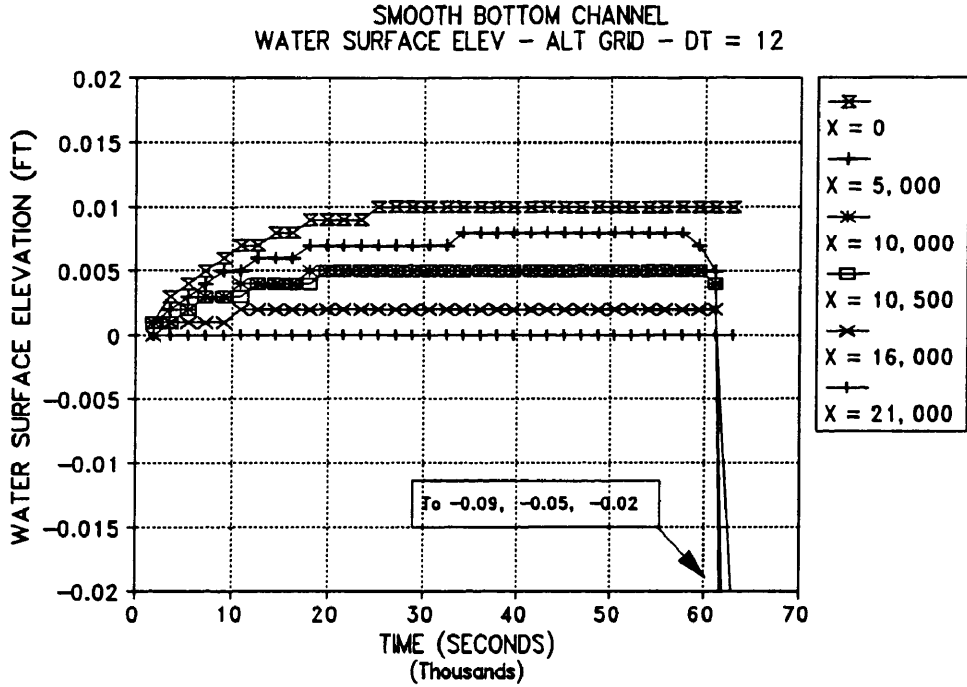


(a) Water Surface Elevation

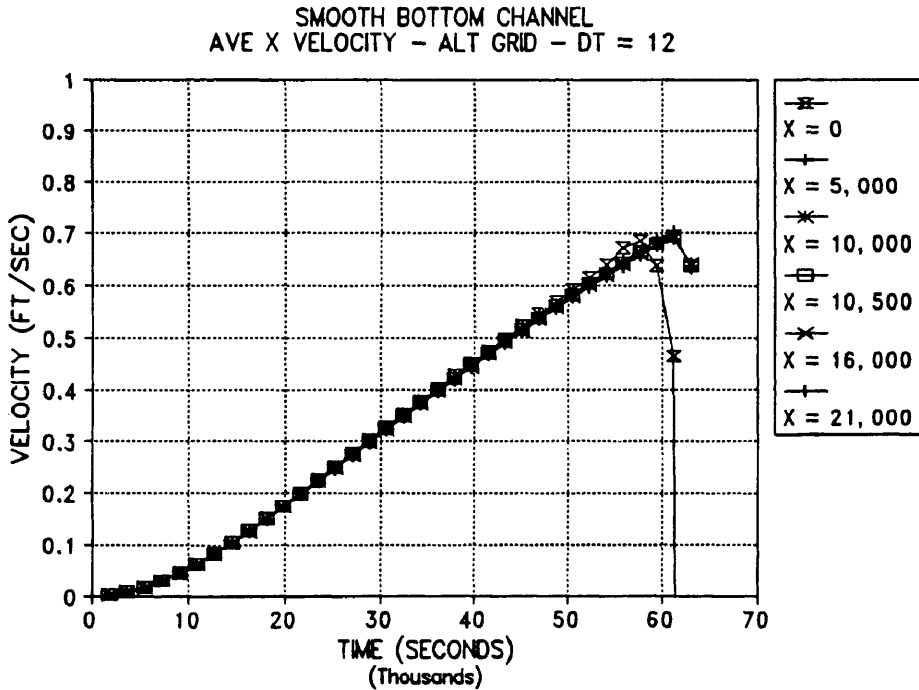


(b) Velocity

Fig. 115. Time Series Plots of Water Surface Elevation and Velocity for 2DDI Model (Version 11.01) with Head of 0.01 Feet and with 12 Second Time Step. Plotted Values Represent Every 125th Time Step.

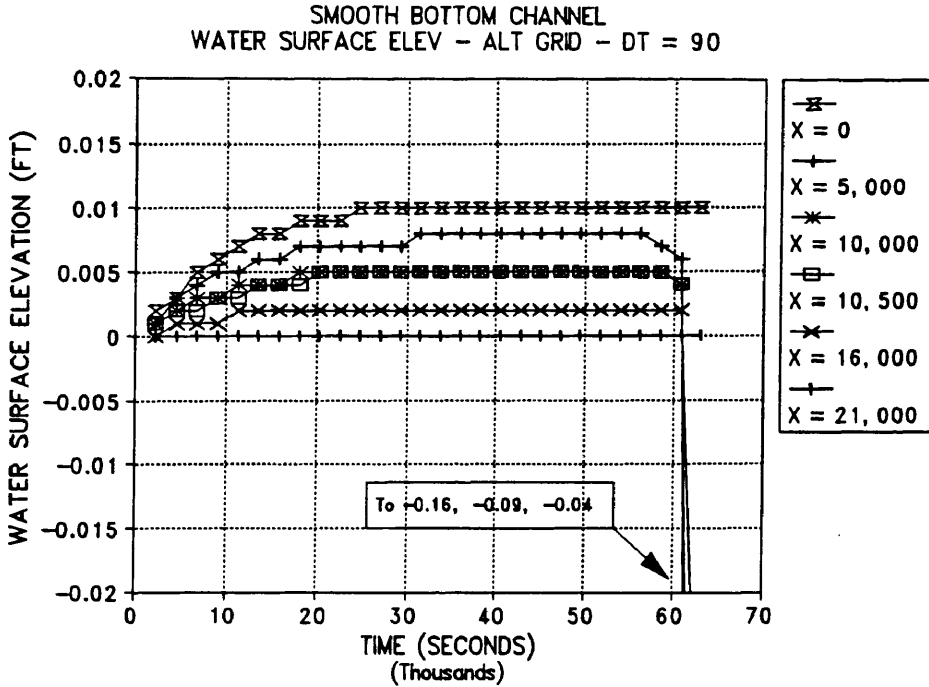


(a) Water Surface Elevation

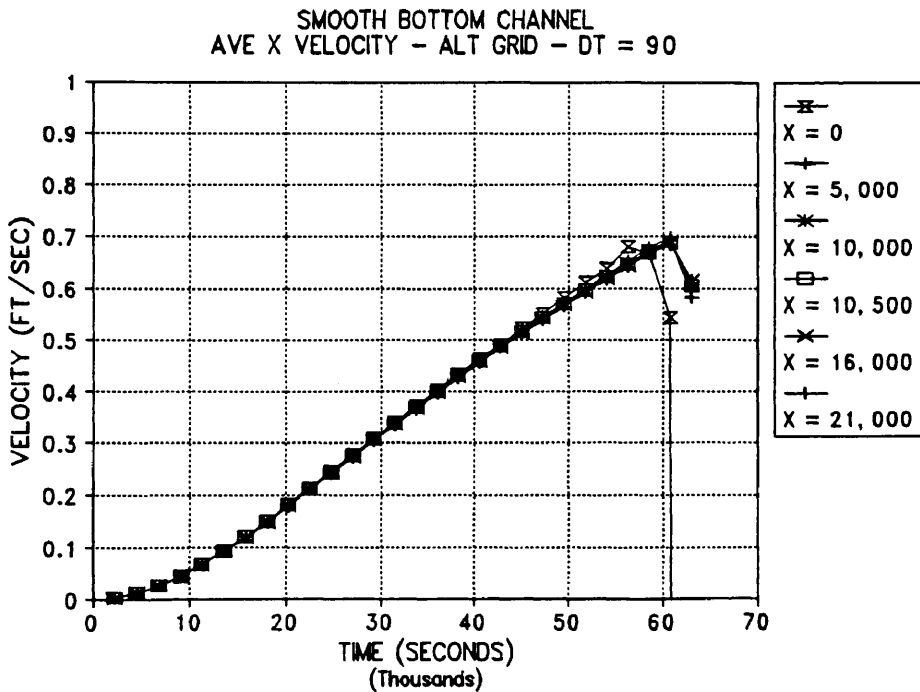


(b) Velocity

Fig. 116. Time Series Plots of Water Surface Elevation and Velocity for 2DDI model (Version 19.11) with Head of 0.01 Feet with 12 Second Time Step.



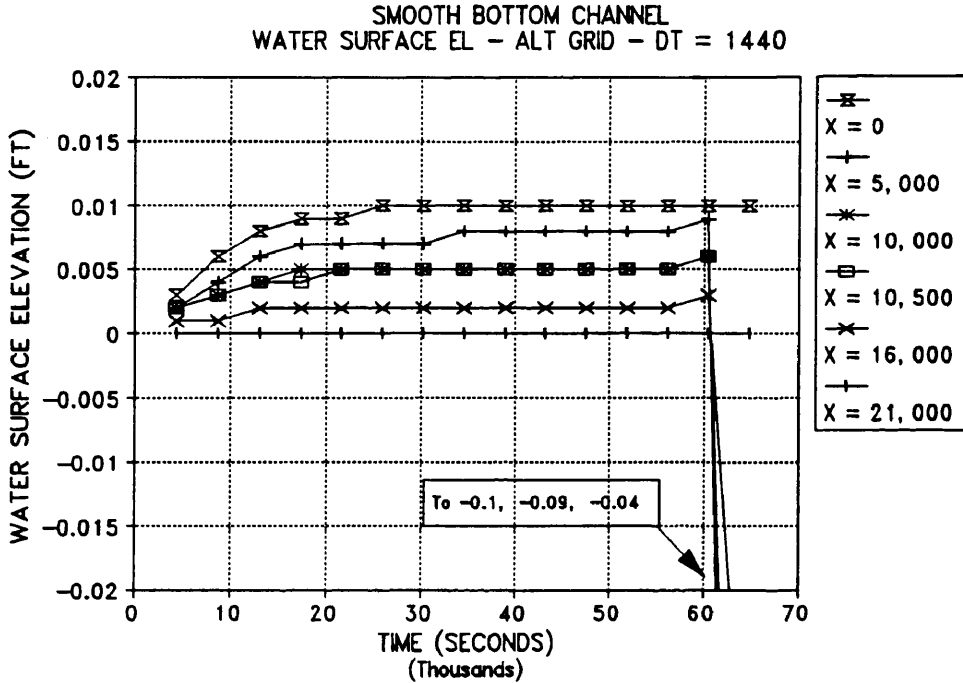
(a) Water Surface



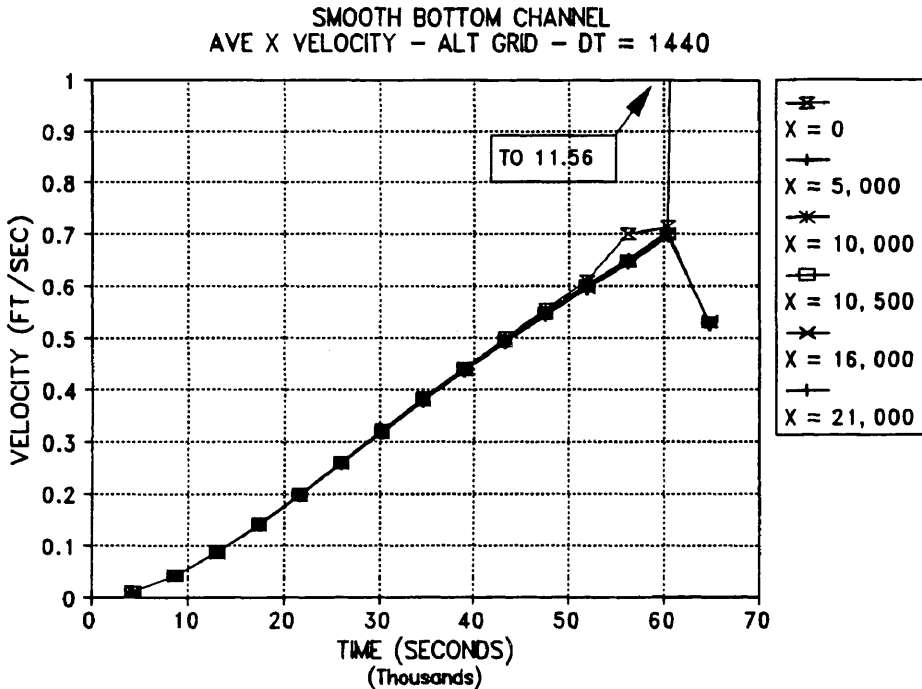
(b) Velocity

Fig. 117. Time Series Plots of Water Surface Elevation and Velocity for 2DDI Model (Version 19.11) with a Head of 0.01 Feet for a Time Step of 90 Seconds.





(a) Water Surface Elevation



(b) Velocity

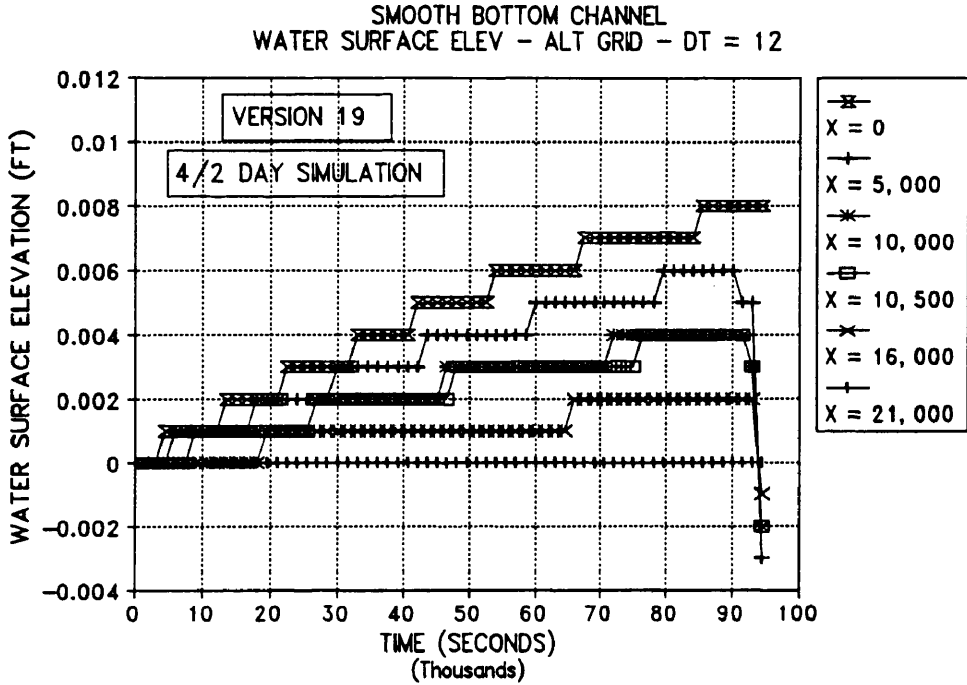
Fig. 118. Time Series Plots of Water Surface Elevation and Velocity for 2DDI Model (Version 19.11) with Head of 0.01 Feet with 1440 Second Time Step.

the model blowing up. It should be noted that due to the large number of time steps involved in the 12 and 90 second tests that not every time step value is plotted for all of the runs. For the 12 second tests every 125th step is shown with every 25th time step for the 90 second test and every 5th step for the 1440 second test. An effort was made to assure that odd and even steps were alternated to view any oscillations in time that may have occurred. Plots with all steps included also showed no  $2\Delta t$  oscillations in the solutions.

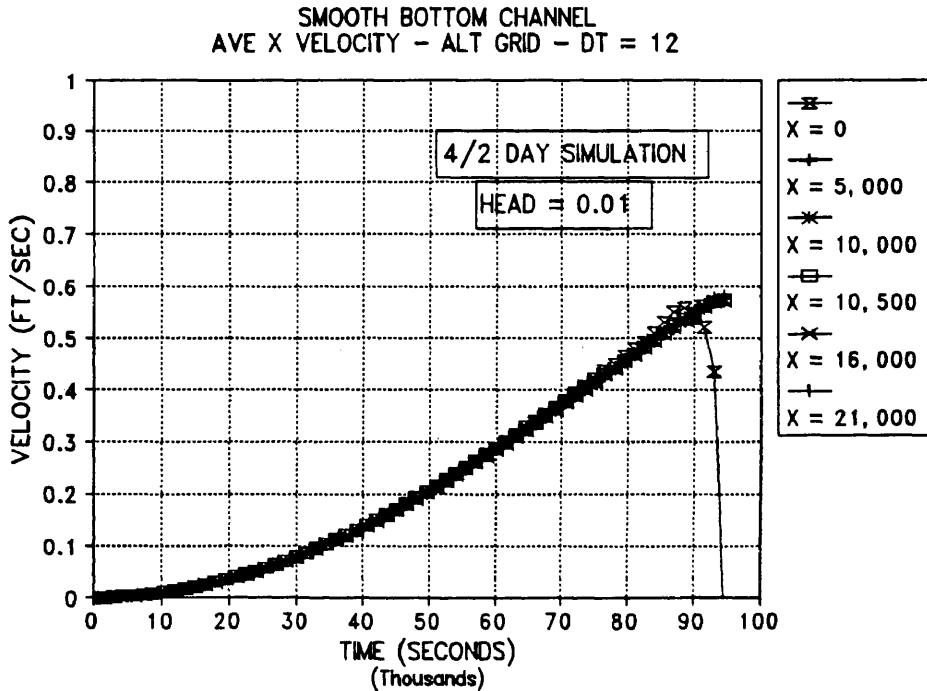
In an attempt to view the effect of ramp length vs model stability a run was made using a ramp up time of 2.0 days and a total simulation length of 4.0 days. A 12 second time step was used for this simulation and the results are shown in Fig. 119. Again only every 125th time step is plotted to allow discernment of individual data points. Immediately noticeable is the lower water surface and velocities in the model when it became unstable. For this simulation water surface was not fully ramped up before the model became unstable and velocity is less than 0.6 feet per second as compared to 0.7 feet per second for the shorter value of the ramp.

A very short ramp of 0.05 days was then used to produce results shown in Fig. 120. Some instabilities can be seen in the water surface elevation plot for this test. These were probably caused by the short duration of the ramp which allowed higher surface waves to form in the solution. The maximum velocity obtained prior to model instability is still 0.7 ft/sec - identical to that obtained with a ramp period of 0.2 day as shown in Figs. 115 to 118.

For a test with a water surface slope of 1.0 feet across the length of the channel the model performs similarly as shown in Fig. 121. For a test with a  $\Delta t$  of 12 seconds the time series velocity plot is nearly identical to those for the 0.01 foot head test with the exception of the

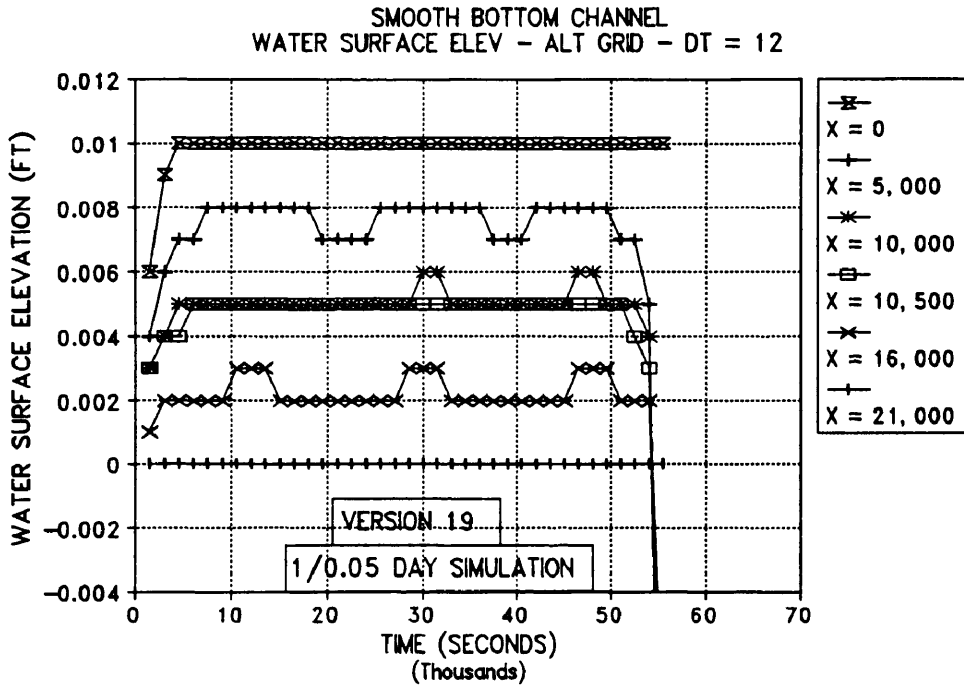


(a) Water Surface Elevation

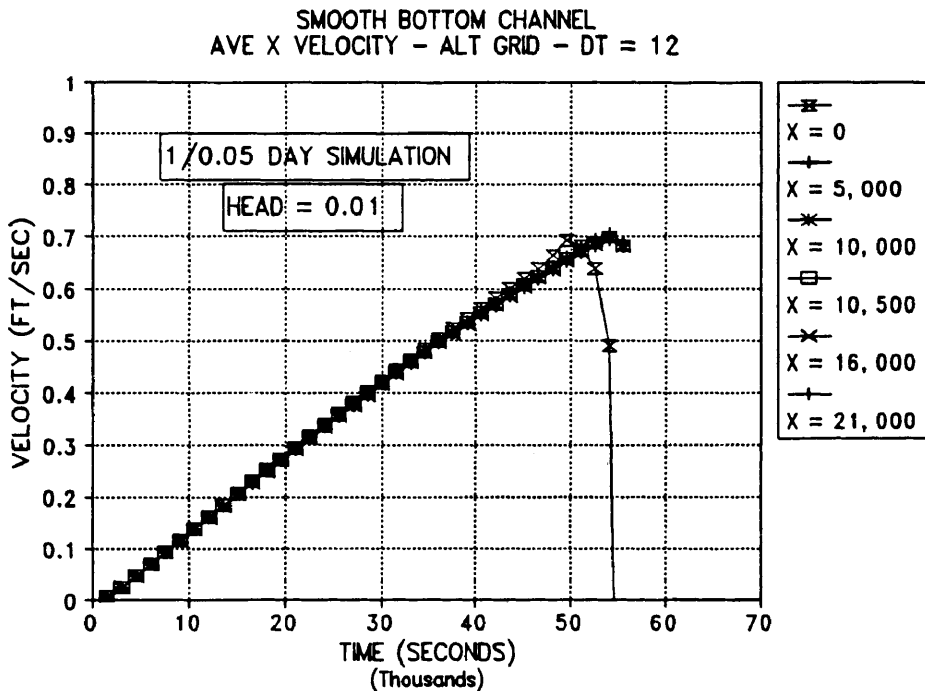


(b) Velocity

Fig. 119. Time Series Plot of Water Surface Elevation and Velocity for 2DDI Model (V. 19) with 0.01 Ft. Head, 12 Second Time Step, and Ramp Length of 2 Days.

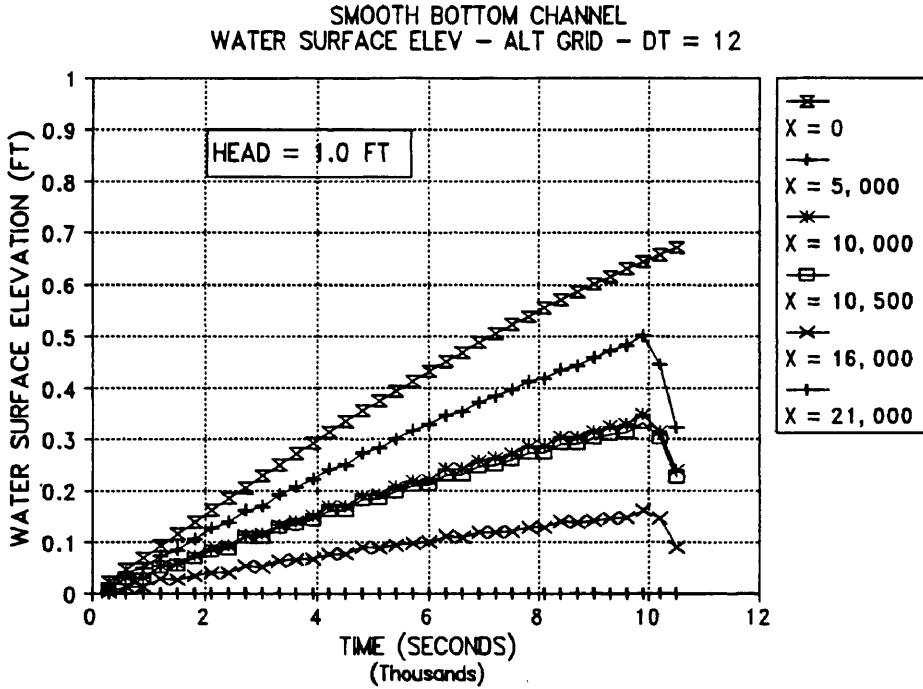


(a) Water Surface Elevation

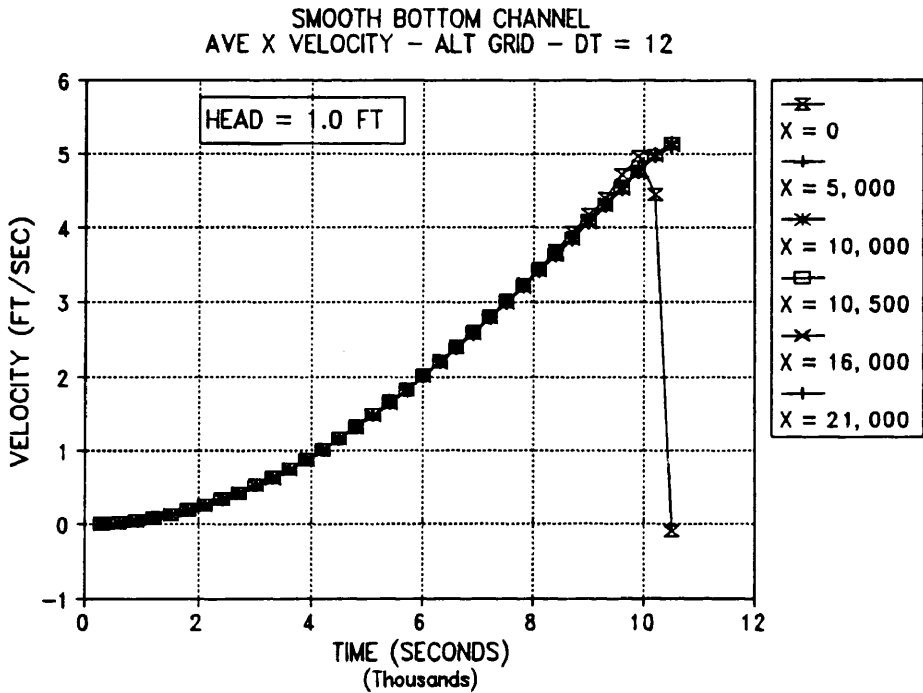


(b) Velocity

Fig. 120. Time Series Plots of Water Surface Elevation and Velocity for 2DDI Model (V. 19) with Head of 0.01 Ft., with 12 Second Time Step, and Ramp Length of 0.05 Days.



(a) Water Surface Elevation



(b) Velocity

Fig. 121. Time Series Plots of Water Surface Elevation and Velocity for 2DDI Model (Version 19.11) with Head of 1.0 Feet with 12 Second Time Step.

scale values and the length of the simulation. The time series water surface elevation plot in Fig. 121 increases smoothly with respect to time but the model becomes unstable prior to reaching the end of the ramp.

Using a HEC-2 model of the smooth bottom channel (or calculating normal flow based on Manning's Equation) the predicted velocities for the channel are approximately 1.0 ft/sec for the test with 0.01 foot head and 11.63 ft/sec for the 1.0 foot head test (Manning's Equation yielded 1.01 ft/sec and 10.34 ft/sec). It appears that the fully non-linear model begins to become unstable at about 40 to 70% of the actual velocity for the smooth bottom channel tests. The point where the model becomes unstable seems to depend on how fast the water surface is rising and how long the ramp is. The length of the time step used does not appear to have a major impact on the point where the model becomes unstable.

As a result of the above tests the fully non-linear model appeared to be unstable for all of the "simple test cases" and probably for all river applications. Thus tests were begun to determine if the model would be stable in any form for the simple test channels. Conversations with Dr. Westerink indicated that the instability problem for the fully non-linear model in flows with significant velocities had been known to the model developers for several months at that point and efforts were being planned during summer 1992 to address the problem.

This posed a serious dilemma for continued research with the model. If the fully non-linear model was not usable in the class of problems represented by rivers, would further research with the linear model be beneficial and worthwhile? After several discussions with Dr. Westerink and others it was determined that while testing could not be accomplished with the fully non-linear model at least some insight could be obtained by comparing RMA-2V with the

linear form of the 2DDI model. Accordingly the linear form of the model was then applied to the smooth bottom channel to view the properties of the model with the troublesome non-linear terms eliminated from the calculations.

#### THE LINEAR 2DDI MODEL

The initial versions of the 2DDI model (7.03 and 11.01) allowed the modeler to select a solution technique which neglected only the convective terms. This resulted in the removal of the following non-linear terms from the wave continuity equation and the x and y momentum equations:

x momentum equation:

$$u \frac{\partial u}{\partial x} + v \frac{\partial u}{\partial y} \quad (107)$$

y momentum equation:

$$u \frac{\partial v}{\partial x} + v \frac{\partial v}{\partial y} \quad (108)$$

Thus the linear option still include the non-linear bottom friction terms, the finite amplitude terms, the linear wave model - i.e. all of the terms in the full form of either the RMA-2V or 2DDI model except those shown in the above equations. (Both the time and spatial derivatives of the terms in Equations 107 and 108 were eliminated using this option.) The advective (lateral diffusion, eddy viscosity, or turbulent exchange) terms can also be used in either the fully non-linear or linear mode.

Some of the modification made to the 2DDI program for version 19.11 included simplified methods of specifying which terms are included in the calculations. For version 11.01 the non-linear terms were dropped by specifying a NOLI = 2. For version 19.11 each set of terms can be turned off or on individually. For this test the convective terms were

turned off by specifying NOLICA and NOLICAT equal to zero. This turned off both the time and spatial derivatives of the convective acceleration terms. (Westerink, Luettich, Blain and Scheffner 1992) The model would not run in this mode due to an internal data check and required the finite amplitude terms also be turned off to maintain continuity and consistency.

The finite amplitude terms account for the difference between the actual water surface elevation and the zero elevation water surface - i.e. height above or below mean sea level in ocean modeling. In the fully non-linear model the depth used in the solution is given as:

$$H = h + \zeta \quad (109)$$

While in the linear model depth is approximated by  $h$  which is the depth from sea level to the bed (i.e. bathymetry) at each node (See Fig. 2). If the difference in the water surface elevation and the zero datum used in the model is small with respect to the bathymetry this assumption is valid, but in the case of rivers where the depths can be shallow and the water surface highly sloped this assumption will often not be valid.

When the finite amplitude terms were also turned off the model did not converge to a near steady state result within the 0.75 day time frame for all time steps evaluated. Since the model was still displaying water surface waves after 0.75 days the simulation was lengthened to 2 days. This resulted in greatly reduced surface waves and improved continuity down the channel. While the time had to be lengthened, the linear model did converge to a solution that was very near the desired steady state solution.

To obtain a flow rate of 500,000 cfs in the smooth bottom channel the head was set to 0.167 feet with the lateral diffusion terms set at 0.0. This head is less than



that predicted by Manning's Equation (0.214 ft) but higher than that predicted by RMA-2V for this same test (0.10 ft).

The linear model was tested at time steps of 5 to 1440 seconds and the linear model would converge at either extreme of the Courant numbers tested. For the high values of the Courant number convergence in the linear model was rapid as most disturbances created by model start-up could pass through the model prior to the next time step. For the low Courant numbers numerous waves could be traced moving through the model and but were eventually damped out to give a very nearly steady state solution.

Continuity down the channel was good for the smooth bottom channel test with the linear model. The continuity values for time steps of 12, 90, and 1440 seconds ( $\Delta t = 1.5, 10.5, \text{ and } 167.7$ ) are shown in Fig. 122. Continuity can be seen to vary only slightly, from a minimum of 99.97% to a maximum of 100.13% with the average value down the channel equal to about 100.05%. This is a good representation of actual flow in the channel but not as good as the RMA-2V model which includes the convective terms. The values for the RMA-2V solution are also shown in Fig. 122 for comparison and were all identically equal to 100%.

With the head set at a constant 0.167 feet the lateral diffusion (eddy viscosity) terms were varied from 0.0 to 0.001. At a diffusion value of 0.00015 the model began to become unstable as shown in Fig. 123. At lateral diffusion values of 0.00015 or less maximum continuity deviations in the channel were less than 0.2% which is an acceptable value.

When lateral diffusion was increased to 0.00015 the maximum continuity deviation was increased to over 3% - unacceptably high for a straight smooth channel of this nature. At a momentum diffusion value of 0.001 the presence of the undamped surface wave accounted for nearly a 20% loss in continuity in the model. At a differing time step this

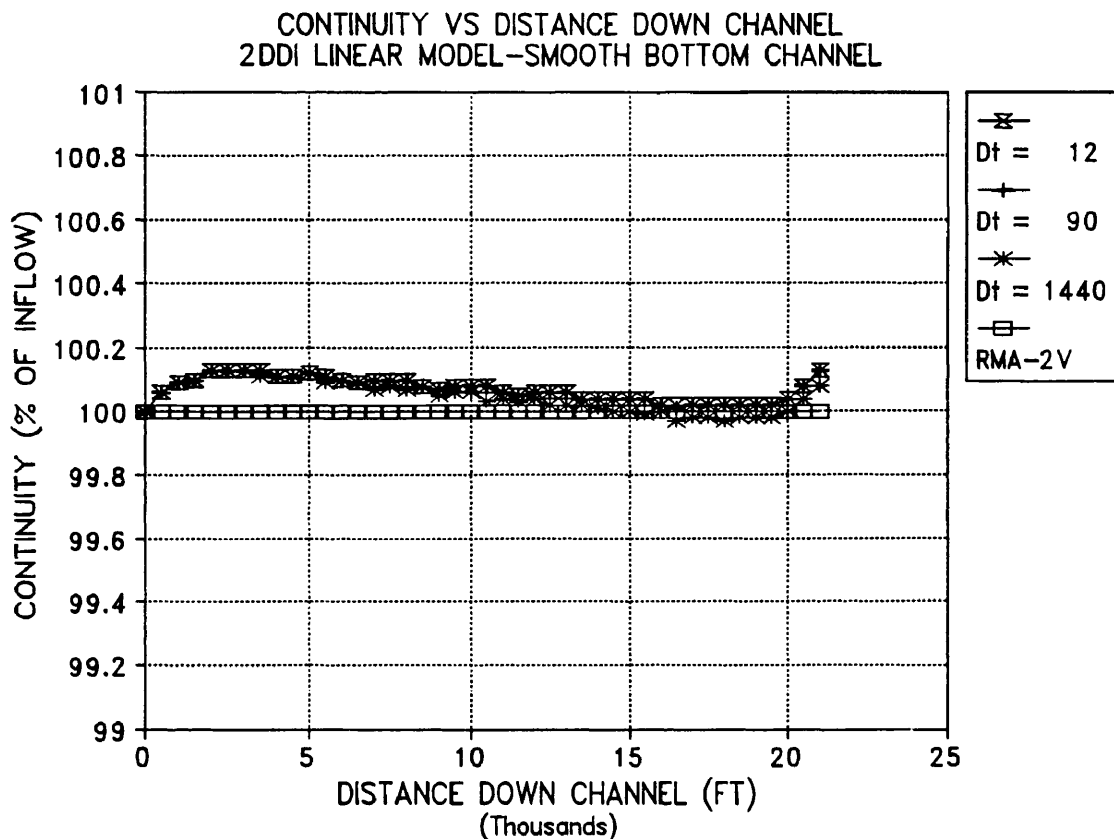
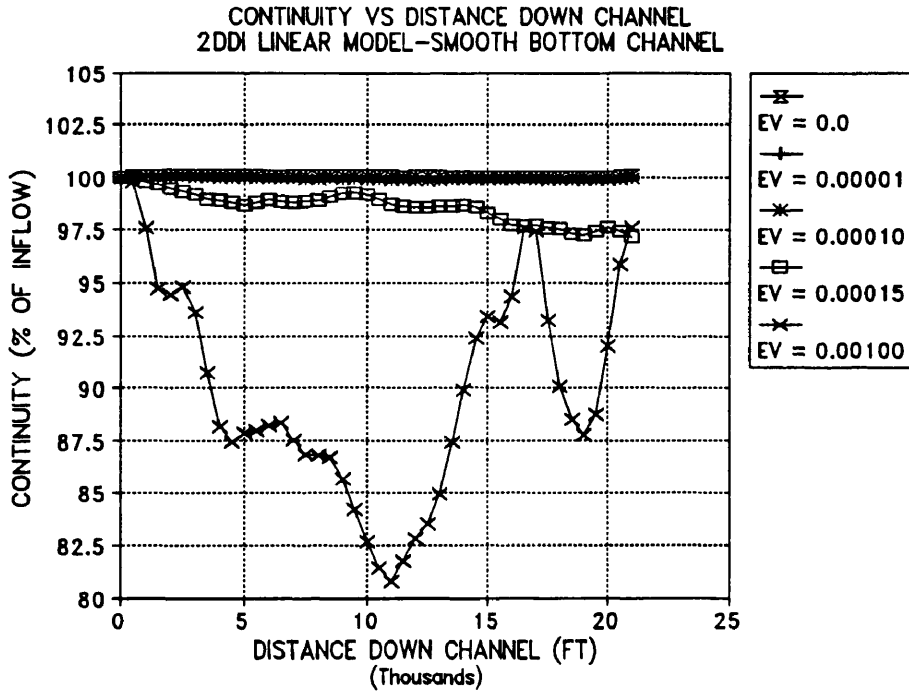


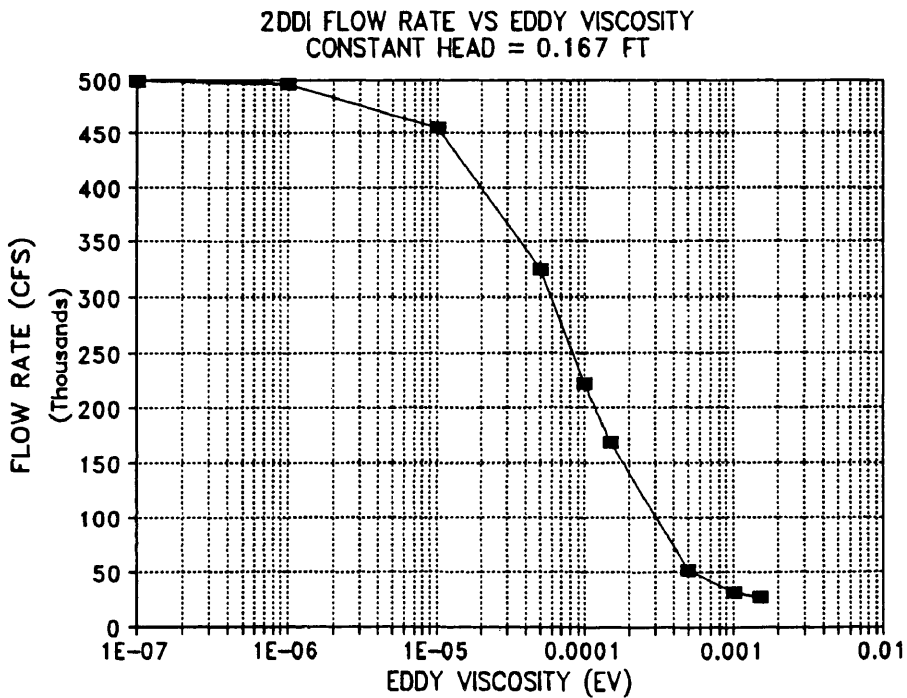
Fig. 122. Continuity in Smooth Bottom Channel for Linear 2DDI Model with Flow Equal to Approximately 500,000 cfs for  $\Delta t$  Equal to 12, 90, and 1440 Seconds. RMA-2V Results Included for Comparison.

value would probably be a 20% gain which gives a 40% range in continuity values. It must be noted that this continuity difference is not due to model oscillations but undamped surface waves being reflected between the fixed boundary conditions at the ends of the model.

As the lateral diffusion was increased with a constant head, flow in the channel was reduced due to higher momentum dissipation in the channel as shown in Fig. 123(b). The flow varied less than 500 cfs (0.1%) from a lateral diffusion value of 0.0 to 1.0 E-07. The model began to behave unacceptably (in terms of continuity) with the diffusion terms set to 0.00015 or larger which corresponded to a flow rate of about 160,000 cfs or 32% of the desired



(a) Continuity Vs Distance for Various Values of EV



(b) Eddy Viscosity vs Flow Rate

Fig. 123. Effects of Varying Lateral Diffusion (Eddy Viscosity) for Constant Head of 0.167 Ft with Time Step of 12 Seconds and Simulation Length of 2.0 Days for Linear 2DDI Model and Smooth Bottom Flume.

flow. It is interesting to note that the lateral diffusion terms showed no indication of increasing model stability at any of the tested levels of lateral momentum diffusion, but served as a sink for flow momentum only as would occur with turbulence in a natural flow situation. This also means that the momentum diffusion terms can be applied without sacrificing model response - i.e without overdamping the solution.

The fact that the diffusion can be varied so widely with no appreciable effect on continuity would allow the tuning of the model to match observed water surface elevations while using the same Manning's n values used in one-dimensional river modeling. This would be especially useful when using flux boundary conditions at inflow boundaries - an option not yet available. The fact that flow conditions can be varied so widely with only changes in the lateral momentum diffusion terms may also allow the linear model to give a good approximation of the non-linear conditions if the assumptions inherent in neglecting the finite amplitude portion of the flow are met.

Upon the completion of the initial runs with the linear and fully non-linear models it was determined that testing should continue with the linear form of the model as a general basis for comparing the two formulations. Since the model showed some promise it was felt that a significant amount of insight into wave equation behavior could be obtained by testing the model with the planned simple test cases. This obviously could not be a fair comparison of the two basic formulations, but would give insight into the relative behavior, stability and accuracy of the two models. The fact that the linear model could arrive at a solution for this class of tests was encouraging in itself.

Testing in the other planned cases (the Riprap Test Facility and Redeye crossing) would have to be considered

carefully, however, to insure that assumptions inherent in the linear model were not being violated.

Testing on all of the test cases thus proceeded based on the assumption that even without the non-linear terms, some idea could be obtained of the applicability of the model to river problems with the hope that the testing might aid in the determination of additional areas needing development if the fully non-linear 2DDI model or some modification thereof is to be adapted for use in river modeling.

#### SUDDEN DEPTH REDUCTIONS WITH 2DDI

The grids used for the RMA-2V sudden depth reduction tests were converted to the 2DDI format by a short routine which also specified nodes on the boundaries and generated a friction coefficient ( $C_f$ ) for each node. A grid editor developed by Center for Coastal and Land-Margin Research (1991) could also specify boundaries for more complicated geometries but was not used for the simple test case grids.

Since the  $\phi$  number varies as a function of depth and grid resolution it was necessary to calculate the maximum allowable time step for the differing grids and depths in the grids. The maximum time step values which maintain  $\phi$  less than 1.5 are presented in Table 1. It should be noted that stability in the linear model is not controlled by the Courant number but accuracy considerations still warrant time steps of the same order to maintain accuracy in time dependent studies. (Westerink, Luettich, Blain, Scheffner 1992)

The very small time steps for the high resolution grids indicate the importance of changing resolution with depth in the 2DDI model rather than only with the amount of flow variation as done in the use of the RMA-2V model. The variation of resolution with depth makes sense for ocean

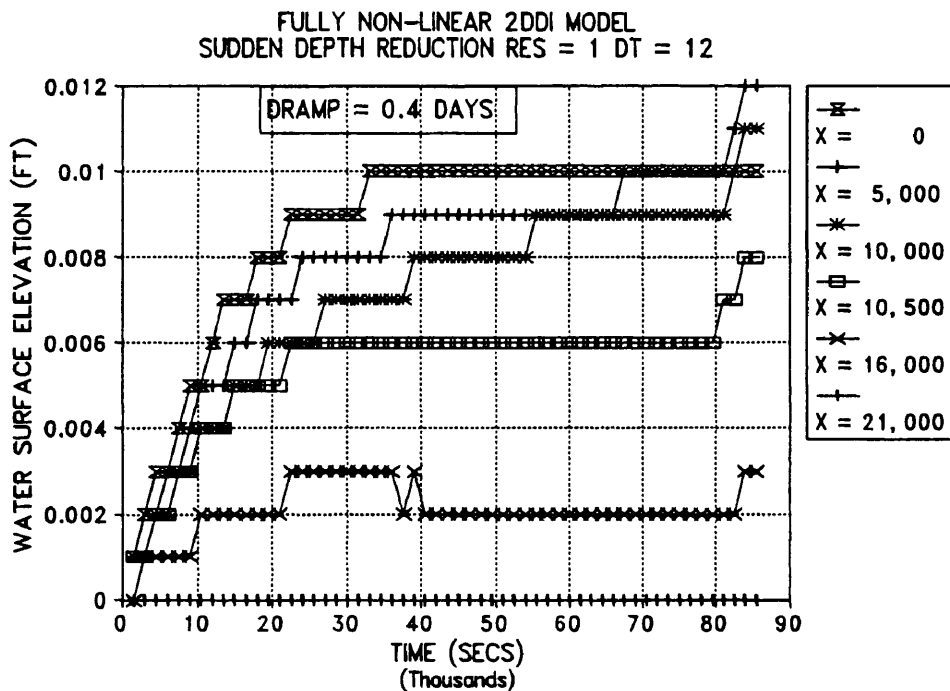
Table 1. Time Step Limits for 2DDI Model with Simple Test Grids for Maximum Expected Depths and Tested Grid Resolutions.

Courant Numbers for Expected Depths and Resolutions				
$\Delta x$ (ft) Resolution	500 1	250 2	125 4	62.5 8
Depth	Maximum Time Step for $C \leq 1.5$			
60.	17.06	8.53	4.27	2.13
110.	12.60	6.30	3.15	1.58
Step Used	12	6	3	1.5

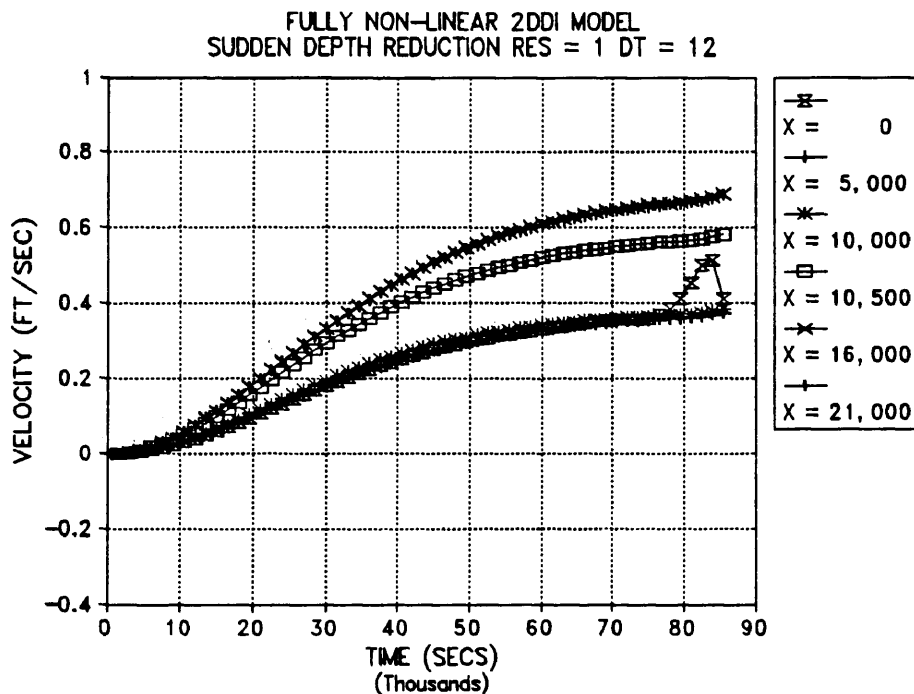
modeling where wave celerity varies with depth and where it is not common to have very large changes in velocity and flow characteristics within a very small area as occurs in river modeling.

Only three of the test grids used with the RMA-2V model could be used with the 2DDI model as the 2DDI model is not adapted for the use of quadrilateral elements. Thus only the regular, alternating and "C" grids could be tested with the 2DDI model.

The initial test with the 2DDI model for the sudden reduction in depth again used the fully non-linear version of the model. The results were again unstable and did not converge to a steady state solution. Fig. 124 shows a time history plot of the water surface elevation and velocity for 6 nodes with the head difference along the channel set to 0.01 feet. It can be seen that the water surface elevation at the inlet had completed "ramping up" when the model became unstable and aborted prior to velocity reaching its steady state value. The model ran to the completion of the 1 day simulation but had not reached steady state and was in the late stages instability as indicated by the velocity at the inlet ( $X = 0$ ) on Fig. 124(b). The water surface can also be seen to be diverging from the "true" solution during



(a) Water Surface Elevation



(b) Velocity

Fig. 124. Time History Plots of Water Surface Elevation and Velocity for Sudden Reduction in Depth with Fully Non-linear 2DDI Model for Head = 0.01 Ft and a 12 Second Time Step.

the last several data points. This behavior is identical to that noted for the smooth bottom channel test.

Continuity is shown in Fig. 125 for five time steps from the 0.01 foot head non-linear test. The time steps of 40,500., 51,000., 72,000., 79,500., and 85,500 seconds were selected to be after the model was fully "ramped up" - i.e. after the water surface had reached the full 0.01 head differential - and prior to or during the process of becoming unstable. The relative positions of the time steps can be noted by referring to Fig. 124. It can be noted in Fig. 125 that continuity across the sudden reduction in depth (between 10,000 and 10,500 feet) shows a large oscillation which varies very little through the simulation prior to the start of model instability and varies only slightly as the instability builds. Continuity oscillations vary from +8% to -15% over the sudden depth reduction but damp out extremely rapidly which was not the case in RMA-2V

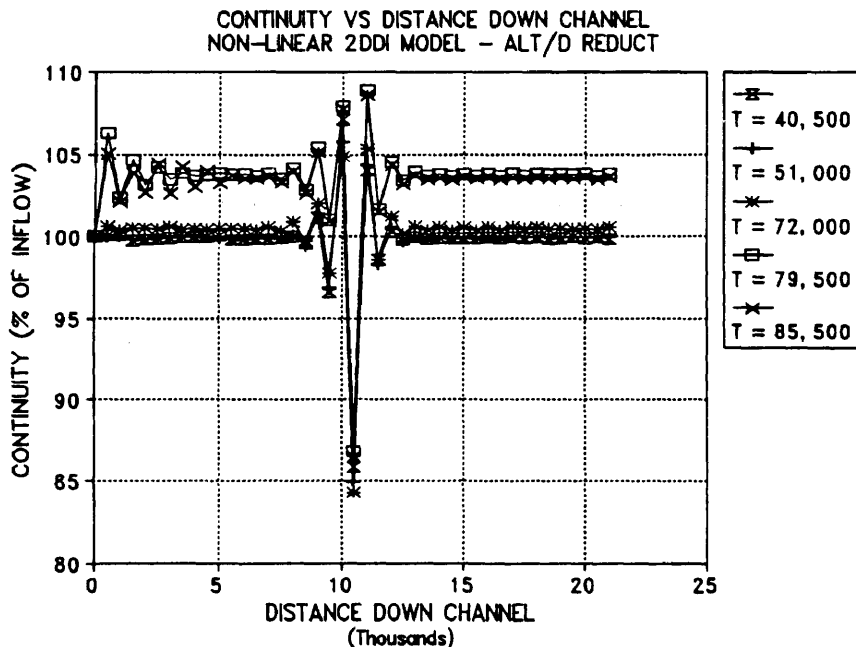


Figure 125. Continuity in Channel vs Distance and Time for Fully Non-linear 2DDI Model for a Head of 0.01 Feet for a Sudden Reduction in Depth with Resolution = 1.



at very low values for the turbulent exchange coefficients (EV or lateral diffusion).

The last two time steps show oscillations building from the inflow in the direction of flow. This wave form was observed as the model became unstable in all fully non-linear tests previously completed. Continuity farther down the channel is also increasing as a result of the increase in water surface elevation at the interior nodes. It should be noted that the two  $\Delta x$  wave form that is exhibited near the channel inlet during the two later two time steps, while increasing in amplitude over previous time steps, was not passed down the channel or moved laterally by the model - i.e. as time progressed the amplitude of the standing wave builds until the model became too unstable to continue calculations.

Since the model operated with no lateral diffusion - i.e. no momentum losses due to turbulence - and no non-linear terms other than friction, tests were performed to determine the proper head specification at the upstream boundary in order to obtain the desired flow rate. A head of 0.75 feet produced the desired flow rate of approximately 500,000 cfs which compared to a head of 1.56 feet from the RMA-2V simulation with EV = 5 and to a predicted head of 1.59 feet from HEC-2 (HEC 1990). This difference in water surface elevation is substantial between the 2DDI and the RMA-2V and HEC-2 models.

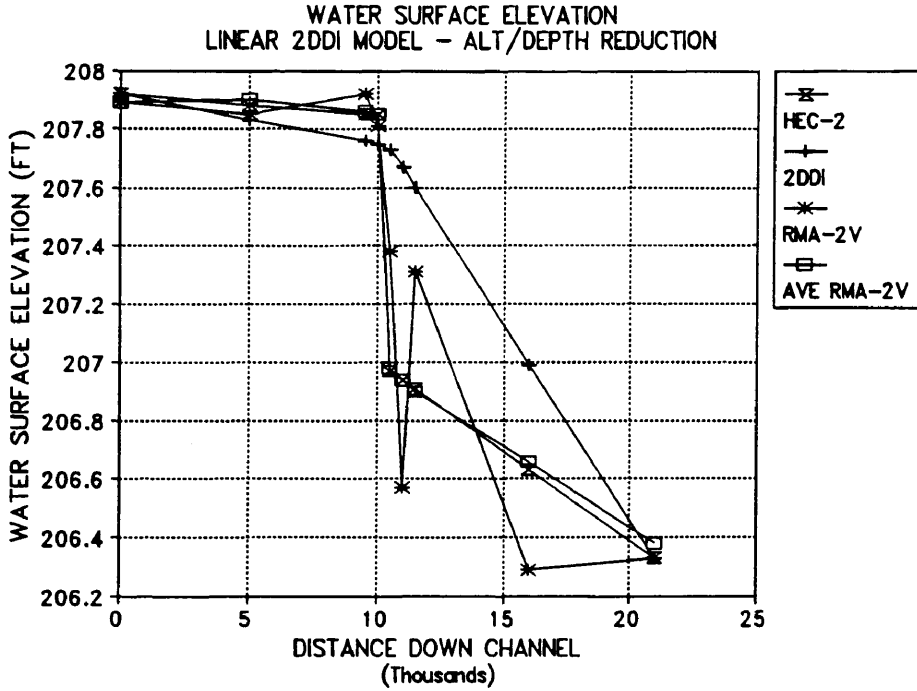
Since the water surface difference across the model was less than 50% of that predicted by HEC-2 and RMA-2V an attempt was made to force the model to match the water surface profile from HEC-2 and RMA-2V. To do this the head on the 2DDI model was raised to 1.59 feet and the lateral diffusion (EV) was raised to produce sufficient losses to match the predicted upstream water surface elevation from HEC-2. This required a diffusion value of 0.000195 which was determined by trial and error. This value was applied

to all nodes in the grid. This produced a water surface elevation (labeled 2DDI) as shown in Fig. 126(a). The direct comparison of water surface elevations required that the 2DDI datum be adjusted by +206.33 feet such that downstream water surface elevations for both models start at the same elevation. The water surface value obtained from the HEC-2 model (labeled HEC-2) is also shown in Fig. 126(a) as are both the RMA-2V output and a RMA-2V data set that was averaged to remove water surface oscillations from the results (RMA-2V and AVE RMA-2V, respectively).

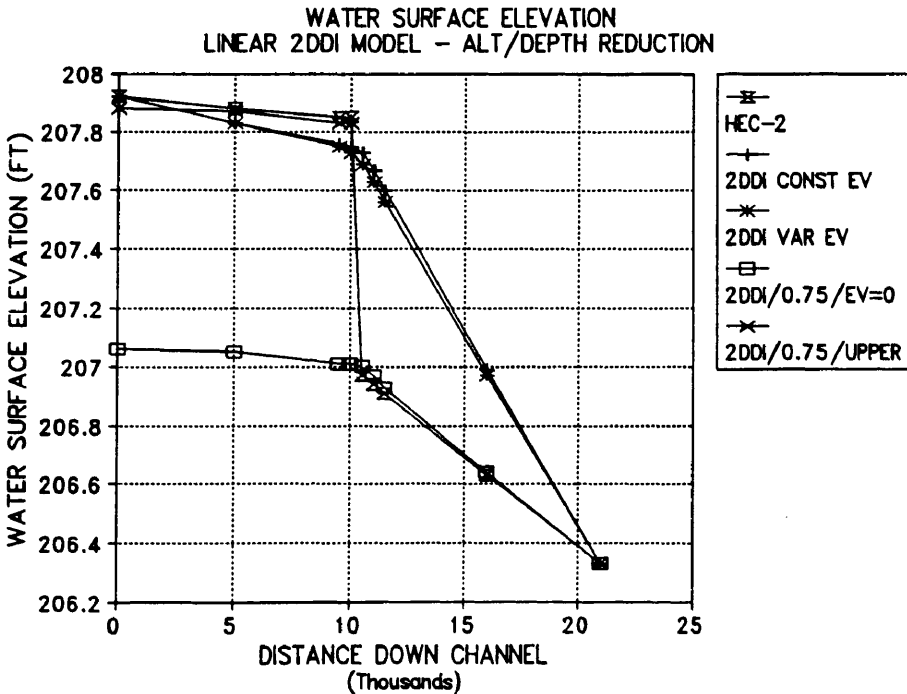
Since the water surface elevations were still substantially different an attempt was then made to fine tune the lateral diffusion values in the 2DDI model to give a better picture of the loss upstream of the sudden depth reduction and to model the water surface elevation change at the sudden reduction in depth. To get some idea of the magnitude of the change that could be made by varying the lateral diffusion, the lateral diffusion upstream and downstream of the sudden depth reduction was set to 0.00001 and the value for the nodes along the change in depth was set to 0.01. This resulted in the slight difference in water surface elevation near the change in depth as shown in Fig. 126(b) (labeled 2DDI VAR EV).

The difference in water surface elevations is equal to the difference in velocity head ( $V^2/2g$ ) for this tests and is 1.17 feet downstream of the reduction in depth and 0.35 feet upstream. The net difference is 0.82 ft which corresponds closely with the change in water surface elevation across the bump in the HEC-2 model in Fig 126.

When the velocity heads are taken into account for the three models, the net energy head across the models is calculated to be 0.76 feet - equal to the head required to produce a flow rate of 500,000 cfs in the 2DDI model. The fact that the linear 2DDI model does not model the change in water surface elevation due to velocity head is a direct



(a) Water Surface Elevations - HEC-2, RMA-2V, and 2DDI



(b) EV = 0.00001 Above and Below Depth Change and 0.1 on Depth Change

Fig. 126. Water Surface Elevations for 2DDI Model as Compared with HEC-2 and RMA-2V Models for Alternating Grid with Head = 1.59 Feet.

result of the elimination of the non-linear terms.

When the calculated 2DDI water surface for  $EV = 0.0$  and head = 0.76 was plotted (after datum adjustment) the line identified as 2DDI/0/0.75 in Fig. 126(b) was obtained. This data plots almost exactly on the RMA-2V and the HEC-2 model results until the change in depth is reached. If the data upstream of the depth change is then adjusted (increased) for the difference in velocity head (0.82 ft), the line identified as 2DDI/0.75/UPPER is obtained. It can be seen that both of these lines follow almost exactly the results from the RMA-2V and HEC-2 models when the effect of velocity head is removed (or included in - depending on your point of view) from the calculated water surface elevations. The fact that driving the model with the net energy head will produce the proper results is an exoneration of the basic physics of the model but does not help in situations where the water surface elevation is important and when velocity head is significant as often occurs in river modeling.

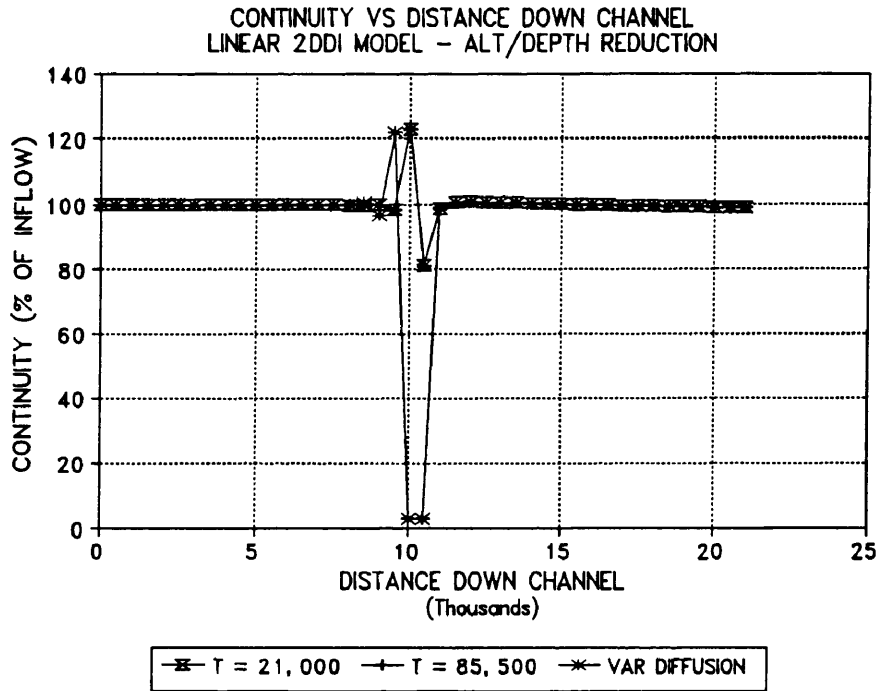
When the lateral diffusion in the model was increased to 0.01 across the depth change to attempt to force the model to match the non-linear water surface profile, as described above, continuity down the channel was again checked. The continuity for the variable EV case is plotted in Fig. 127(a) along with the continuity for the case where lateral diffusion is equal (0.000195) for all nodes in the grid. It can be seen that at the change in depth where the lateral diffusion is extremely high, continuity is extremely low - less than 3% of the inflow. The two time steps for the constant lateral diffusion case ( $EV = 0.000195$ ) - one at 21,000 seconds (5.833 hours) into the simulation and one at 85,500 seconds or near the end of the run (23.75 hours of 24 hours) - show much better continuity but still show 20% continuity oscillations. These two continuity values plot almost identically on top of one another with only a few very minor exceptions.

In Fig. 127(b) the effect of constant lateral diffusion (constant over the entire grid) on channel flow rate for a constant head of 1.59 is shown. It can be seen that changes in the lateral diffusion (EV) can drastically change the flow rate in the channel. The maximum flow rate with EV = 0.0 was about 720,000 cfs. It should also be noted that the model converged at all diffusion values used in this particular case but it is evident from the preceding discussion that the linear model cannot be manipulated to accurately model the change in water surface for cases with sudden changes in bedform where the velocity head is important.

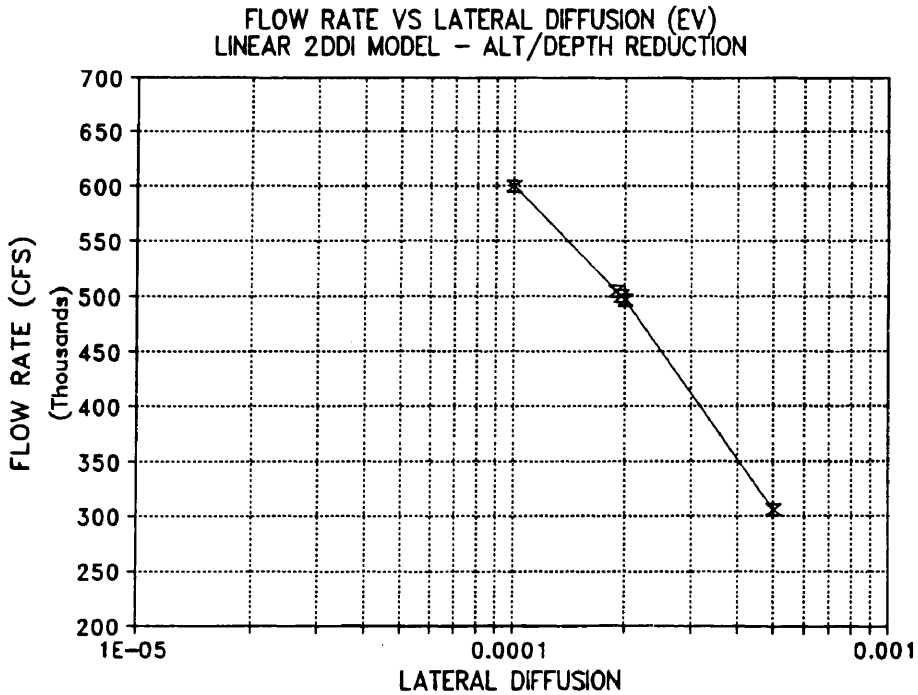
Since a major change in the lateral diffusion on the sudden depth reduction resulted in only a slight change in water surface elevation at the depth reduction and destroyed the model continuity, no further tests were performed with lateral diffusion being set to different values - i.e. all nodes in the grid were assigned the same value for lateral diffusion during the ensuing testing. Even though the model matched the desired flow rate of 500,000 cfs with EV set to 0.0, it was decided to run the remaining single resolution depth reduction tests with EV at 0.000195 to view any additional the effects of high lateral diffusion on the 2DDI model.

Tests were next run for the other two grids being tested with the 2DDI model - the "C" and the regular grids. Continuity values for these grids are shown in Fig. 128. It can be noted by comparing Fig. 127(a) and Fig. 128 that continuity values are similar for the regular and alternating grids but that due to the continuity drift of about 2.5% for the "C" grid, the "C" grid deviations are shifted somewhat higher. Other than this drift continuity values are within a few percentage points.

Three dimensional water surface elevation plots for all three grids are shown in Fig. 129. The water surface

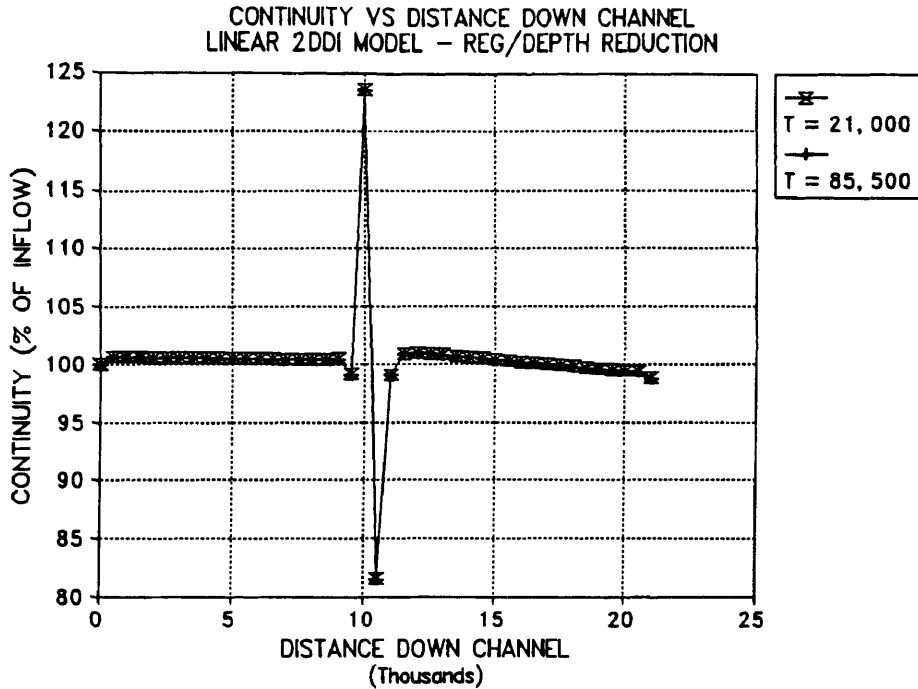


(a) Continuity vs Distance Down Channel

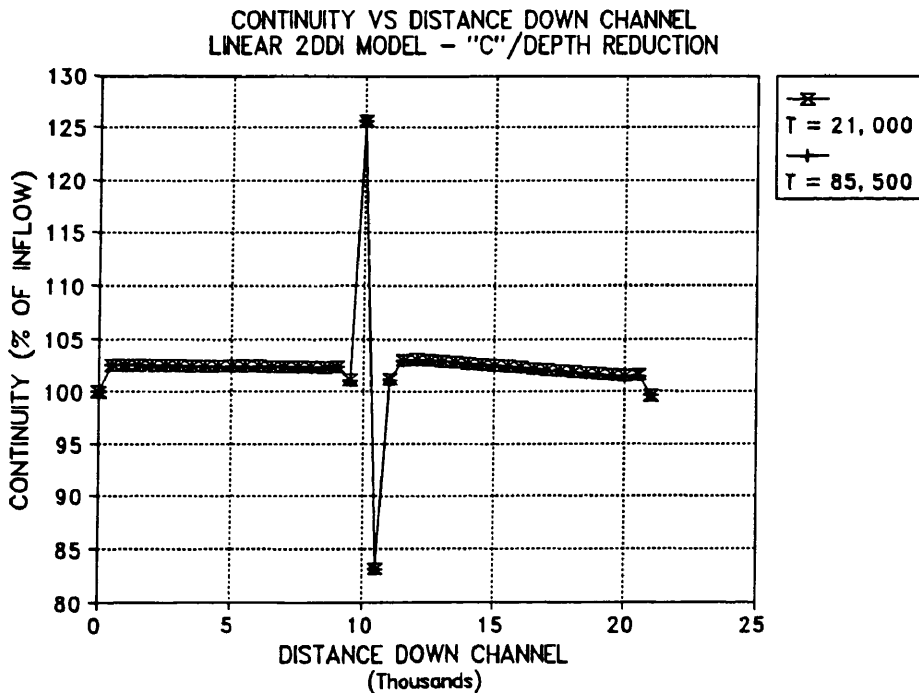


(b) Flow Rate vs Lateral Diffusion (EV)

Fig. 127. Continuity for Linear 2DDI Model and Flow Rate vs Lateral Diffusion for Alternating Grid with Resolution = 1 and Head = 1.59 Feet.

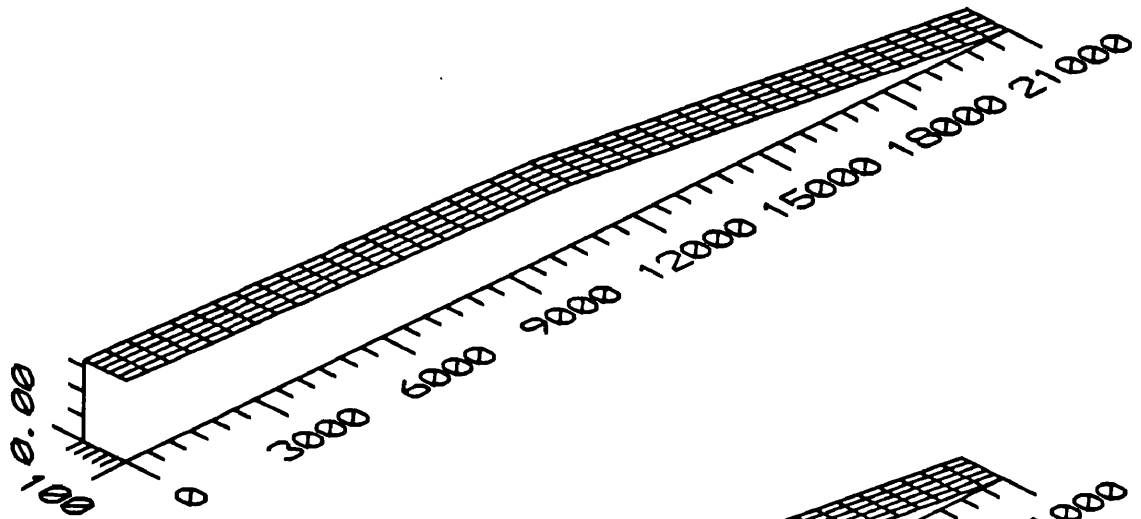


(a) Regular Grid

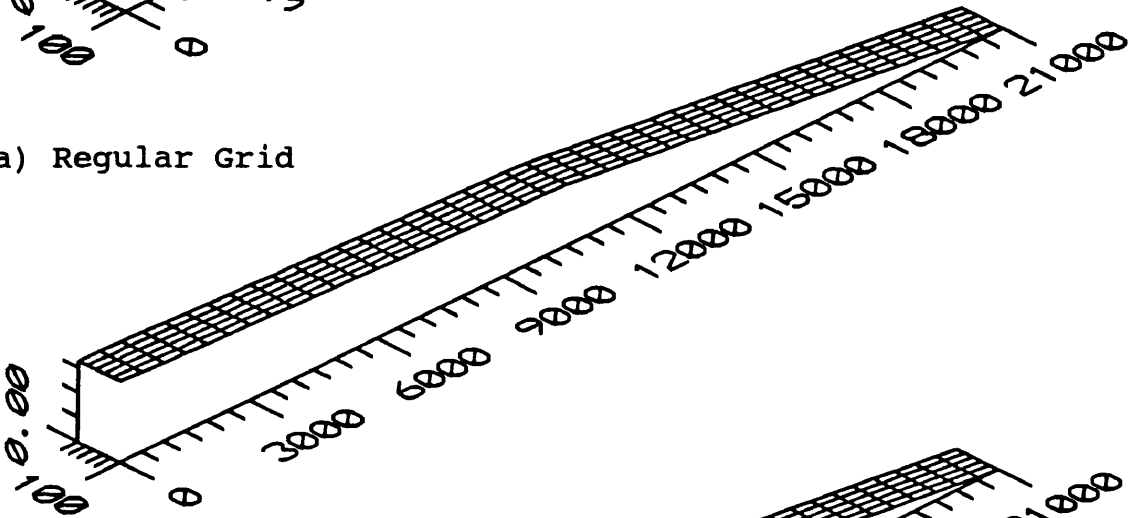


(b) "C" Grid

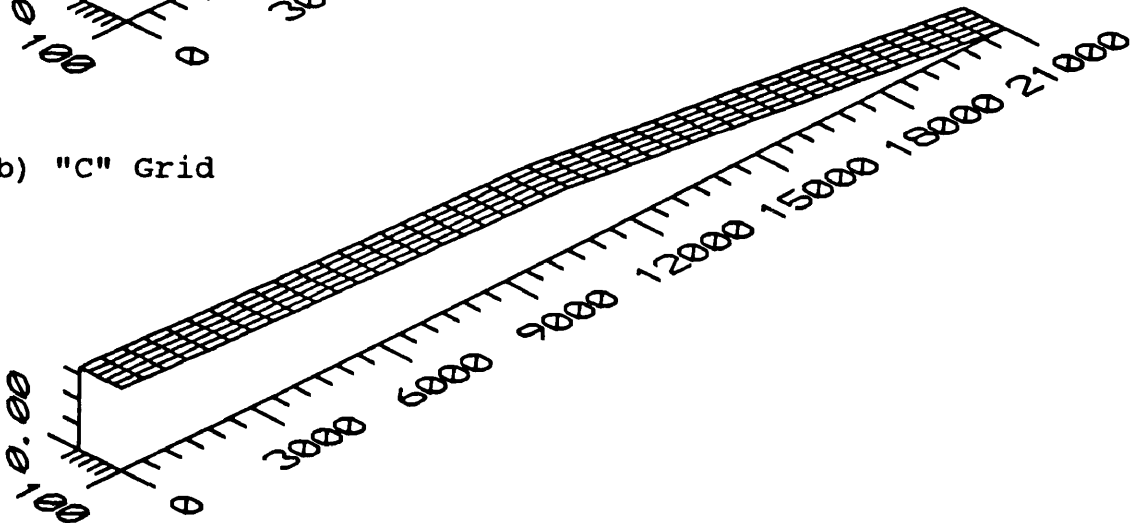
Fig. 128. Continuity vs Distance Down Channel for Linear 2DDI Model for Regular and "C" Grids for Single Resolution Test with Head = 1.59 Feet and EV = 0.000195.



(a) Regular Grid



(b) "C" Grid



(c) Alternating Grid

Fig. 129. Three Dimensional Water Surface Elevation Plots for Linear 2DDI Model for Test Grids with a Head of 1.59 Feet and  $EV = 0.000195$ .

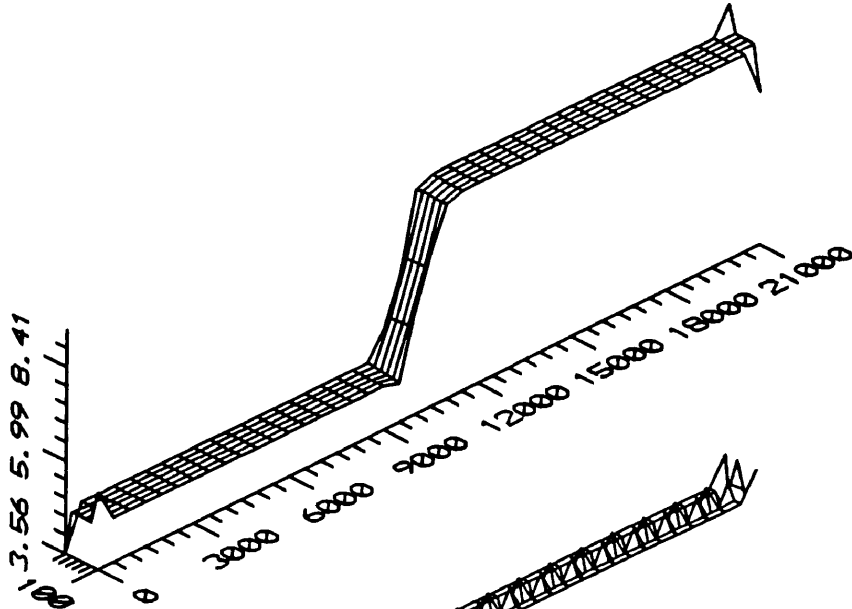


elevations are almost perfectly smooth for these grids but do not match the HEC-2 water surface profiles as previously shown in Fig. 126. Slight differences exist between the three grids but nothing that could be considered problematic in this type of modeling if the water surface including velocity head could be modeled accurately.

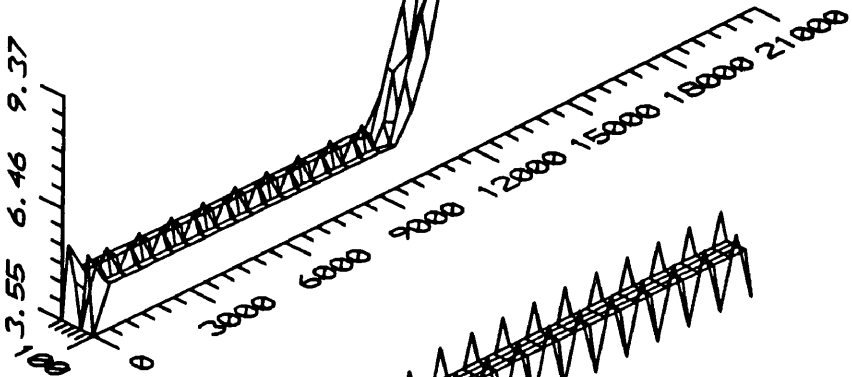
The corresponding three dimensional velocity surface plots shown in Fig. 130 and show less than perfect results. All plots are for a lateral diffusion (EV) equal to 0.000195 at all nodes in the grid. The regular grid performs the best performance with the "C" and alternating grids showing significant velocity oscillations throughout the length of the grid. The regular grid shows velocity peaks and spikes only at the inlet and at the outlet and a slight increase in velocity along the descending right bank near the depth reduction. There is also a corresponding decrease in velocity along descending left bank near the depth reduction. The "C" grid shows a smooth pattern along the walls but oscillates at all points where the diagonals of the triangular elements switch directions.

The continuity oscillations along the walls of the alternating grid are offsetting - when the left bank is high the right bank is low so continuity is still good at the cross section even though serious velocity oscillations are occurring. The magnitude of these oscillations in the alternating grid is on the order of 1.5 ft/sec as compared with a flow velocity of approximately 4.7 ft/sec upstream of the depth reduction and 8.7 ft/sec downstream. The oscillations in the "C" grid velocities account for the continuity "drift" discussed above.

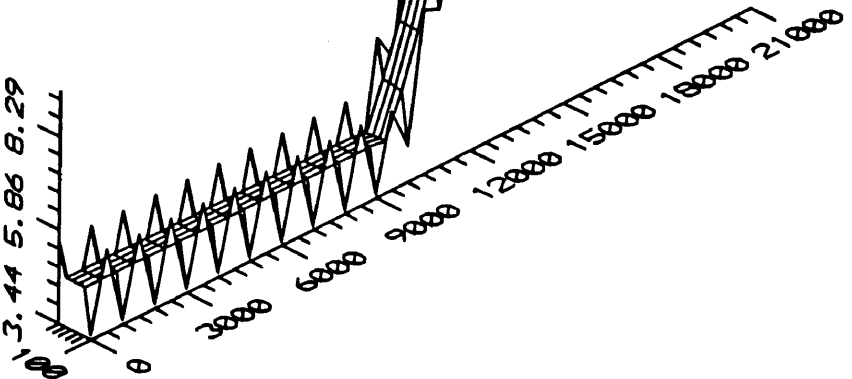
This continuity deviation seems to be tied specifically to grid type and the direction of the diagonals since the only difference in the three test grids and boundary condition files is the orientation of the diagonals within the grids. To determine the effect of lateral diffusion on



(a) Regular Grid



(b) "C" Grid



(c) Alternating Grid

Fig. 130. Three Dimensional Velocity Surface Plot for Linear 2DDI Model for Test Grids with Head = 1.59 Feet,  $EV = 0.000195$ , and Resolution = 1.

the oscillations, lateral diffusion was varied from 0.0 to 0.000195 as shown in Fig. 131. Fig. 131(a) shows a relatively smooth velocity surface with some slight skewing near the depth reduction for  $EV = 0.0$ .

As  $EV$  was increased to 0.00001 (Fig. 131(b)) oscillations are beginning to form along the side walls and skewing of flow across the sudden depth reduction becomes more noticeable. The next increase in  $EV$  to 0.000195 (Fig. 130(c)) gives significant oscillations all along the side walls and on the reduction in depth. The fourth plot (Fig. 131(c)) shows the case where  $EV$  was set to 0.00001 upstream and downstream of the reduction in depth and  $EV = 0.01$  on the change in depth. The extreme reduction in velocity accounts for the continuity loss previously discussed (Fig. 127(a)). It should be noted that the water surface elevation is unchanged - at least the water surface elevation plots for this run (not shown) and those shown in Fig. 129 are indistinguishable.

Since the use of the 1.59 ft head with and  $EV$  of 0.000195 created significant oscillations along the wall, and given the fact that the 0.76 ft head with an  $EV$  of 0.0 gives accurate results when the velocity head is neglected, the single resolution test cases were again run with a head of 0.76 feet and  $EV = 0.0$ . Continuity results for  $EV = 0.0$  and a head of 0.76 feet are shown in Fig. 132. The continuity values are almost identical to those shown for the test grids with  $EV = 0.000195$  and a head of 1.59 feet (Figs. 127(a) and 128).

The three dimensional velocity surface plots shown in Fig. 133 for  $EV = 0.0$  and a head of 0.76 feet continue to show oscillations at the sudden reduction in depth for all three grids. Of the three grids the alternating seems to be the best behaved with some slight skewing occurring on the reduction in depth and a slight oscillation just prior to the beginning of the reduction in depth. None of the

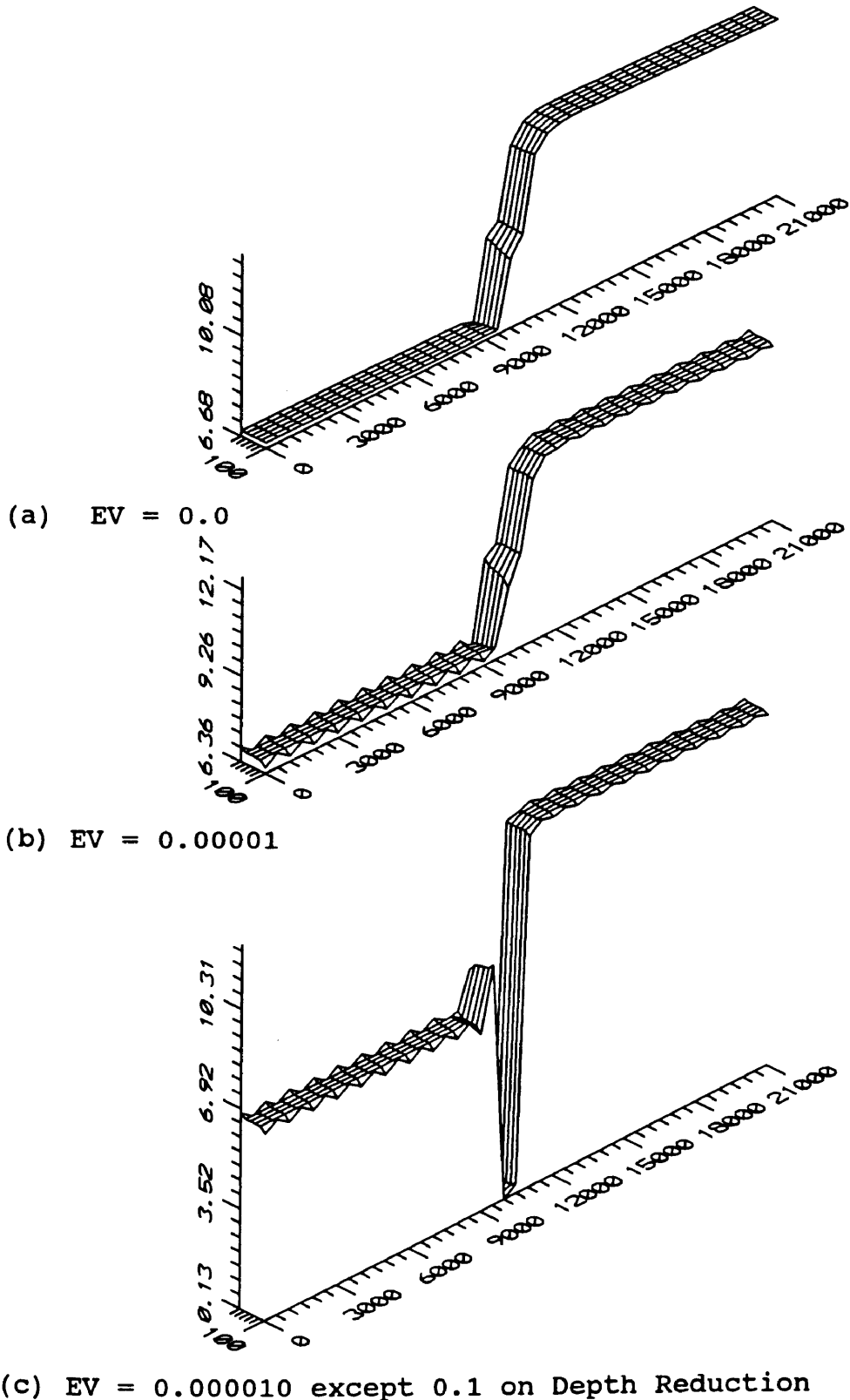


Fig. 131. Three Dimensional Velocity Surface Plots for Linear 2DDI Model for Alternating Grid for Increasing Lateral Diffusion with Head of 1.59 Feet and 12 Second Time Step.

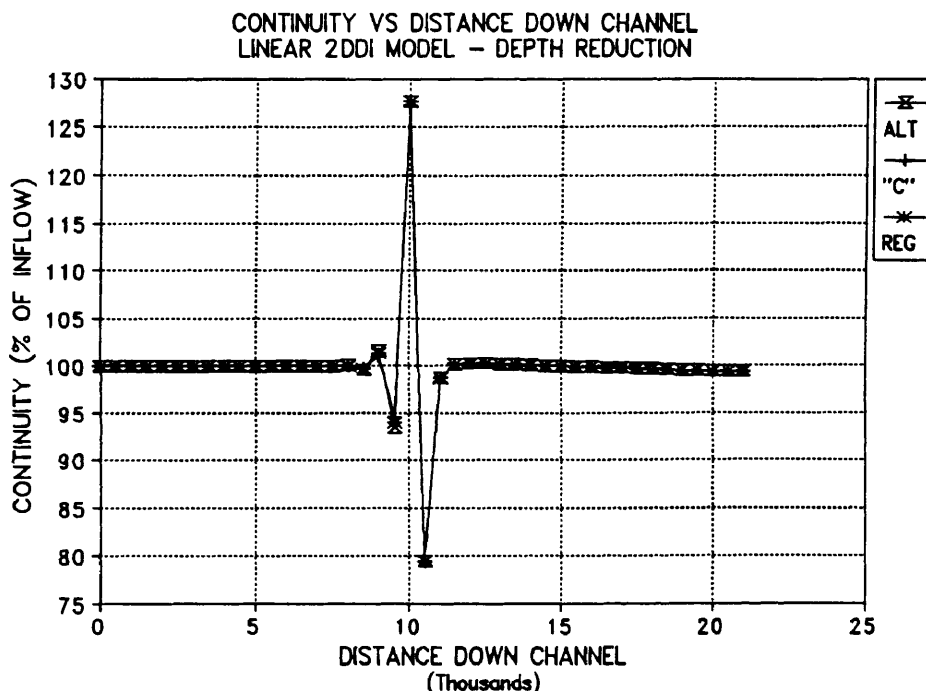
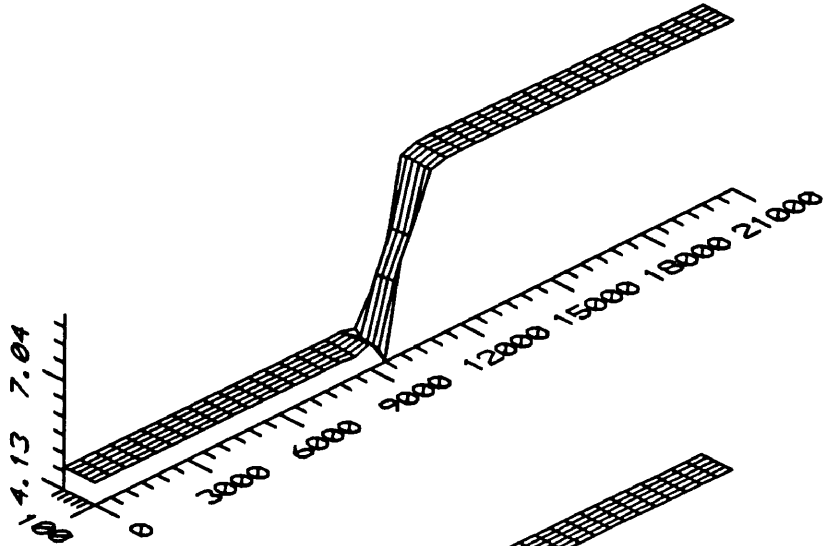


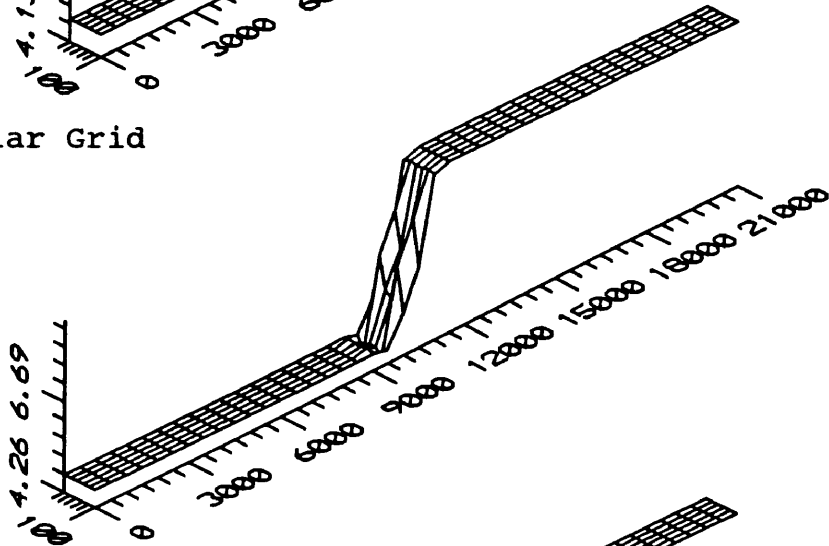
Fig. 132. 2DDI Continuity vs Distance Down Channel for Test Grids with Sudden Reduction in Depth for Resolution = 1, EV = 0.0 and Head = 0.76 Ft.

solutions are particularly good given the continuity oscillations shown previously.

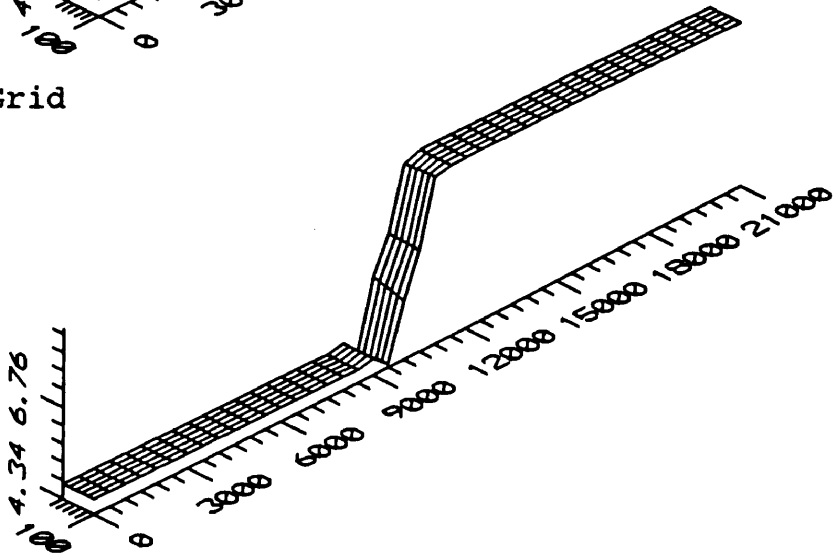
Increased Resolution on Depth Reductions with 2DDI. Next the grid resolution was doubled to 2 elements on the sudden reduction in depth as had been done for the RMA-2V model previously. A value of 0.000195 was again used for EV with a time step of 12 seconds ( $\Delta t > 1.5$ ) since time accuracy is not as important for a steady state run and time steps of an order of magnitude above the Courant limit did not effect linear model convergence in preliminary tests.  $\tau$  was left at 0.0003 and all other values were left at previously tested values. This test again resulted in a flow rate of about 500,000 cfs. For this case the continuity deviation remained relatively unchanged for the positive side (over +20%) but reduced from about -18% for the single resolution case to about -4% to -6% on the negative side for this case



(a) Regular Grid



(b) "C" Grid



(c) Alternating Grid

Fig. 133. 2DDI Three Dimensional Velocity Surface Plots for Test Grids with  $EV = 0.0$ , Head = 0.76 Ft, and Time Step = 12 Seconds.

as shown in Fig. 134(a). The various grids performed in almost an identical manner as they did in the single resolution case with the "C" grid showing about a 2.5% positive drift compared to the alternating and regular grid.

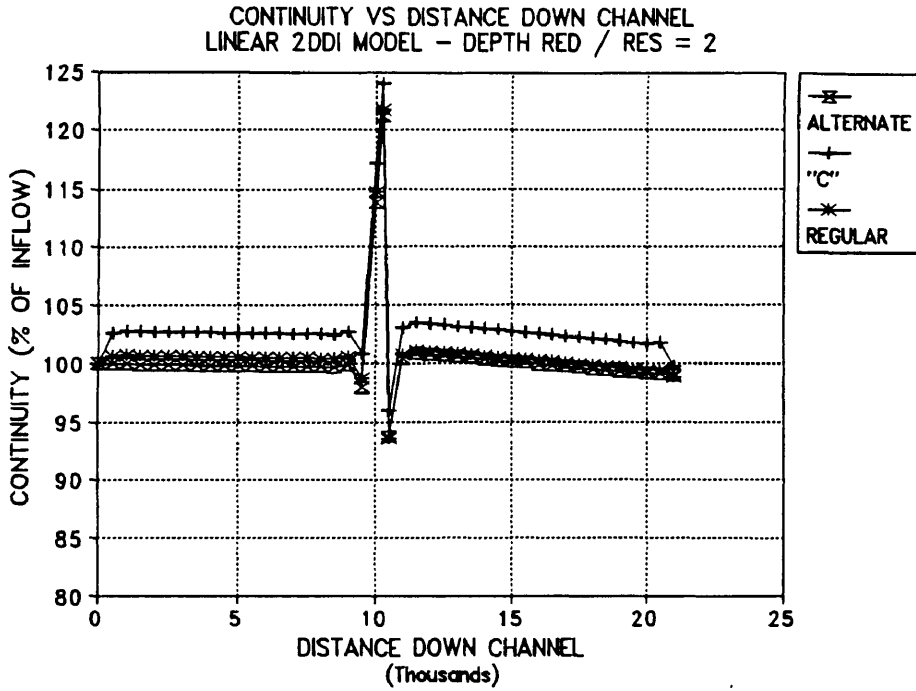
The model was then tested with a head of 0.76 ft and  $EV = 0.0$  for all three grids. The results are shown in Fig 134(b) and it can be noted that the continuity oscillations are more centered around the desired 100% line.

Oscillations are between +10% and -13.5% - a significant reduction from the single resolution case. For this case with no lateral diffusion it can be seen that all three grids plot nearly identically.

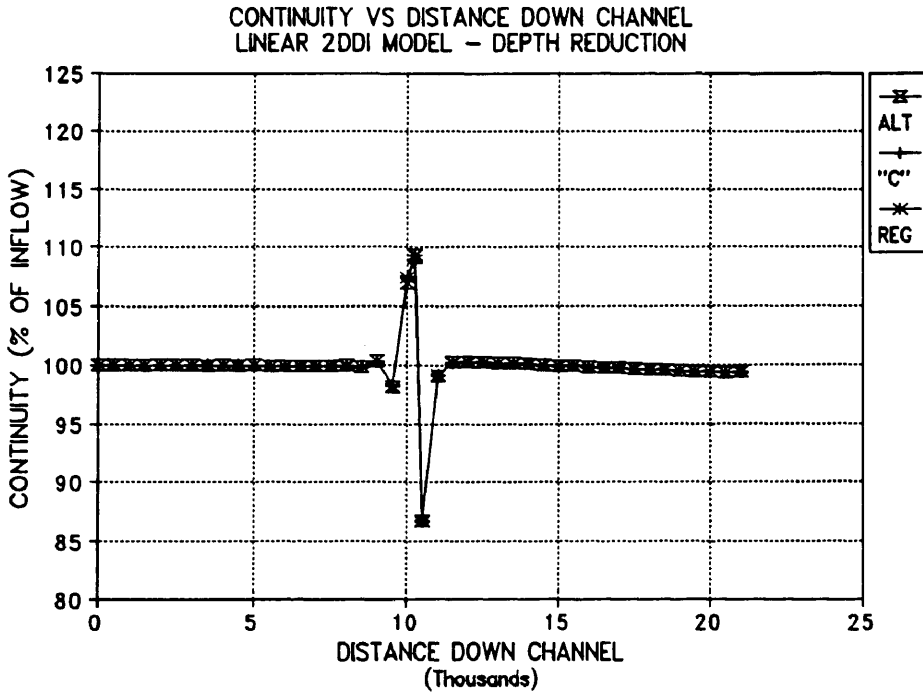
When the resolution on the sudden depth change was increased to 4, with  $EV = 0.000195$  and head = 1.59, all negative deviations disappeared but the positive deviations are still 15% or higher as shown in Fig. 135(a). It should be noted that the x scale is not constant in this figure and that each tic mark on the axis is the location of a data point, not an equal distance down the channel. The data was plotted in this manner to make it possible to view the model behavior on the reduction in depth.

Tests were then run with  $EV = 0.0$  and a head of 0.76 feet. These results are shown in Fig. 135(b) and it can be noted that continuity oscillations are greatly reduced over the single resolution test as well as the previous resolution = 4 test in Fig. 135(a). Maximum deviation in this case is less than 8%.

Resolution was then increased to 8 elements on the reduction in depth with  $EV = 0.000195$  and a head of 1.59 ft with the results are shown in Fig. 136(a). It is interesting to note that while the wave form has changed, that the maximum continuity deviation remains at about +15% and that the negative deviation is again non-zero and approximately -6% to -8%. This tends to indicate that this method of increasing resolution with high EV values does not



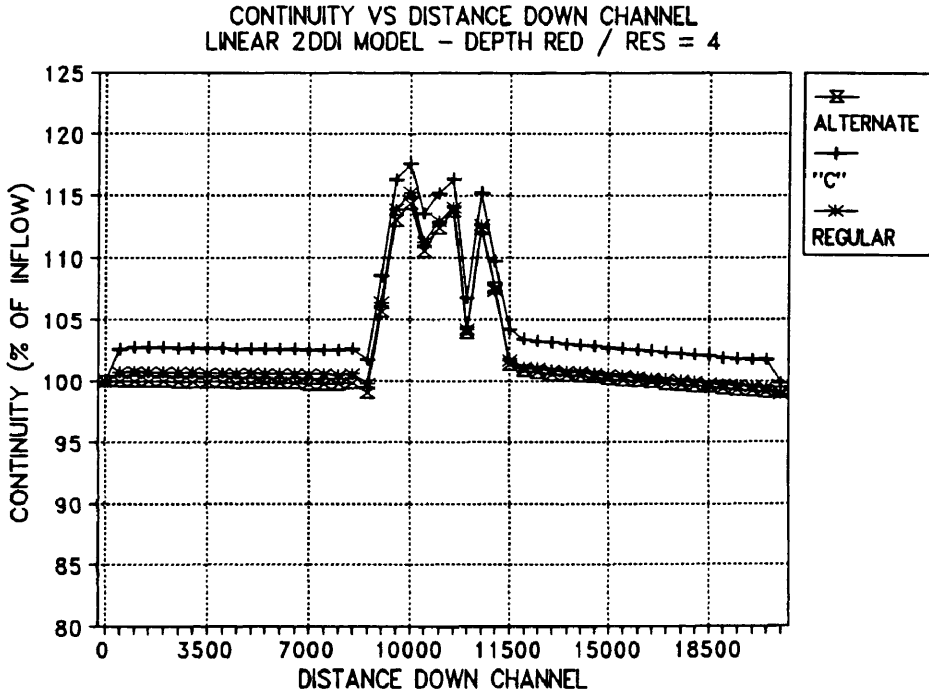
(a) EV = 0.000195 and Head = 1.59 Ft



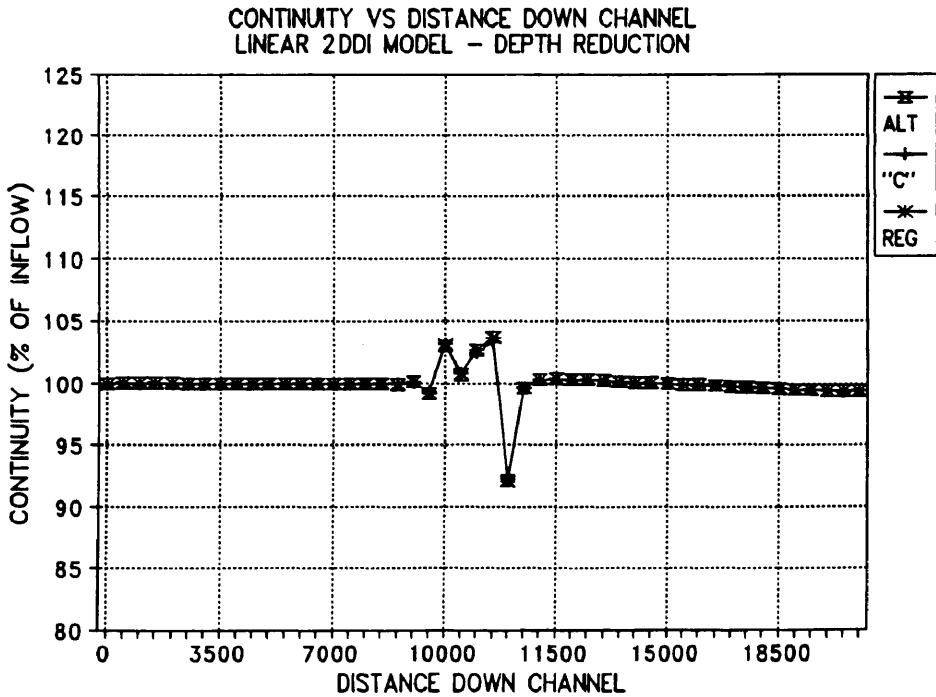
(b) EV = 0.0 and Head = 0.76

Fig. 134. 2DDI Channel Continuity for Sudden Depth Reduction Test Grids for Resolution = 2 with 12 Second Time Step.



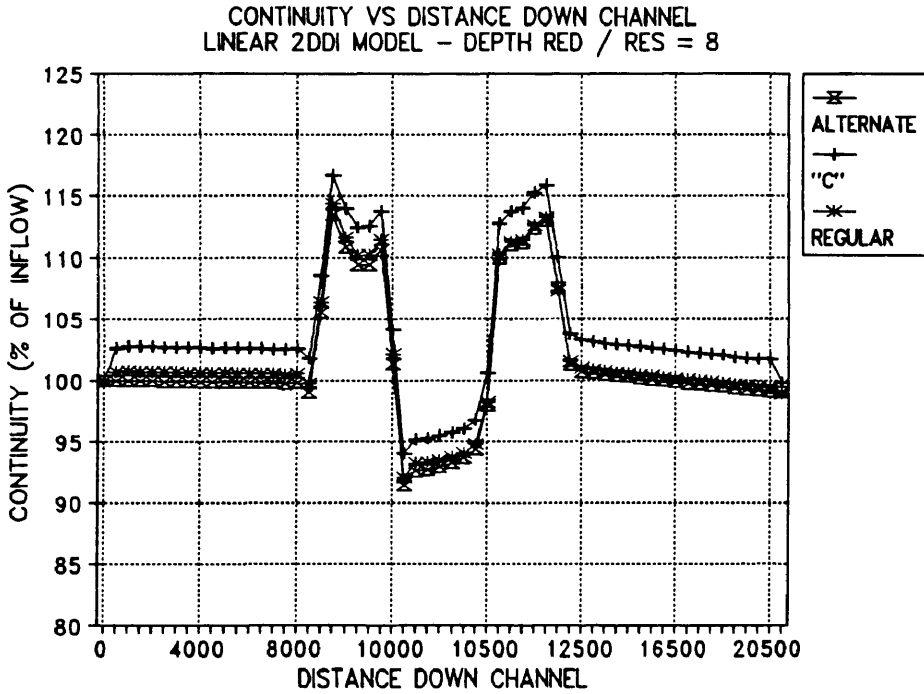


(a)  $EV = 0.000195$  and Head = 1.59 Ft.

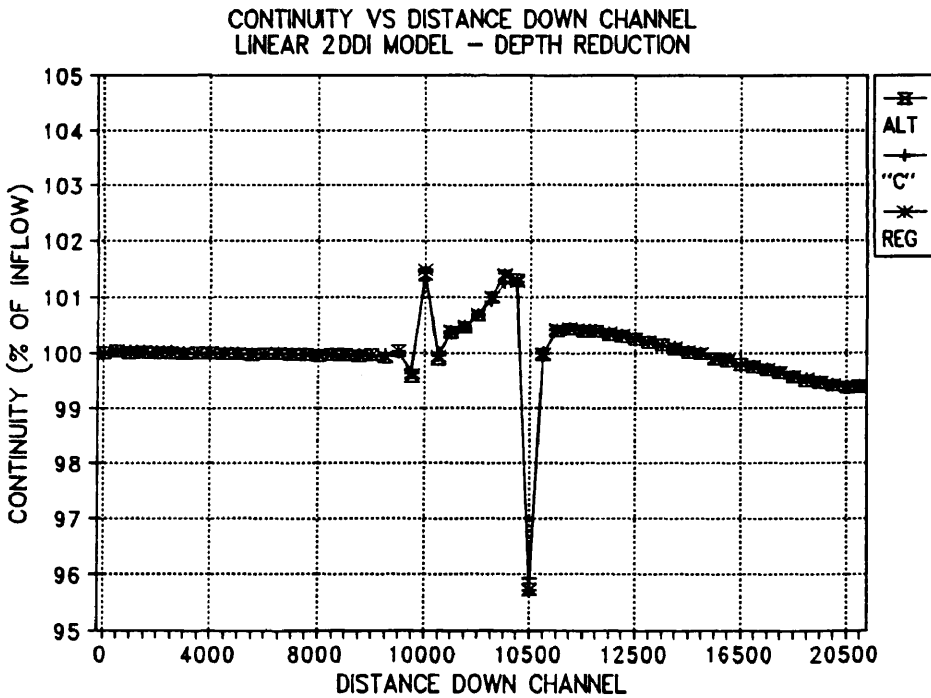


(b)  $EV = 0.0$  and Head = 0.76 Ft

Fig. 135. 2DDI Channel Continuity for Sudden Depth Reduction Test Grids for Resolution = 4 with a 12 Second Time Step.



(a) Resolution = 8, EV = 0.000195, Head = 1.59



(b) EV = 0.0 and Head = 0.76

Fig. 136. 2DDI Continuity for Sudden Depth Reduction Test Grids with a 12 Second Time Step for Resolution = 8.

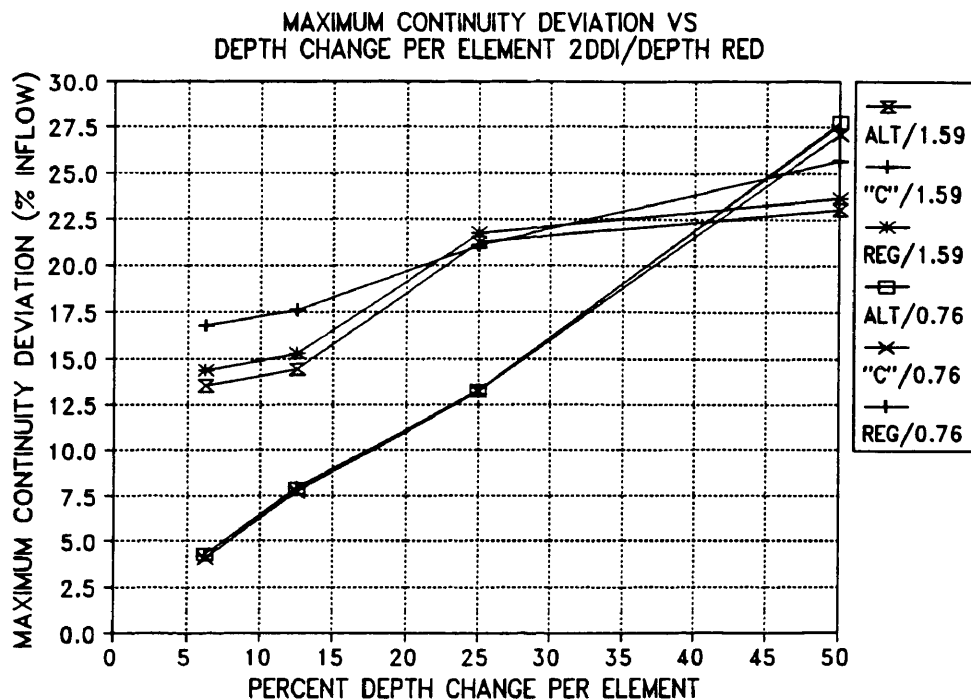
reduce continuity oscillations to near zero as was the case with RMA-2V.

The value for EV was then reduced to 0.0 and the model head reduced to 0.76 (500,000 cfs) and continuity values again plotted to determine if the relatively high value of EV was contributing to the large continuity oscillations for the resolution = 8 case. This data is presented in Fig. 136(b) for all three test grids. The extreme difference in y scales should be noted between Fig. 136(a) and (b). The continuity deviations for (a) are from -8% to +17% while those for (b) are only from -4.2% to +1.5% - a very significant reduction due to the elimination of lateral diffusion (EV).

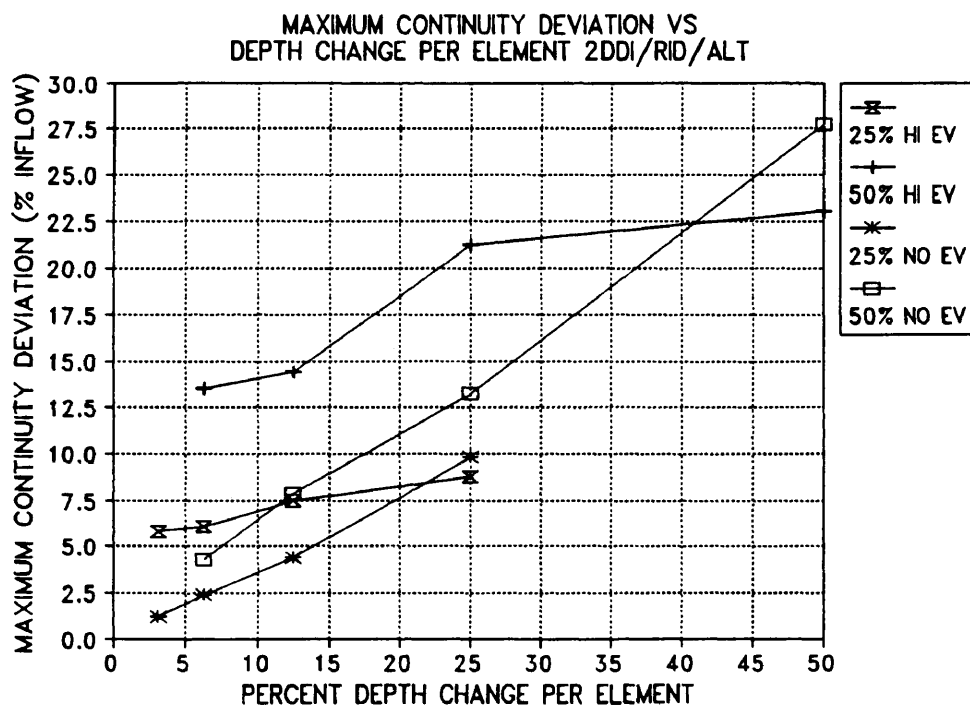
From this series of plots for resolutions of 1 to 8, it is apparent that continuity oscillations for these models are influenced to a large extent by the advective terms - i.e. the lateral diffusion terms. The fact that increasing the EV also increases the continuity deviations (except at a resolution of 1) is the direct opposite of RMA-2V for this test case where increased lateral diffusion (EV) results in increased model stability.

When comparing the two models even the continuity loss of about 5% with the resolution = 8 grid is excessive - especially considering the high resolution involved. This same problem solved with the RMA-2V model produced less continuity deviations for both the 4 and 8 resolution case. Even the resolution = 2 case did not produce higher maximum deviations in the RMA-2V model although the oscillations produced carried to the end of the channel.

The maximum deviation results for the various grids are plotted in Fig. 137(a). The difference between the EV = 0.0 cases and the EV = 0.000195 (high EV) cases is very noticeable in this plot. The high EV tests do not show the same pattern as do the EV = 0.0 tests which show nearly a linear relationship between the maximum continuity deviation



(a) 50% Reduction in Depth Tests for EV = 0.0 and 0.000195



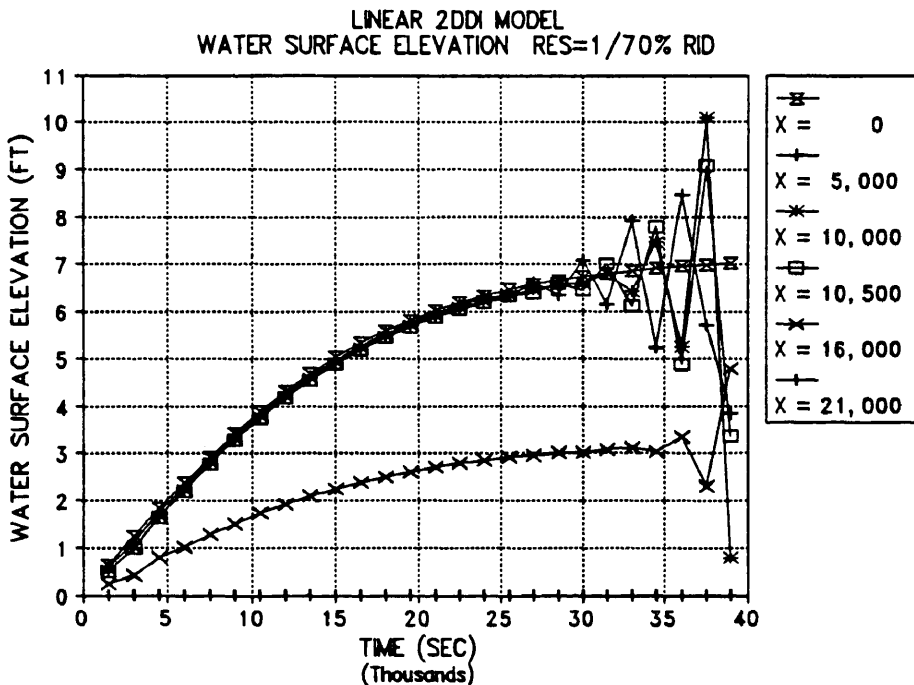
(b) 25% and 50% Depth Reduction Tests

Fig. 137. Linear 2DDI Model Maximum Continuity Deviation vs Percent Change in Depth per Element for 50% and 25% Reduction in Depth for 500,000 cfs Flowrate for EV = 0.0 and 0.000195.

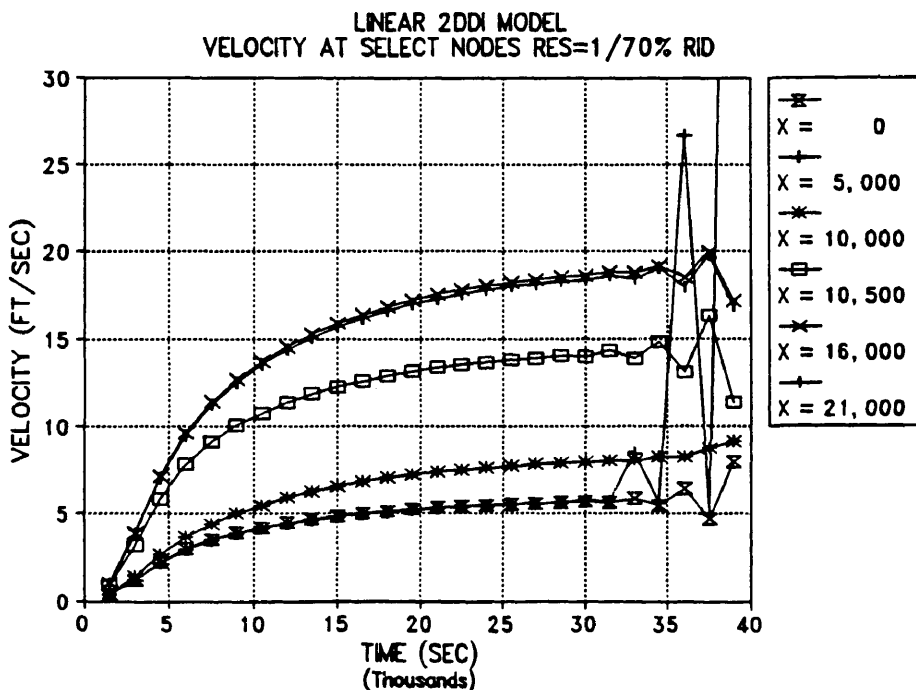
and the percent change in depth per element with all grid types producing nearly identical maximums. The high EV cases show significant differences between the various grids at both high and low resolutions with the alternating grid producing the best results at both extremes.

Next the model was run approximately 25% and 75% depth reductions for the alternating grid as had previously been done for the RMA-2V model. The 75% reduction test would not converge with EV set to 0.000063 - the value that produced the proper flow in the channel for the 25% test. In an attempt to get the model to converge the ramp was lengthened from 0.1 days to 0.8 days. The results for the 0.4 and 0.8 day ramps are shown in Figs. 138 and 139. It can be seen that even though the ramp length is doubled that the model instability starts in about the same time in the simulation and the model stops due to instability at approximately the same time. With EV at 0.0 and head at 4.40 the model reached steady state for a flow rate of 500,000 cfs and produced the maximum deviation results shown in Fig. 140(a). The data from the similar RMA-2V test is also included here for comparison purposes. It can be easily noted that the 2DDI model has produced much higher maximum deviations than the RMA-2V model for the 75% reduction in depth. The RMA-2V data is with EV = 5 - the worst case for RMA-2V at a high percentage of depth reduction per element and the best case at a small amount of depth change per element.

The 25% reduction test (EV = 0.000195 and head = 1.59 ft) converged and produced substantially better continuity results than the 50% depth reduction test as shown in Fig. 140(b). This was also true of the EV = 0.0 and head = 0.76 as shown in Fig. 140(b). The influence of total depth reduction appears to be nearly as important in determining maximum continuity deviations as the amount of depth change per element for the 2DDI model. For the RMA-2V model the values for the 25% and 50% depth reductions tended to the

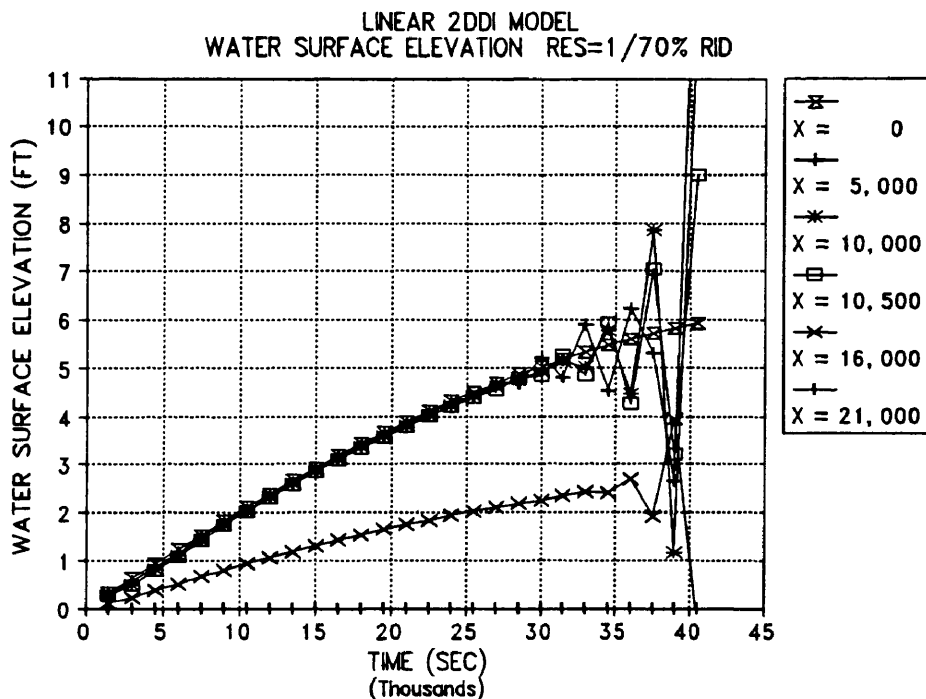


(a) Water Surface Elevation

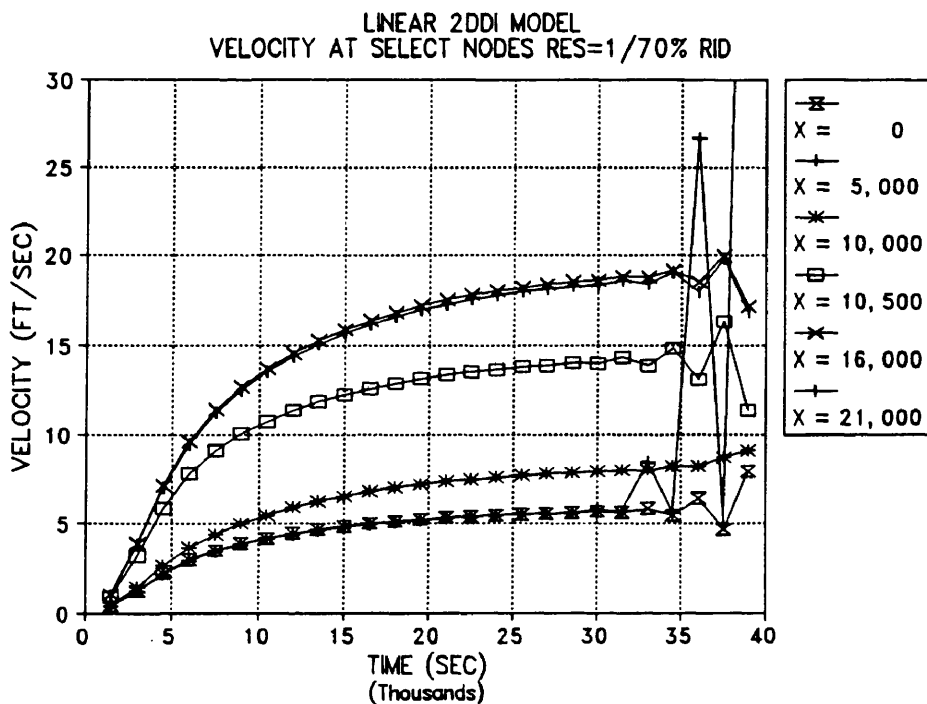


(b) Velocity

Fig. 138. 2DDI Water Surface Elevation and Velocity for Selected Nodes for Alternating Grid with 75% Depth Reduction with 0.4 Day Ramp. EV = 0.000063, Head = 7.18 Ft, and DT = 12 Seconds.

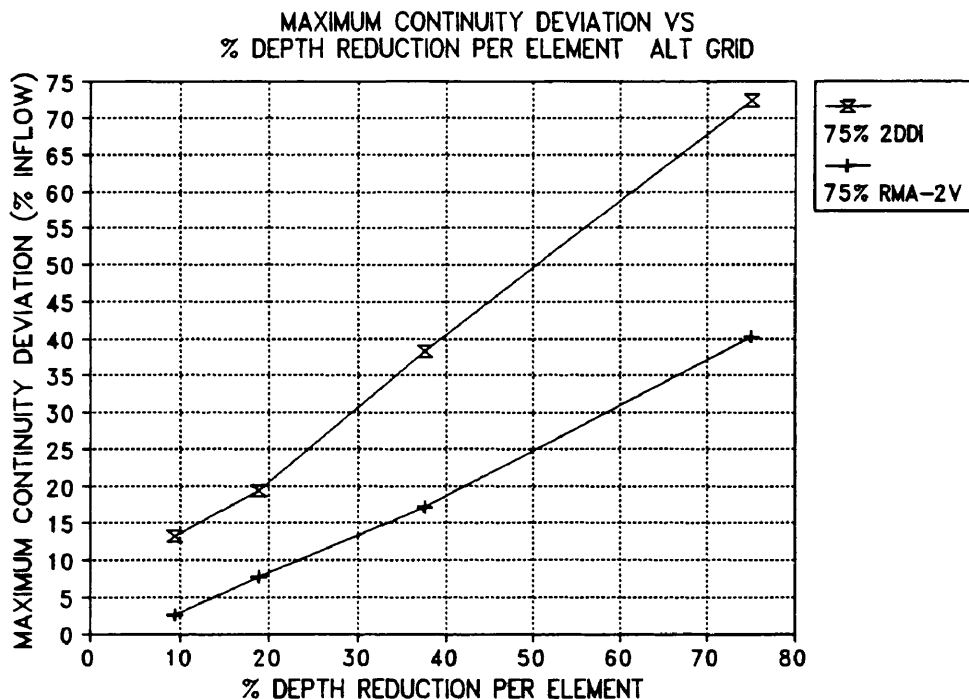


(a) Water Surface Elevation

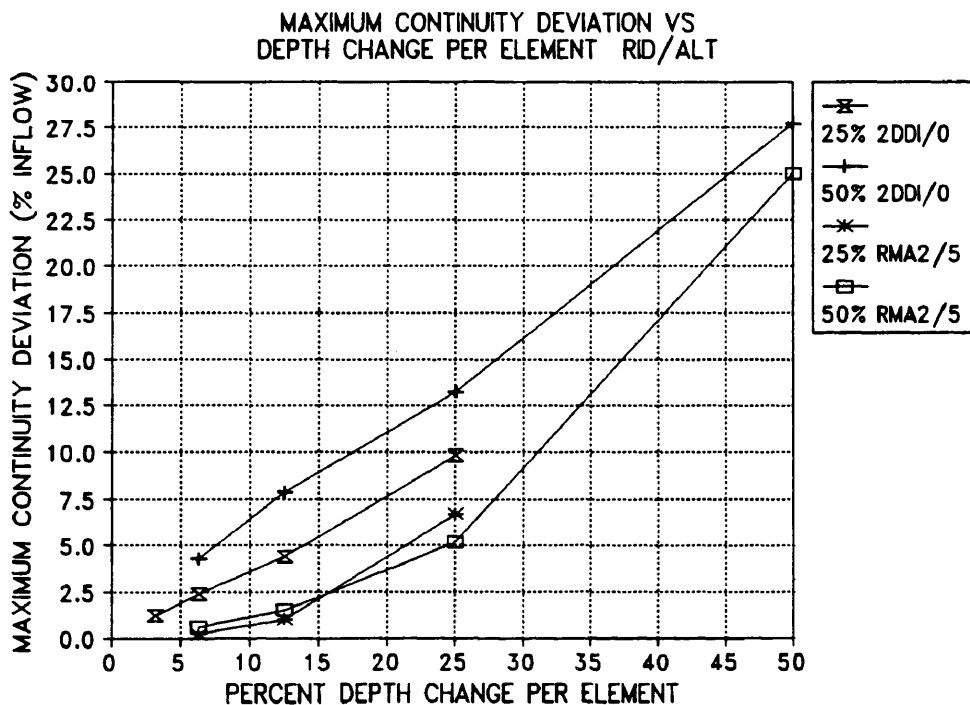


(b) Velocity

Fig. 139. 2DDI Water Surface Elevation and Velocity for Selected Nodes for Alternating Grid with 75% Depth Reduction with 0.8 Day Ramp. EV = 0.000063, Head = 7.18 Ft, and DT = 12 Seconds.



(a) 2DDI 75% Compared to RMA-2V



(b) 2DDI 25% and 50% Compared to RMA-2V with EV = 5

Fig. 140. 2DDI Maximum Deviation vs Percent Reduction in Depth for 25% to 75% Depth Reductions Compared to RMA-2V Results. RMA-2V Results are with EV = 5.

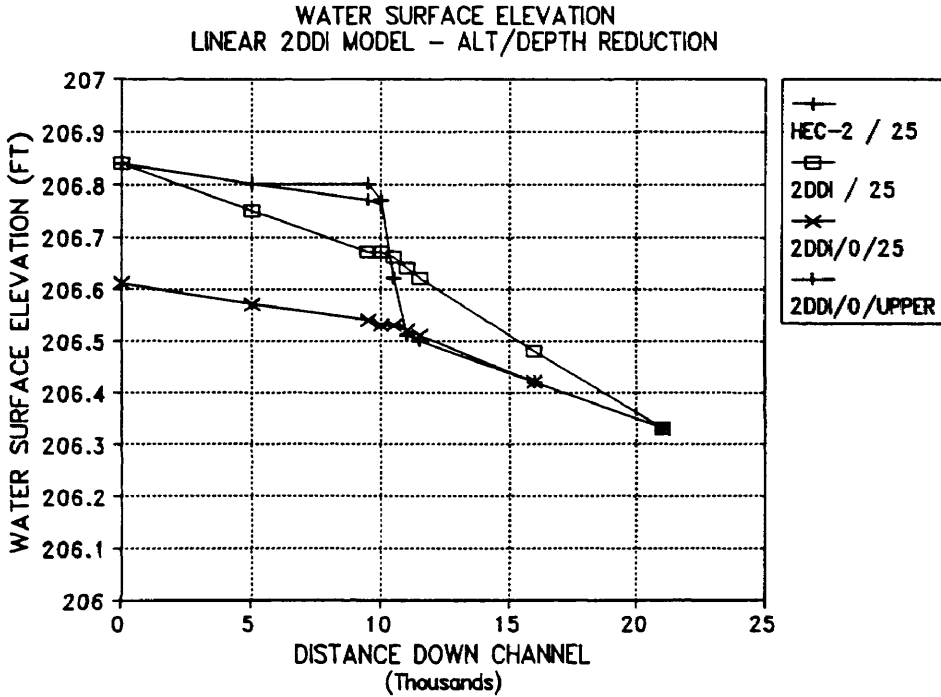


same line as resolution increased - also shown in Fig. 140(b). For the 2DDI model the pattern is similar for the 25% and 50% but the values do not converge to the same values as the resolution increases. Values are also substantially higher than for RMA-2V at all grid resolutions.

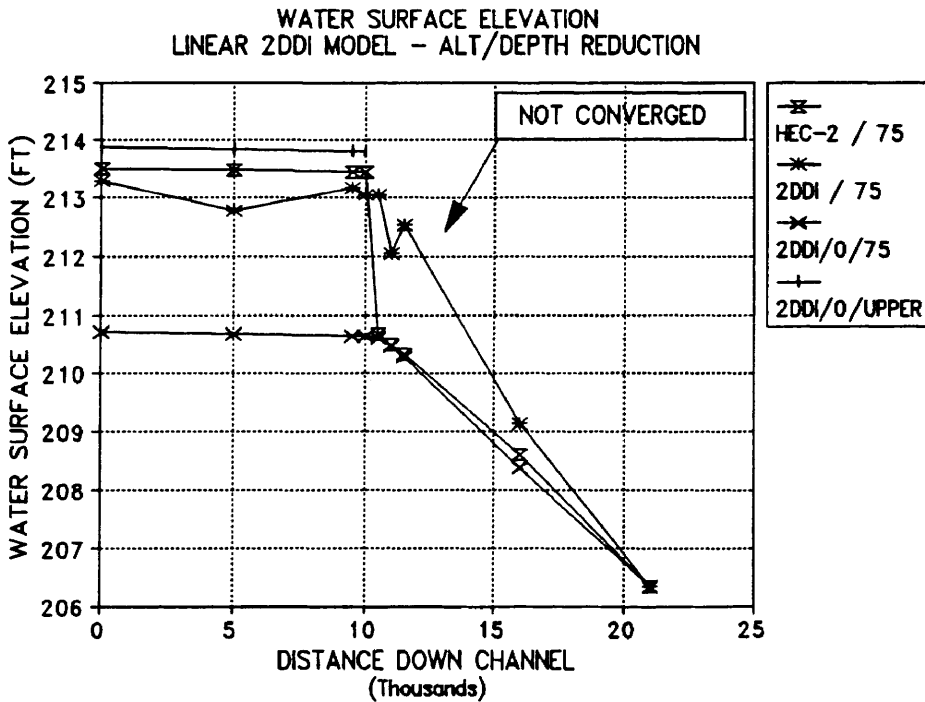
If the water surface elevations for the 25% reduction in depth test are compared with the HEC-2 results, the two values are still not in agreement for the  $EV = 0.000195$  test due to the elimination of the non-linear terms - shown in Fig. 141(a) (labeled HEC-2/25 and 2DDI/25 respectively). With  $EV = 0.0$ , water surface adjusted for datum, and results plotted; the elevations agree very closely with the HEC-2 data as also shown by the 2DDI/0/25 label in Fig. 141(a). When the 2DDI data is adjusted for velocity head the results plotted as 2DDI/0/UPPER in Fig. 141(a) are obtained. These results follow the HEC-2 results very closely with the exception of just upstream of the sudden reduction in depth where there is a slight difference in water surface elevation.

The water surface for the 75% reduction in depth test with  $EV = 0.000195$  and a head of 7.18 ft shows surface waves that continued to move back and forth through the model and prevented the model from reaching a steady state condition. The water surface created by these waves is shown in Fig. 141(b) and is labeled 2DDI/75. The NOT CONVERGED identifier indicates that the solution has not reached steady state.

When  $EV$  was set to 0.0 a water surface elevation of 4.40 feet was found to give just over 500,000 cfs as the flow rate for the channel. The datum adjusted water surface elevation for the  $EV = 0.0$  and head = 4.4 (2DDI/0/75) is again in very good agreement with the HEC-2 results up to the sudden reduction in depth where the difference in velocity head is neglected by the model. When velocity head is taken into account the agreement is fairly good although



(a) 25% Depth Reduction



(b) 75% Depth Reduction

Fig. 141. 2DDI Water Surface Elevation vs HEC-2 Model Predictions for 25% and 75% Depth Reductions with Alternating Grid for 500,000 cfs. Water Surface for 75% Depth Reduction not Converged to Steady State.

the 2DDI model is predicting a slightly higher water surface elevation upstream of the sudden depth reduction than the HEC-2 model. This data is identified by the 2DDI/0/UPPER label in Fig. 141(b).

The water surface elevation plots discussed above show the same pattern for water surface elevation for the  $EV = 0.000195$  test that was shown in the 50% reduction in depth test (Fig. 126). These results indicate that the linear 2DDI model cannot be forced to match the water surface elevation in a channel when the velocity head changes by any significant amount. This indicates that the linear 2DDI model is not applicable to a large abrupt reduction in depth when velocities are significant and accurate water surface elevations are important. None of the sudden reduction tests were adequately modeled using the linear 2DDI code when water surface elevation was considered and the non-linear code was unstable for all tests made to date. The RMA-2V model was superior for all sudden depth reduction tests as water surface is accurately modeled and the maximum continuity deviations were smaller. The oscillations in the RMA-2V and 2DDI models indicate that more research is needed into stable formulations of the shallow water equations for river applications where sudden depth reductions occur.

#### SUDDEN DEPTH INCREASES WITH 2DDI

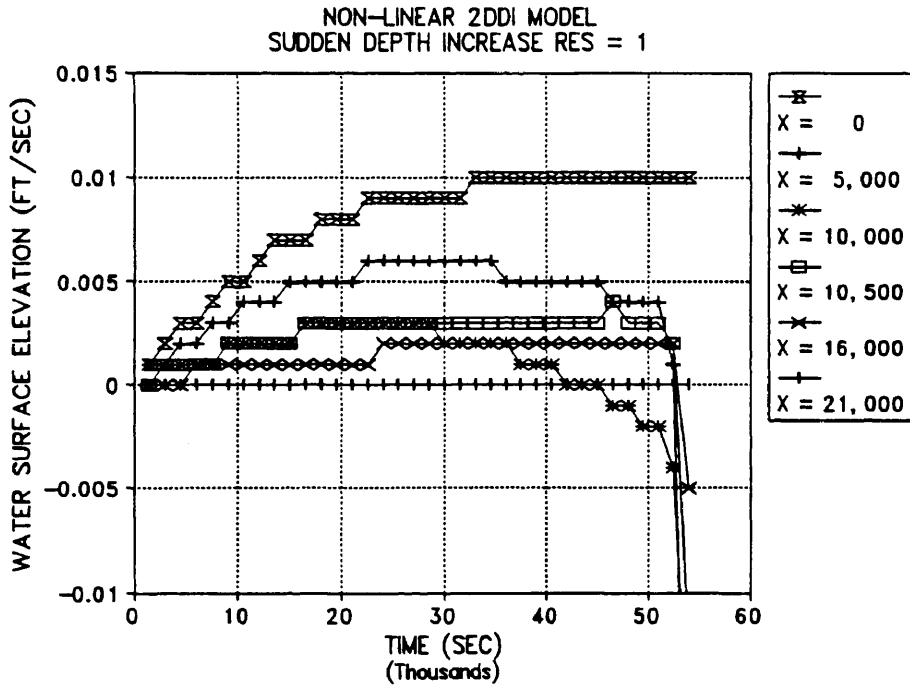
The sudden depth increase grids were again converted from the RMA-2V grids by linearization (removal of midside nodes) and reformatted to be acceptable to the 2DDI model. Test values used for these grids were identical to the values used for the tests with RMA-2V. Manning's  $n$  values were used to calculate  $C_f$  based on depth as previously described and other values were identical to those used for RMA-2V and for the 2DDI sudden depth reduction test.

The first tests were again run using the FULLY NON-LINEAR form of the model. The time history plots for water surface elevation and velocity for a test with a head of 0.01 feet across the model and a time step of 12 seconds are shown in Fig. 142. The water surface elevation shown in Fig. 142(a) indicates that the model did not reach a stable water surface at the plotted nodes prior to becoming unstable. At about 30,000 seconds into the simulation the water surface elevation starts to drop at  $X = 10,000$  feet down the channel. This occurs while the water surface at the head of the channel is still "ramping up". The result is a model that goes unstable prior to reaching steady state conditions.

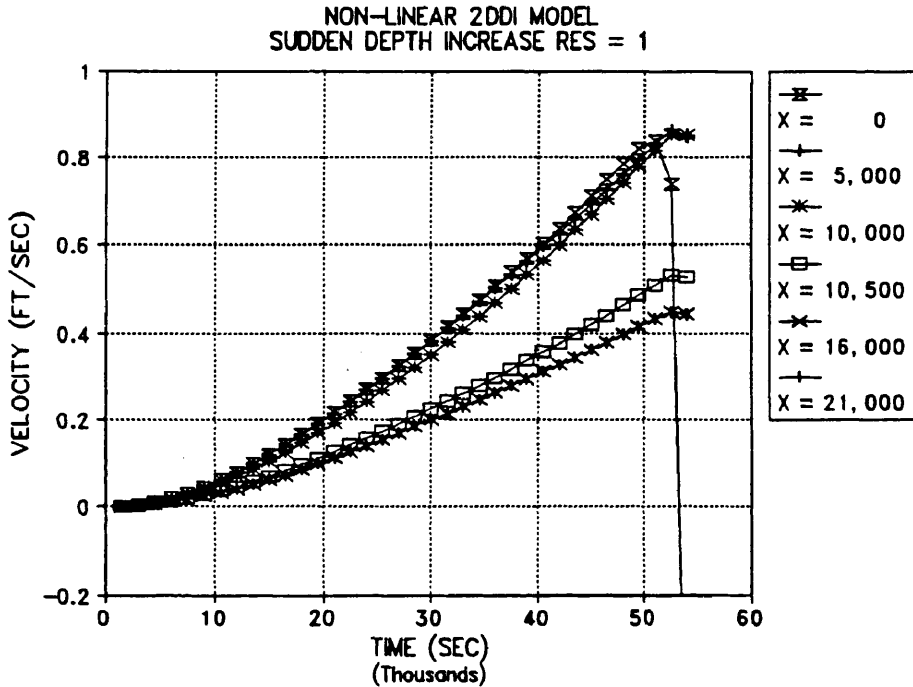
The velocity plot in Fig. 142(b) shows very similar results to the smooth bottom channel results (Fig. 116) and the sudden depth reduction test (Fig. 124). There are some differences in maximum velocity and time of model instability but the mode of failure is the same in all three tests.

The continuity of the model for 3 time steps near the end of the sudden depth increase simulation is shown in Fig. 143. Again it can be noted that instabilities build at the inlet to the model and continuity values are shifted vertically prior to model failure. In this plot it can be noted that the continuity oscillation across the depth increase also tends to increase as the model approaches terminal instability but the oscillation is increasing more slowly than the increase in the continuity drift. The term terminal instability will be used to define the point when the maximum velocity becomes greater than 100.0 ft/sec and the model is stopped by internal logic.

The LINEAR form of the model was then used for the same conditions tested with the RMA-2V model. For the RMA-2V model the upstream water surface elevation was 206.14 ft while the downstream elevation was 206.33 ft. This yields a



(a) Water Surface Elevation



(b) Velocity

Fig. 142. Non-linear 2DDI Model Water Surface Elevation and Velocity for Sudden Depth Increase, Alternating Grid with 0.01 Ft Head, 0.4 Day Ramp, and EV = 0.0.

negative slope on the water surface due to the effect of the velocity head of the water. This velocity head accounts for about 1.26 feet of head at the channel entrance and 0.30 feet at the exit. If we use these values to adjust the head to have a positive slope across the model we obtain a head of 0.77 ft. With this value for the head and with  $EV = 0.0$  the model produced a flow rate of 507,000 cfs in the channel.

When the model head was reduced to 0.75 ft the flow in the channel was 498,000 cfs which was deemed sufficiently close to the desired 500,000 cfs rate. To insure that the model had reached a steady state condition the water surface elevation and velocity were plotted for the six nodes along the centerline of the channel as shown in Fig. 144. For this case it can be seen that the linear 2DDI model reached a steady state solution very rapidly and no oscillations or drift can be noted in this data.

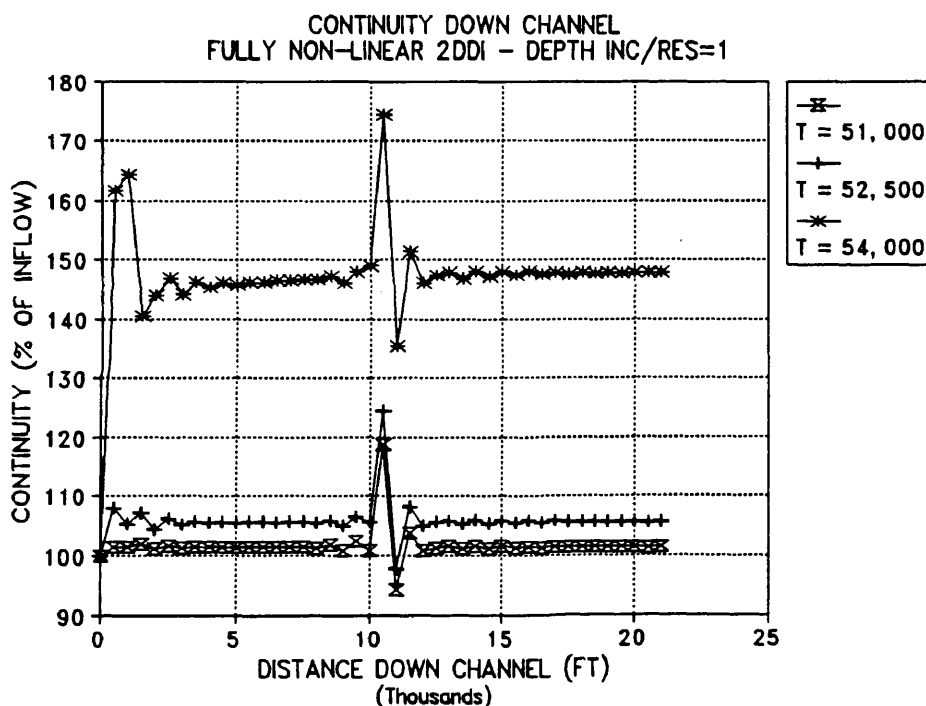
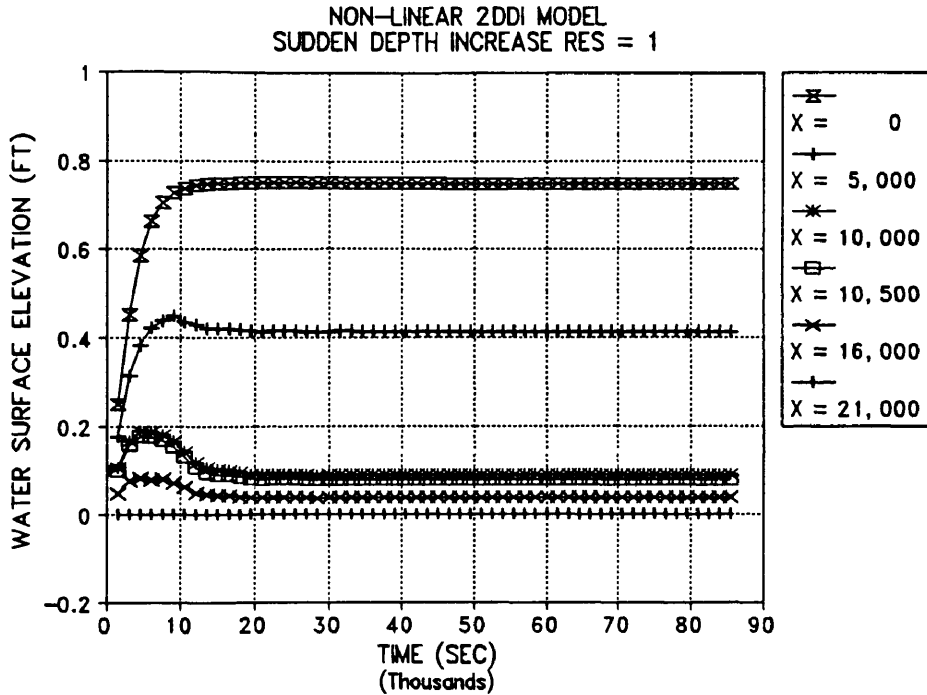
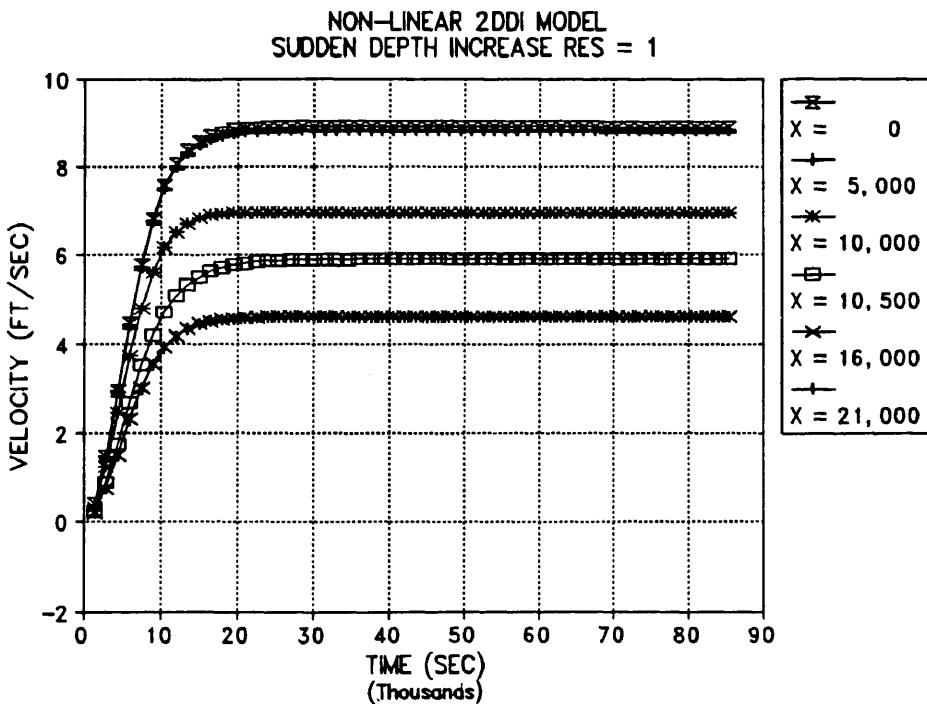


Fig. 143. Non-linear 2DDI Model Continuity Results for Sudden Depth Increase, Alternating Grid with  $EV = 0.0$ , Ramp = 0.4 Days, and Head at 0.01 Ft.



(a) Water Surface Elevation



(b) Velocity

Fig. 144. Linear 2DDI Model Water Surface Elevation and Velocity for Selected Nodes for Sudden Depth Increase, Alternating Grid with Resolution = 1, Head = 0.75 Ft, EV = 0.0, and 12 Second Time Step.

The continuity was then checked for the three grids with step resolution equal to 1 as shown in Fig. 145(a). All three grids show nearly identical results for this test with  $EV = 0.0$ . The maximum continuity deviations are approximately  $\pm 25\%$ . A slight continuity drift can be seen as flow moves down the channel.

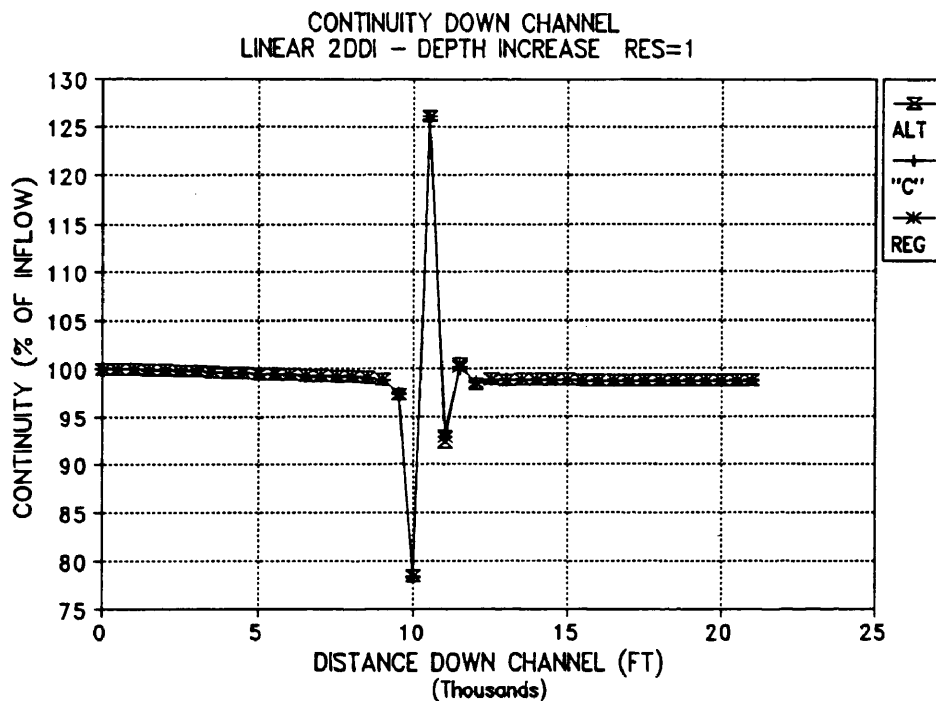
The water surface elevations as calculated by 2DDI, HEC-2 and RMA-2V were then compared for the sudden depth increase as shown in Fig. 145(b). Again the 2DDI water surface did not follow the HEC-2 and RMA-2V water surfaces due to the elimination of the non-linear terms from the calculations. The RMA-2V data was averaged to remove the oscillations which were shown in Fig. 47. The RMA-2V data used for comparison was with  $EV = 5$  and resolution = 1. When the 2DDI data was adjusted for velocity head the values fell almost exactly on the values computed by the HEC-2 model as shown in the plot by the lines labeled 2DDI/LOWER and 2DDI.

The three dimensional water surface elevations for all three test grids as calculated by the 2DDI model are presented in Fig. 146. The extremely smooth water surface is typical of those observed to date in the linear 2DDI model but again do not include any effect of velocity head.

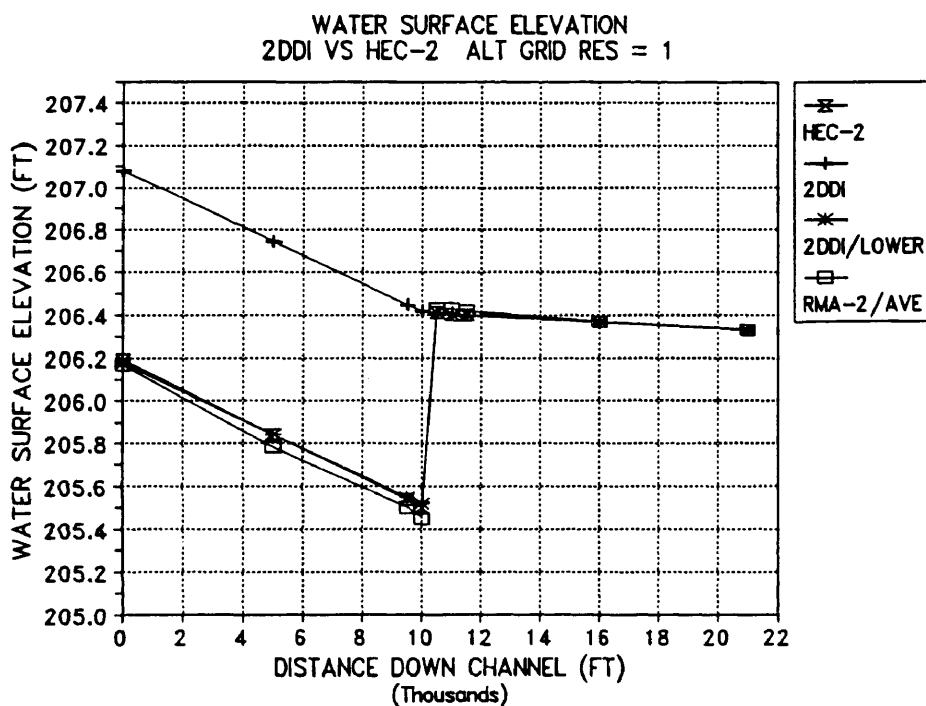
Three dimensional velocity surface plots are shown in Fig. 147. The velocities are very smooth except at the sudden depth increase where some oscillations and skewing are present for all three grid types. It should be noted that both the top and bottom surfaces of the plots are visible in this figure which allows a better understanding of how velocity varies across the depth increase for each of the three grids.

The grid resolution was next increased to two elements on the step face. This produced the continuity results shown in Fig. 148(a) while tests with a resolution of 4 produced the results in Fig. 148(b). The continuity



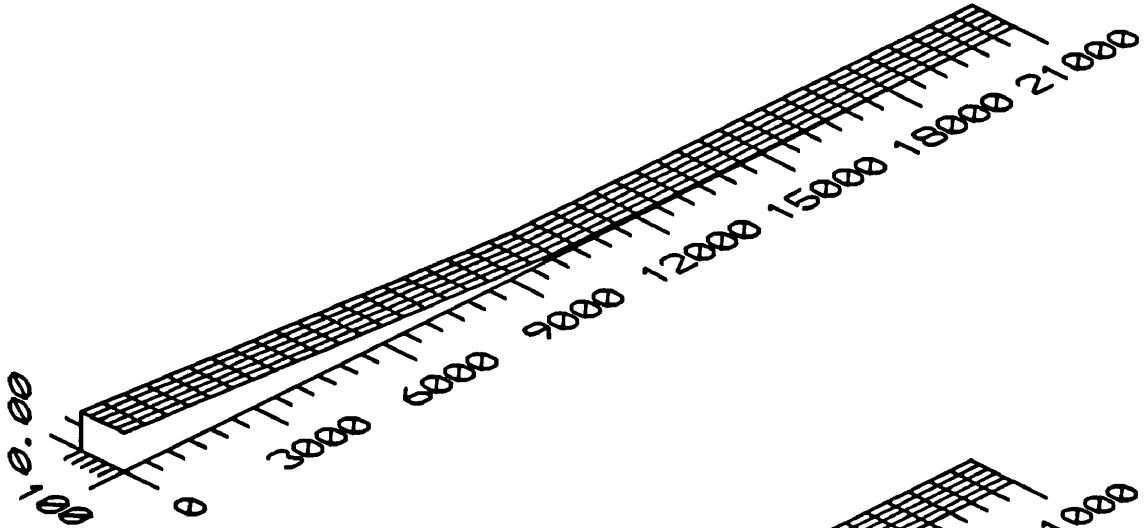


(a) 2DDI Continuity for Resolution = 1

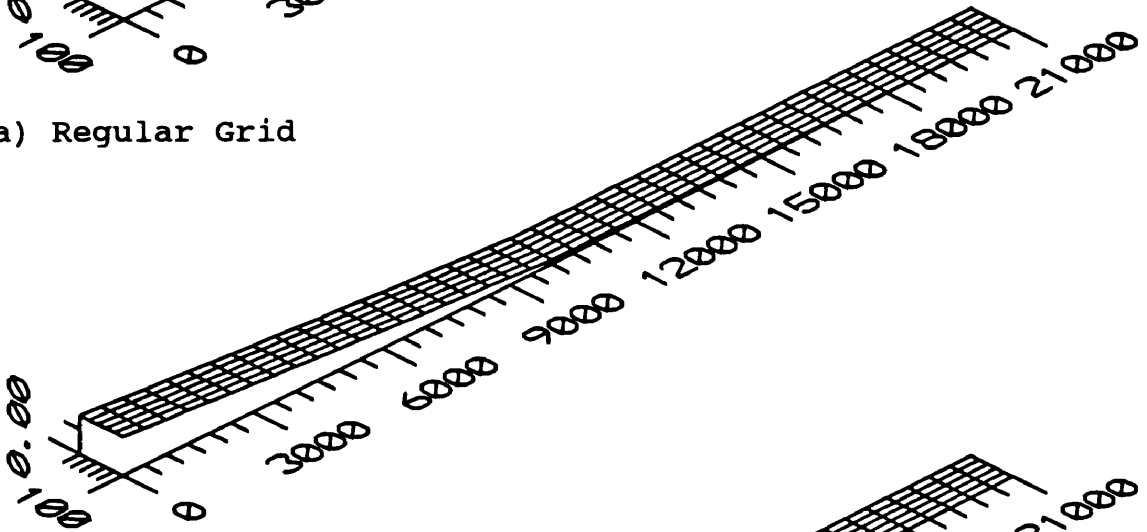


(b) 2DDI Water Surface Elevation Compared with HEC-2 Profile.

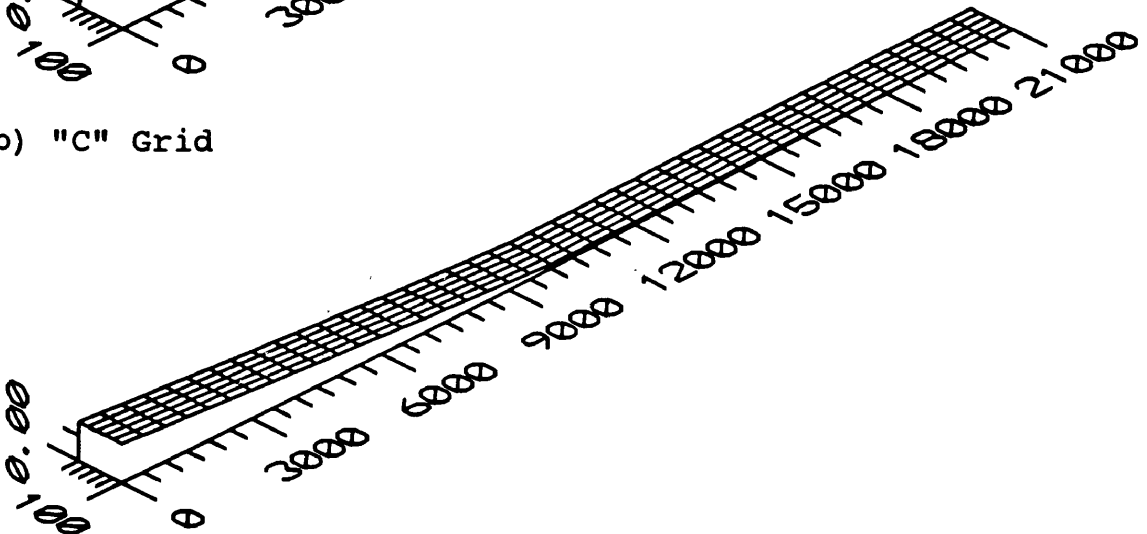
Fig. 145. Linear 2DDI Continuity vs Distance Down Channel and 2DDI Water Surface Elevation with EV = 0.0 and 0.75 Ft. Head vs HEC-2 and RMA-2V. RMA-2V Data is Averaged, EV = 5.



(a) Regular Grid

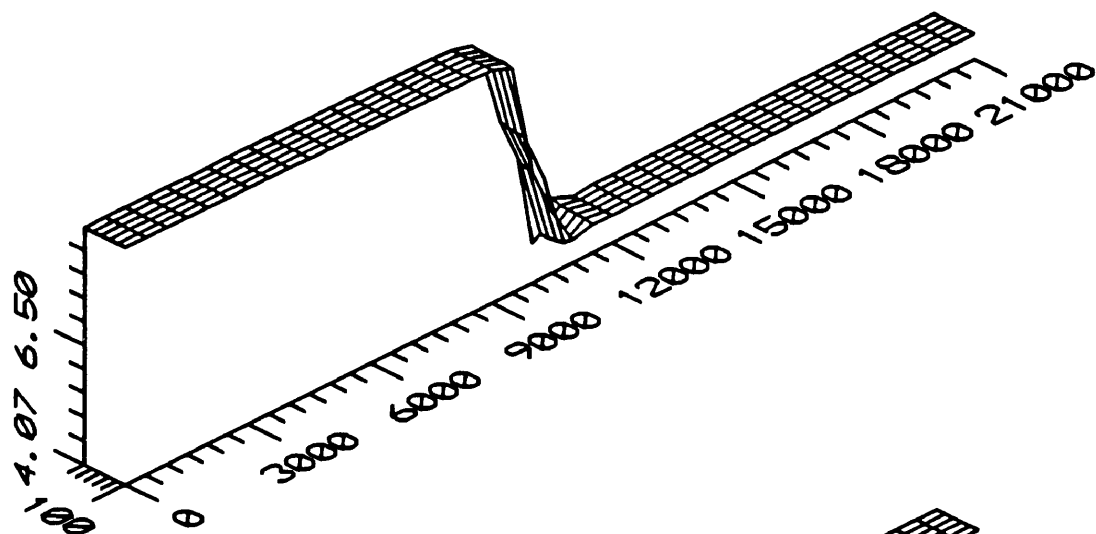


(b) "C" Grid

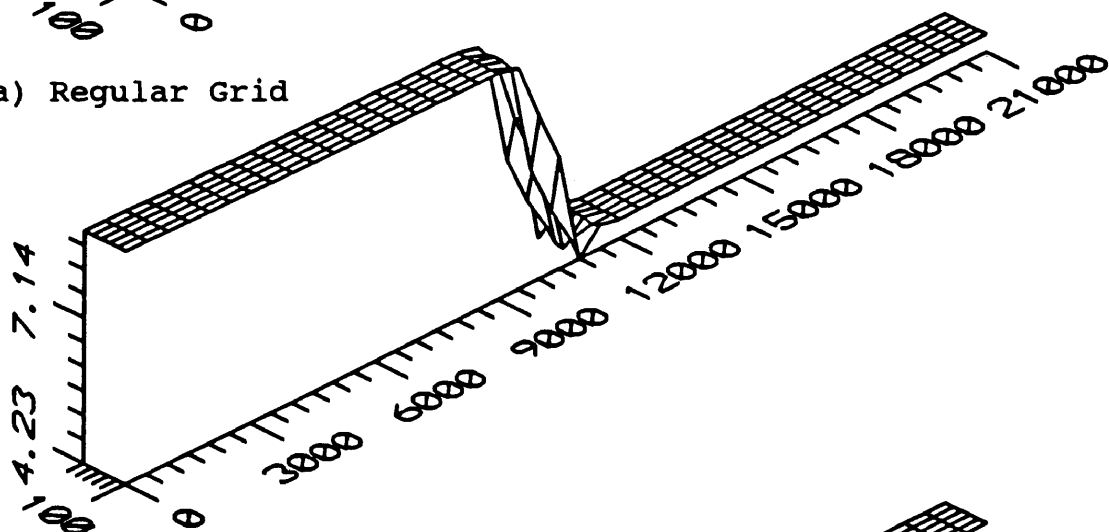


(c) Alternating Grid

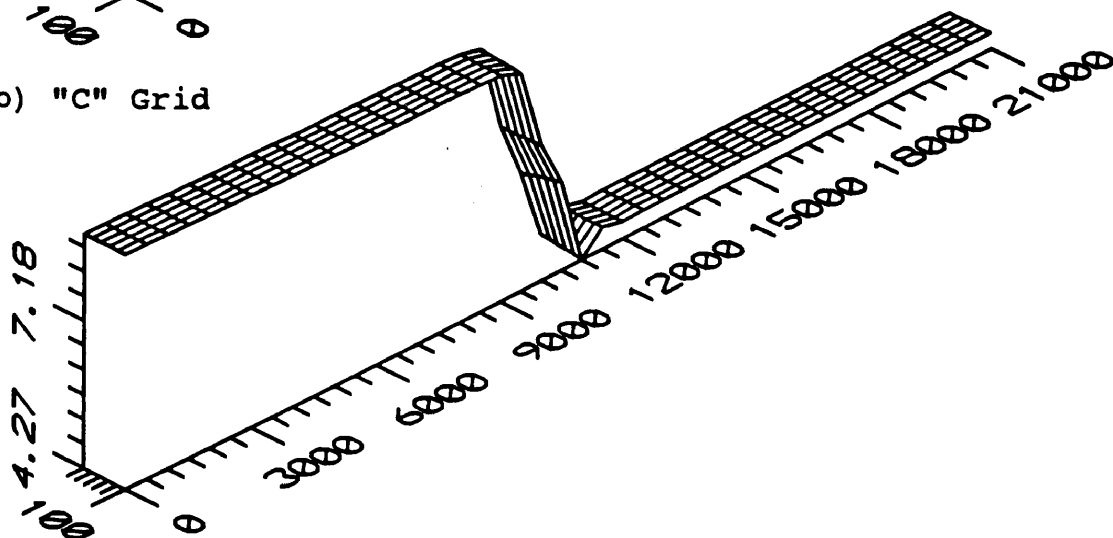
Fig. 146. Linear 2DDI Three Dimensional Water Surface Elevation Plots for Sudden Depth Increase Test Grids with  $EV = 0.0$ , Head = 0.75, Resolution = 1, and Time Step = 12 Seconds.



(a) Regular Grid

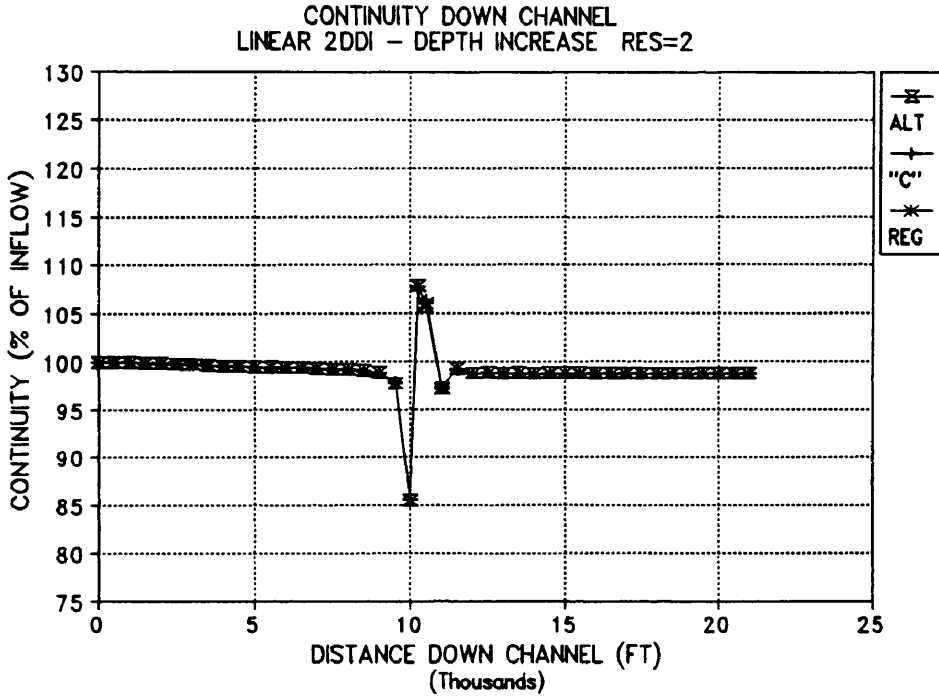


(b) "C" Grid

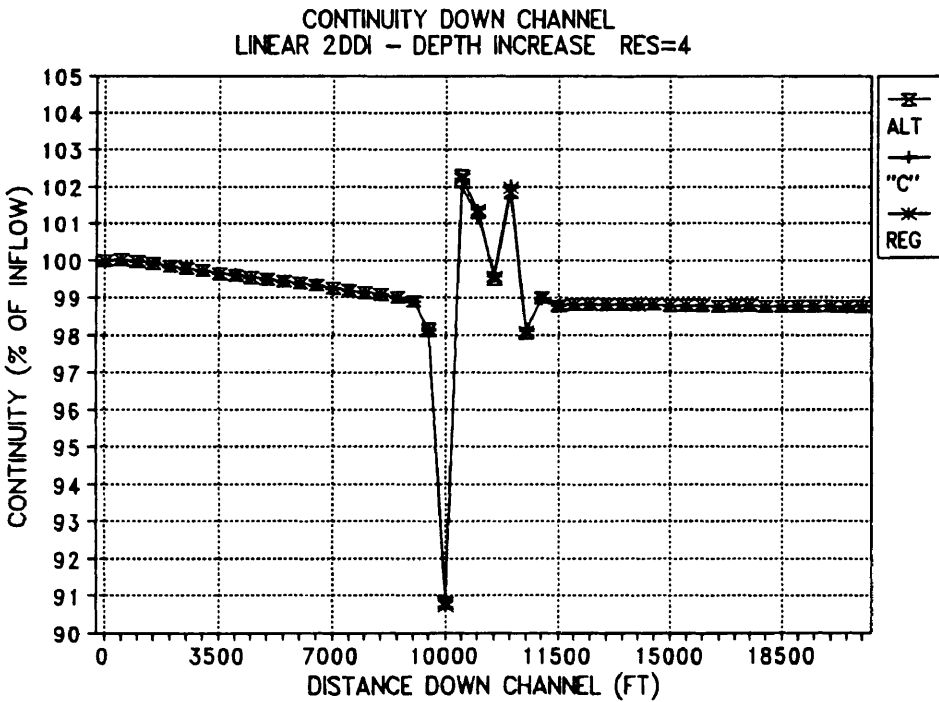


(c) Alternating Grid

Fig. 147. Linear 2DDI Three Dimensional Velocity Surface Plots for Sudden Depth Increase Test Grids with  $EV = 0.0$ , Head = 0.75, Resolution = 1, and Time Step = 12 Seconds.



(a) Resolution = 2



(b) Resolution = 4

Fig. 148. Linear 2DDI Continuity vs Distance Down Channel for Sudden Depth Increase Test Grids, Resolution = 2 and 4, EV = 0.0, Head = 0.75 Ft, and a 12 Second Time Step.

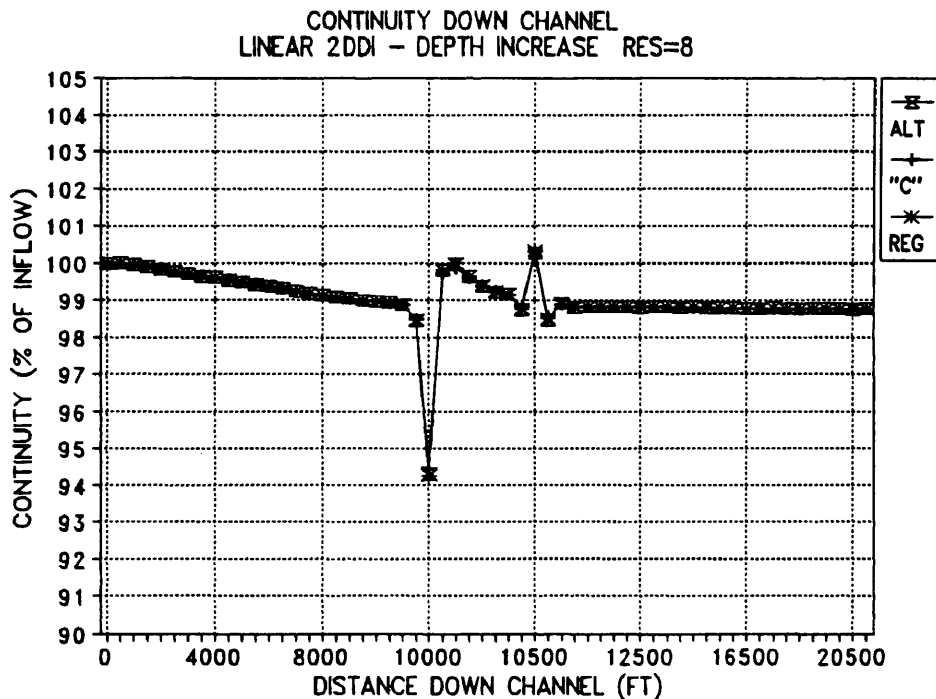
oscillation is significantly reduced in the resolution = 2 test as compared to the single resolution test. The reduction is nearly 20% for the positive side of the oscillation and about 7% for the negative side.

When the resolution was increased to 4 elements the oscillation was reduced even further. Continuity oscillations for this case were between -9% and +2.5%. The three grids continued to show almost identical behavior for continuity with some very slight exceptions at the change in depth.

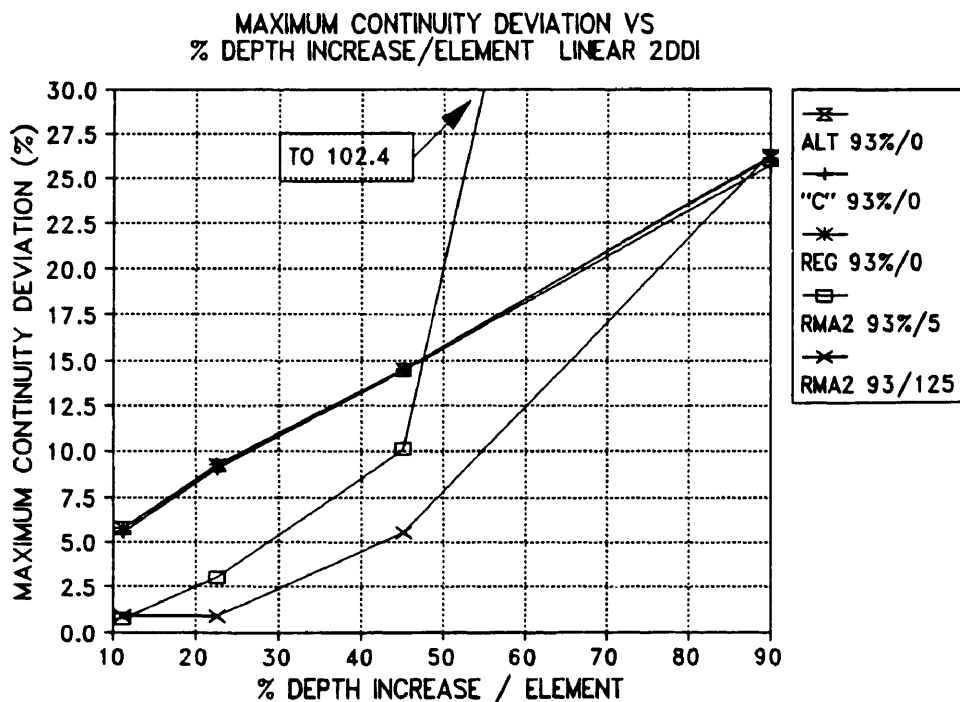
When the resolution on the step was increased to 8 elements Fig. 149(a) was obtained. It can be noted that the continuity oscillation is again reduced but that a continuity drift of approximately 1% is unchanged for all resolutions.

The maximum continuity deviation vs the percent depth change per element is plotted in Fig. 149(b) for all three grid types. It again can be noted that all three grids behave almost identically and exhibit an almost linear relationship between the maximum deviation and percent depth increase per element. The RMA-2V results are also plotted on the graph and show that with the exception of the single resolution case (93% depth increase) the EV = 5 case (labeled RMA2 93%/5) produces significantly lower maximum deviations than the 2DDI model. When EV was increased to 125 - in the range normally used in modeling rivers of this size - all of the RMA-2V values are as good or better than the 2DDI results.

The step height was then adjusted to a 25 foot step which resulted in approximately a 30% depth increase as flow moved from the shallow portion of the model to the deeper portion. The model was also run with the step height set at 75 feet which produced a 238% depth increase. These values are the identical step heights used for the sudden reduction in depth case. The two cases are simply the same step



(a) Resolution = 8



(b) 2DDI Maximum Continuity Deviation vs % Depth Increase / Element

Fig. 149. 2DDI Continuity for Resolution = 8 and Maximum Continuity Deviation vs % Depth Increase for 93% Depth Increase. EV = 0.0, Head = 0.75, and 12 Second Time Step.

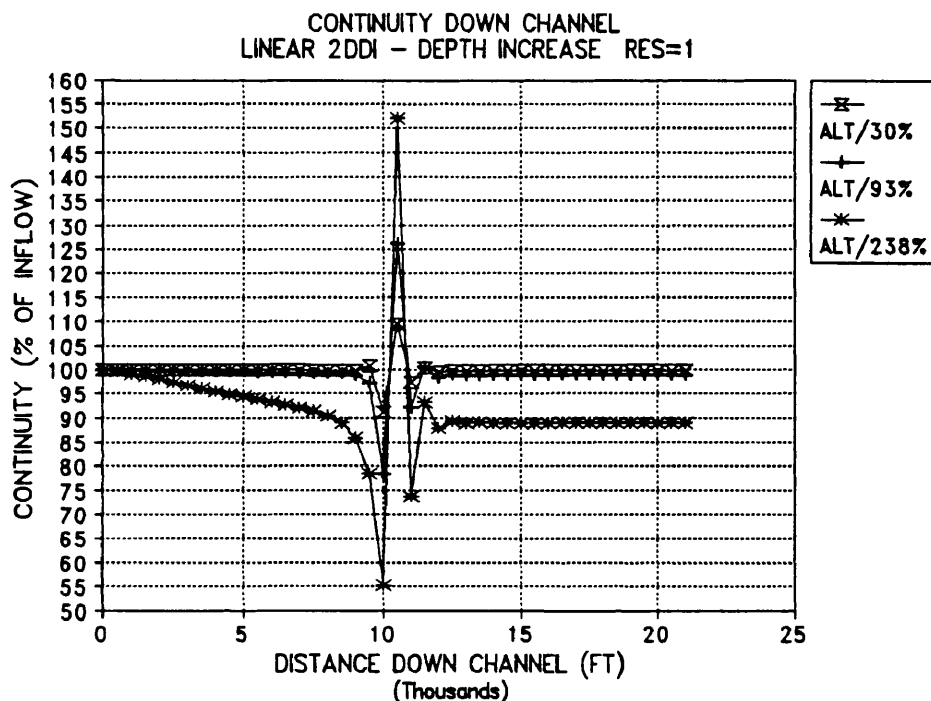
reversed and a down channel slope of 1 foot in 10,000 feet imposed on the channel to give a slight down channel gradient to the bed. The continuity results for these tests with a resolution of 1 are shown in Fig. 150(a). When resolution was increased to 8 the results obtained in Fig. 150(b) were obtained. (Note scale change between plots in Fig. 150(a) and (b).)

From these two plots it can be noted that the continuity drift for the 2DDI model seems to be associated with the height of the step for this case. Drift was not effected by increasing model resolution. Resolution again affects the magnitude of the maximum deviation as is readily apparent from the two plots. For the 30% depth increase the maximum deviation for the resolution = 8 case is less than 2%.

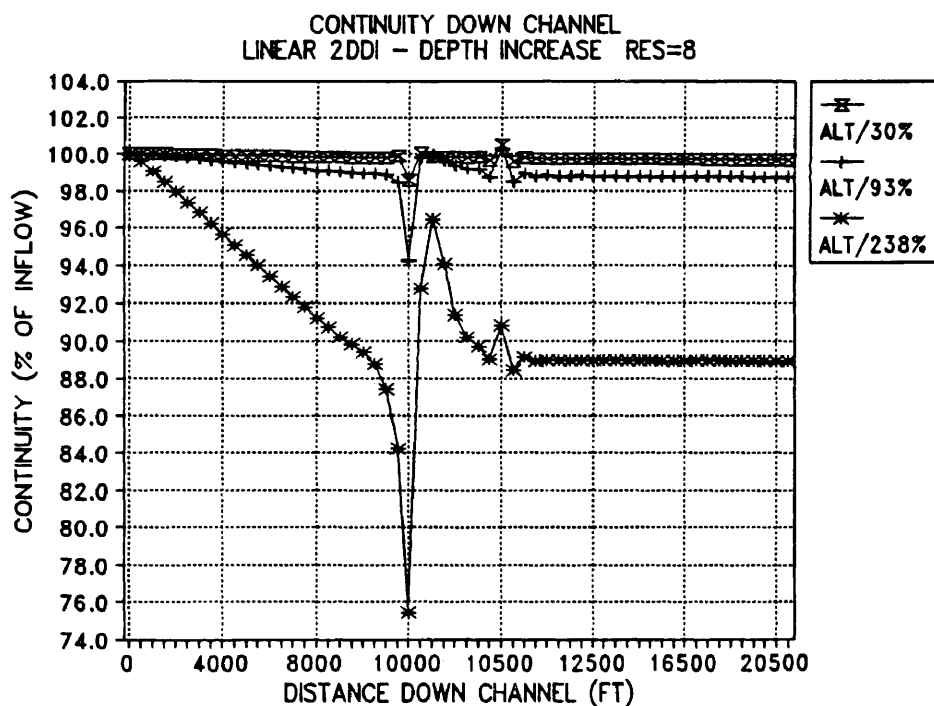
When the maximum deviation was plotted for the 30% depth increase tests the data shown in Fig. 151(a) was obtained. The RMA-2V data is also plotted here for reference. Again it can be noted that the continuity deviation vs percent depth increase per element is nearly linear for the 2DDI model but that the RMA-2V values are better at all values except the EV = 5 single resolution test.

The maximum deviation data for the 238% depth increase case is shown in Fig. 151(b). The magnitude of the oscillations for this test indicate that the 2DDI model is not performing at all well - but is substantially better than the RMA-2V model at low resolutions. At resolutions of 4 and 8 the RMA-2V model significantly out performs the 2DDI model. It should be noted that the RMA-2V model did not converge until EV was raised to 125 for this case. Even with an EV of 500 the 2DDI model outperformed the RMA-2V model for resolutions of 1 and 2.

These results indicate that the RMA-2V model while not perfect gives superior results when compared to the 2DDI



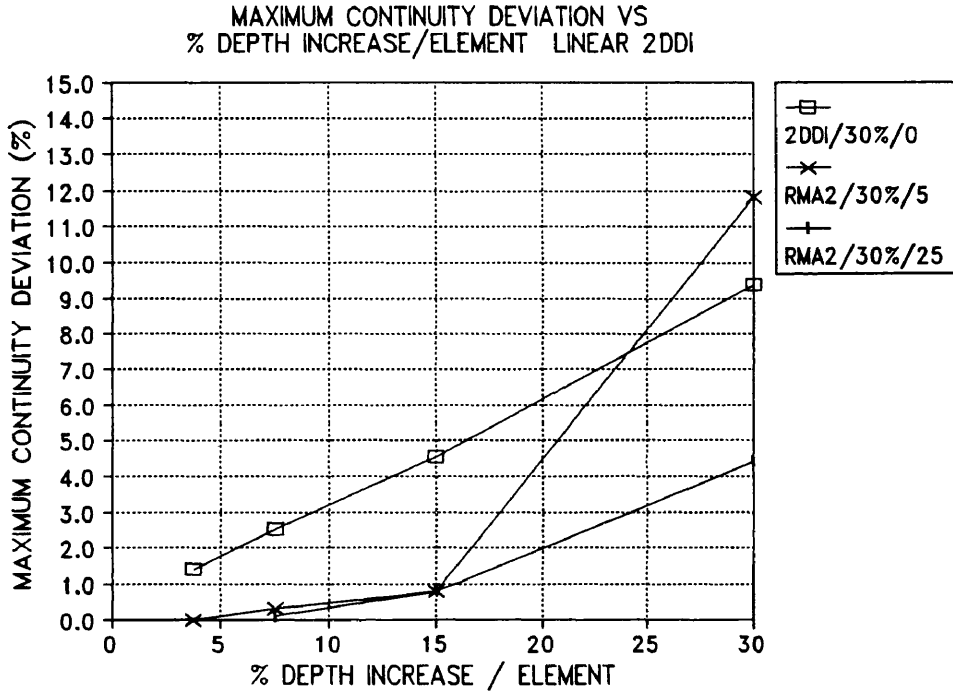
(a) Resolution = 1



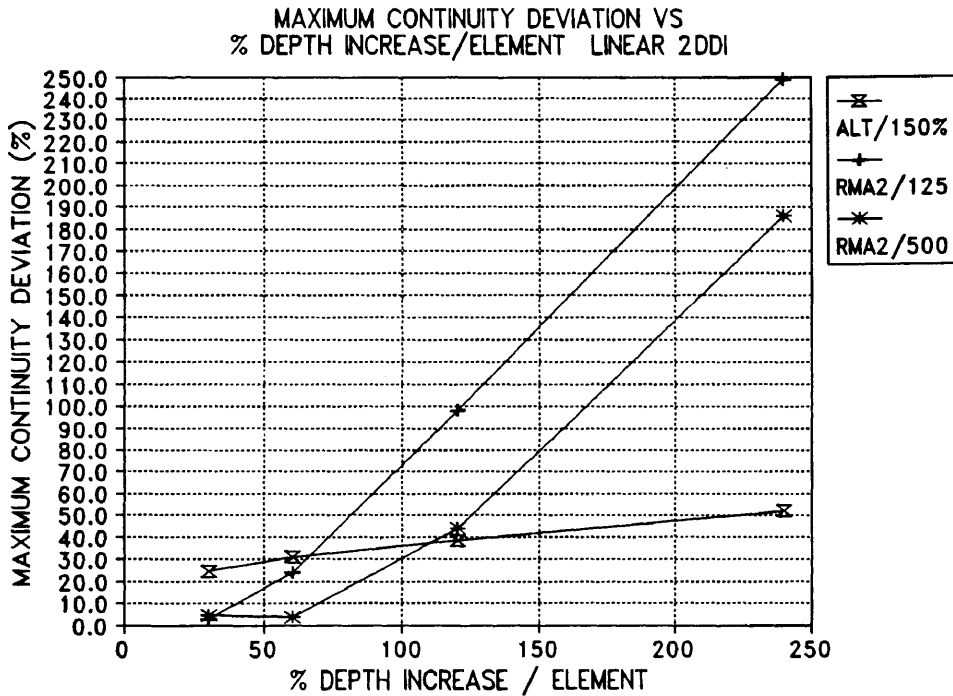
(b) Resolution = 8

Fig. 150. 2DDI Channel Continuity for 30%, 93% and 238% Depth Increase, Alternating Grid, Resolution = 1 and 8, EV = 0.0, 12 Second Time Step. Note Change in Vertical Scale Between Resolutions.





(a) 30% Depth Increase



(b) 238% Depth Increase

Fig. 151. 2DDI Maximum Deviation Data for 30%, and 238% Depth Increase Alternating Grid with EV = 0.0, and 12 Second Time Step Compared with RMA-2V Data.

model for this test case. The 238% depth increase is obviously too severe a test for both models since both exhibited unacceptably high maximum deviations and oscillations.

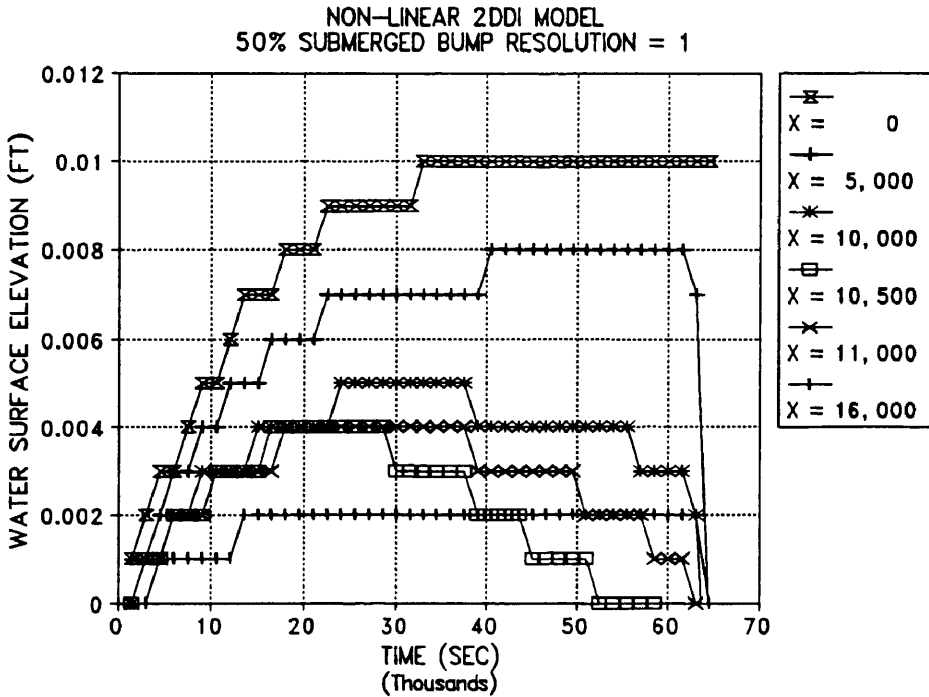
#### SUBMERGED BUMPS WITH 2DDI

The RMA-2V test grids for a submerged bump were converted to be acceptable to the 2DDI model and the identical values in the boundary condition file were used for this test as were used for the submerged bump test in RMA-2V and in the preceding two tests with the 2DDI model. The bump height was again set at 50 feet which produced approximately a 50% (47%) reduction in depth followed by a 93% depth increase.

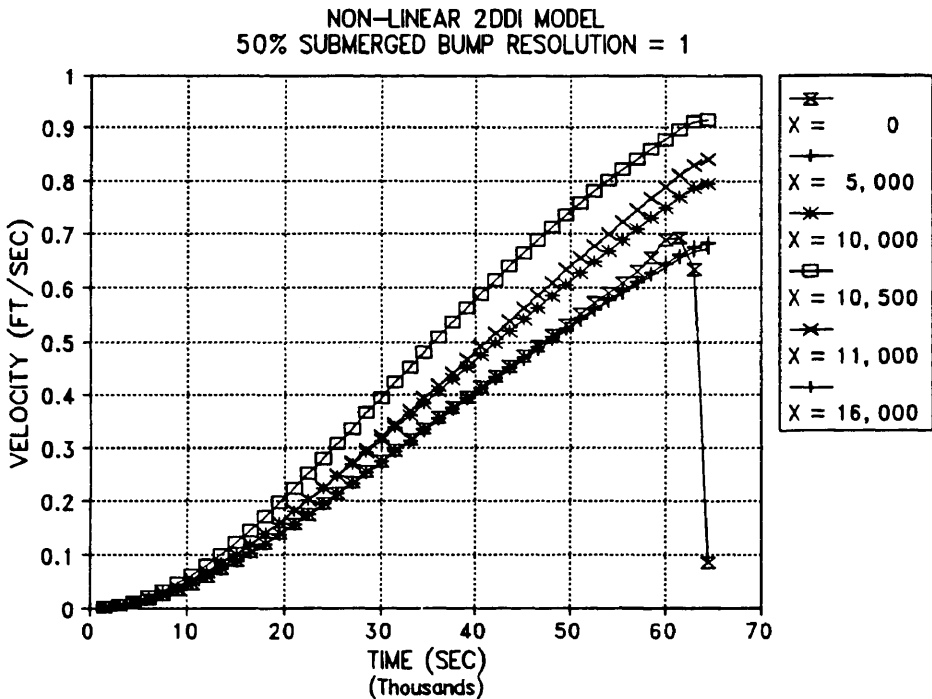
The FULLY NON-LINEAR model was again run to view its ability to converge for this type of problem. The model would not converge and the water surface elevation and velocity at the standard six center-line nodes in the channel are plotted in Fig. 152. It can be seen that the water surface elevations never stabilize and prior to the completion of the ramping up process the interior water surface elevations are beginning to lower. The velocity plots are again almost identical to the previous fully non-linear test results.

Continuity in the channel for this test is shown in Fig. 153. It can again be noted that as time passes the channel continuity increases as the model begins to blow up. The continuity oscillations on the submerged bump also tend to increase as time passes. The location of time steps in Fig. 153 can be referenced from Fig. 152.

The LINEAR model was then run using the same model input parameters with the exception of the ramp length which was shortened to 0.1 days from the 0.4 days used in the non-linear model. The water surface elevations and velocities



(a) Water Surface Elevation



(b) Velocity

Fig. 152. Non-linear 2DDI Model Water Surface Elevation and Velocity for Submerged Bump Alternating Grid with 0.01 Ft Head, 0.4 Day Ramp, and EV = 0.0.

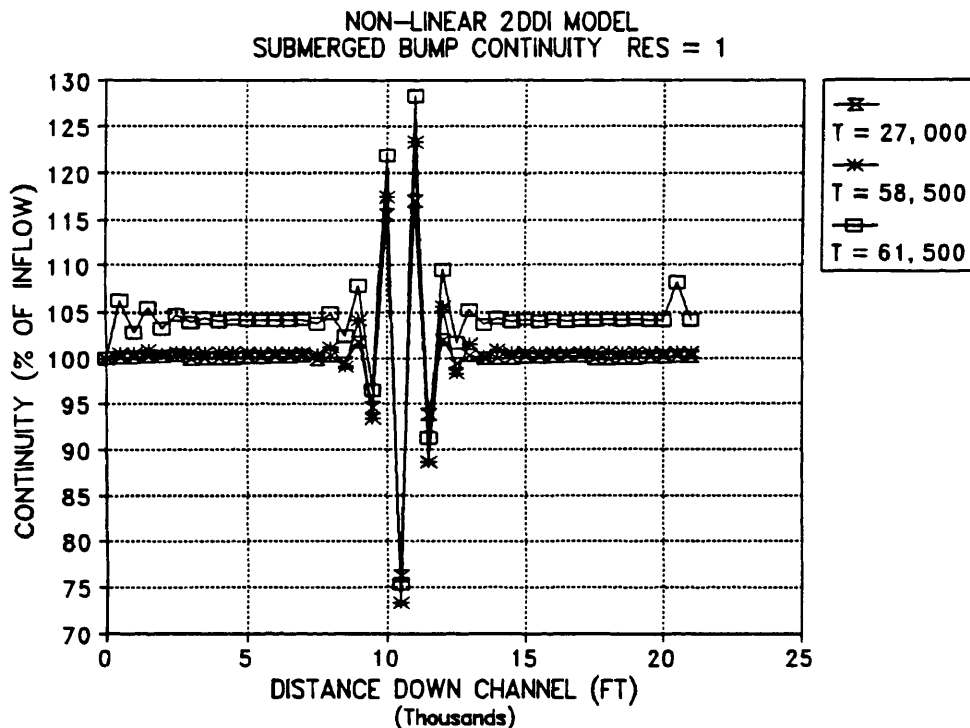
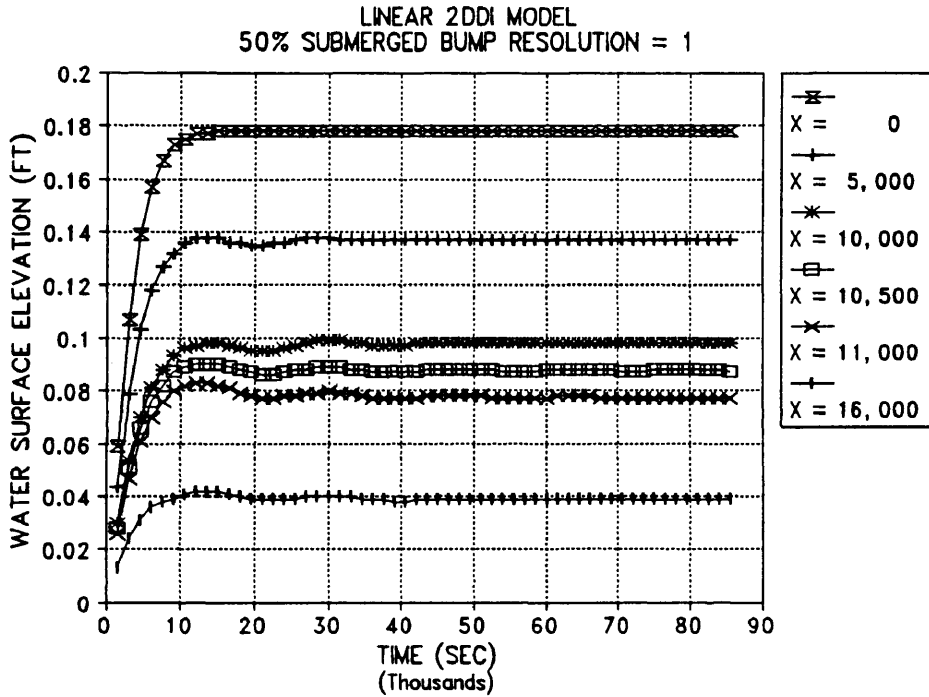


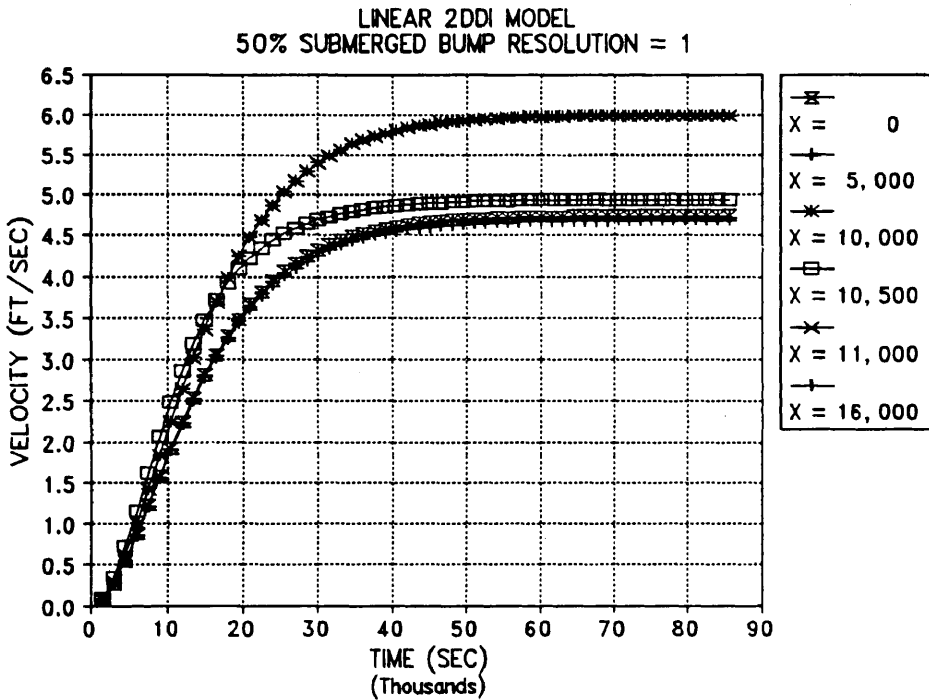
Fig. 153. Non-linear 2DDI Model Continuity Results for Submerged Bump, Alternating Grid with  $EV = 0.0$ , Ramp = 0.4 Days, Head at 0.01 Ft, and 12 Second Time Step.

for six center line nodes for the single resolution test are shown in Fig. 154. It can be seen that while the water surface showed some instabilities - perhaps due to the short ramp length - that the model reached a very nearly steady state solution by the end of the 1.0 day simulation.

The velocity on the crest of the bump can be seen in Fig. 154(b) and is labeled as X - 10,500. The model appears to be unable to accurately model this velocity since the value is approaching those upstream and downstream of the bump. The value should be higher than those on each end of the bump (X = 10,000 and X = 11,000) which both plot higher than the value on the bump crest. In short the model over predicts the values at the upstream and downstream toe of the bump and drastically under predicts the value at the crest. This accounts for the very high continuity oscillations at the submerged bump for the single resolution



(a) Water Surface



(b) Velocity

Fig. 154. Linear 2DDI Model Water Surface Elevation and Velocity for Selected Nodes for Submerged Bump Alternating Grid with Resolution = 1, Head = 0.178 Ft, EV = 0.0 and 12 Second Time Step.

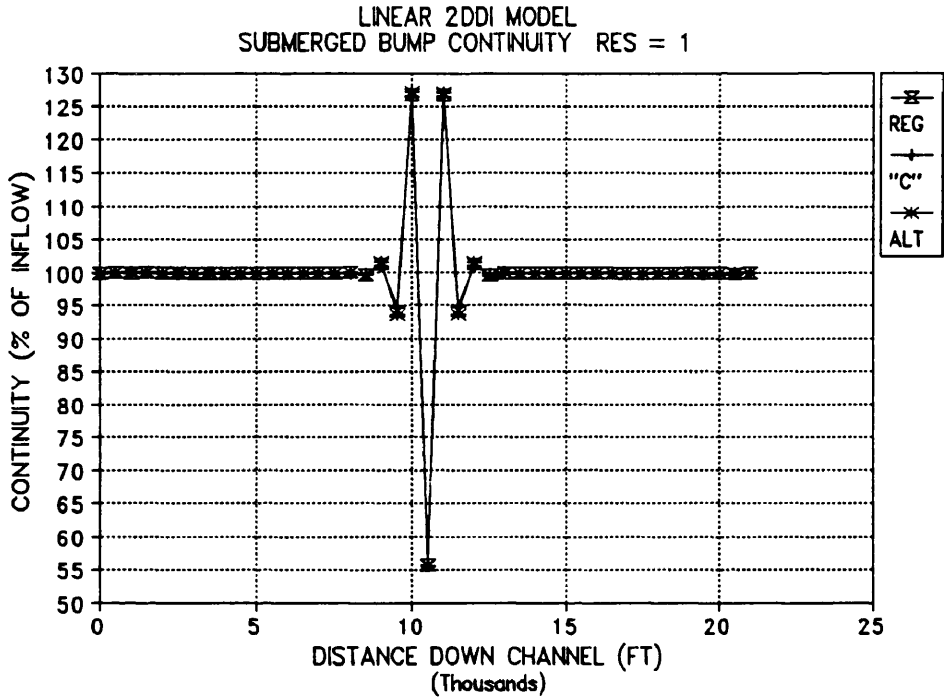
test as shown in Fig. 155(a). It can again be noted that the three grids perform almost identically as far as continuity is concerned. Only very slight differences exist in the area of the submerged bump.

The water surface elevation at several locations down the channel is plotted in Fig. 155(b) for the 2DDI model as well as the HEC-2 model and the RMA-2V model. The RMA-2V data has not been manipulated or averaged in any way before plotting. It can be seen that the 2DDI model again does not predict the velocity head due to the absence of the non-linear terms. The RMA-2V model also under predicts the reduction in water surface elevation at the crest of the submerged bump which would account for the loss of continuity on the bump by the RMA-2V model.

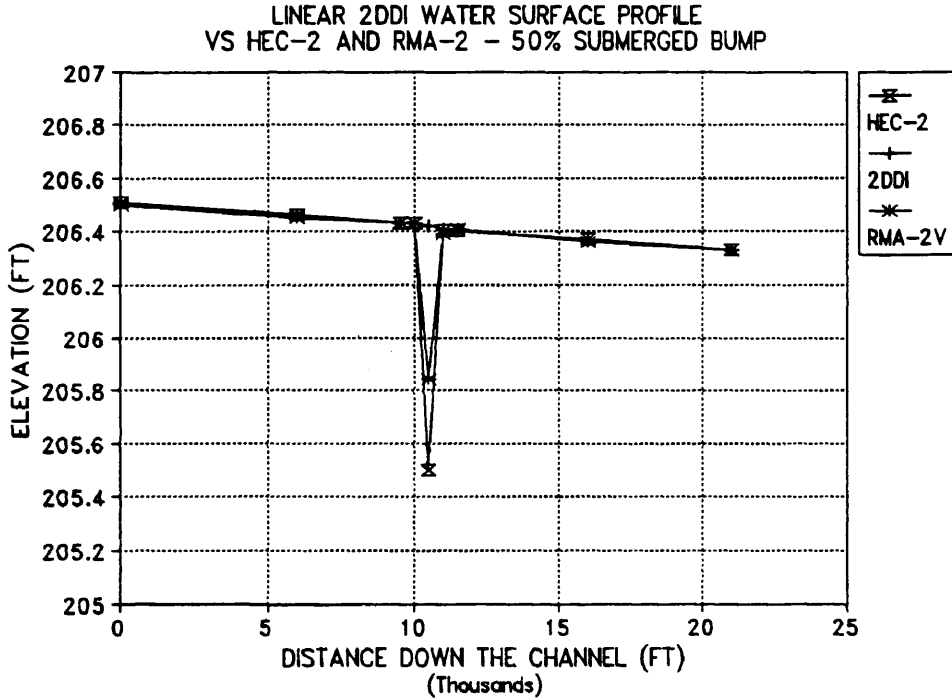
The three dimensional water surface elevation and velocity surface plots for the 2DDI model are shown in Figs. 156 and 157 respectively. The water surface elevations are very smooth for all three test grids as has been the case previously. The velocity surface plots continue to show a high amount of grid sensitivity in areas where velocities are rapidly changing producing patterns similar to those noted in the previous test cases.

When the resolution on both faces of the step was increased to 2, the continuity results shown in Fig. 158(a) were obtained. It can be noted that the increase in resolution reduced the continuity oscillations substantially - from a maximum of about 45% to less than 30%. Again there are only slight differences in the continuity behavior of the three grids.

When the resolution was increase to 4 elements per bump face the maximum continuity deviation was further reduced to about 16% as shown in Fig. 158(b). The x scale is again expanded for this plot to allow a better view of the behavior of the model on the submerged bump.

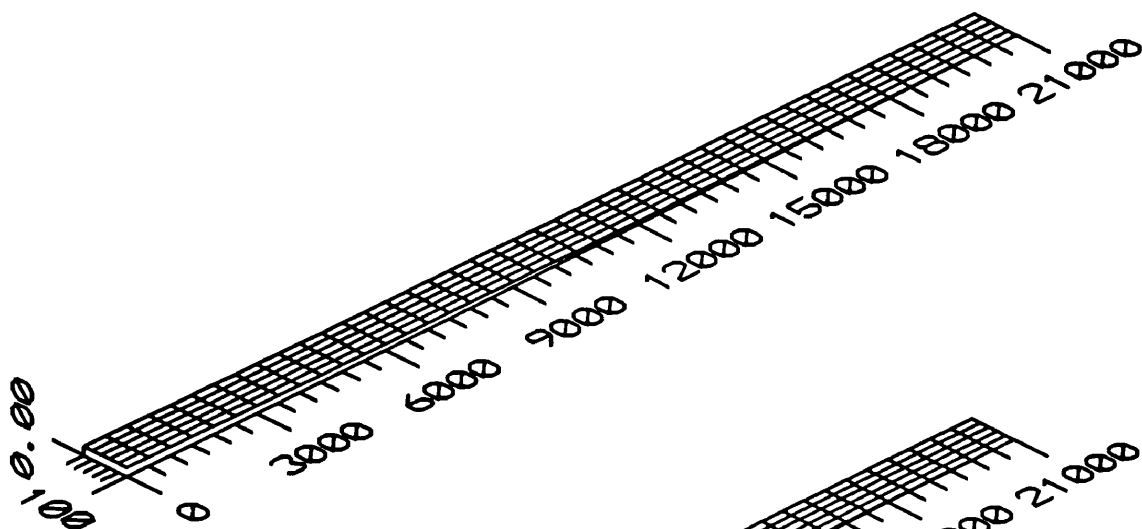


(a) 2DDI Continuity for Resolution = 1

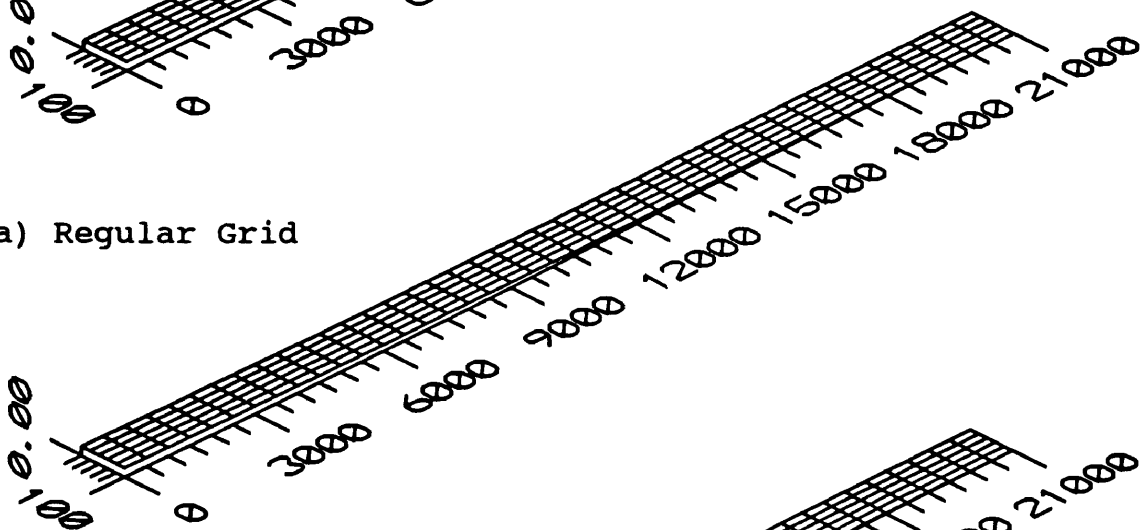


(b) 2DDI Water Surface Elevation Compared with HEC-2 Profile

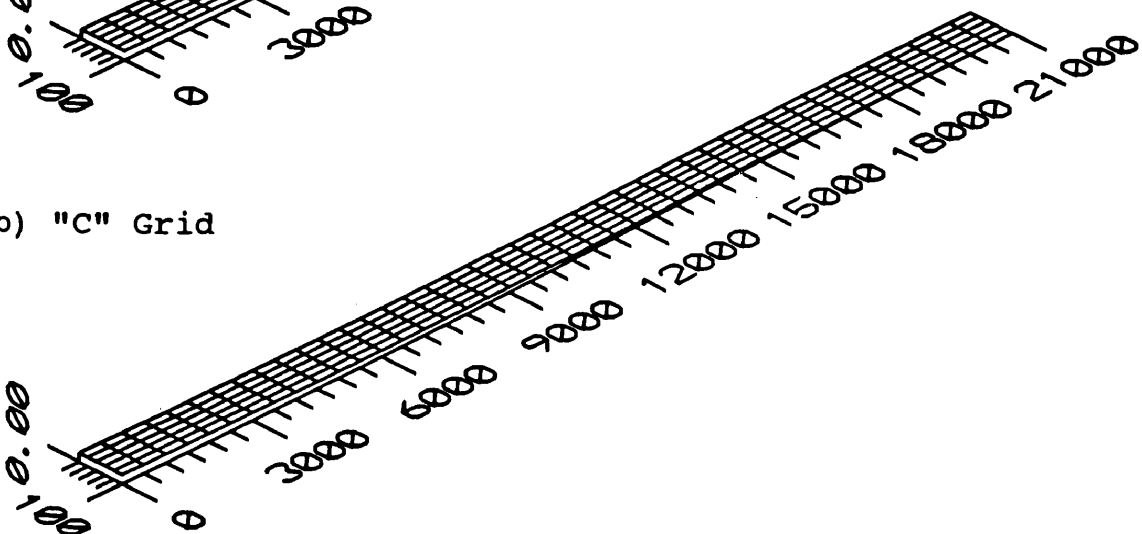
Fig. 155. Linear 2DDI Continuity vs Channel Distance with EV = 0.0, Ramp = 0.1 Day, Head = 0.178 Ft, 12 Second Time Step, and Water Surface Elevation Compared with HEC-2 and RMA-2V.



(a) Regular Grid



(b) "C" Grid



(c) Alternating Grid

Fig. 156. Linear 2DDI Three Dimensional Water Surface Elevation Plots for Submerged Bump Test Grids with  $EV = 0.0$ , Head = 0.178 Ft, Resolution = 1, and Time Step = 12 Seconds.



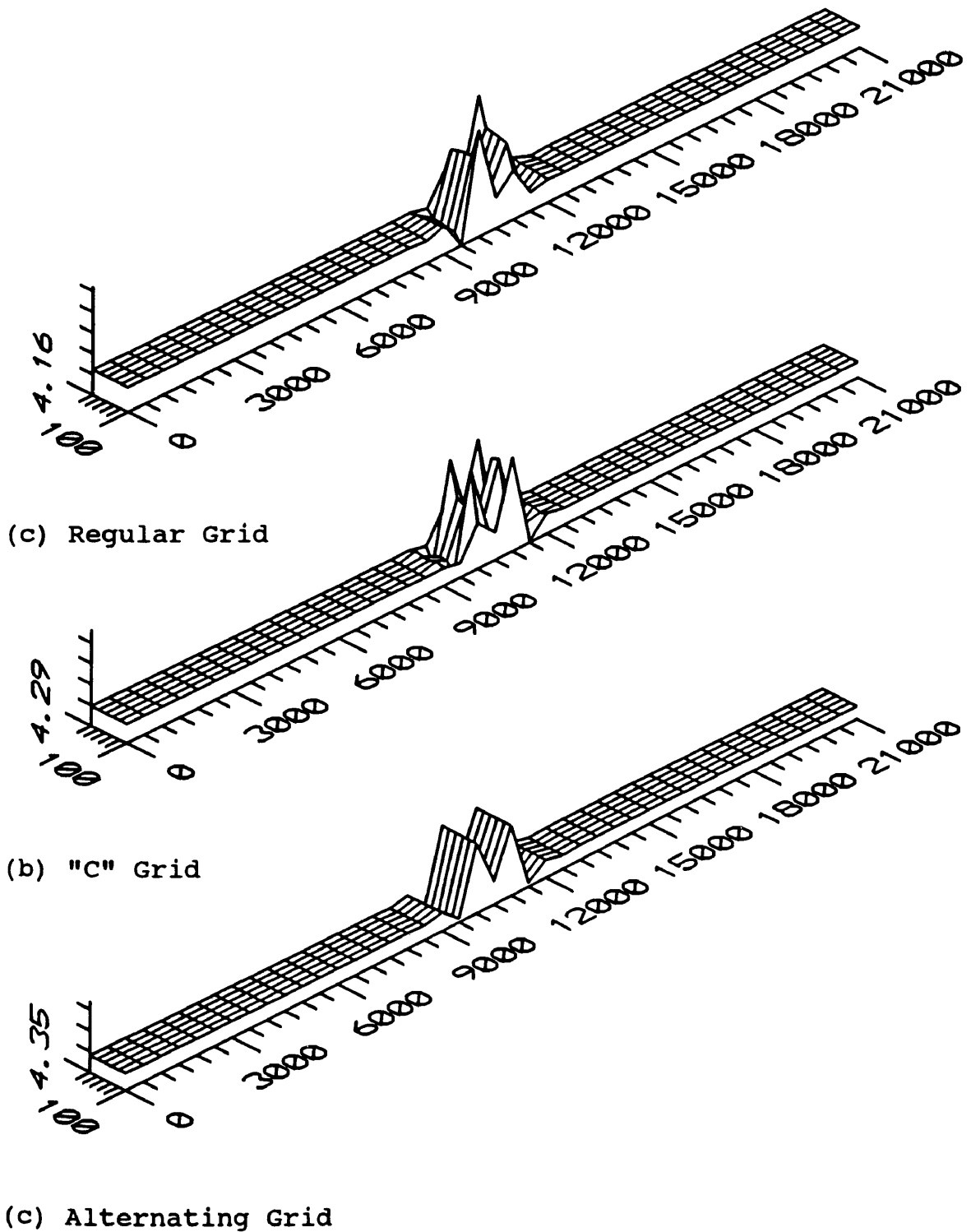
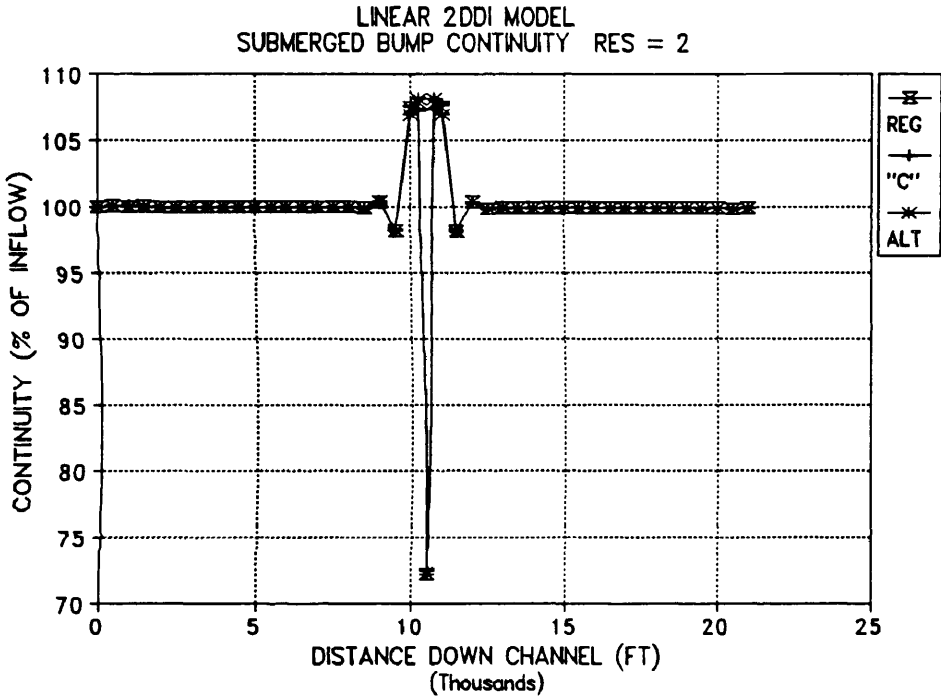
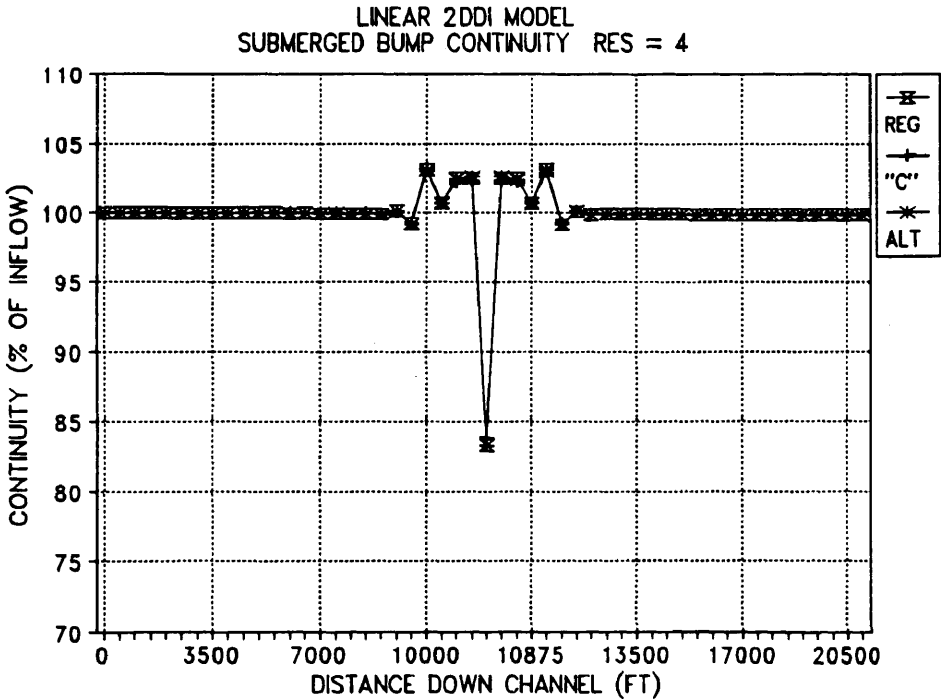


Fig. 157. Linear 2DDI Three Dimensional Velocity Surface Plots for Submerged Bump Test Grids with  $EV = 0.0$ , Head =  $0.178$ , Resolution =  $1$ , and Time Step =  $12$  Seconds.



(a) Resolution = 2



(b) Resolution = 4

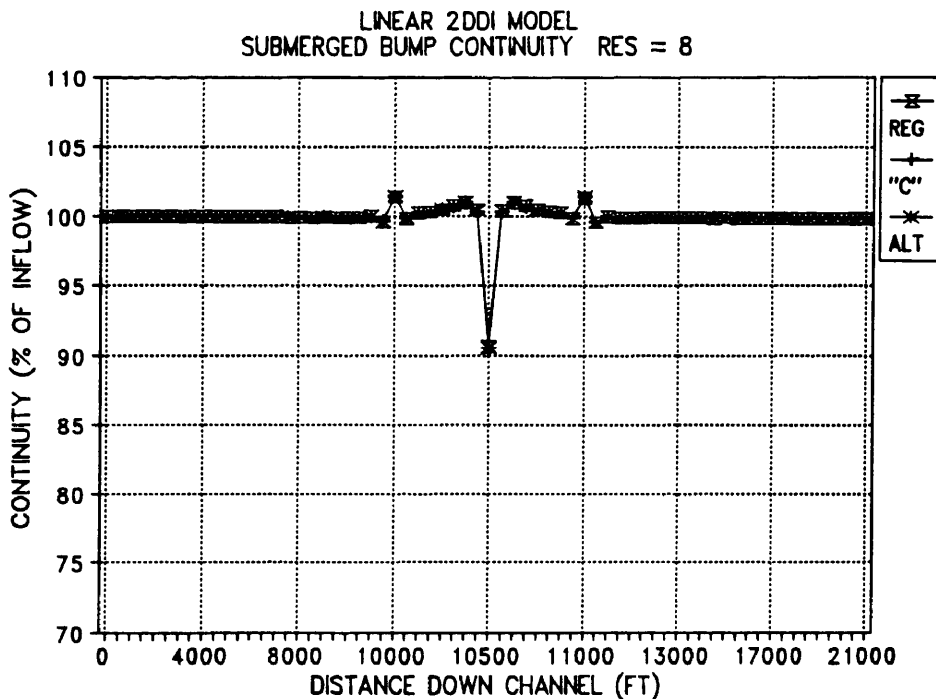
Fig. 158. Linear 2DDI Continuity vs Distance Down Channel for Submerged Bump Test Grids, Resolution = 2 and 4, EV = 0.0, Head = 0.178 Ft, and a 12 Second Time Step.

The resolution was then increased to 8 as shown in Fig. 159(a). This resulted in the further reduction of the maximum continuity deviation to just less than 10%. With the exception of the oscillation at the crest of the bump the other oscillations are less than 2% and would be within an acceptable range. In all tests for the submerged bump the maximum continuity deviation is at the crest of the bump.

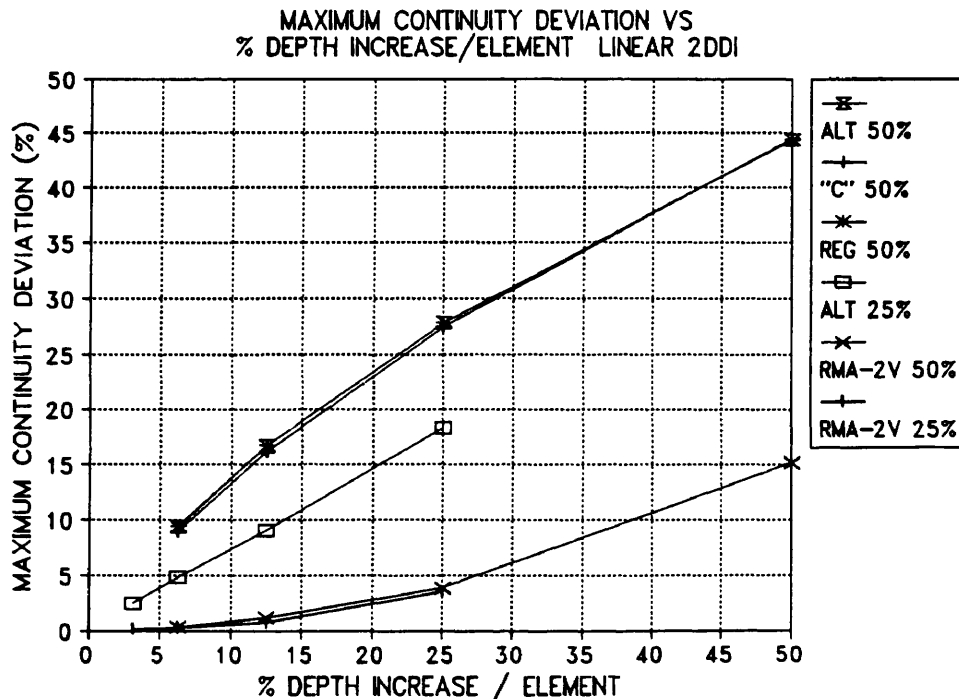
The maximum continuity deviation plotted against the percent reduction in depth per element is plotted in Fig. 159(b). When comparing the 50% values it can be seen that the RMA-2V model substantially out performs the 2DDI model even with an EV of 5 for the RMA-2V model.

When the bump height was reduced to 25 feet (25%) the maximum deviations shown in Fig. 159(b) labeled as 25% results were obtained. With a bump height of 75 feet (75%) the results plotted in Fig. 160(a) were obtained. The RMA-2V model produces significantly reduced maximum deviations as can be seen in Figs. 159(b) and 160(a) and outperforms the linear 2DDI model.

In the 75% test an interesting phenomenon occurred involving the flow rate in the channel. As the resolution was increased flow rate in the channel was reduced. After the runs were completed it was noticed that the channel flow had varied substantially for the 75% bump test with a resolution of 8 elements. The flow results are plotted in Fig. 160(b) and show that for the 75% bump test the flow rate in the channel varied 10% from the flow for the single resolution test. The 25% test showed no flow variation while the 50% test exhibited about a 1% change in flow as resolution increased. This change in flow for the 75% test had little effect on the maximum continuity deviation. When the head on the 75% bump test with resolution = 8 was increased to 0.227 from 0.186, the flow rate was increased to 499,193 cfs at the inflow and the maximum continuity

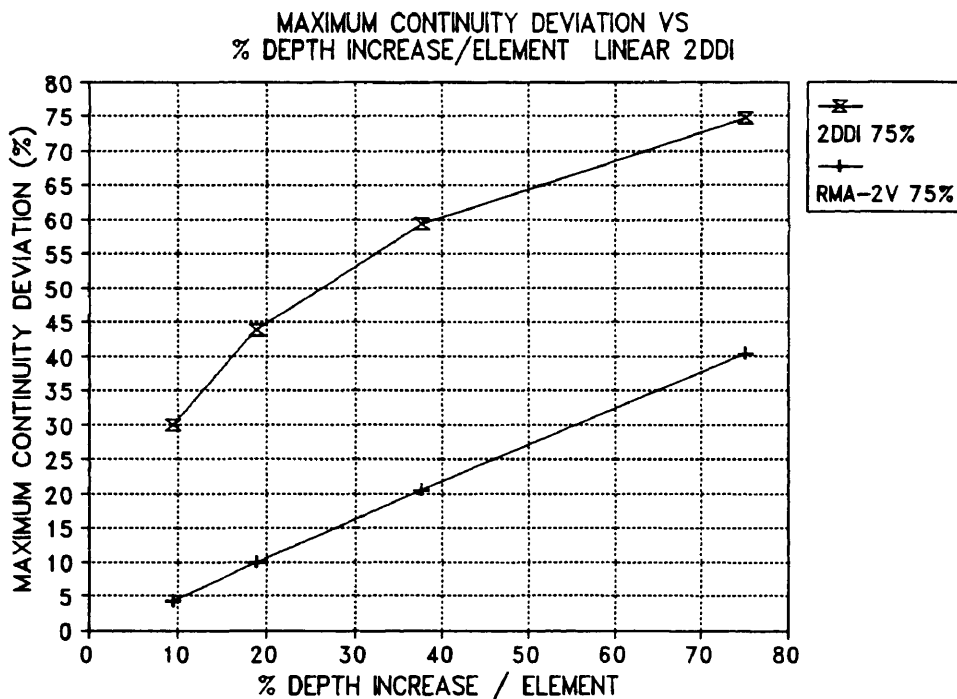


(a) Resolution = 8

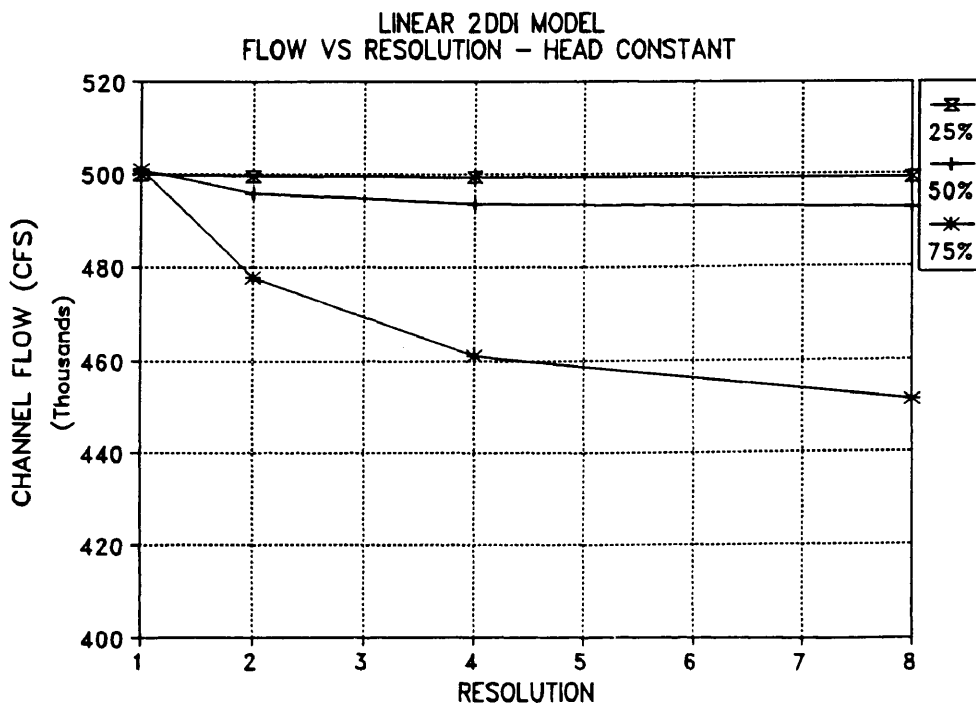


(b) 25% and 50% Bump Height

Fig. 159. 2DDI Continuity for Resolution = 8 and Maximum Continuity Deviation for 25% and 50% Submerged Bump with EV = 0.0 and 12 Second Time Step.



(a) 2DDI Maximum Continuity Deviations with 75% Bump Height



(b) Flow Rate vs Resolution

Fig. 160. 2DDI Maximum Continuity Deviations for 75% Submerged Bump and Channel Flow Rate vs Resolution of Submerged Bump with  $EV = 0.0$  and 12 Second Time Steps.

deviation increased from 29.9% to 30.7%.

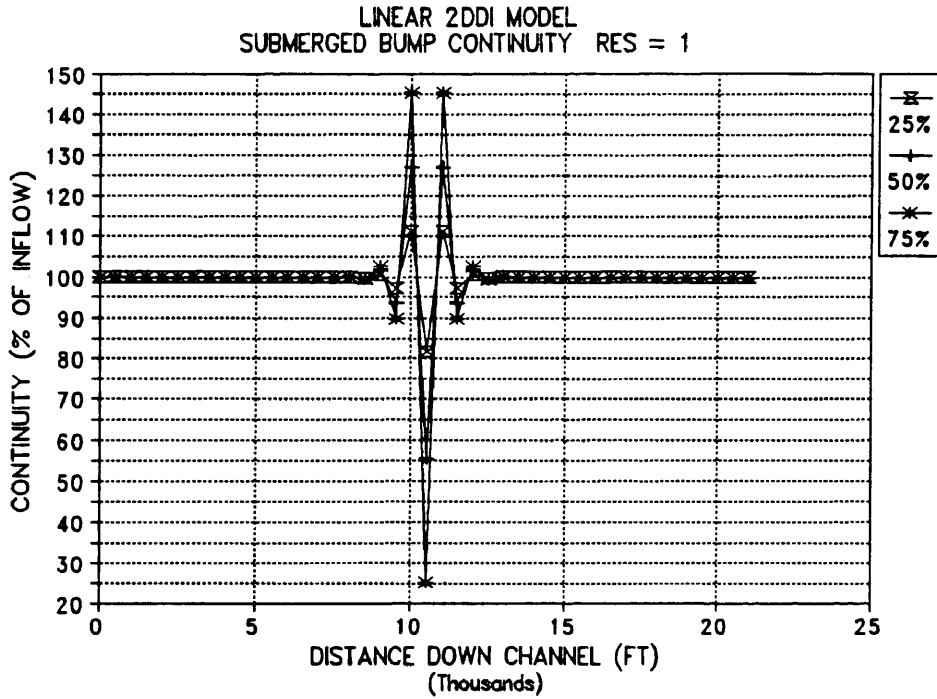
The channel continuity for the 25%, 50% and 75% submerged bump tests are shown in Fig. 161 for resolutions of 1 and 8 elements per bump face. It can be noted that the continuity values for the 75% tests are extremely bad at the crest of the dike and immediately upstream and downstream of the crest. None of the bump heights produce acceptable results for the single resolution case (Fig. 161(a)). For the 8 element resolution case the continuity values are unacceptable for all cases except the 25% bump case. The 25% bump case would be an adequate solution if the water surface draw down could be modeled - i.e. if the non-linear model was stable and could give answers at least as good as the linear model.

#### SUDDEN WIDTH REDUCTIONS WITH 2DDI

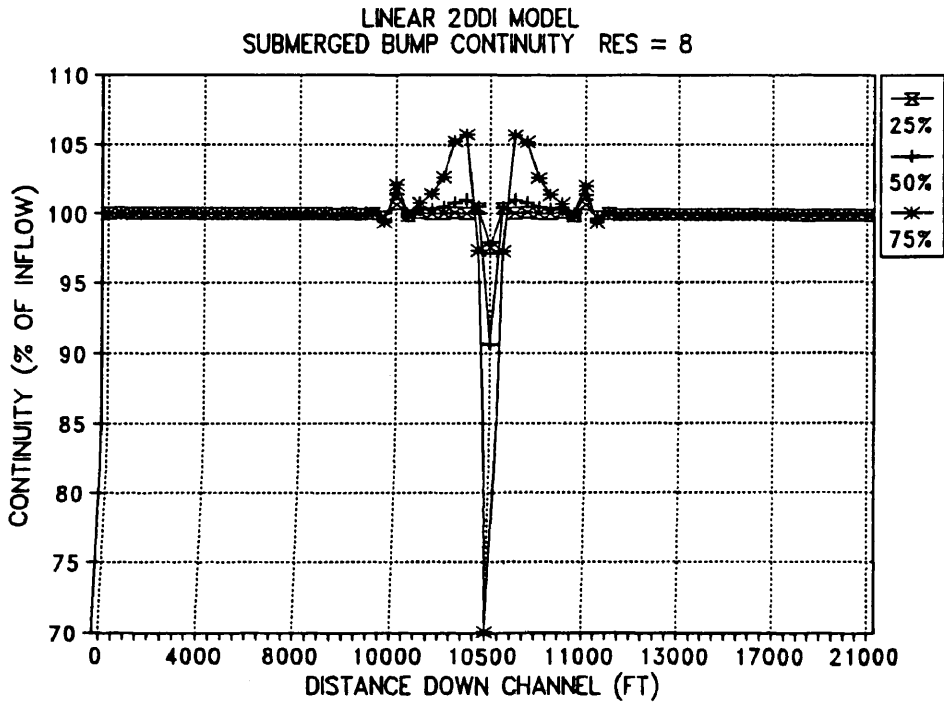
The sudden width reduction grids were translated from the RMA-2V format and prepared for the 2DDI model. Boundary conditions were identical to those used in the previous simple test cases. The only change to the boundary condition file was the deletion of boundary conditions for nodes that were eliminated when the channel width was reduced. The standard width reduction was 40% - identical to the value used for the RMA-2V tests.

At this point the "C" grid was eliminated from further testing due to its inferior performance when compared to the regular and alternating grids. This did not present a problem in model comparison since the grid had also been dropped from the RMA-2V testing at the beginning of the bump tests.

The FULLY NON-LINEAR model was again run with the standard resolution at the sudden reduction in depth (See Fig. 81). This produced the water surface elevation and velocity results shown in Fig. 162. The nodes plotted are

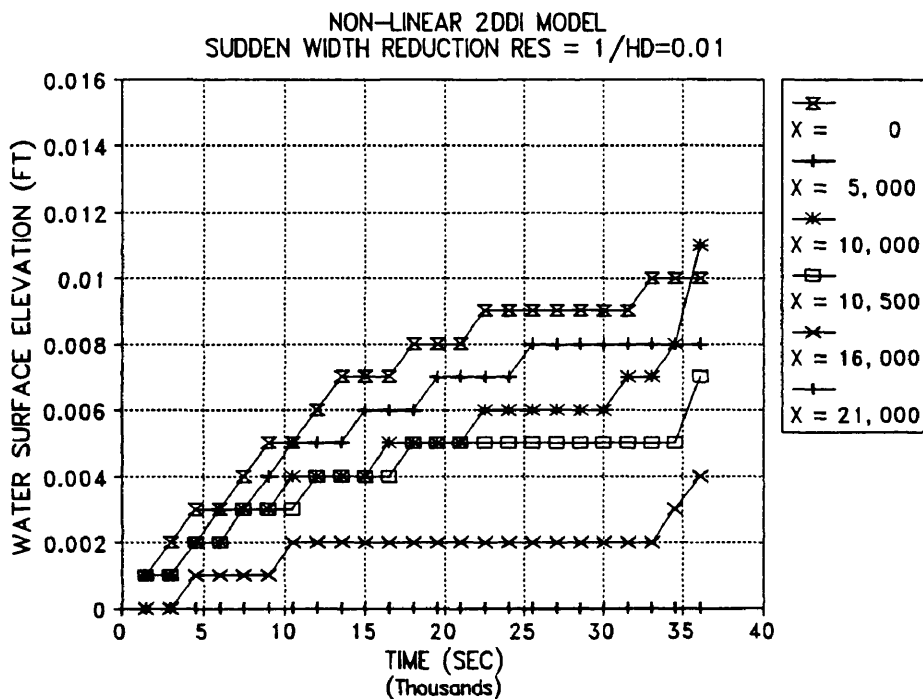


(a) Resolution = 1

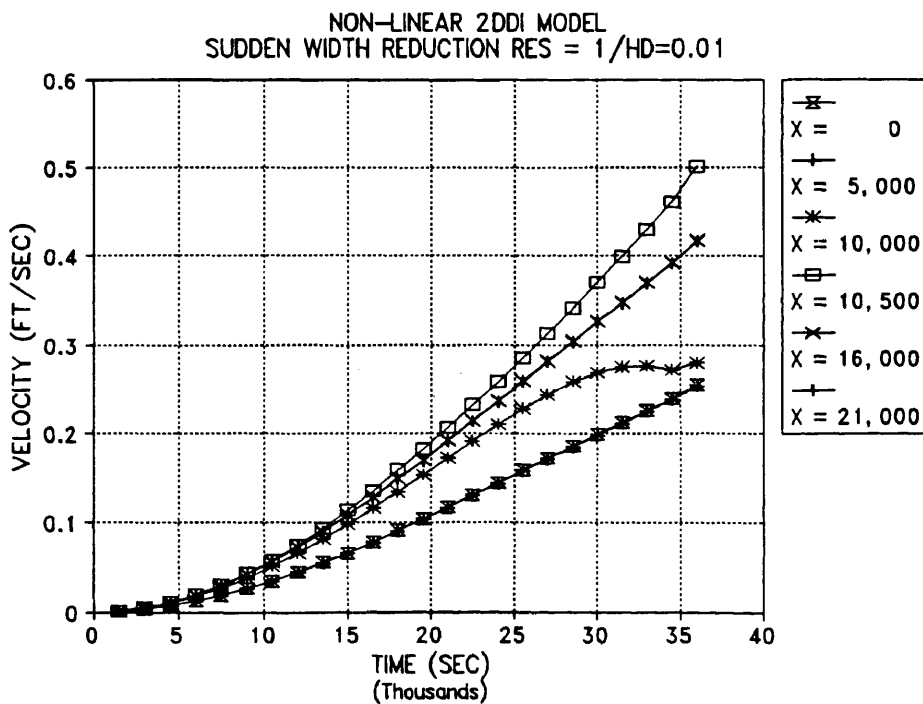


(b) Resolution = 8

Fig. 161. Linear 2DDI Continuity vs Channel Distance for 25%, 50% and 75% Submerged Bump, Alternating Grid, Resolution = 1 and 8, EV = 0.0, 12 Second Time Steps. Note X Scale Variation.



(a) Water Surface Elevation



(b) Velocity

Fig. 162. Non-linear 2DDI Model Water Surface Elevation and Velocity for 40% Width Reduction with Alternating Grid, 0.01 Ft Head, 0.4 Day Ramp, and EV = 0.0.



all on the center line of the channel. For this case the velocity is more unstable at the change in geometry than for previous tests. The water surface elevation again becomes unstable at all interior nodes just prior to terminal instability. The continuity results for this test are shown in Fig. 163. It can be noted that the continuity is extremely constant over time with the exception of the area at the width reduction where the maximum deviation grows rapidly only as the model is becoming unstable.

Since the model appeared much more stable (continuity wise) than in the previous tests, a test was run with resolution = 8 in the x and y grid directions. Since the model was running in the fully non-linear mode the time step was shortened to 1.5 seconds to be within the Courant stability criteria previously discussed (Table 1). All

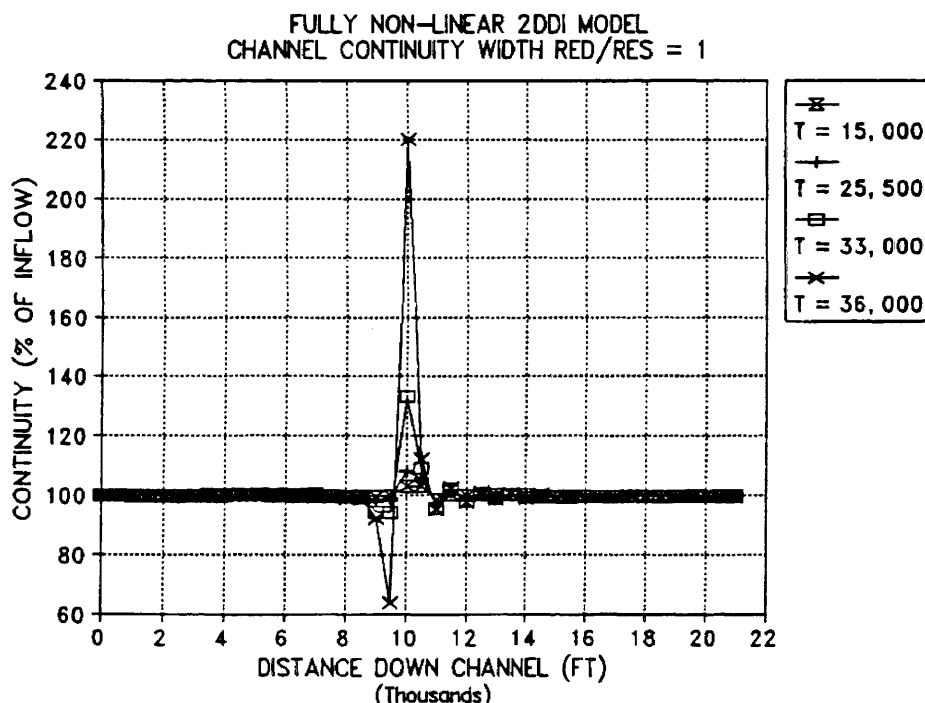


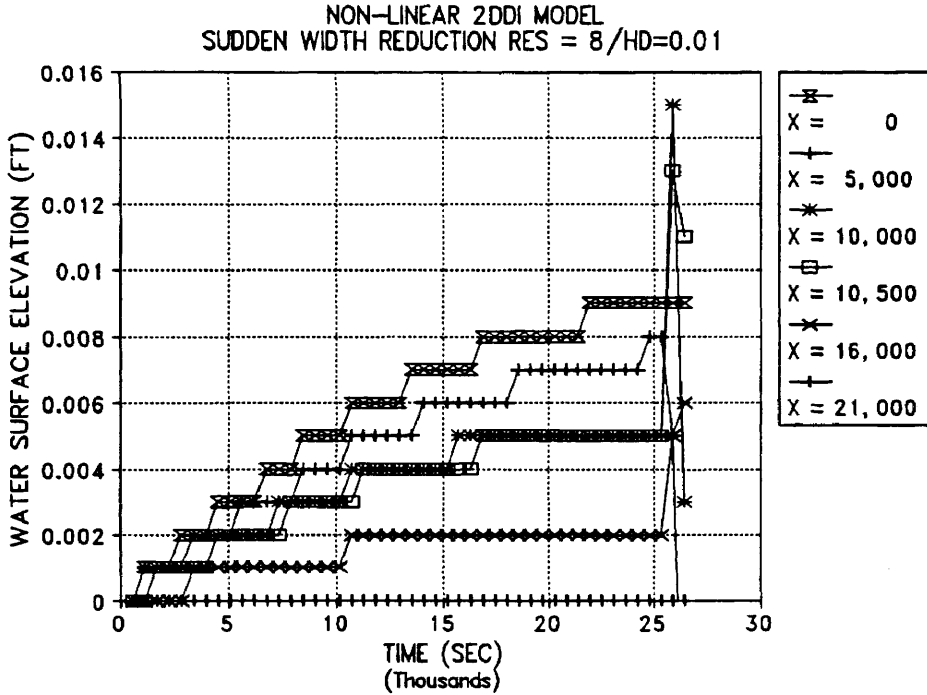
Fig. 163. Non-linear 2DDI Model Continuity vs Channel Distance for Alternating 40% Width Reduction Grid at  $t = 15,000, 25,500, 28,500, 33,000,$  and  $36,000$  Seconds with 0.01 Ft Head, 0.4 Day Ramp and  $EV = 0.0$ .

other values were left at the same values as for the single resolution test. The time history plots of water surface elevation and velocity at the selected channel nodes are plotted in Fig. 164. For this case the velocity does not increase uniformly - i.e. the velocity increase shows what appears to be the effects of waves moving through the model.

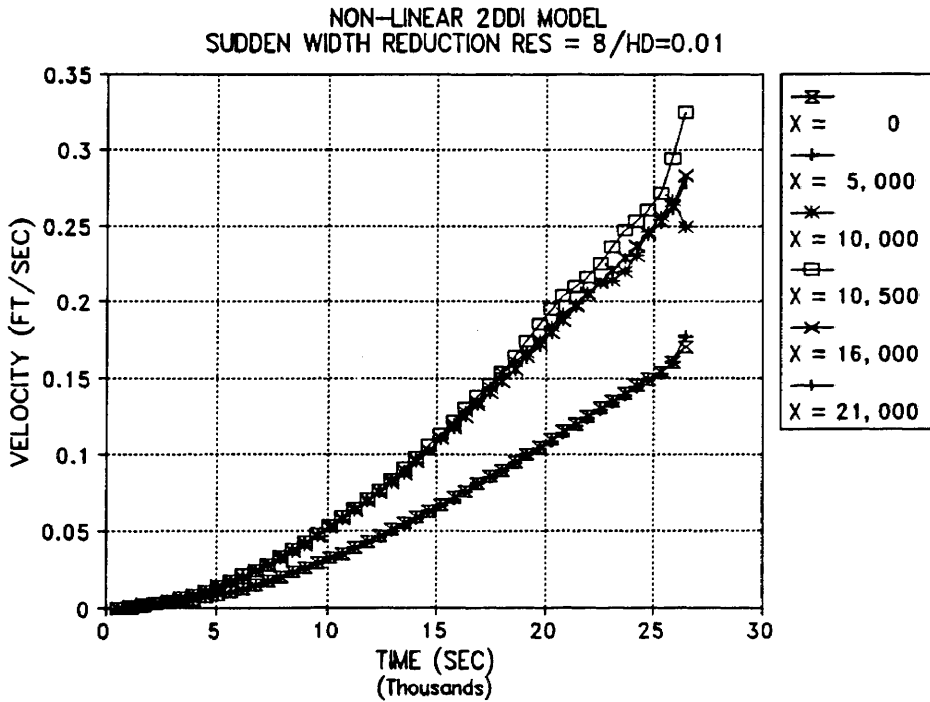
It was thought that perhaps this could be a result of a ramp length that was too short. The length of the ramp was accordingly lengthened to 1.4 days and the simulation lengthened to 4.0 days to give a slow smooth increase in the water surface elevation and flow rate for the 2DDI model. The results of this test showed no significant improvement and aborted at a lower velocity than the above test with the shorter ramp. This differences in model performance were very similar to those shown in the discussion of the fully non-linear model at the beginning of this chapter.

The continuity results for the 8 resolution test with a 1.5 second time step and a 0.4 day ramp are shown in Fig. 165. Fig. 165(a) shows the values at 4 time steps while Fig. 165(b) shows only values at time values of 18,000 seconds and 22,500 seconds - prior to the start of severe instabilities. It can be noted that the continuity values rapidly deteriorate near the end of the simulation but show significant instabilities even at the 18,000 second point in the simulation. From reviewing the program output it appears that the instabilities start in the area just upstream of the width reduction.

The model was then switched to its linear mode and run with resolution equal to 1 at the width reduction. The water surface elevation and velocity results are plotted in Fig. 166. It can be noted that while there are some oscillations in the water surface as time passes they are damped out and a steady state solution is obtained by about 50,000 seconds into the simulation.

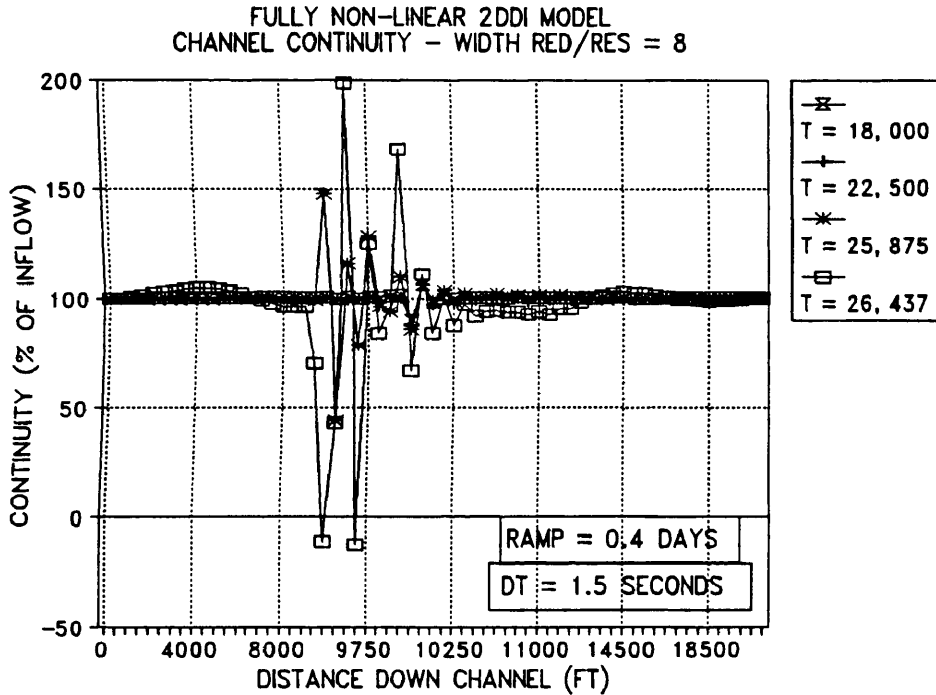


(a) Water Surface Elevation

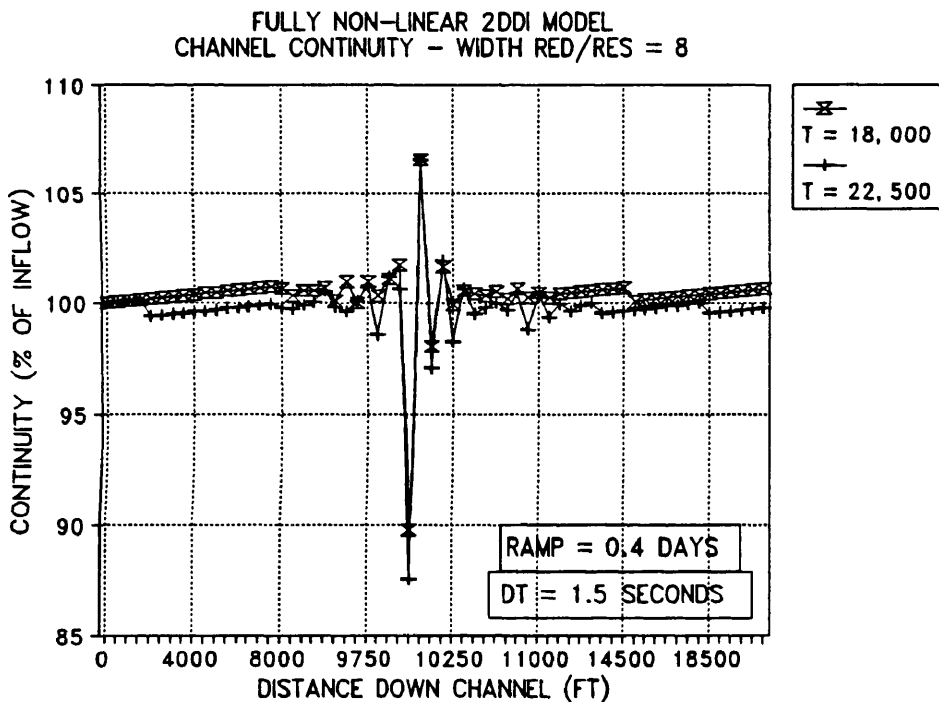


(b) Velocity

Fig. 164. Non-linear 2DDI Model Water Surface Elevation and Velocity for 40% Width Reduction with Alternating Grid, 0.01 Ft Head, 0.4 Day Ramp, EV = 0.0, and 1.5 Second Time Step.

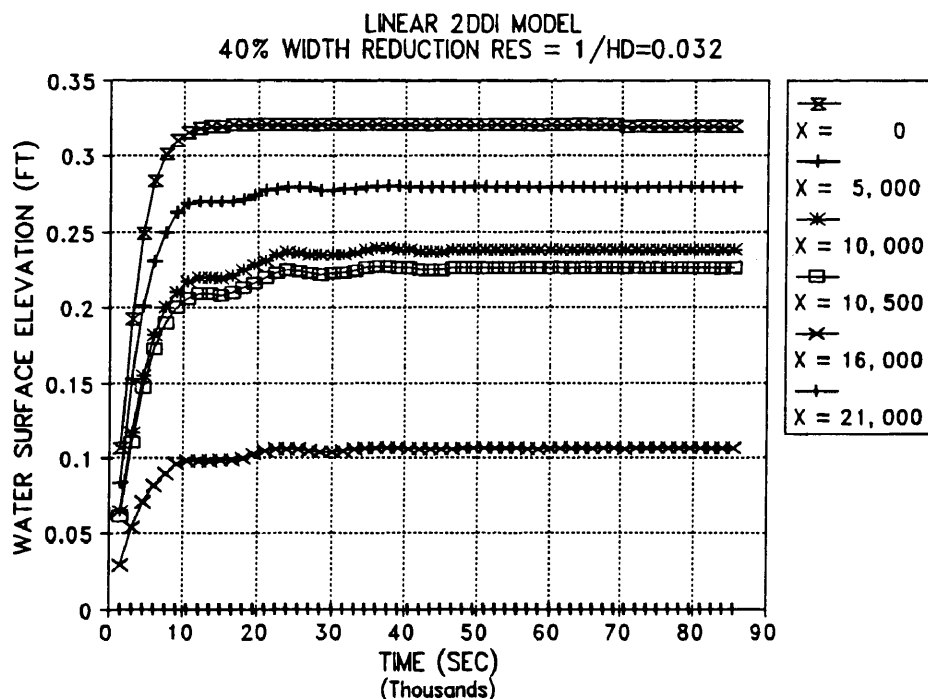


(a) Continuity at 4 Time Steps

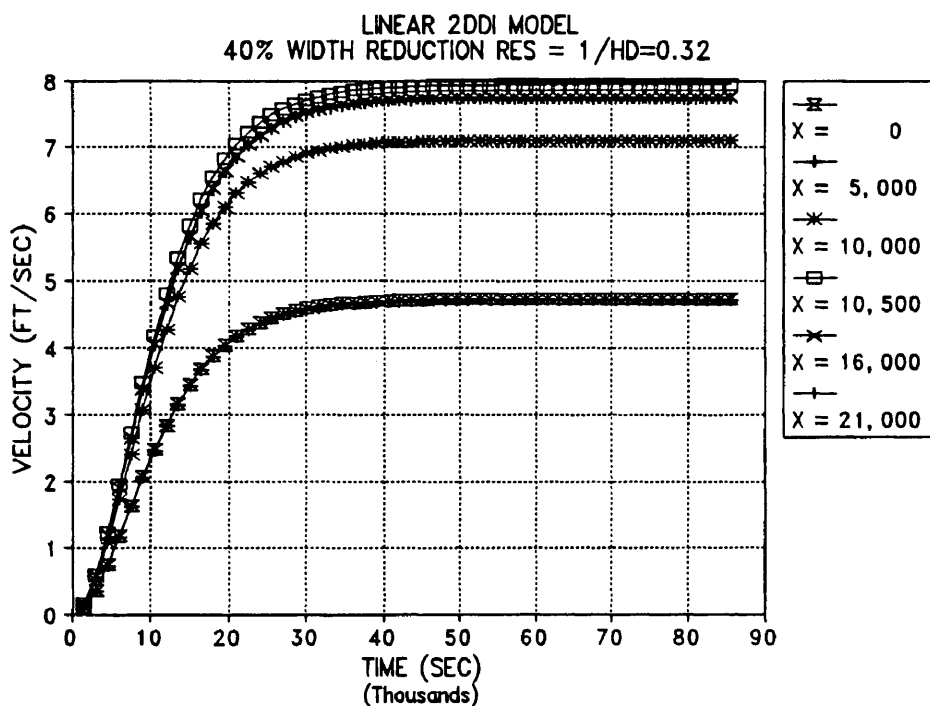


(b) Continuity Values Prior to Severe Instabilities

Fig. 165. Non-linear 2DDI Model Channel Continuity for 40% Width Reduction Alternating Grid at Simulation Times of 18,000, 22,500, 25,875, and 26,437 Seconds. Ramp = 0.4 Days.



(a) Water Surface Elevation



(b) Velocity

Fig. 166. Linear 2DDI Water Surface Elevation and Velocity for 40% Width Reduction Alternating Grid with Resolution = 1, Head = 0.32 Ft, EV = 0.0, and 12 Second Time Step.

The continuity values in the channel for the linear, single resolution test are shown in Fig. 167(a). The continuity is very good with only about a 3% deviation at the location of the width reduction at  $X = 10,000$  feet.

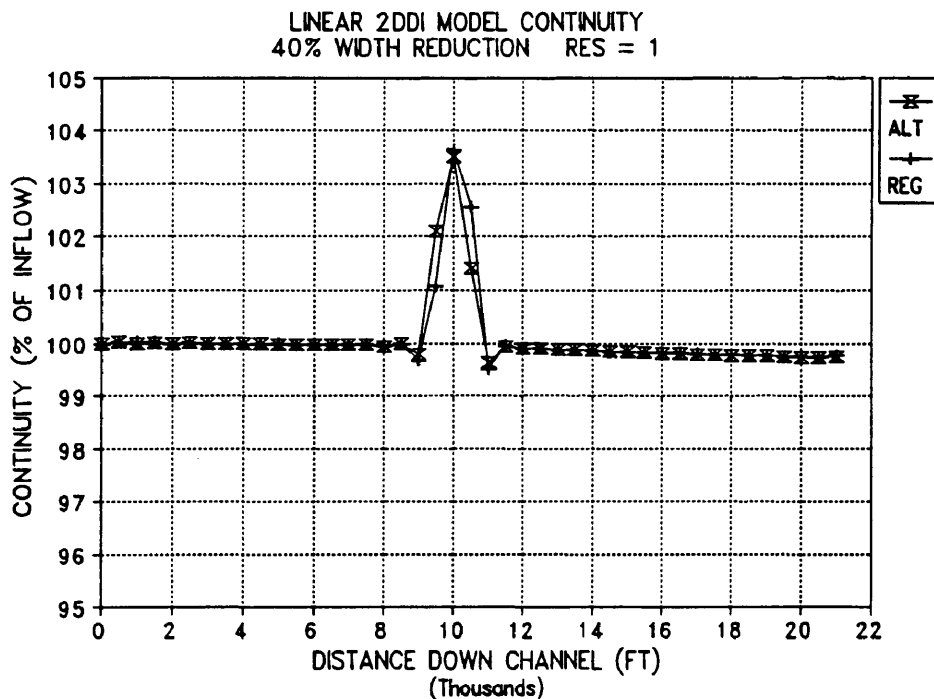
The calculated water surface elevation was compared to the HEC-2 elevations and the RMA-2V computed elevations as shown in Fig. 167(b). When the 2DDI water surface elevation is adjusted for velocity head the values are very close to those obtained from HEC-2. The RMA-2V values can be seen to oscillate badly but when averaged to remove the oscillations (RMA-2V/AVE) match the HEC-2 profile almost exactly.

The three dimensional water surface elevations and velocity surface plots are shown in Figs. 168 and 169 respectively. The water surface elevation plots are again extremely smooth - in fact too smooth since the stagnation head at the width reduction is not included due to the elimination of the non-linear terms. The line of data along the right front of the plot with a head 0.0 is the area outside the boundary of the model in this test.

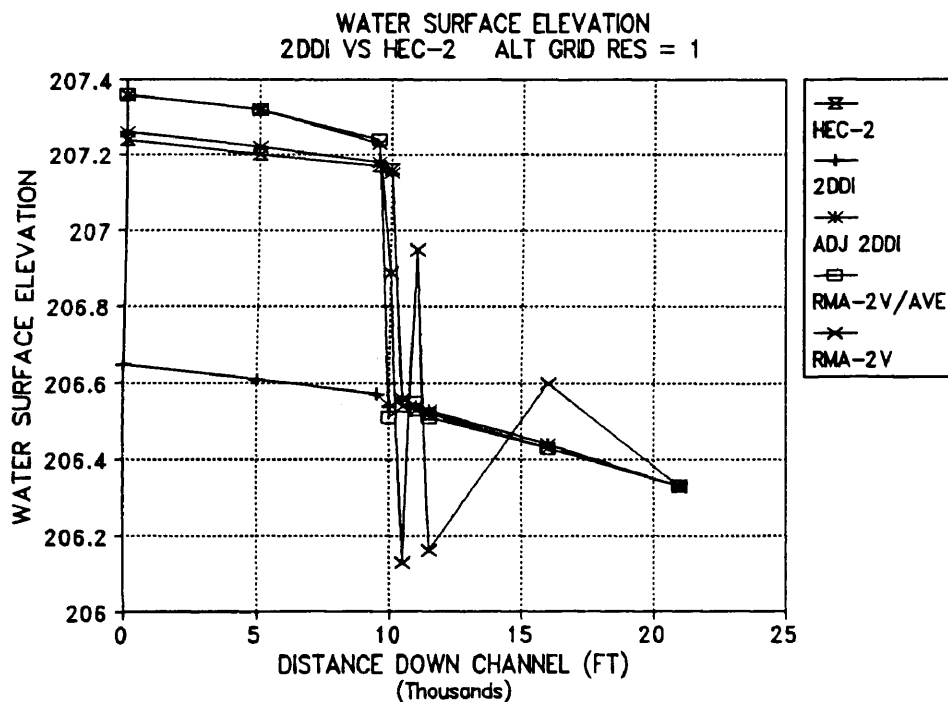
The velocity surface plots are also very smooth and show only minor oscillations through the area of the sudden reduction.

Next the resolution was doubled in the areas just upstream and downstream of the reduction in width. The resolution was first increased in the x direction only, as had been done for the RMA-2V testing. This produced the continuity results shown in Fig. 170(a). The width reduction case was then tested with increased grid resolution in the y direction only and then with increased resolution in both the x and y directions as shown in Fig. 170(b) and (c) respectively. Again the test with increased resolution in both the x and y directions showed the lowest deviations and best model performance.

The maximum continuity deviations are significantly lower than those obtained with the RMA-2V model but some

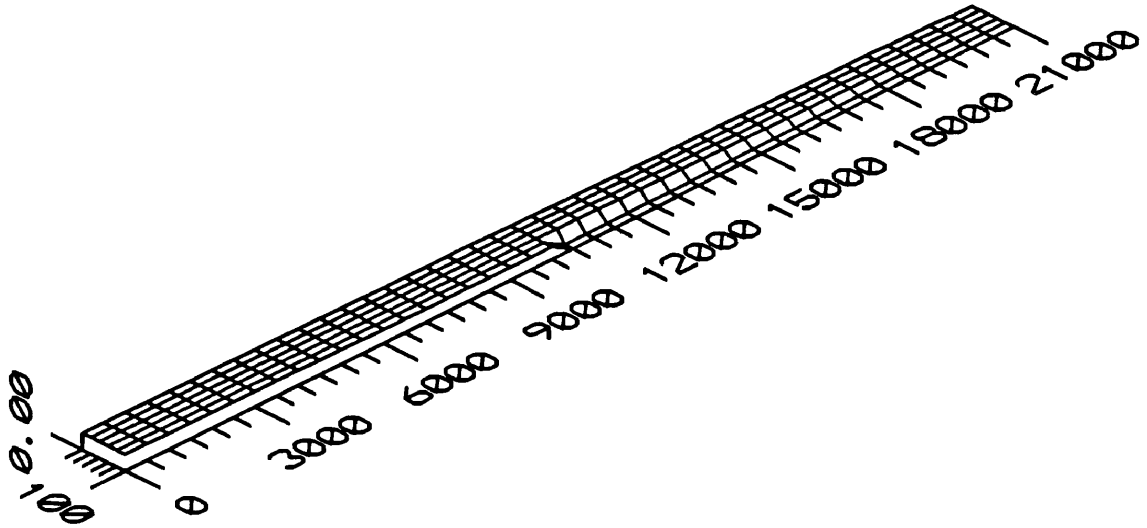


(a) 2DDI Continuity for Resolution = 1

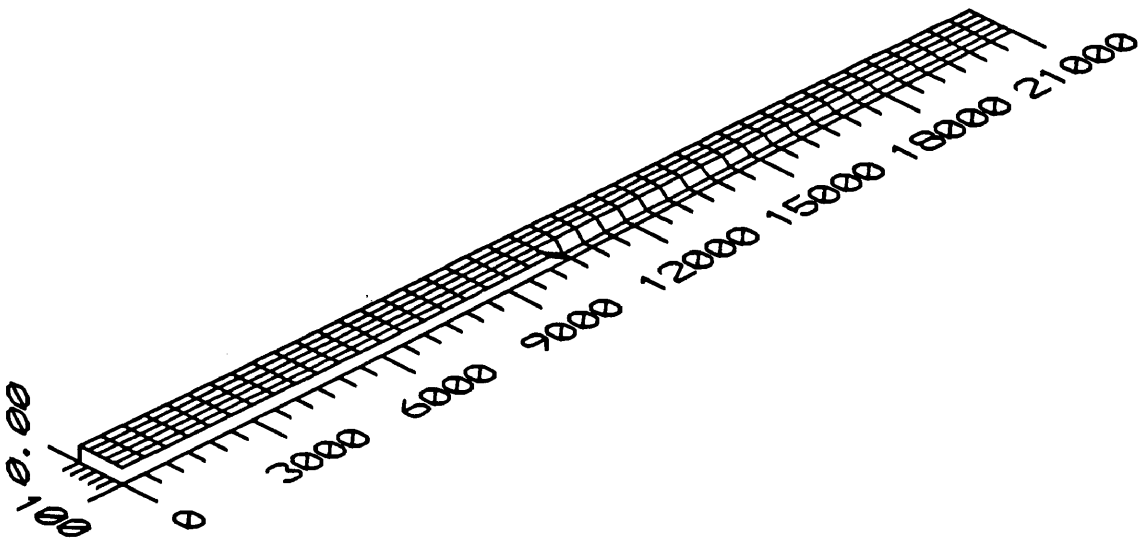


(b) 2DDI Water Surface Elevation Compared with HEC-2 Profile

Fig. 167. Linear 2DDI Continuity vs Channel Distance and Water Surface Elevation Compared to HEC-2 and RMA-2V for EV = 0.0 and 0.32 Ft Head.



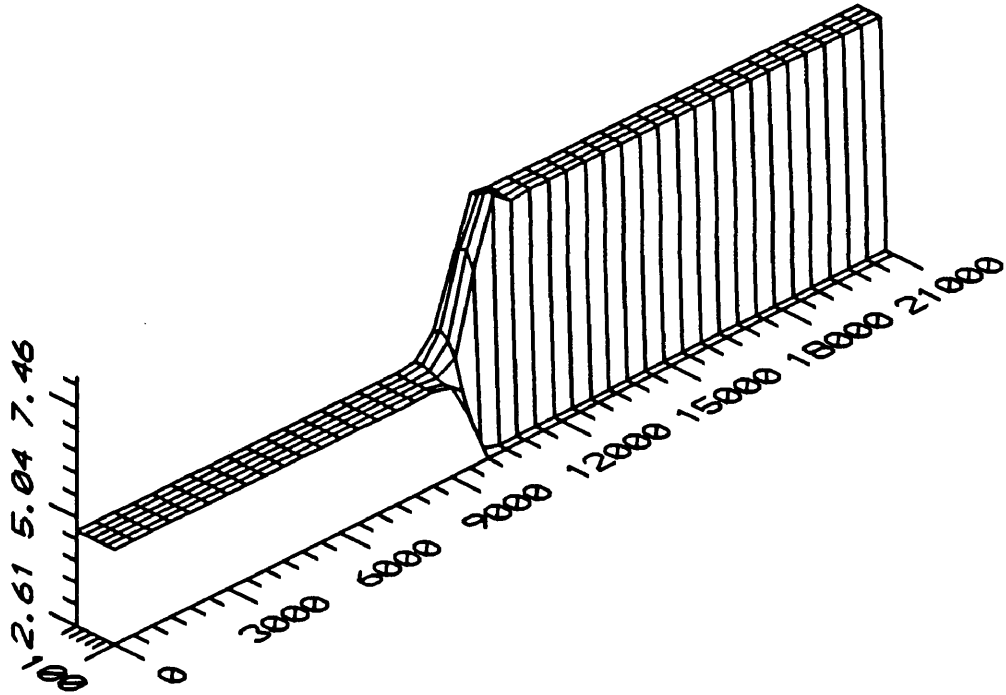
(a) Regular Grid



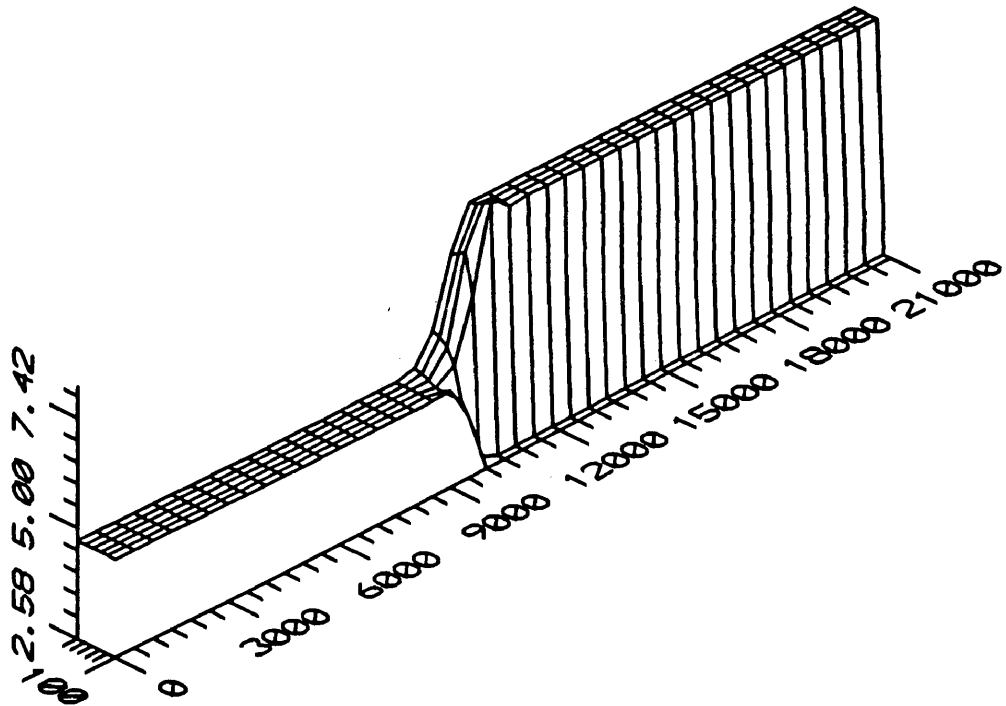
(b) Alternating Grid

Fig. 168. Linear 2DDI Model Three Dimensional Water Surface Elevations for 40% Width Reduction Test Grids with  $EV = 0.0$ , Head = 0.32 Ft, Resolution = 1, and a 12 Second Time Step.



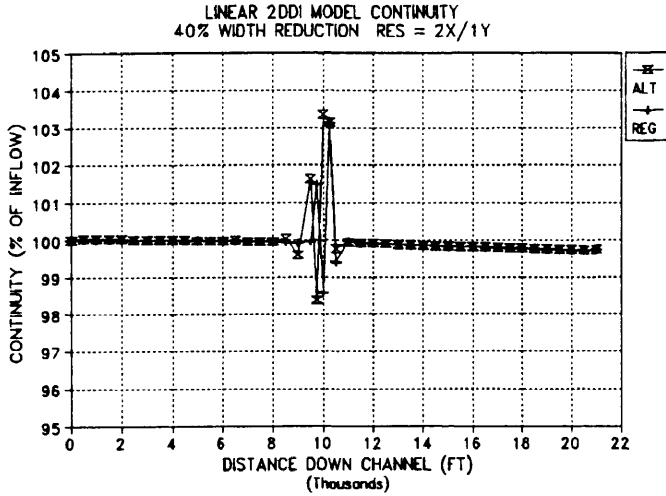


(a) Regular Grid

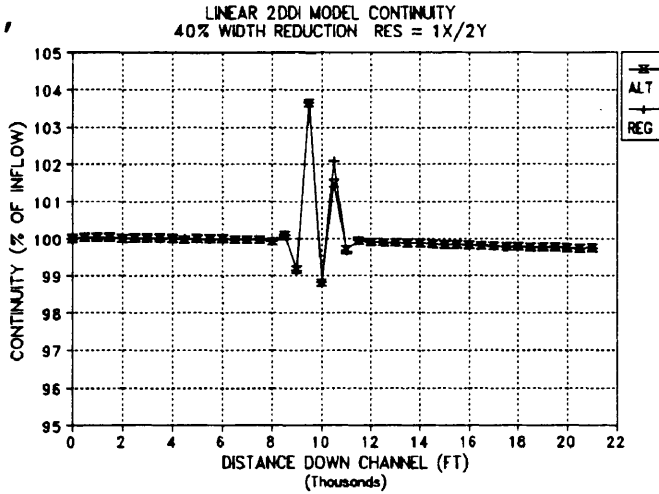


(b) Alternating Grid

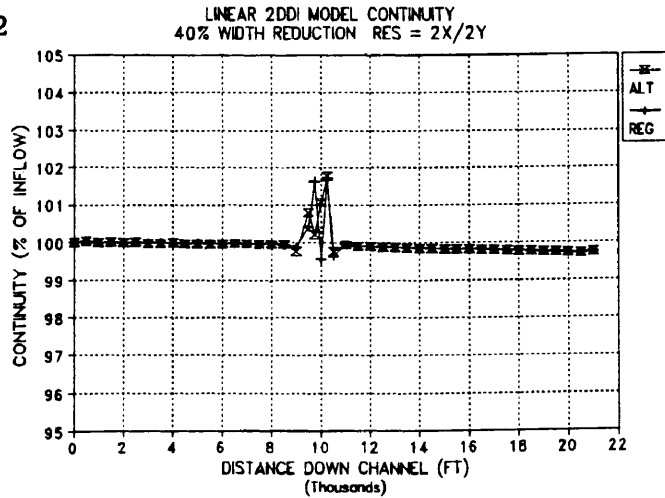
Fig. 169. Linear 2DDI Model Three Dimensional Velocity Surface Plot for 40% Width Reduction Grids with  $EV = 0.0$ , Head = 0.32 Ft, Resolution = 1, and Time Step = 12 Seconds.



(a) X Res = 2,  
Y Res = 1



(b) X Res = 1, Y Res = 2



(c) X Res = 2, Y Res = 2

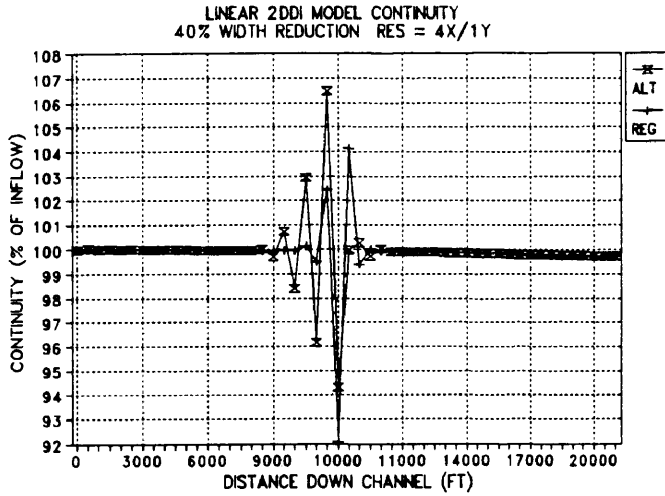
Fig. 170. Linear 2DDI Continuity vs Channel Distance for 40% Width Reduction with Resolution Equal to 2 in X and 1 in Y, 1 in X and 2 in Y, and 2 in Both X and y for Head = 0.32 Ft.

credit must be given RMA-2V due to its fully non-linear form. Maximum continuity deviation is less than 2% for the 2DDI model with both x and y resolution equal to two elements. The RMA-2V model produced deviations on the order of 10 to 15% for this same test depending on the value selected for EV.

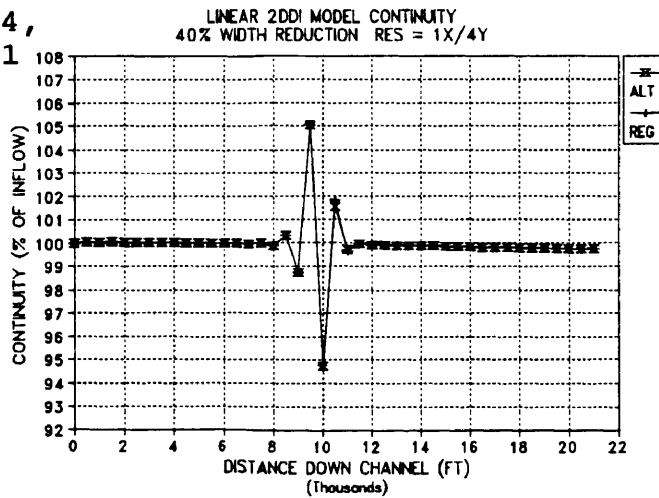
The results obtained when the x, the y, and both resolutions were increased to 4 elements are shown in Fig. 171. It should be noted that the scales have INCREASED from the preceding plots in Fig. 170 due to the increased oscillations present in the  $x = 4, y = 1$  and  $x = 1, y = 4$  tests. The  $x = 4, y = 4$  test shows almost no difference in the magnitude of the maximum continuity deviation when compared to the  $x = 2, y = 2$  case in Fig. 170(c).

When resolution was increased to 8 the results in Fig. 172 were obtained. The only resolutions tested were  $x = 8, y = 1$  and  $x = 8, y = 8$  since the  $x = 1, y = 8$  grid violated gridding criteria selected at the beginning of this study. The continuity oscillations again increased for the unequal resolution test but decreased slightly for the  $x = 8, y = 8$  test case. Maximum continuity deviations are about 1% for both the alternating and the regular test grids with the alternating grid showing more oscillations but lower peak deviations than the regular grid.

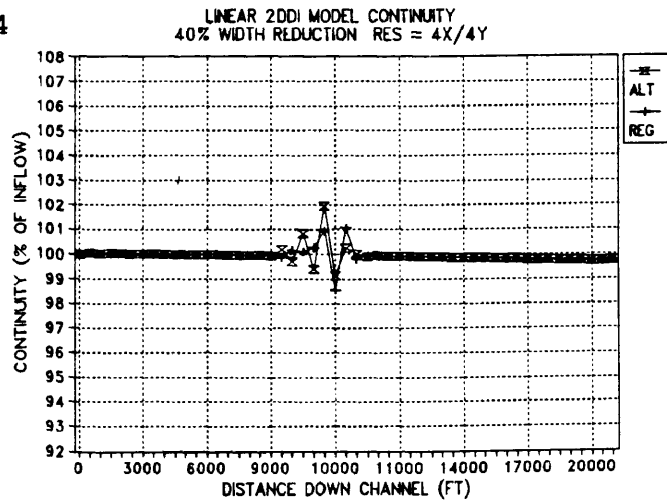
When the maximum deviations were plotted against the percentage of width reduction per element Fig. 173 was obtained. The notation in the legends in Fig. 173 is keyed such that for  $X=1/Y=V$  the data is from x resolution = 1 with variable y resolutions. It can be seen that for the unequal resolution test cases that the maximum deviation increases significantly as resolution is increased unequally. This is especially true when the x resolution is increased but the y resolution is held constant. The best method is increasing both the x and y resolution equally.



(a) X Res = 4,  
Y Res = 1

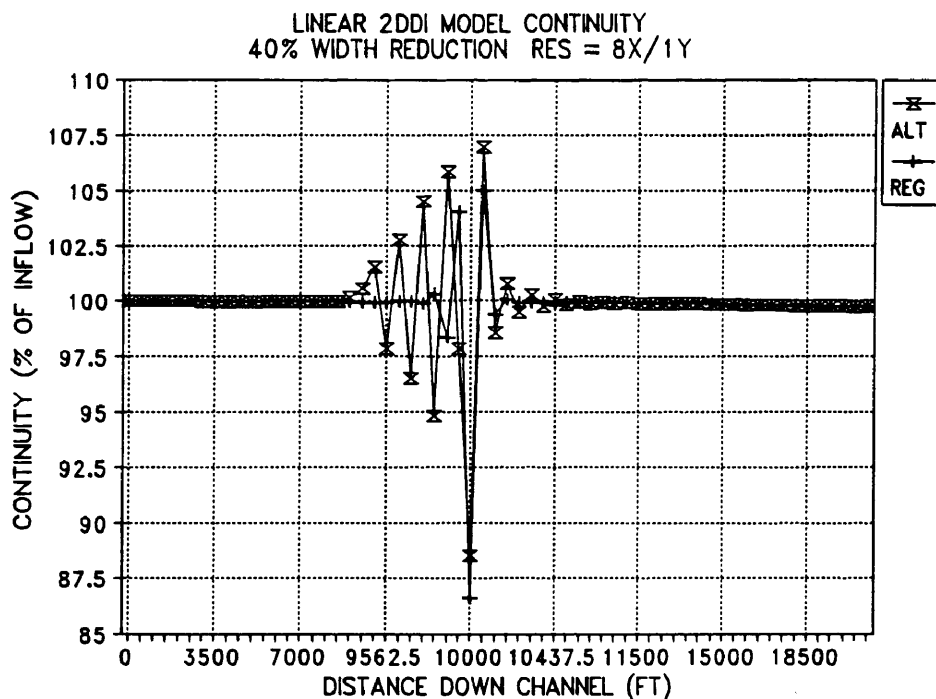


(b) X Res = 1, Y Res = 4

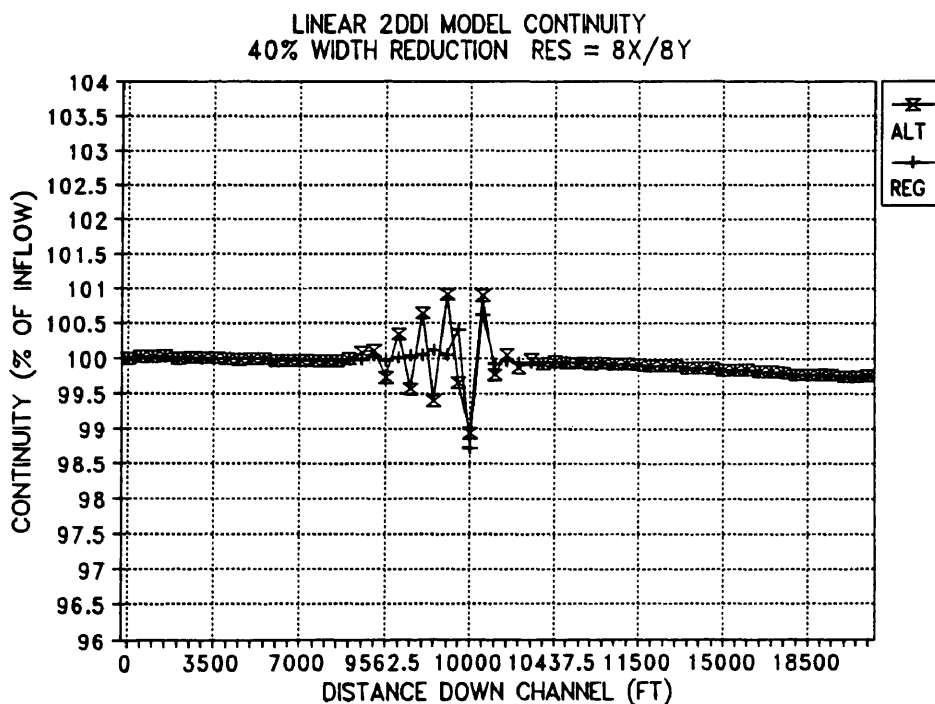


(c) X Res = 4, Y Res = 4

Fig. 171. Linear 2DDI Channel Continuity for 40% Width Reduction with Resolution Equal a) 4 in X and 1 in Y, b) 1 in X and 4 in Y, and 4 in both X and Y for Head = 0.32 Ft.

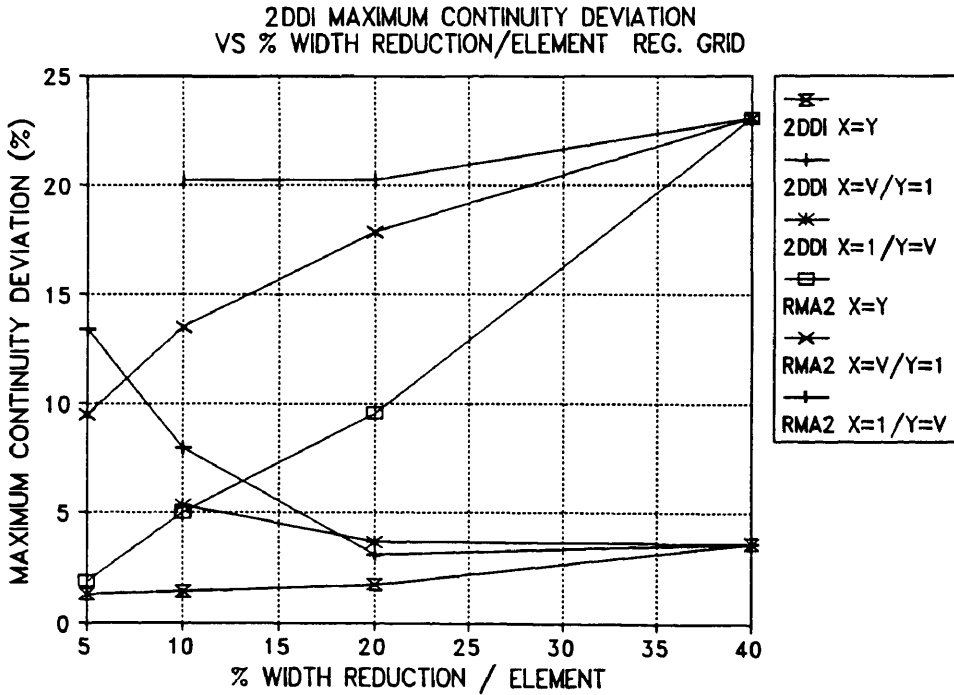


(a) X Resolution = 8, Y Resolution = 1

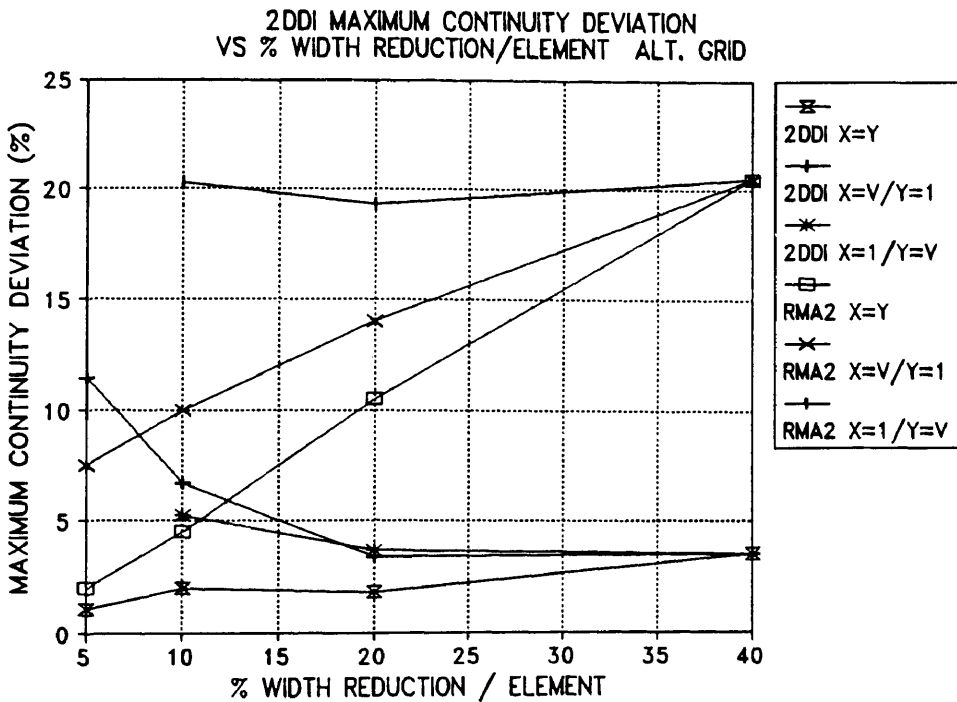


(b) X and Y Resolution = 8

Fig. 172. Linear 2DDI Channel Continuity for 40% Width Reduction with Resolution Equal a) 8 in X and 1 in Y, and b) 8 in Both X and Y for Head = 0.32 Ft with EV = 0.0.



(a) Regular Grid



(b) Alternating Grid

Fig. 173. 2DDI Continuity Deviations vs Percent Reduction in Width per Element for Test Grids with Head = 0.32 Ft, EV = 0.0, Ramp = 0.1 Day, and 12 Second Time Steps.

The results from the RMA-2V model are also plotted on Fig. 173 for comparison. It can be seen that RMA-2V model produces much higher continuity oscillations at low resolutions but approaches or betters 2DDI values at high resolutions when x and y resolutions are equal.

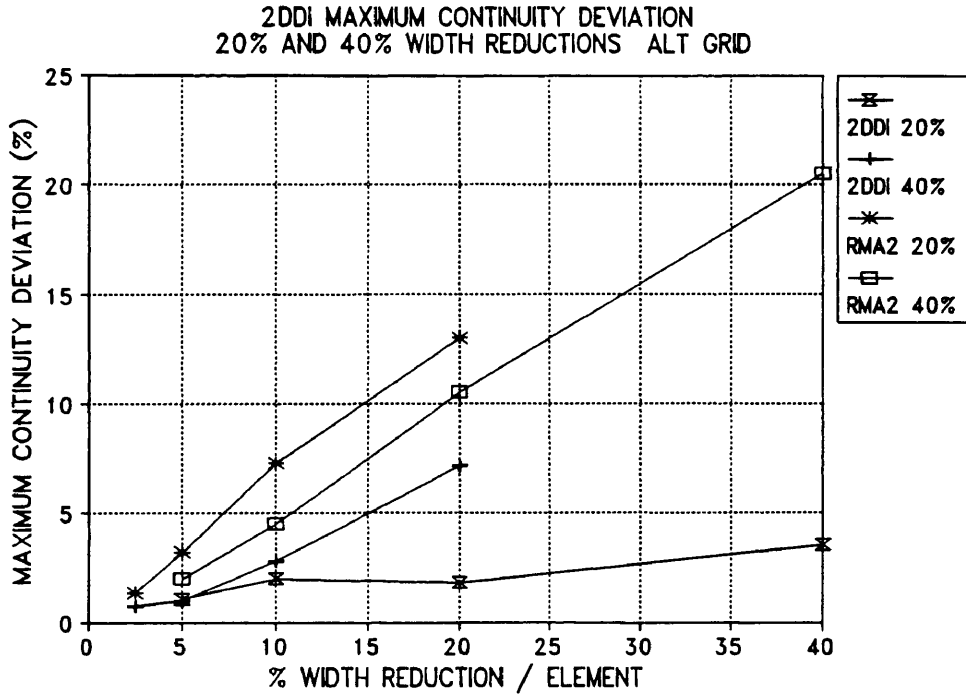
The amount of channel reduction was next varied to 20% and 60% and the maximum continuity deviations plotted in Fig. 174. The values obtained from the RMA-2V model are also plotted on this figure for comparison. It can be noted that the RMA-2V values are again higher but are converging to the same values as the grid resolution is increased.

Channel continuity results for the 20%, 40%, and 60% tests for resolutions of 1 and 8 (x = y resolution) are shown in Fig. 175. For the single resolution case all maximum deviation values are over 3% while for the 8 resolution test all values are less than 1% with the exception of the 60% test where the maximum is just over 2%. Of note is the high maximum deviation value for the single resolution 20% test - even higher than the 60% test. The reason for this anomaly is not clear.

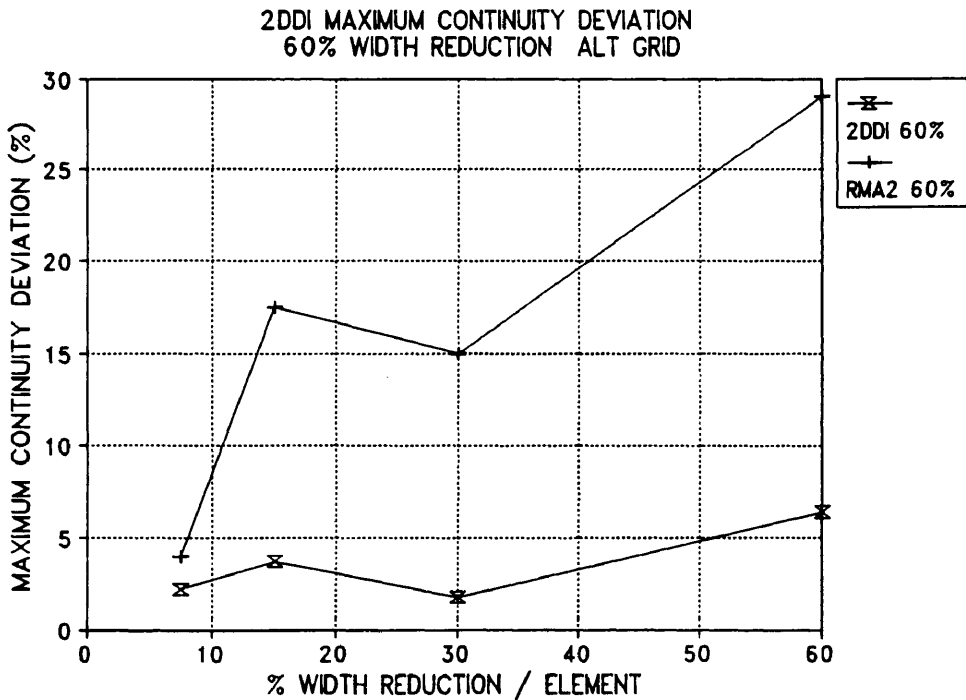
Overall the linear 2DDI model produces lower resolutions than the non-linear RMA-2V model. The fact that the 2DDI model is linearized may account for the reduction in maximum deviations but a direct comparison is not possible.

#### SUDDEN WIDTH EXPANSIONS WITH 2DDI

The grids used previously for the RMA-2V model tests were again translated and identical input values were used in the model. It was found that the identical head values used for the sudden reduction in width again produced a 500,000 cfs flow rate in the model. The width expansion was located at X = 10,500 ft from the upstream end of the model. The expansion location was set to correspond with the



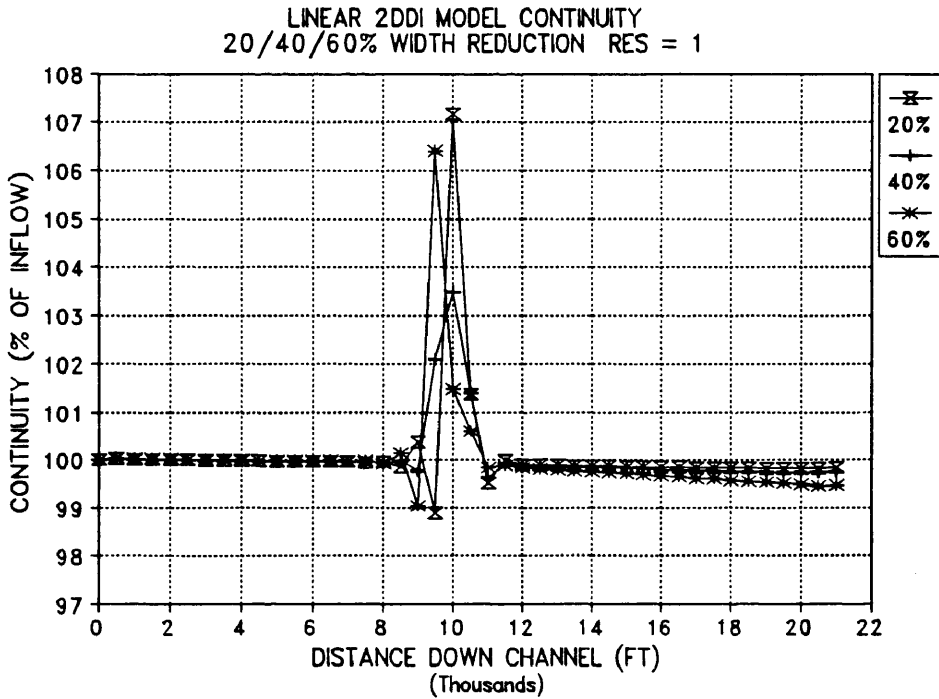
(a) 20% and 40% Width Reductions



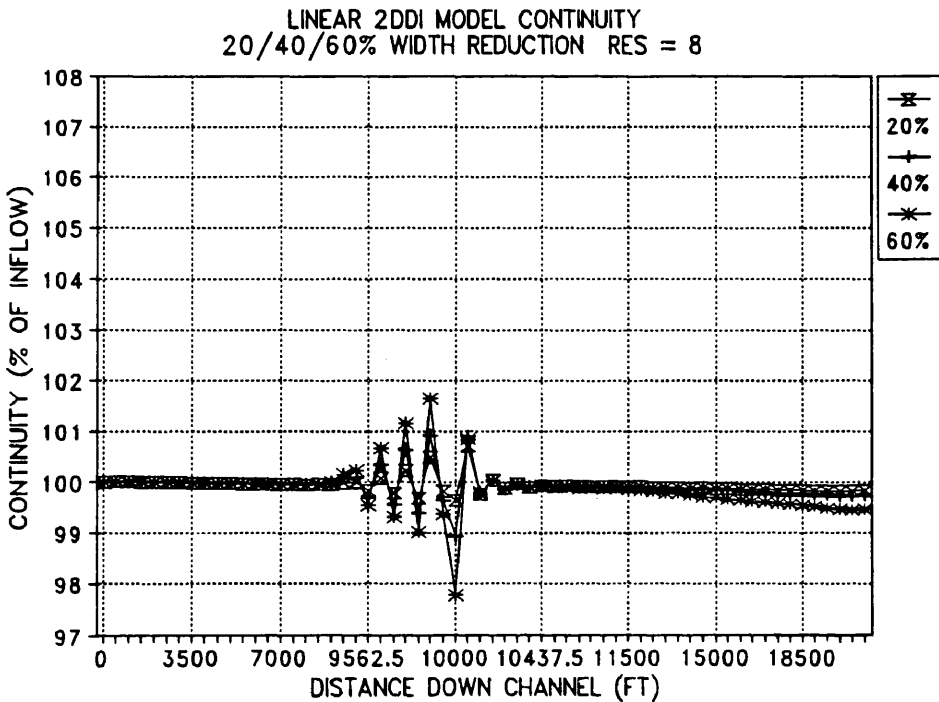
(b) 60% Width Reduction

Fig. 174. 2DDI Maximum Continuity Deviations vs Percent Width Reduction per Element for 20%, 40% and 60% Width Reductions with RMA-2V Data Plotted for Comparison. RMA-2V Data is at EV = 125.





(a) Resolution = 1



(b) Resolution = 8

Fig. 175. Linear 2DDI Channel Continuity for 20%, 40%, and 60% Width Reduction Alternating Grid for Resolutions of 1 and 8, EV = 0.0, 12 Second Time Steps and 0.1 Day Ramp.

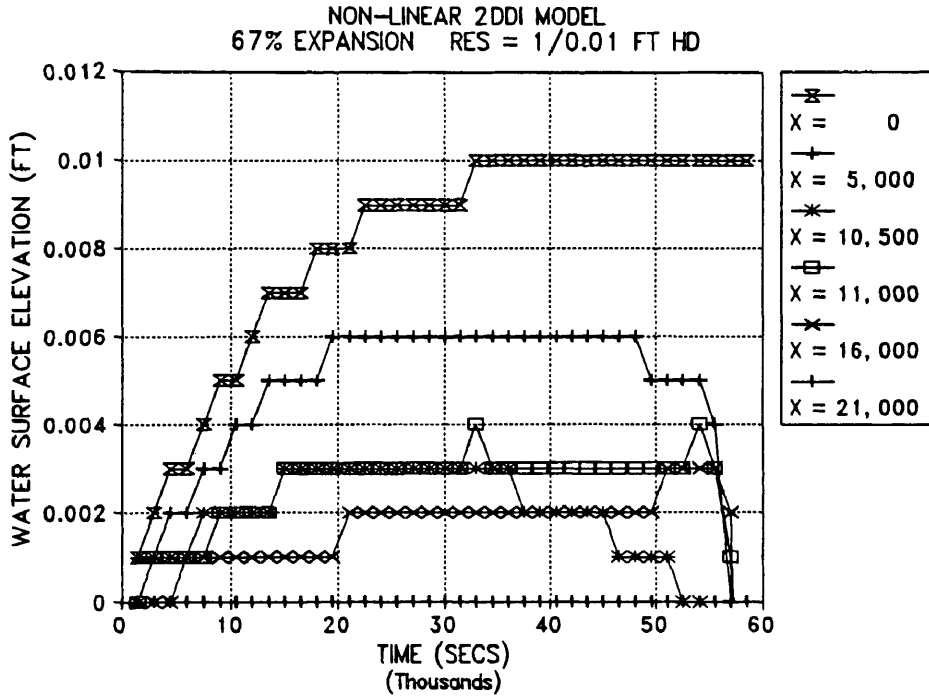
downstream face (expansion) of the abutment test which was to be run following the width reduction and the width expansion tests.

The non-linear form of the model was again tested and produced values shown in the time series plots of Fig. 176. The model was again unstable and aborted when the water surface began to oscillate over the entire length of the channel. The continuity in the channel is shown in Fig. 177 and shows oscillations growing downstream of the expansion and continuity increasing along the entire length of the channel as the model becomes unstable. It can be noted that as the instabilities grow they also begin to carry to the downstream end of the model at  $T = 51,000$  seconds.

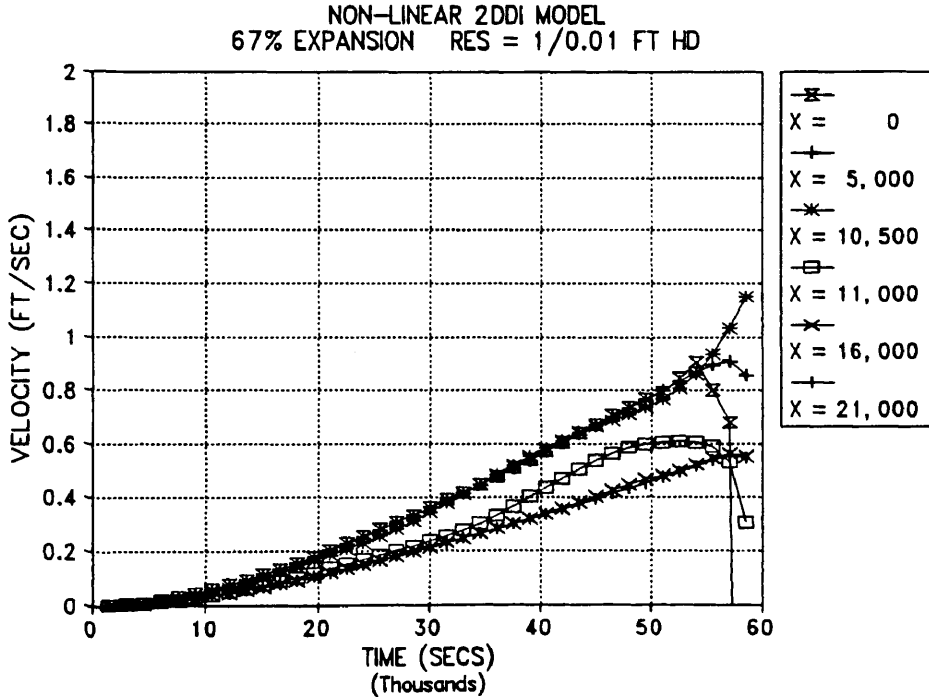
The linear model was then run and produced water surface elevations and velocities as shown in Fig. 178. Again it can be seen that while some instabilities exist early in the simulation during and shortly after ramping up, overall the model is very stable and has converged to a steady state solution by about 40 to 50 thousand seconds into the simulation.

Continuity for the linear test with  $EV = 0.0$  and a 0.32 ft head on the model is shown in Fig. 179. Also shown is the calculated water surface for this test compared with that predicted by HEC-2 and RMA-2V. The model continuity has a definite spike at the beginning of the expansion which accounts for just over 7% of the inflow.

The water surface elevation again shows the lack of the non-linear terms and does not show the velocity head upstream of the expansion. When adjusted for the velocity head (labeled ADJ 2DDI) the data follows very closely to the value predicted by HEC-2. The RMA-2V data shows the effect of the eddy downstream and its effect on velocity in the main portion of the channel. The water surface upstream of the expansion is also high - about 0.17 feet. This is probably due to the effect of the high EV values needed for



(a) Water Surface Elevation



(b) Velocity

Fig. 176. Non-linear 2DDI Model Water Surface Elevation and Velocity for 67% Width Expansion with Alternating Grid, 0.01 Ft Head, 0.4 Day Ramp, and EV = 0.0.

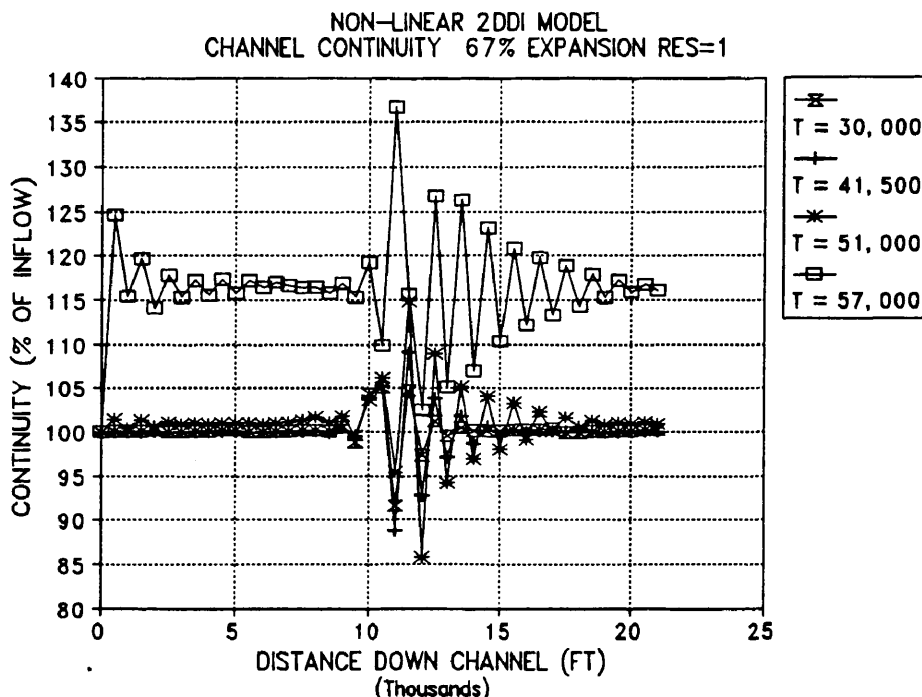


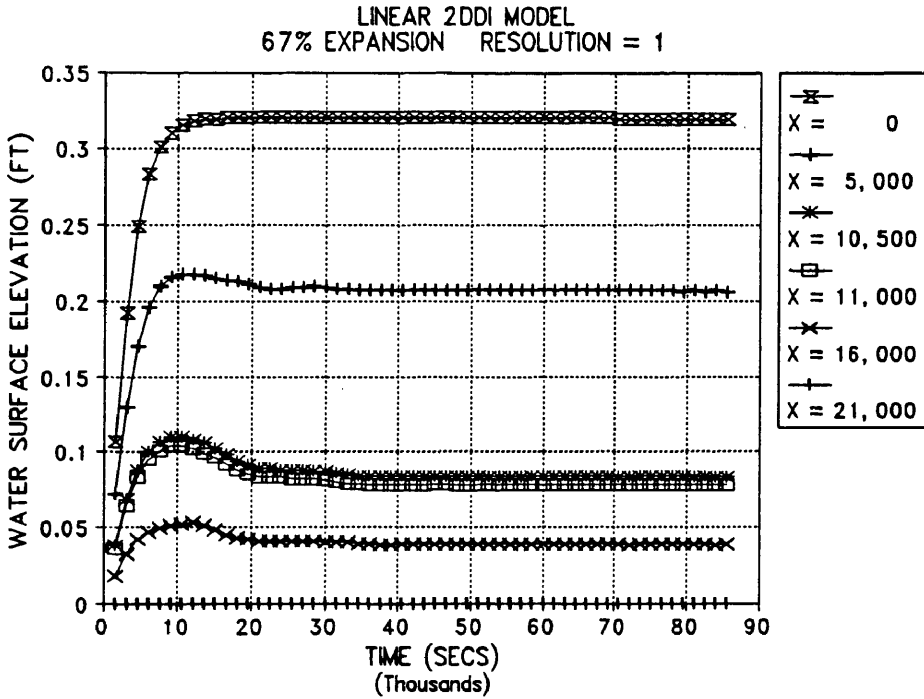
Fig. 177. Non-linear 2DDI Model Channel Continuity for Alternating Grid 67% Width Expansion at  $t = 30,000, 41,500, 51,000,$  and  $57,000$  Seconds with  $0.01$  Ft Head,  $0.4$  Day Ramp, and  $EV = 0.0$ .

model stability and may account for need to reduce Manning's  $n$  values from values used in one dimensional calculations as noted by those using the model (Thomas, 1992).

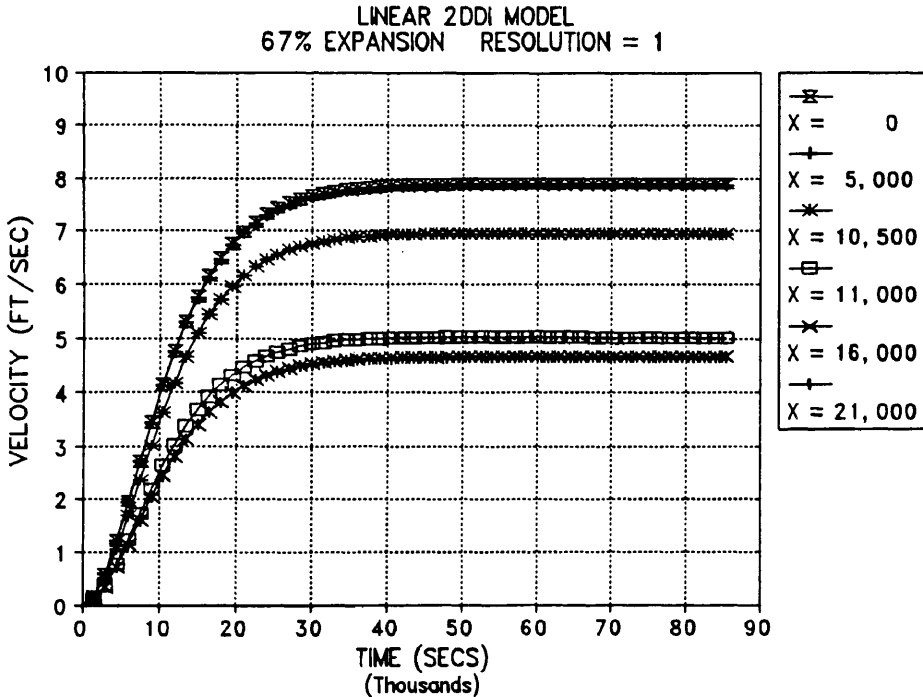
The three dimensional water surface elevation plots for the regular and alternating grids are shown in Fig. 180 with the three dimensional velocity surface plots shown in Fig. 181. The water surface elevation plot is very flat - a result of neglecting the non-linear terms in the model. The velocity surfaces show some minor oscillations at the expansion but are very smooth over the rest of the channel.

The resolution was next doubled and produced the results in Fig. 182(a). It can be noted that by increasing the resolution to 2 that the maximum deviation is reduced to under 2% for both grid types.

When the resolution was again doubled to 4 elements the results in Fig. 182(b) were obtained. For this plot the two

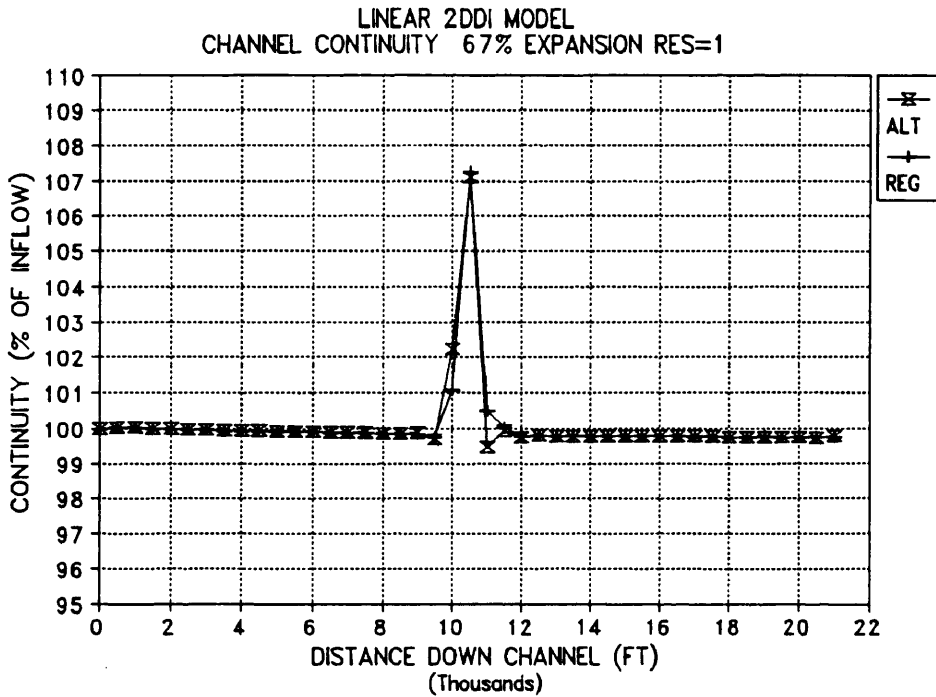


(a) Water Surface Elevation

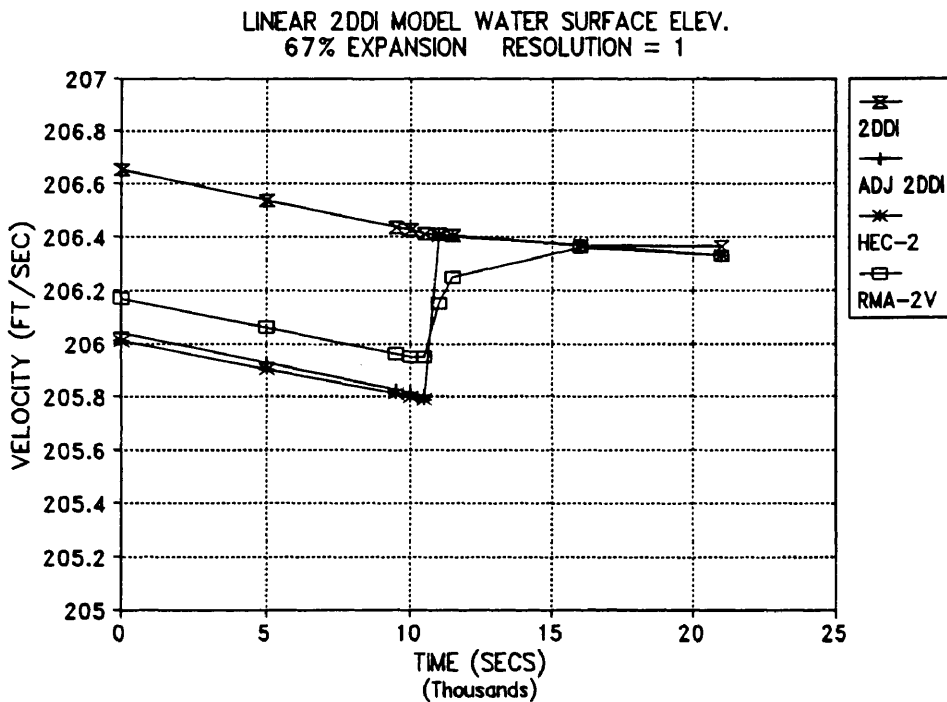


(b) Velocity

Fig. 178. Linear 2DDI Model Water Surface Elevation and Velocity for Selected Nodes for 67% Width Expansion Alternating Grid with Res = 1, Head = 0.32 Ft, and EV = 0.0.

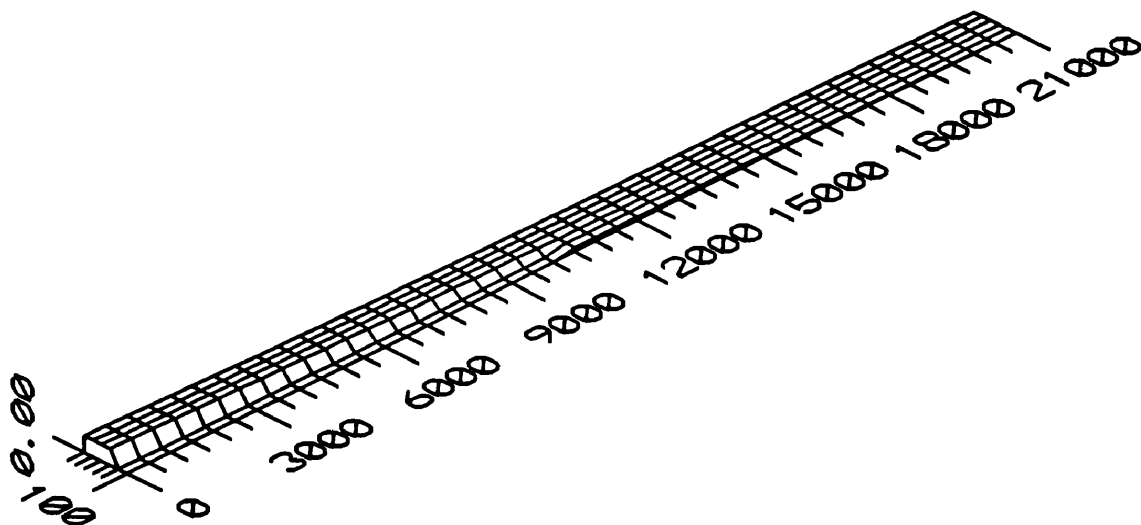


(a) 2DDI Continuity for Resolution = 1

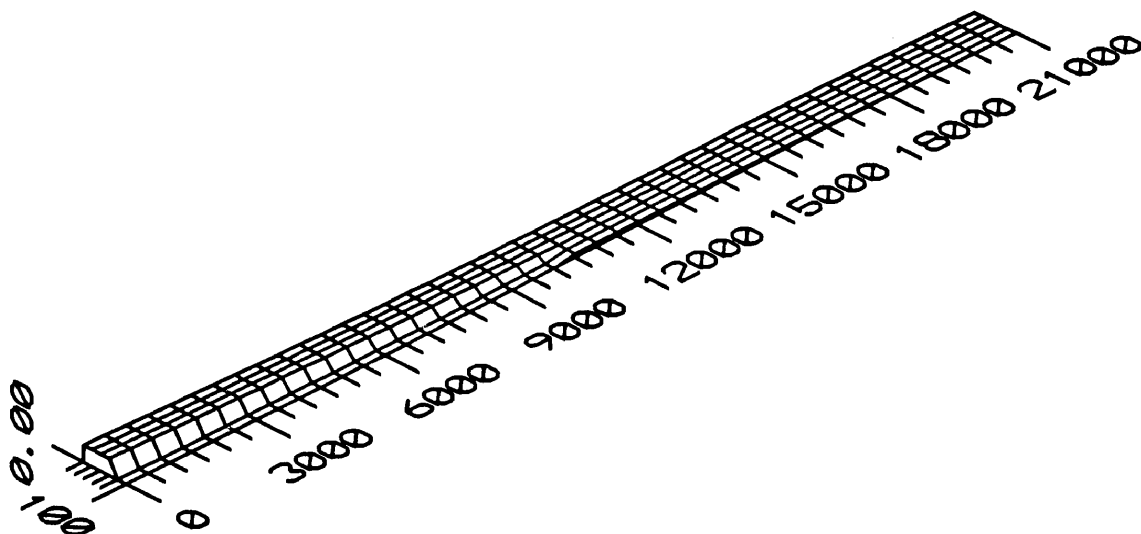


(b) 2DDI Water Surface Elevation Compared with HEC-2 Profile

Fig. 179. Linear 2DDI Continuity vs Channel Distance with EV = 0.0, Ramp = 0.1 Day, Head = 0.32 Ft, 12 Second Time Step, and Water Surface Elevation Compared with HEC-2 and RMA-2V.

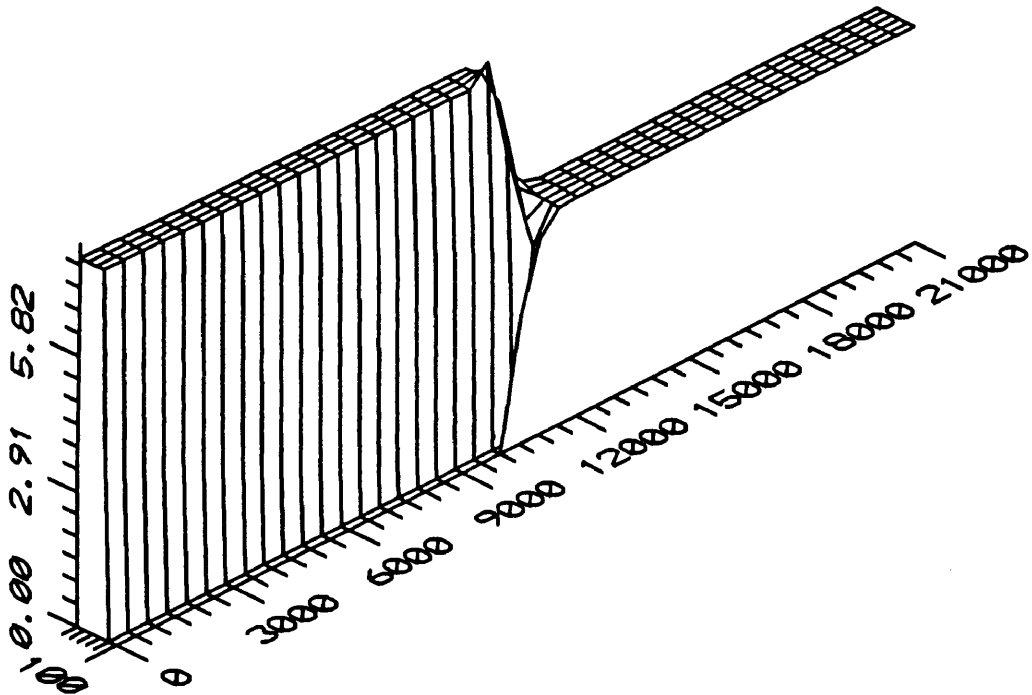


(a) Regular Grid

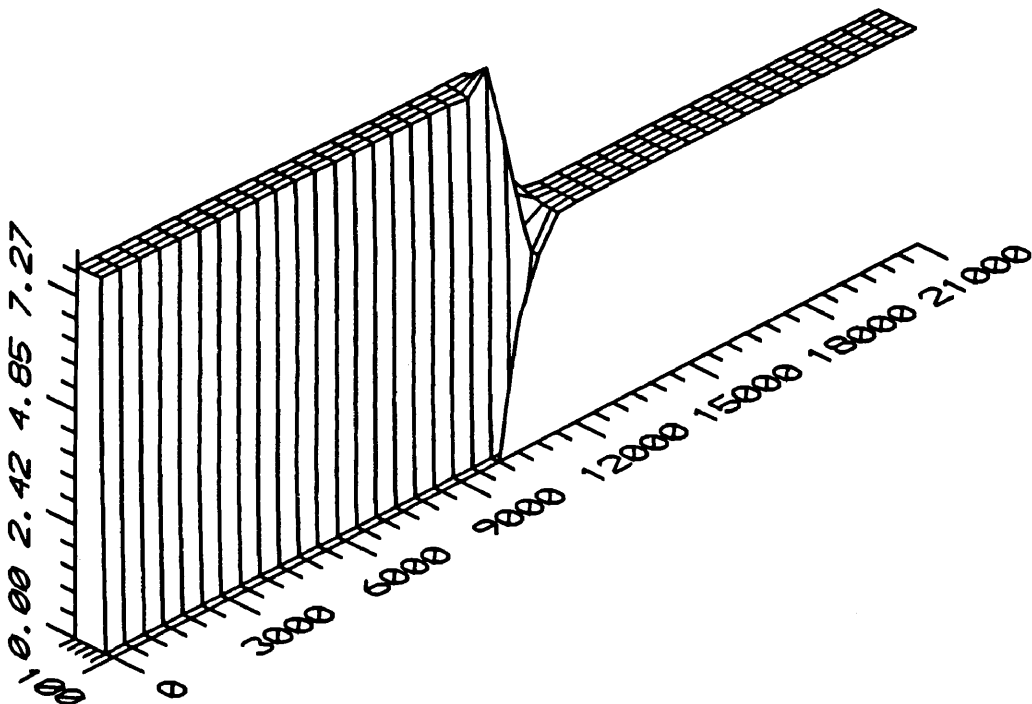


(b) Alternating Grid

Fig. 180. Linear 2DDI Model Three Dimensional Water Surface Elevations for 67% Width Expansion Test Grids with  $EV = 0.0$ , Head = 0.32 Ft, Resolution = 1, and a 12 Second Time Step.



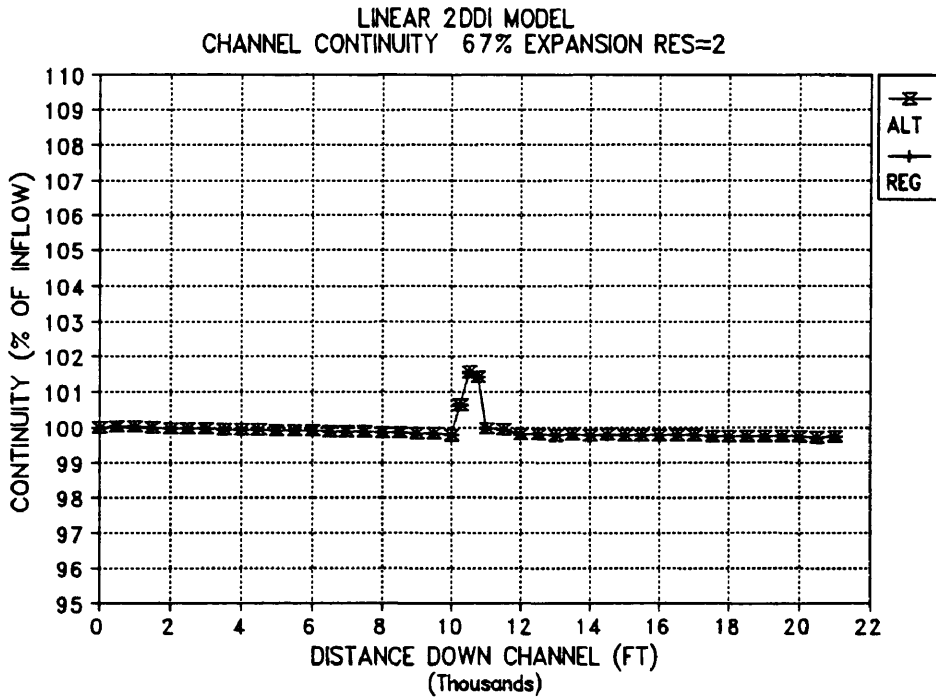
(a) Regular Grid



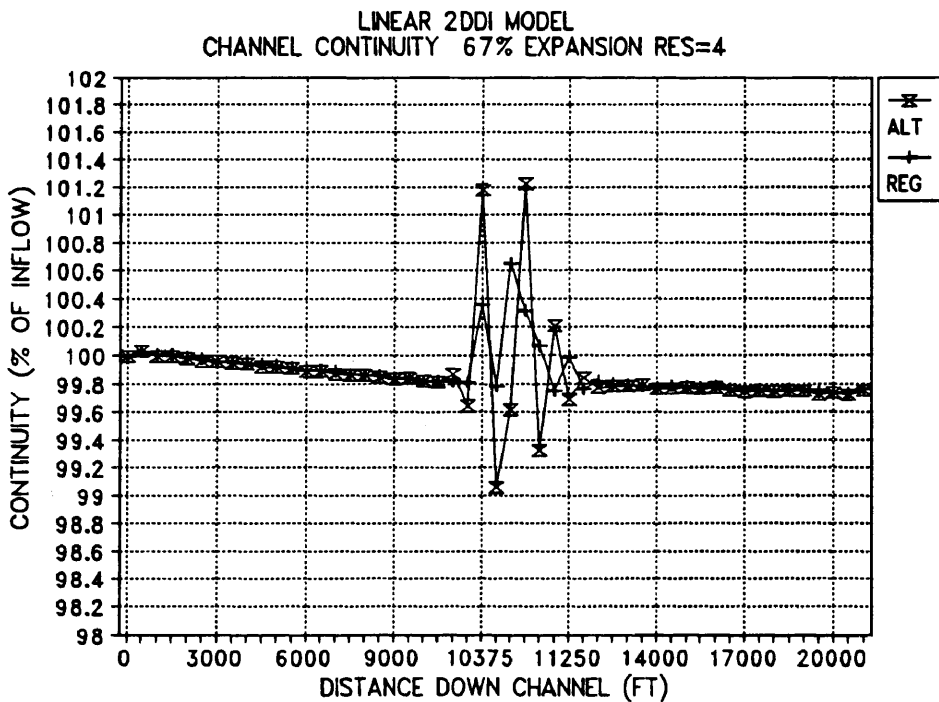
(b) Alternating Grid

Fig. 181. Linear 2DDI Model Three Dimensional Velocity Surface Plot for 67% Width Expansion with  $EV = 0.0$ , Head = 0.32 Ft, Resolution = 1, and Time Step = 12 Seconds.





(a) Resolution = 2



(b) Resolution = 4, Expanded X Scale

Fig. 182. Linear 2DDI Continuity vs Distance Down Channel for 67% Width Expansion Test Grids, Resolution = 2 and 4, EV = 0.0, Head = 0.32 Ft, and a 12 Second Time Step.

grids begin to behave significantly different but the maximum continuity deviation is less than 1.2% for both grids and less than 0.7% for the regular grid.

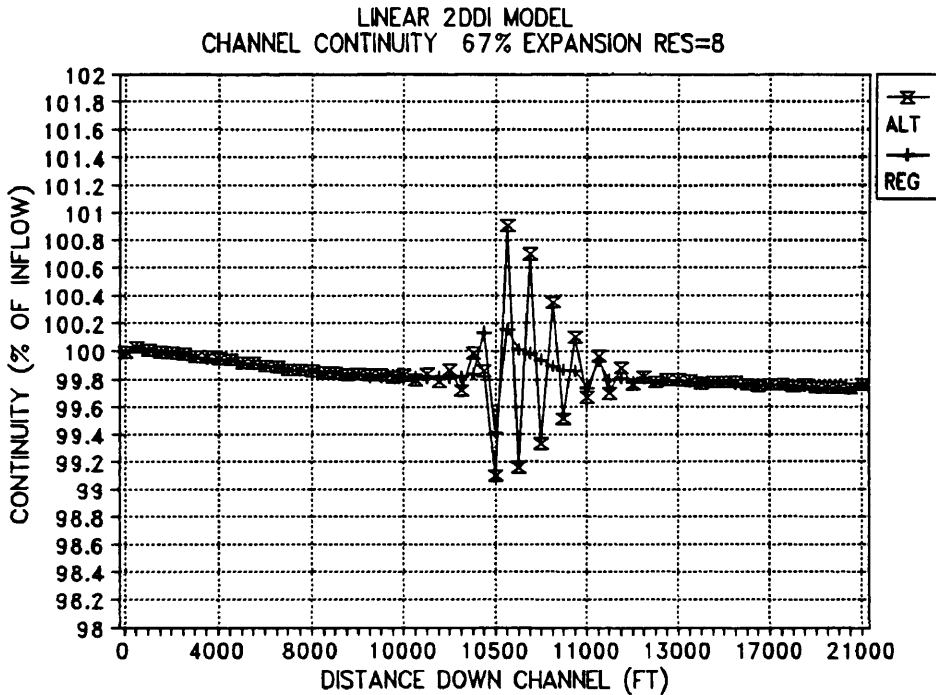
When the resolution was again doubled (to 8 elements per original element) the results in Fig. 183(a) were obtained. A slight improvement was noted for the alternating grid but the regular grid has improved such that the maximum deviation is about 0.2%. Continuity drift in the channel also amounts to about 0.2% - a problem noted in nearly all runs of the 2DDI model.

The maximum continuity deviation for the 67% width expansion is plotted against the percent change in width per element in Fig. 183(b). It is interesting to note that at a resolution of 1 the RMA-2V model performs better than the 2DDI model but at a resolution of 2 the situation is reversed. For resolutions higher than 2 there is no significant difference between the two models.

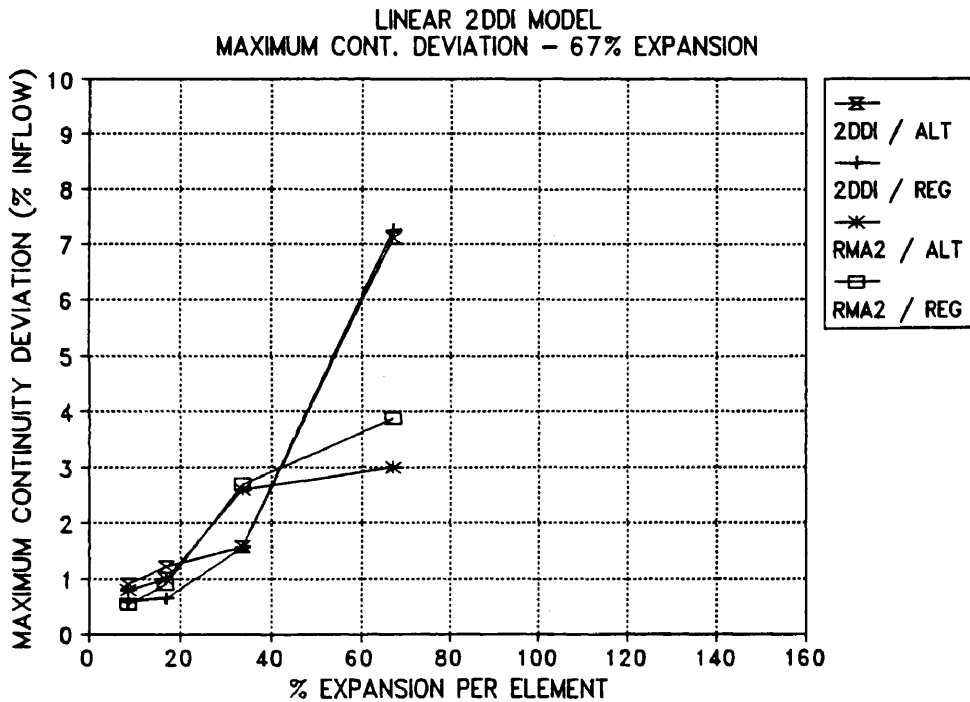
The 2DDI results were next plotted in vector form to determine if the linear 2DDI code could adequately model the separation zone downstream of the expansion. Figs. 184 through 187 show the vector plots for these tests. As would be expected the linear 2DDI results do not capture the flow separation at the abrupt expansion at any of the resolutions. This is again due to the neglecting of the non-linear terms from the shallow water equations.

The maximum deviation values for expansions of 25% and 150% are shown in Fig. 188. It can be noted that the model is very sensitive to resolution for small expansions and that the shapes of the curves for the 2DDI model and the RMA-2V model are similar but the RMA-2V model is much higher at the lower resolutions. This is probably due to the models inability to resolve the separation zone with low resolution.

For the larger (150%) expansion the two models perform similarly at low resolutions but the RMA-2V model



(a) Resolution = 8, X Scale Expanded



(b) Maximum Deviation for 67% Width Expansion

Fig. 183. 2DDI Continuity for Resolution = 8 and Maximum Continuity Deviation for 67% Width Expansion with EV = 0.0, Head = 0.32 Ft, and a 12 Second Time Step. RMA-2V Data Shown for Comparison.

2DDI LINEAR MODEL  
67% WIDTH EXPANSION  
RESOLUTION = 1

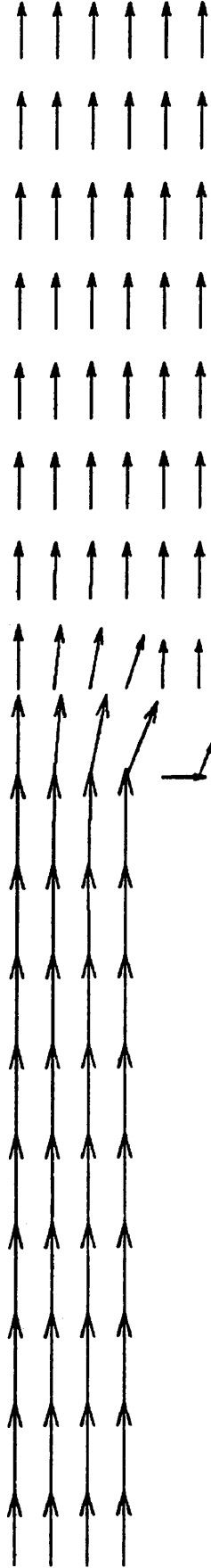


Fig. 184. Linear 2DDI Velocity Vector Plot for 67% Width Expansion with Resolution = 1 and EV = 0.0.

LINEAR 2DDI MODEL  
67% WIDTH EXPANSION  
RESOLUTION = 2

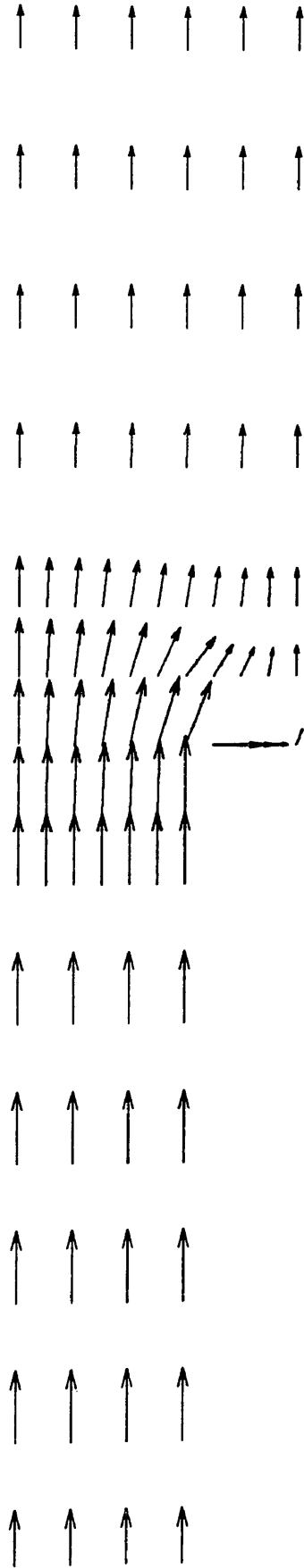


Fig. 185. Linear 2DDI Model Velocity Vector Plot for 67% Width Expansion with Resolution = 2 and EV = 0.0.

LINEAR 2DDI MODEL  
67% WIDTH EXPANSION  
RESOLUTION = 4

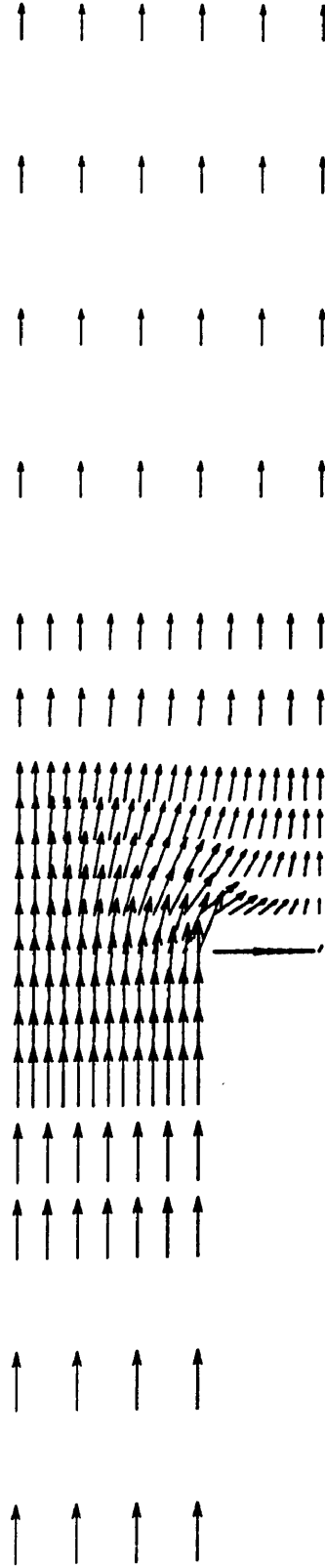


Fig. 186. Linear 2DDI Velocity Vector Plot for 67% Width Expansion with Resolution = 4 and EV = 0.0.

LINEAR 2DDI MODEL  
67% WIDTH EXPANSION  
RESOLUTION = 8

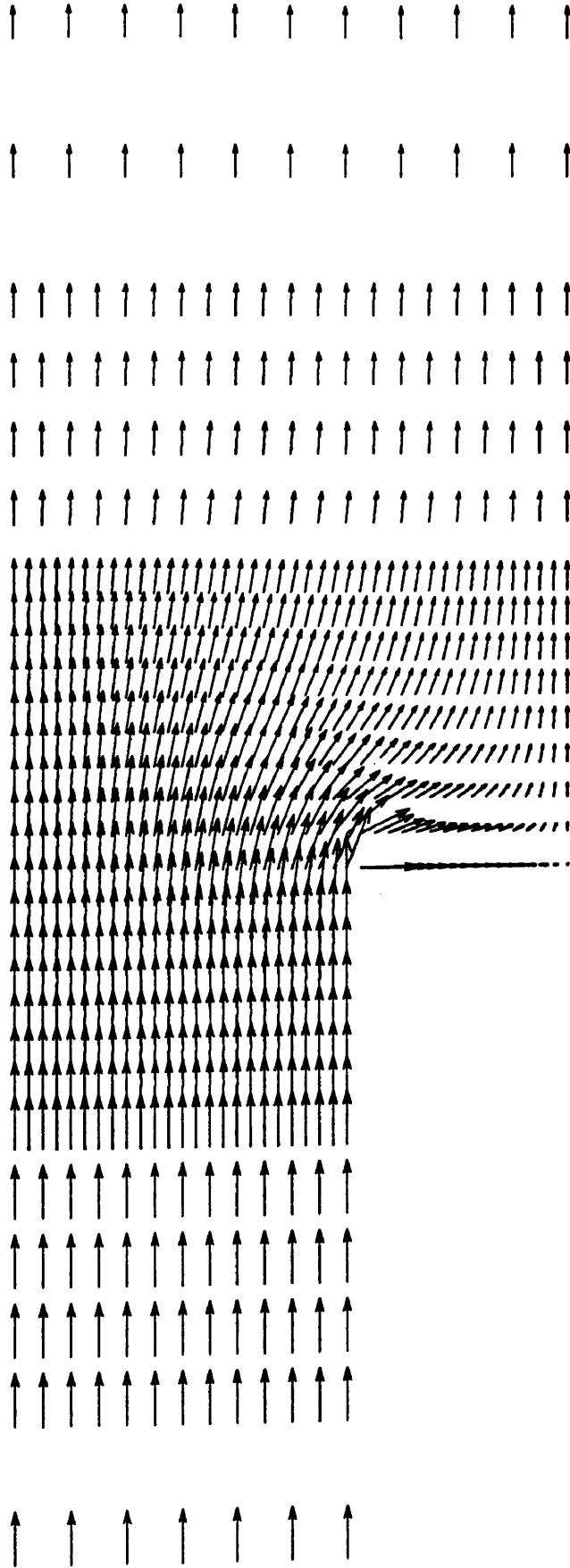
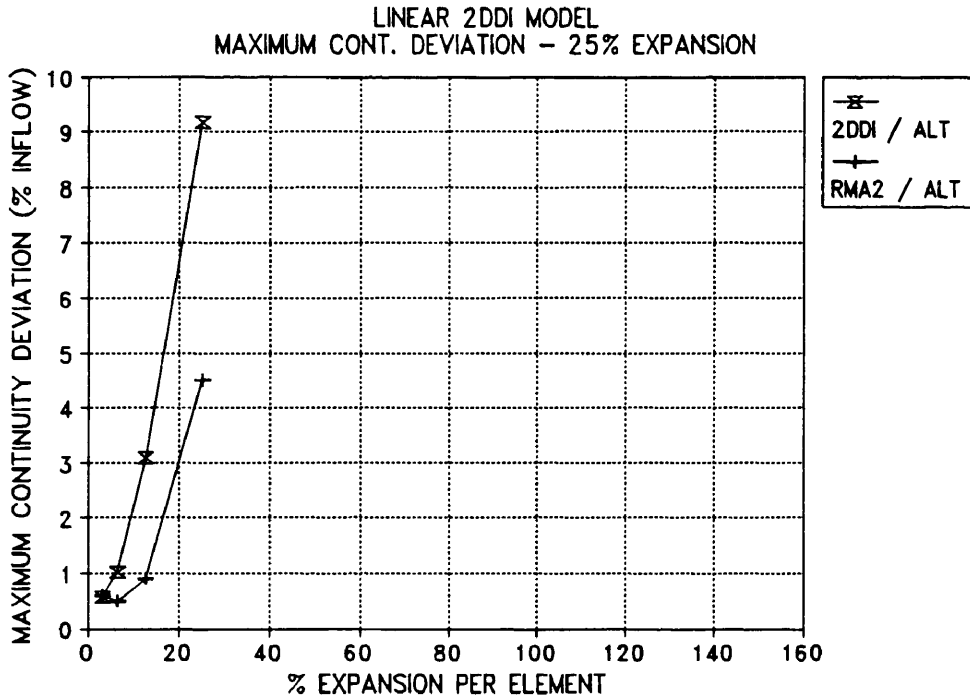
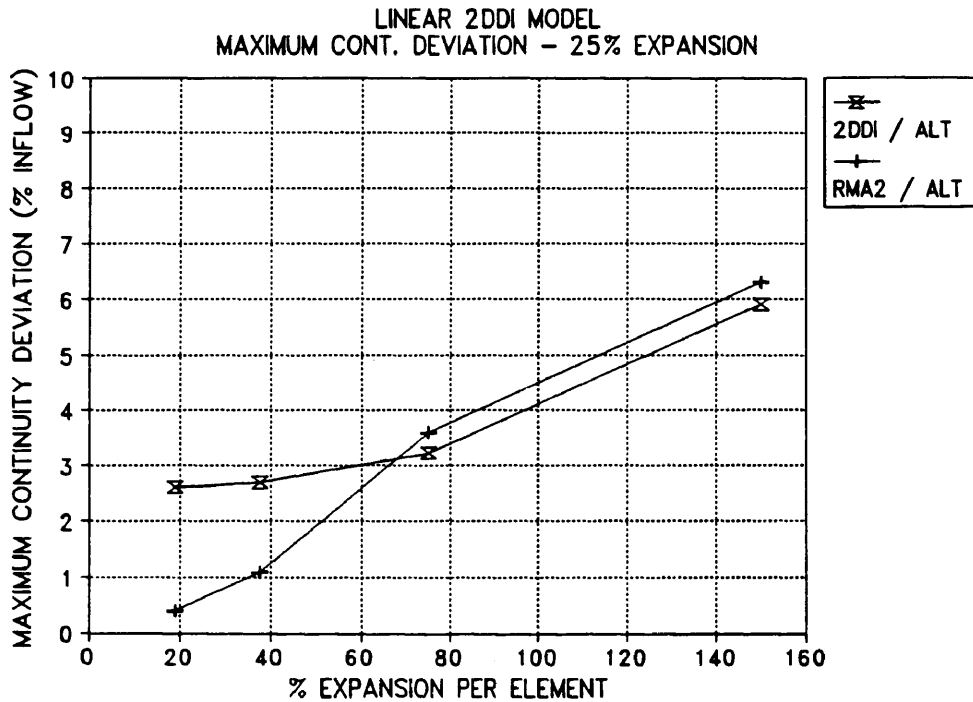


Fig. 187. Linear 2DDI Velocity Vector Plot for 67% Width Expansion with Resolution = 8 and  $EV = 0.0$ .



(a) 25% Width Expansion



(b) 150% Width Expansion

Fig. 188. Linear 2DDI Maximum Continuity Deviation vs Percent Expansion per Element for 25% and 150% Width Expansion Alternating Grid Tests with EV = 0.0 and Flow = 500,000 cfs.



significantly outperforms the 2DDI model at high resolutions.

Channel continuity for the three differing expansions for resolutions of 1 and 8 are shown in Fig. 189. It can be noted that for the single resolution test the 25% expansion produces the highest deviations of the three tested expansions. For the high resolution case the situation is reversed - the 25% expansion produces the lowest continuity deviation while the 150% expansion produces the highest deviation.

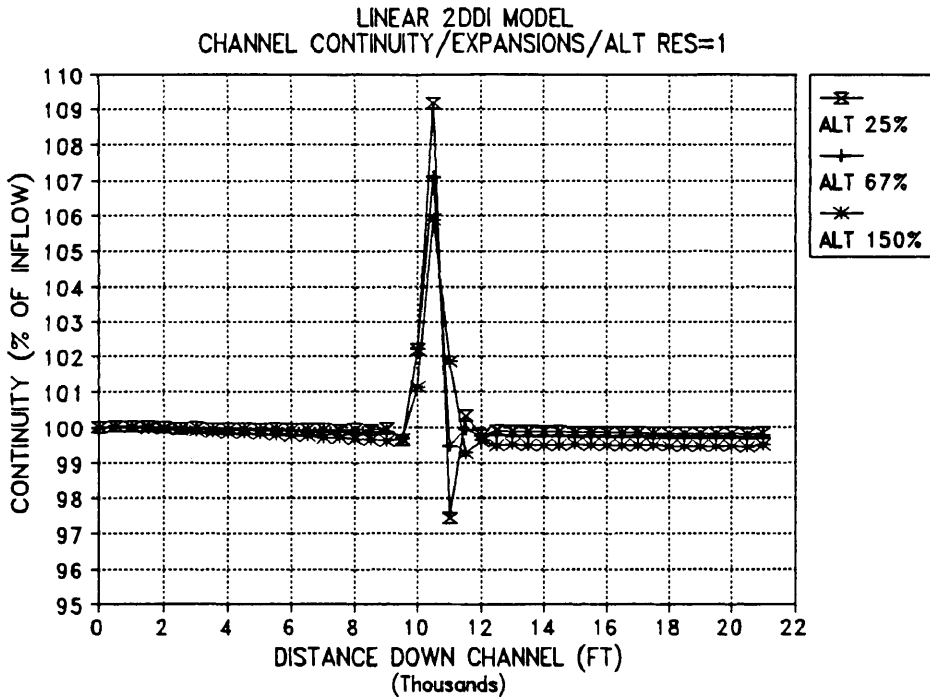
From this series of tests it is apparent that the linear 2DDI model is not suitable for this class of problems where sudden expansions produce separation zones and eddies in the flow field. The modeling of this phenomenon is strictly in the realm of fully non-linear models and while the RMA-2V model is not perfect it does provide adequate solutions to this problem.

#### ABUTMENT REDUCTIONS WITH 2DDI

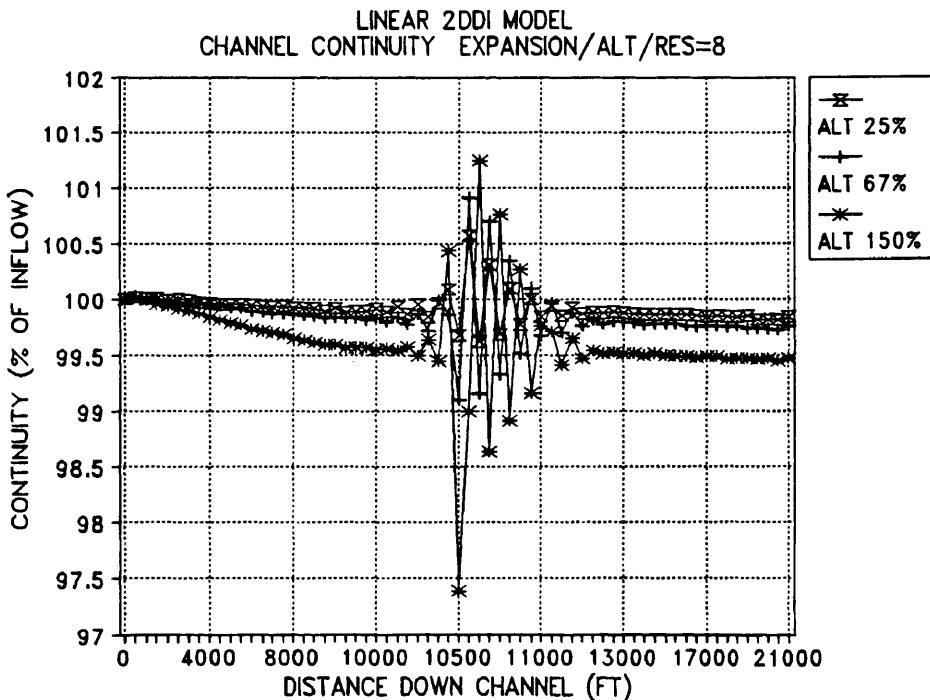
The previously used abutment reduction grids were converted to the 2DDI format and identical boundary conditions and specifications were used for the 2DDI model runs. The head required to produce the desired 500,000 cfs flow rate was found to be 0.18 feet.

The first attempt to run the model for the abutment reduction test used the fully non-linear form of the model with a head of 0.01 feet and a 0.4 day ramp. This resulted in the model aborting at something over 33,000 seconds into the simulation. The water surface elevation and velocity results at the standard nodes for this test are shown in Fig. 190. For this case the water surface did not reach the end of the ramp prior to the model aborting.

Continuity for the non-linear case is shown in Fig. 191. The continuity in the channel remained good until the

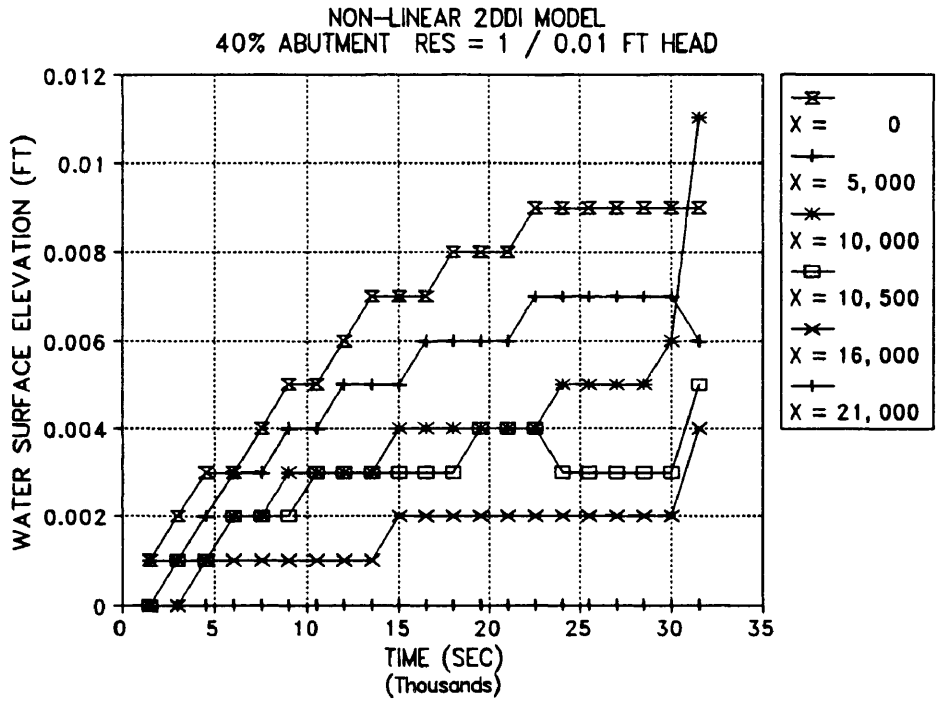


(a) Resolution = 1

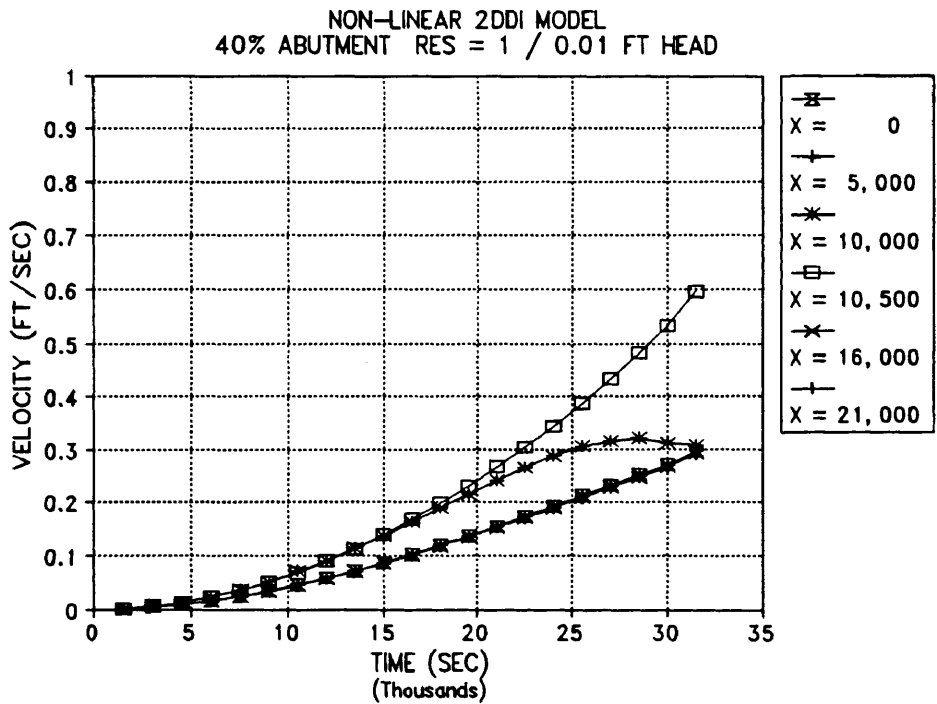


(b) Resolution = 8

Fig. 189. Linear 2DDI Channel Continuity for 25%, 67%, and 150% Width Expansion, Alternating Grid, Resolution = 1 and 8, EV = 0.0, 12 Second Time Steps. X Scale Expanded for Res = 8.



(a) Water Surface Elevation



(b) Velocity

Fig. 190. Non-linear 2DDI Model Water Surface Elevation and Velocity for 40% Abutment Reduction with Alternating Grid, 0.01 Ft Head, 0.4 Day Ramp, and EV = 0.0.

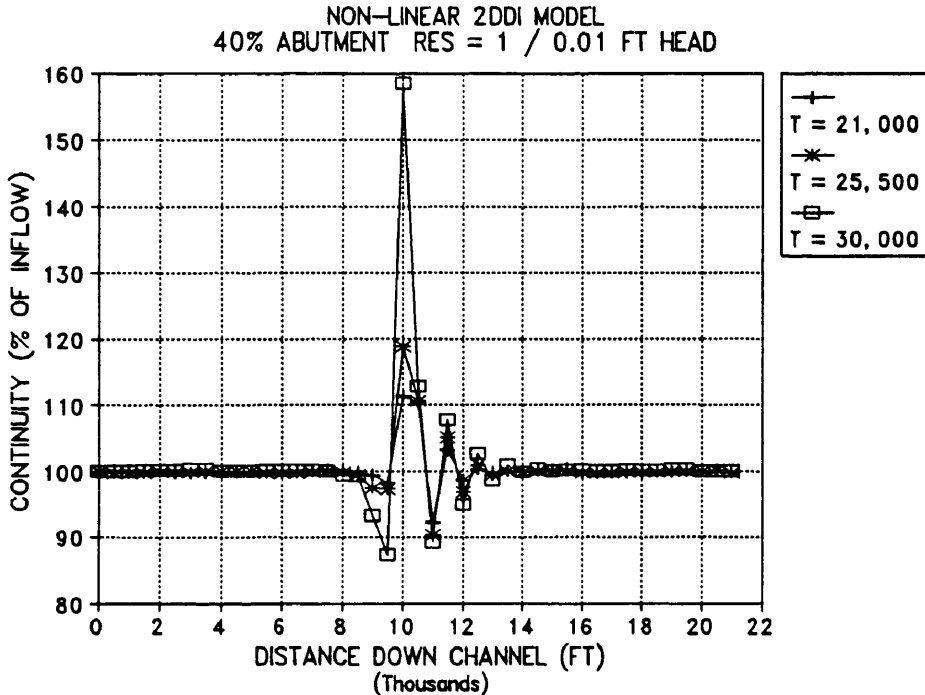
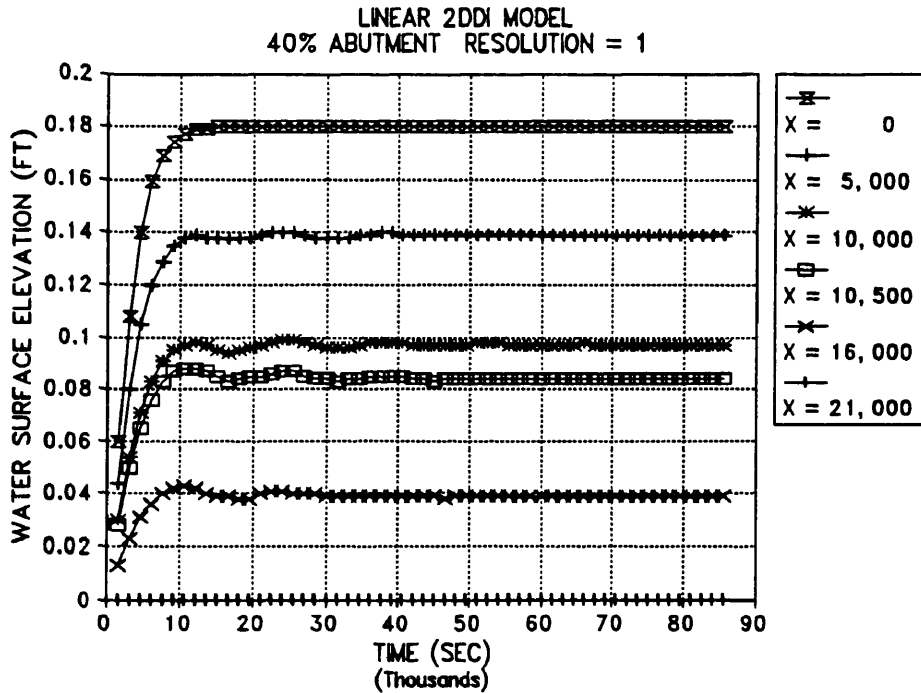


Fig. 191. Non-linear 2DDI Model Channel Continuity for Alternating Grid 40% Abutment Reduction Test at  $T = 21,000$ ,  $25,500$ , and  $30,000$  Seconds with  $0.01$  Ft Head,  $0.4$  Day Ramp, and  $EV = 0.0$ .

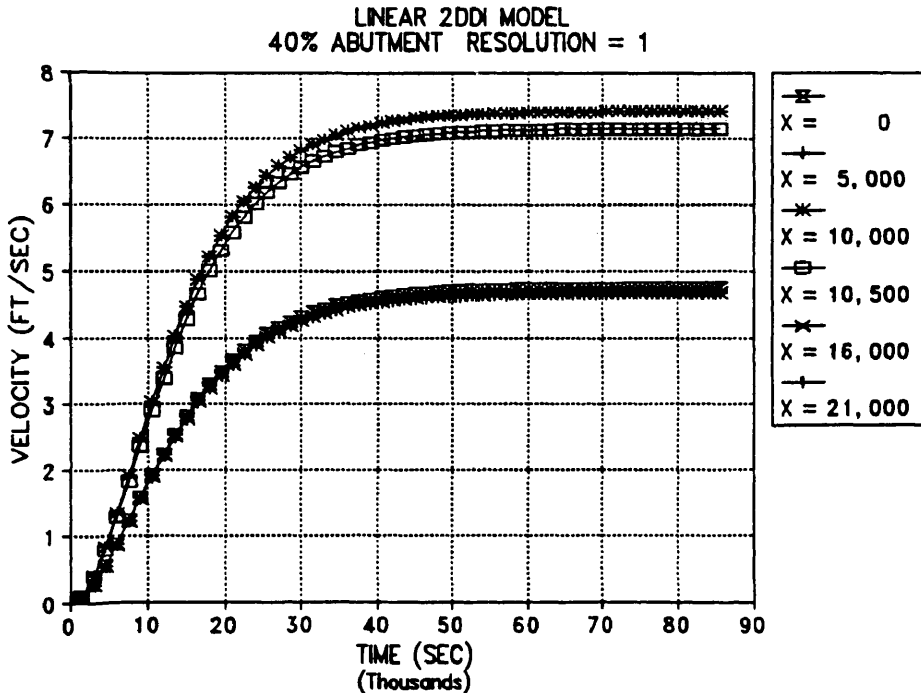
very end of the simulation and only the oscillation at the upstream end of the abutment increased until the model aborted.

The linear form of the model was then run with the head on the model equal to  $0.18$  feet. This run was stable and produced the results shown in Fig. 192. For this case the model again shows some oscillations in water surface but they are mostly damped out by about  $50,000$  seconds ( $13.88$  hours) into the simulation.

Continuity for the single resolution test of the linear model is shown in Fig. 193(a). The maximum continuity deviation is about  $11\%$  for the regular grid and  $9\%$  for the alternating grid. It is interesting to note the single peak of the oscillation. It appears that at this resolution that the expansion has no additional effect on the model continuity.

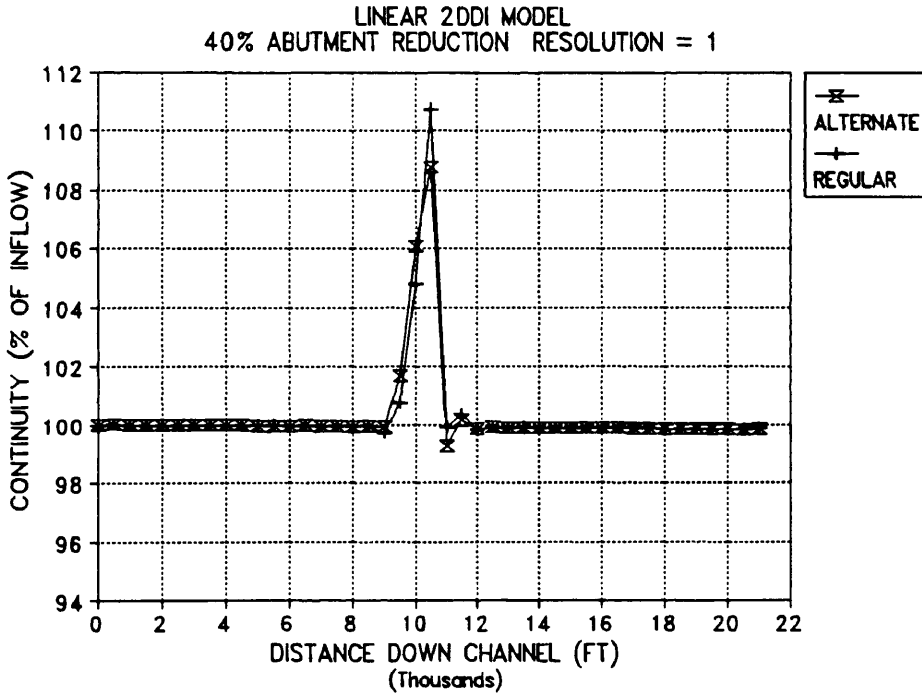


(a) Water Surface Elevation

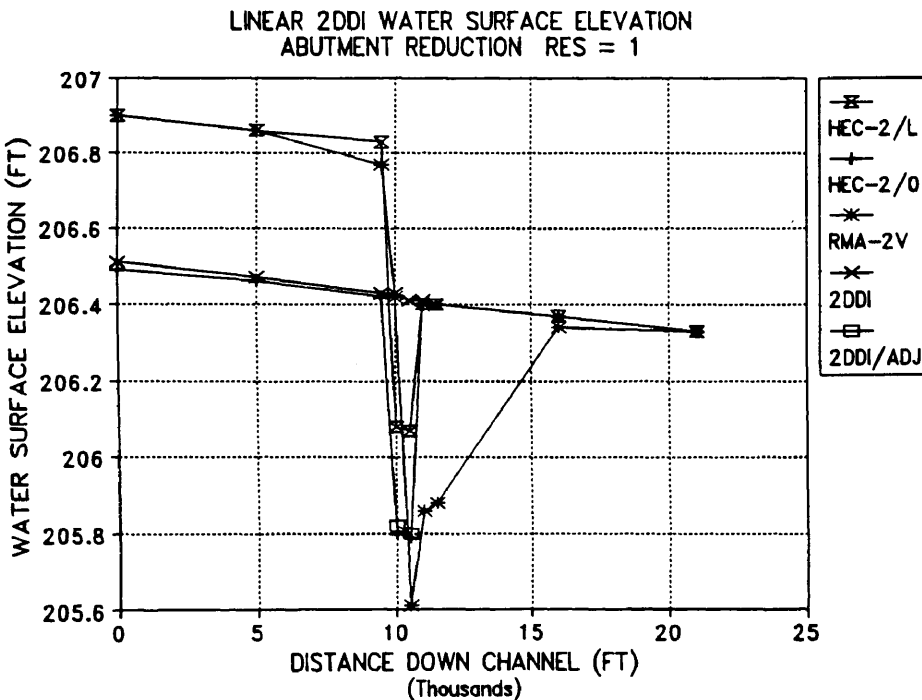


(b) Velocity

Fig. 192. Linear 2DDI Model Water Surface Elevation and Velocity for Standard Nodes for 40% Abutment Reduction Alternating Grid with Res = 1, Head = 0.18 Ft, and EV = 0.0.



(a) Continuity for Resolution = 1



(b) Water Surface Elevation Compared with HEC-2 and RMA-2V

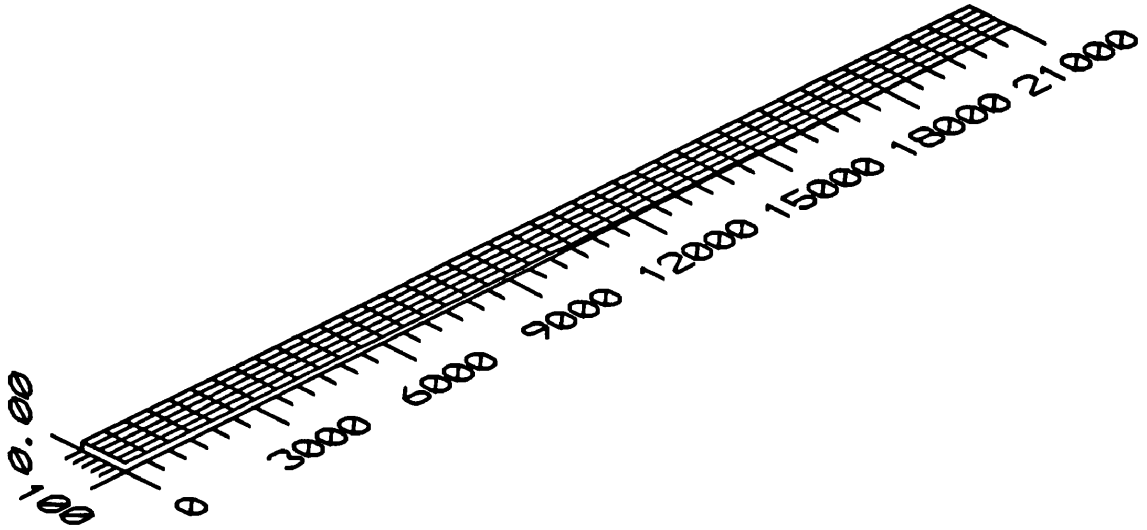
Fig. 193. Linear 2DDI Continuity vs Channel Distance for Res = 1 and Water Surface Elevations for Standard Nodes with EV = 0.0, 0.18 Ft Head, Ramp = 0.1 Day.

The water surface elevations for the linear 2DDI model, the HEC-2 model and the RMA-2V model are shown in Fig. 193(b). Two values are shown for the HEC-2 model - one set of values with the contraction and expansion coefficients (C/E coefficients) set equal to zero (HEC-2/0) and one set with the coefficients set to 0.20 and 0.45 respectively. With the C/E coefficients set to 0.0 the HEC-2 model predicts almost exactly the water surface profile produced by the 2DDI model - with the exception of the velocity head through the contraction. When the C/E coefficients were set to 0.20 and 0.45 the HEC-2 model predicted the identical upstream water surface elevation that the RMA-2V model produced.

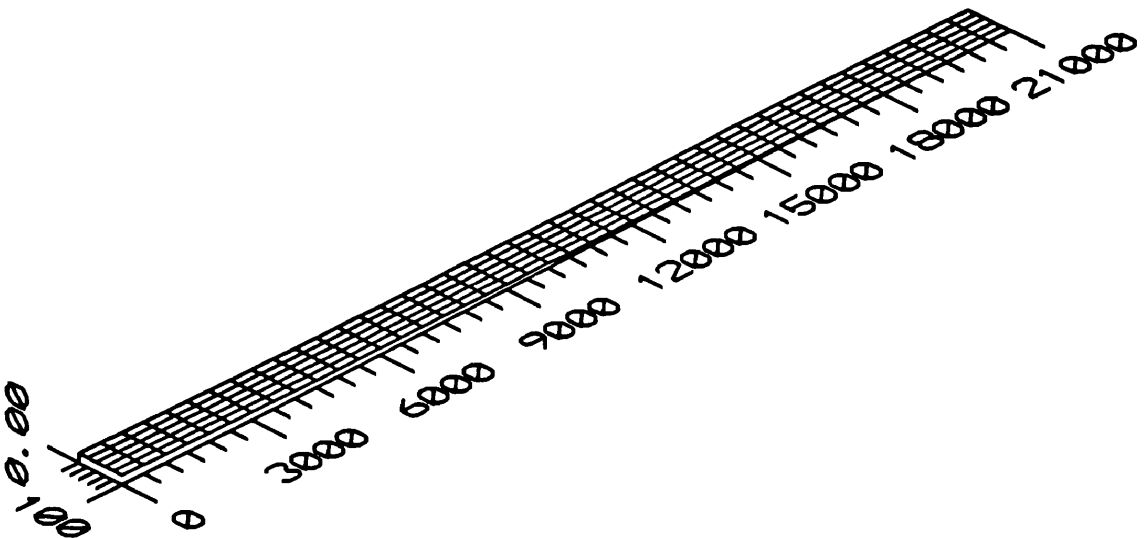
The RMA-2V model over reacted as it moved through the abutment constriction but shows the effect of the effective flow area reduction downstream of the abutment due to the formation of the eddy shown previously in the section dealing with expansions as modeled by RMA-2V. The water surface elevation in RMA-2V probably returns to the value estimated by the HEC-2 model prior to the 15,000 foot point but intermediate points were not used in the HEC-2 model and were not plotted for the RMA-2V and 2DDI solutions.

The three dimensional water surface plots for the alternating and regular grids are shown in Fig. 194. No difference can be seen in the water surface plots and no distinguishing features can be noted. The three dimensional velocity plots are shown in Fig. 195 and show the effect of the contraction due to the abutment. It can be noted that the velocity returns to uniform flow within two element lengths of the lower end of the abutment. A slight difference in velocity patterns is also noticeable at the peaks on the velocity surface due to grid orientation effects.

The resolution was next increased to 2 elements and the continuity results shown in Fig. 196(a) were obtained. The



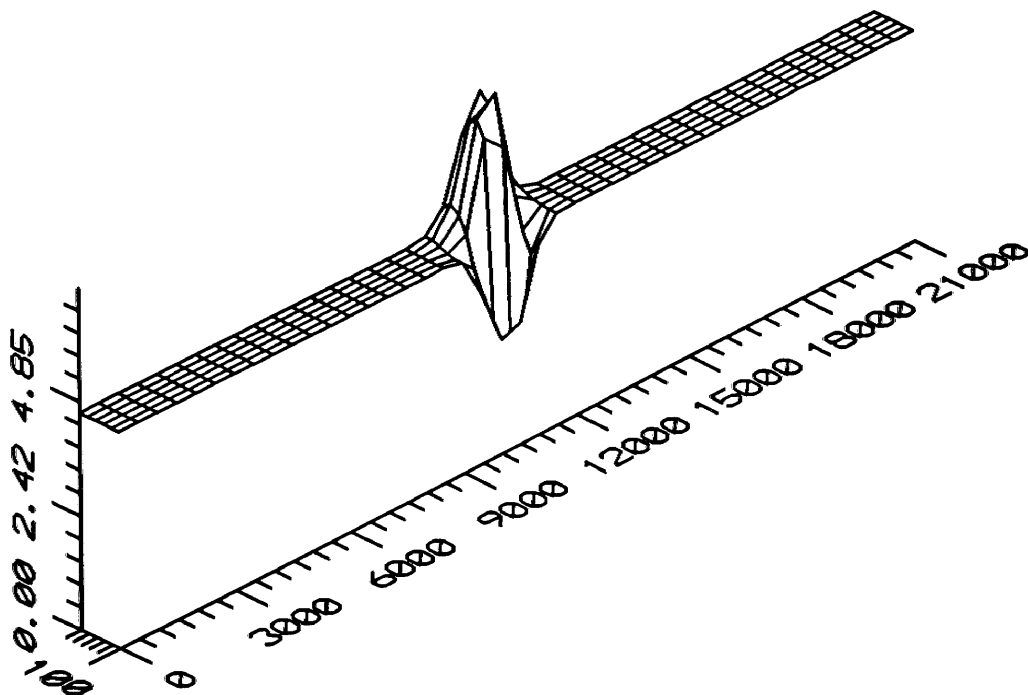
(a) Regular Grid



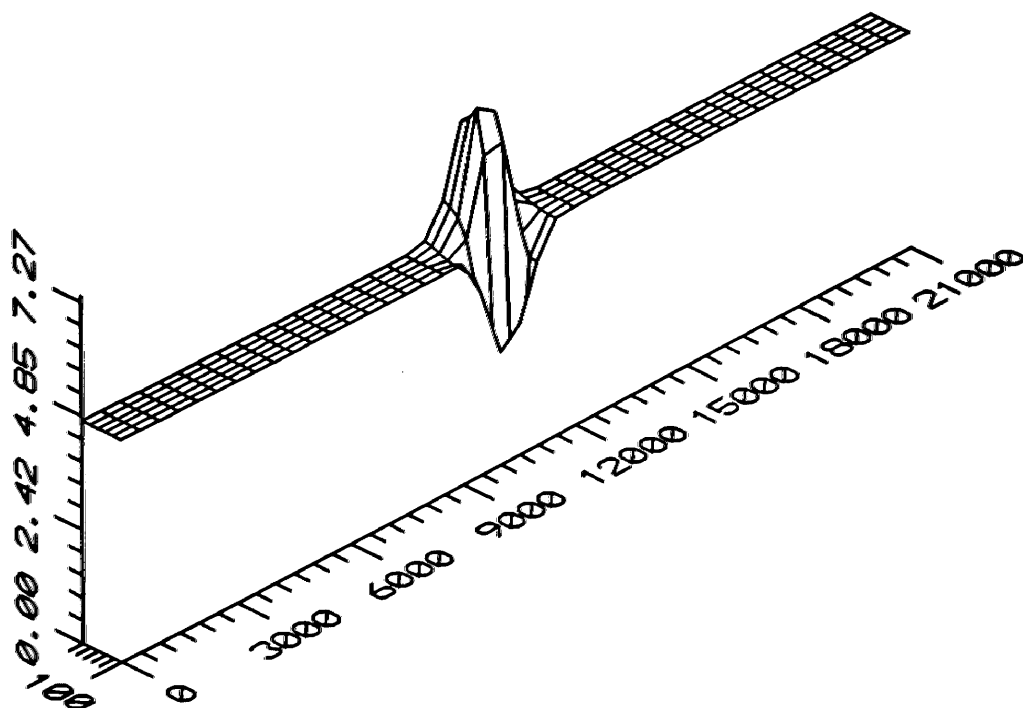
(b) Alternating Grid

Fig. 194. Linear 2DDI Model Three Dimensional Water Surface Elevations for 40% Abutment Reduction with  $EV = 0.0$ , Head = 0.18 Ft, Resolution = 1, and a 12 Second Time Step.



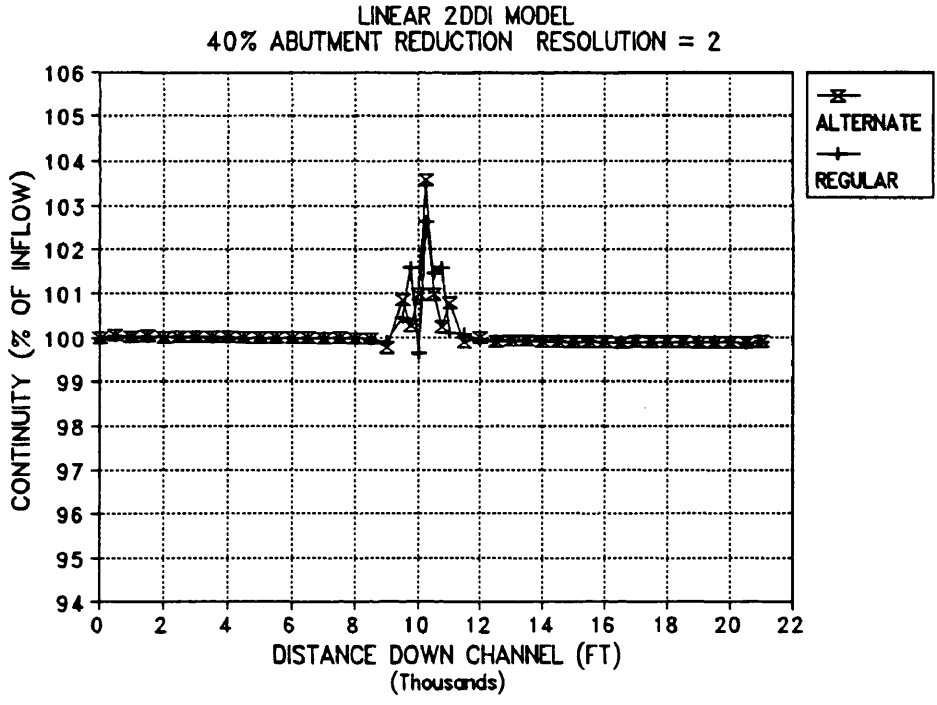


(a) Regular Grid

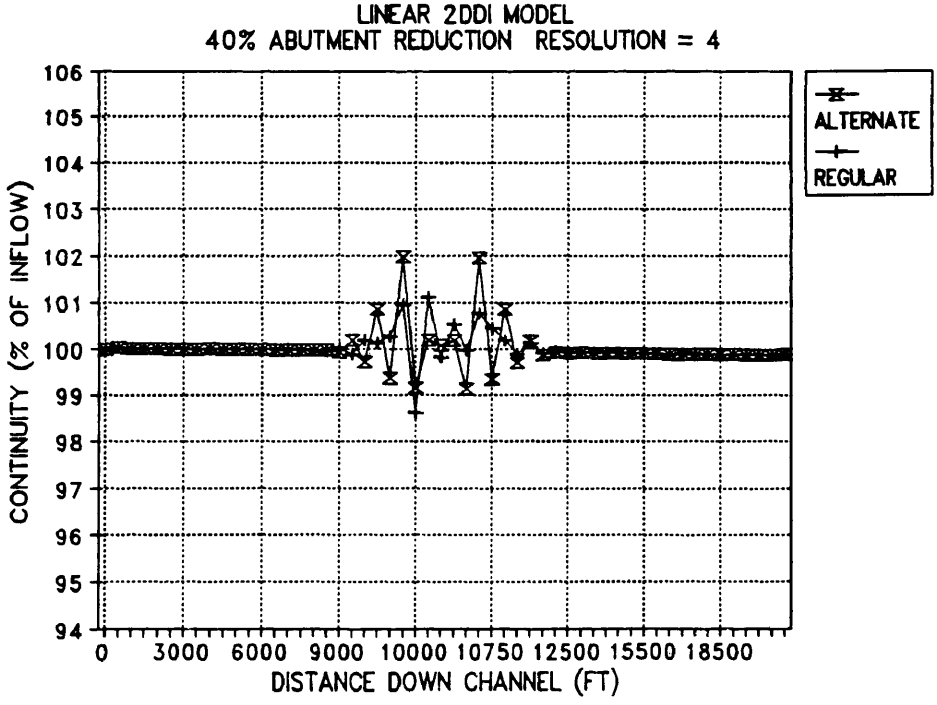


(b) Alternating Grid

Fig. 195. Linear 2DDI Model Three Dimensional Velocity Surface Plots for 40% Abutment Reduction with  $EV = 0.0$ , Head = 0.18 Ft, Resolution = 1, and a 12 Second Time Step.



(a) Resolution = 2



(b) Resolution = 4, X Scale Expanded

Fig. 196. Linear 2DDI Continuity vs Channel Distance for 40% Abutment Reduction with Resolution = 2 and 4, EV = 0.0, Head = 0.18 Ft, and a 12 Second Time Step.

maximum continuity deviation for this test was between 2.8 and 3.7% - a substantial improvement over the single resolution test.

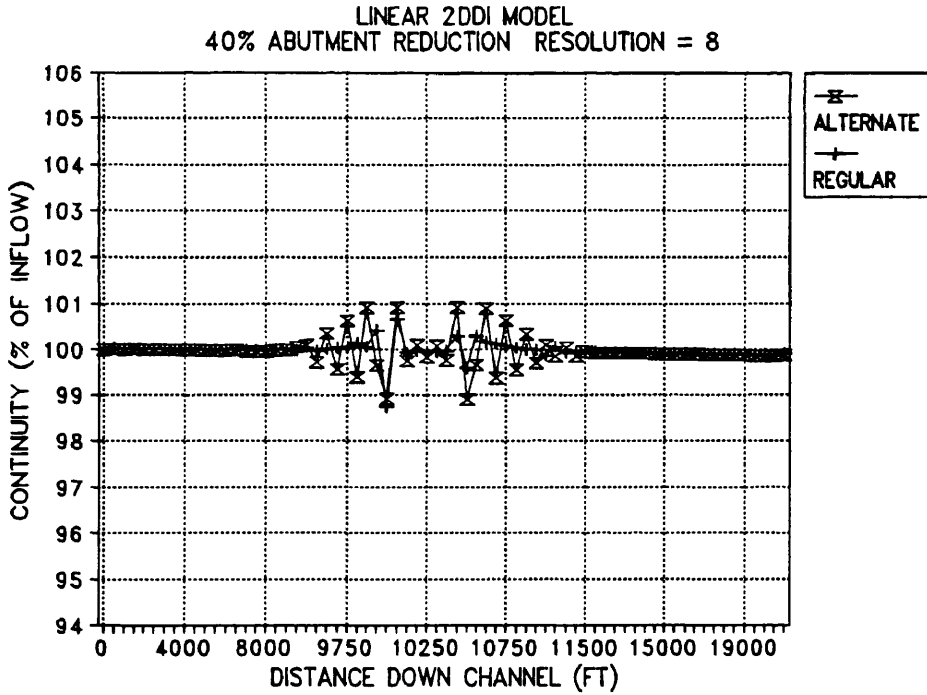
When the resolution was increased to 4 elements (Fig 196(b)) the maximum deviation was reduced to less than 2% for both grids. It should be noted that the x scale is again expanded for resolutions of 4 elements or above.

When the resolution was increased to 8 elements the maximum continuity deviations were reduced to near 1% for both grids as shown in Fig. 197(a). With the increased resolution (4 and 8 elements) distinct oscillation patterns could be seen for both the upstream and downstream ends of the abutment contraction with reduced oscillations through the throat of the contraction.

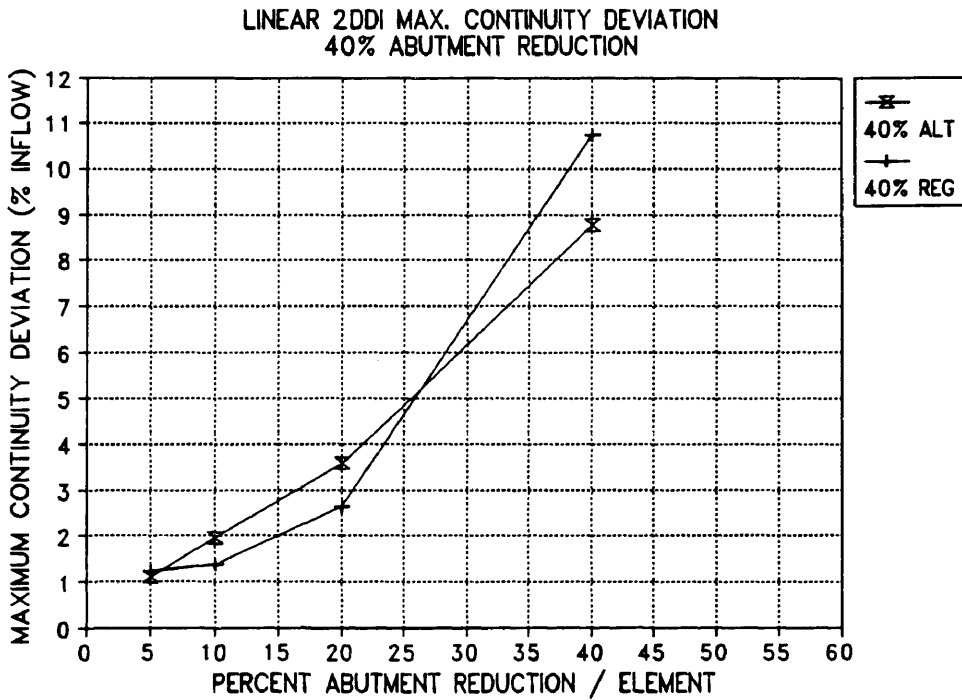
When the maximum continuity deviation was plotted against the percent reduction per element for all of the 2DDI 40% abutment tests, the results in Fig. 197(b) were obtained. It can be seen that there is some differences between grid types at all resolutions except the highest resolution of 8 elements.

The amount of contraction was next varied to 20% and 60% and values were plotted in Fig. 198. The values from the RMA-2V model were also included for comparison. It can be seen that the values for the RMA-2V model was higher at all values but converges to very nearly the same values at resolutions of 8 or above. It can also be noted that the 20% abutment test shows a very strong sensitivity to the amount of contraction and expansion per element. This indicates that even though the amount of contraction is relatively small - even 10% of the total channel width - the importance of proper resolution is very critical. This would also apply where elements are being removed or added by a wetting and drying algorithm.

The channel continuity values for the three values of abutment reduction are shown in Fig. 199. The inversion of

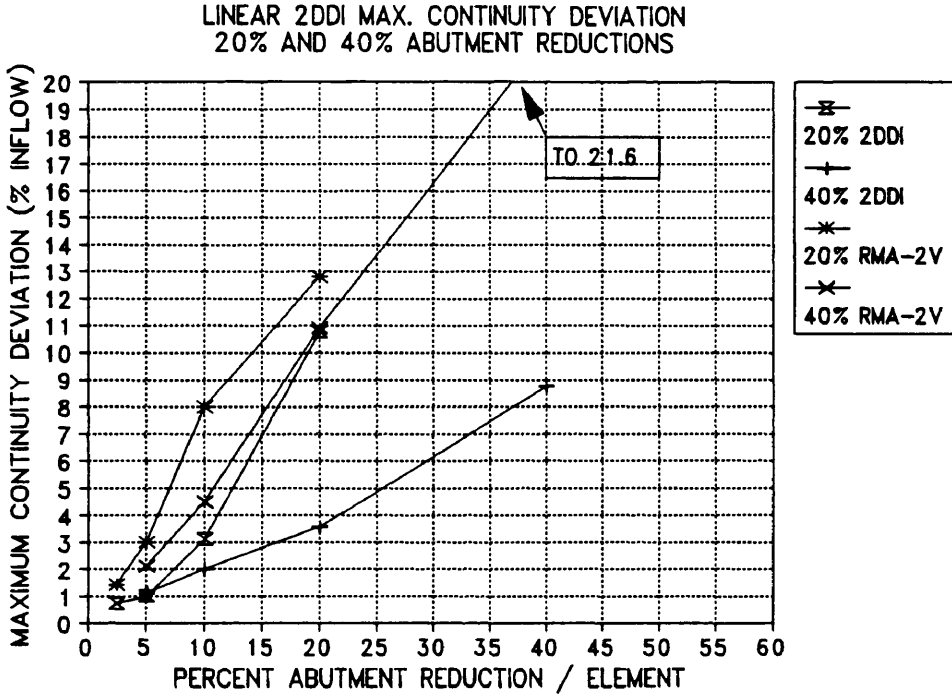


(a) Resolution = 8, X Scale Expanded

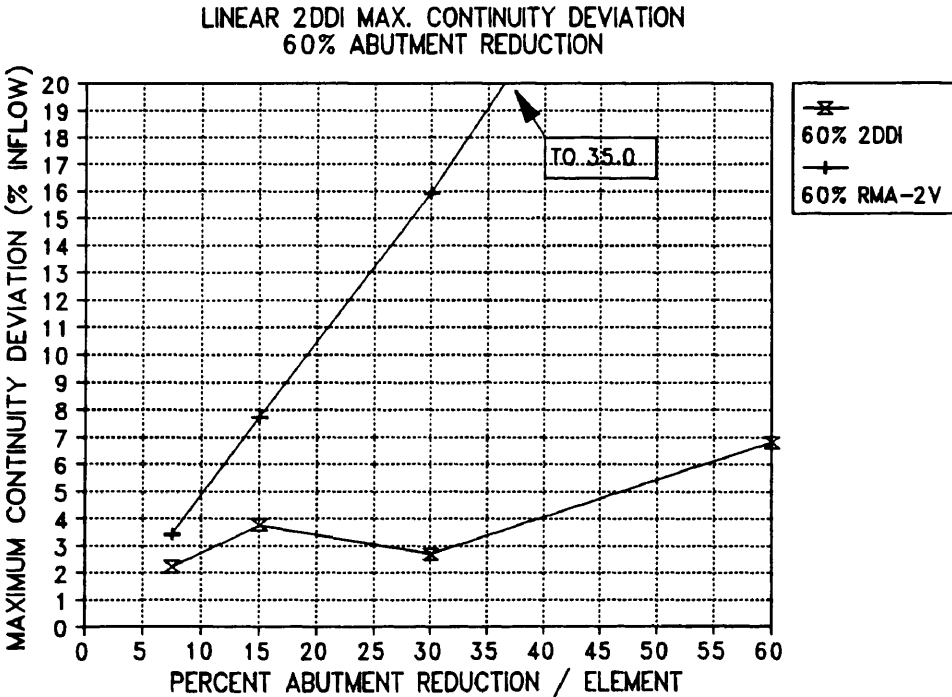


(b) Maximum Deviation for 40% Abutment Reduction

Fig. 197. 2DDI Continuity for Resolution = 8 and Maximum Continuity Deviation for 40% Abutment Reduction with EV = 0.0, Head = 0.32 Ft, and a 12 Second Time Step.

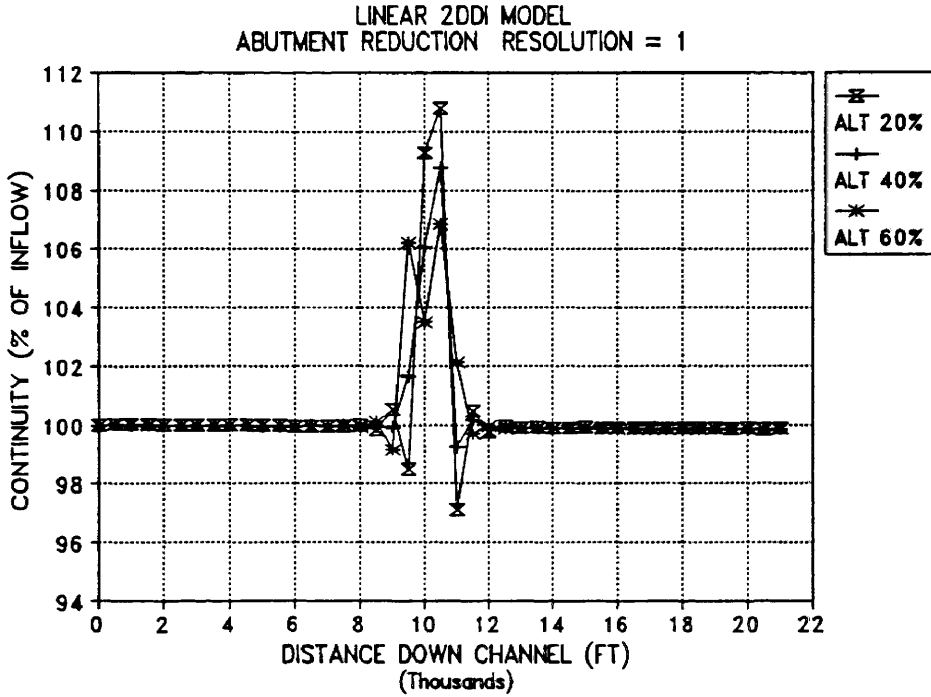


(a) 20% and 40% Abutment Reduction

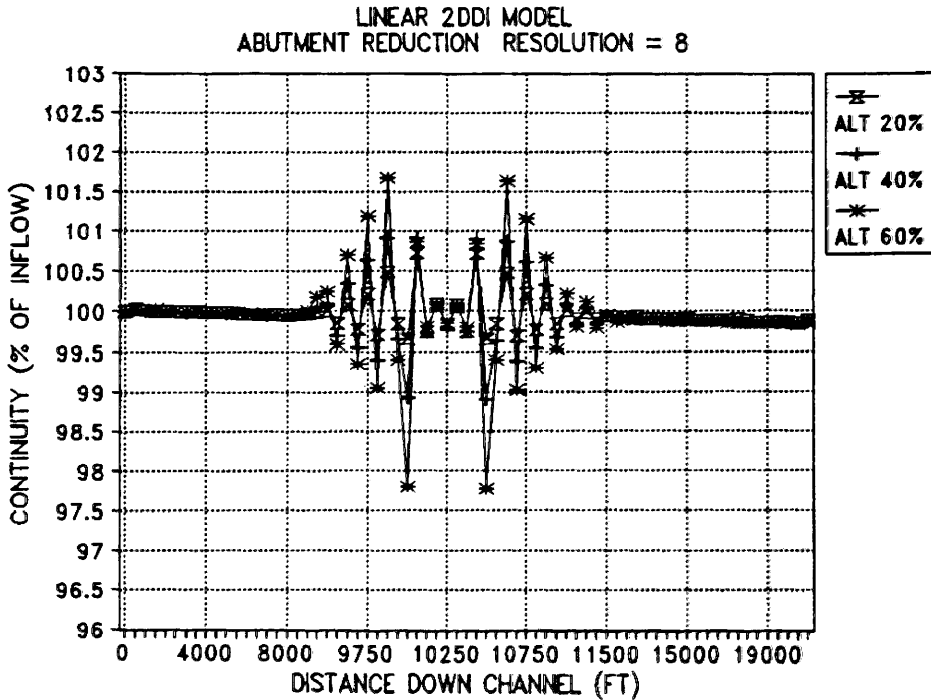


(b) 60% Abutment Reduction

Fig. 198. Linear 2DDI Maximum Continuity Deviation vs Percent Reduction per Element for 20%, 40%, and 60% Abutment Reduction Alternating Grids with EV = 0.0 and a Flow of 500,000 cfs.



(a) Resolution = 1



(b) Resolution = 8

Fig. 199. Linear 2DDI Channel Continuity for 20%, 40%, and 60% Abutment Reduction Alternating Grids, Resolution = 1 and 8, EV = 0.0, and 12 Second Time Steps. X Scale Expanded for Res = 8.

maximum continuity deviation discussed in the sudden expansion section can also be noted here as can the separation of the single continuity oscillation into two distinct oscillations as resolution is increased.

The lack of stability of the non-linear 2DDI model had to this point prevented its successful use for any of the simple test cases and the linear version of the model has been found to be unsuitable due to the lack of the non-linear terms. This stability problem must be addressed prior to any field use of the 2DDI model for problems similar to these tested as simple test cases.

## JOHN L. GRACE, JR. RIPRAP TEST FACILITY

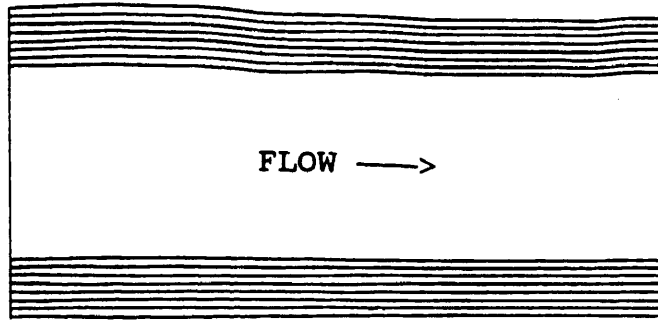
The grid used to represent the John L. Grace, Jr. Riprap Test Facility (riprap facility) was obtained from the work of Abraham (1991). Abraham used the facility to verify the three-dimensional version of RMA-2V known as RMA-10. His grid consisted of 1608 quadrilateral elements with 5117 nodes. The grid was converted to all triangular elements by subdividing each quadrilateral into two triangles. The grids were then manipulated such that the diagonals were aligned in the proper direction for the desired grid type - i.e. regular or alternating.

An additional modification was made to the grids to allow the use of boundary conditions specified by continuity lines for the RMA-2V model. This modification consisted of adjusting nodal elevations at the model inlet and outlet such that none of the nodes on the inlet boundary were above the water surface elevation at any tested flow. The modification amounted to the construction of a headbay and tailbay as shown in Fig. 200 for the inlet and outlet of the test grids. Fig. 200 shows the elevation contours with the top and bottom lines being high and the channel bottom being low. Node locations are shown for the tailbay in Fig. 200(c).

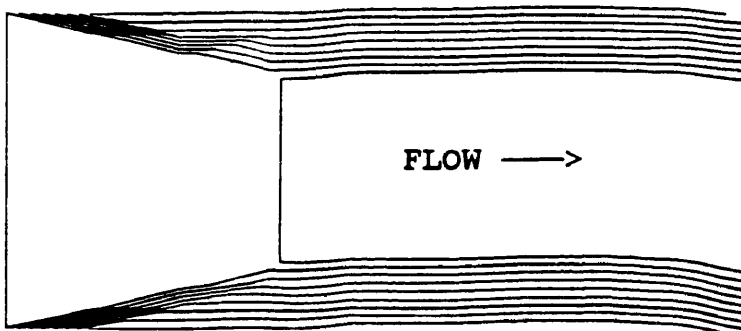
The nodal elevations just downstream were also adjusted for the first three rows for the headbay and upstream for the first four rows for the tailbay to allow a smooth transition from the bays to the trapezoidal section of the riprap test channel.

The grid was initially allowed to wet and dry for the RMA-2V model. This proved to be problematic since small changes in the grid would affect the manner in which the model would wet and dry and cause stability problems in the model. As a result of the wetting and drying problems encountered the elements that would normally be eliminated

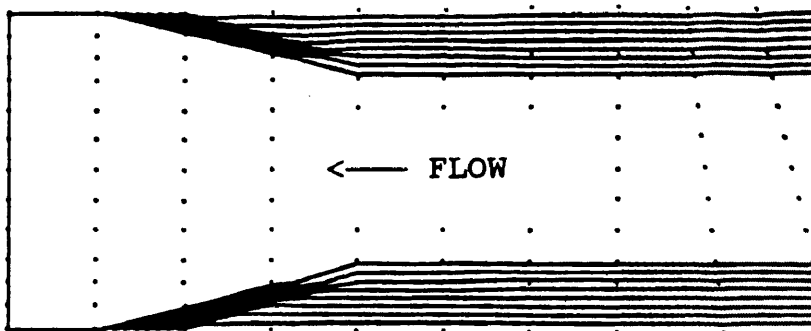




(a) Inlet / Outlet Without Headbay



(b) Inlet with Headbay



(c) Outlet with Tailbay

Fig. 200. Riprap Test Facility Inlet and Outlet Elevation Contours (a) as Modeled by Abraham (1991) Without Headbay or Tailbay, (b) Inlet with Headbay, and (c) Outlet with Tailbay.

by wetting and drying were eliminated from the mesh by either setting the element type to 0 for the RMA-2V model or physically eliminating them for the 2DDI model which does not accommodate wetting and drying.

The RMA-2V and 2DDI models were compared to data obtained from measurements made by Maynard in 1990 at the riprap test facility. The testing process and data limitations are discussed in more detail by Abraham (1991) but measured data were found to be about 5% high based on measured flow in the channel. The reported values used in this study were the "net" values - i.e. the values resulting from the 5% reduction performed by Maynard. The calibrated flowrate was considered to be accurate within  $\pm 2\%$  and water surface elevations within  $\pm 0.01$  feet.

The results obtained by Maynard consisted of velocity measurements in the longitudinal and transverse channel directions at 13 locations along the channel. At each location measurements were taken at up to 15 locations across the channel and up to 15 different depths. Measurements were taken for flow rates of 49.5, 100, and 150 cfs. A flow rate of 49.5 cfs was used in this modeling.

A plan of the facility showing stationing is shown in Fig. 201 and Maynard's longitudinal velocity results at the seventh measured cross section (3+71) are shown in Fig. 202 for a flow of 150 cfs. This data was then depth averaged by summing the flow for each layer measured and dividing by the depth of flow as shown in Fig. 203. This depth averaged velocity data was then used as the standard for comparison for the models.

The RMA-2V model was compared to the observed depth averaged data at the measured cross sections while the 2DDI model was compared to dimensionless velocity data as discussed later in the 2DDI Test Results section. Comparison of the two models used the dimensionless data.

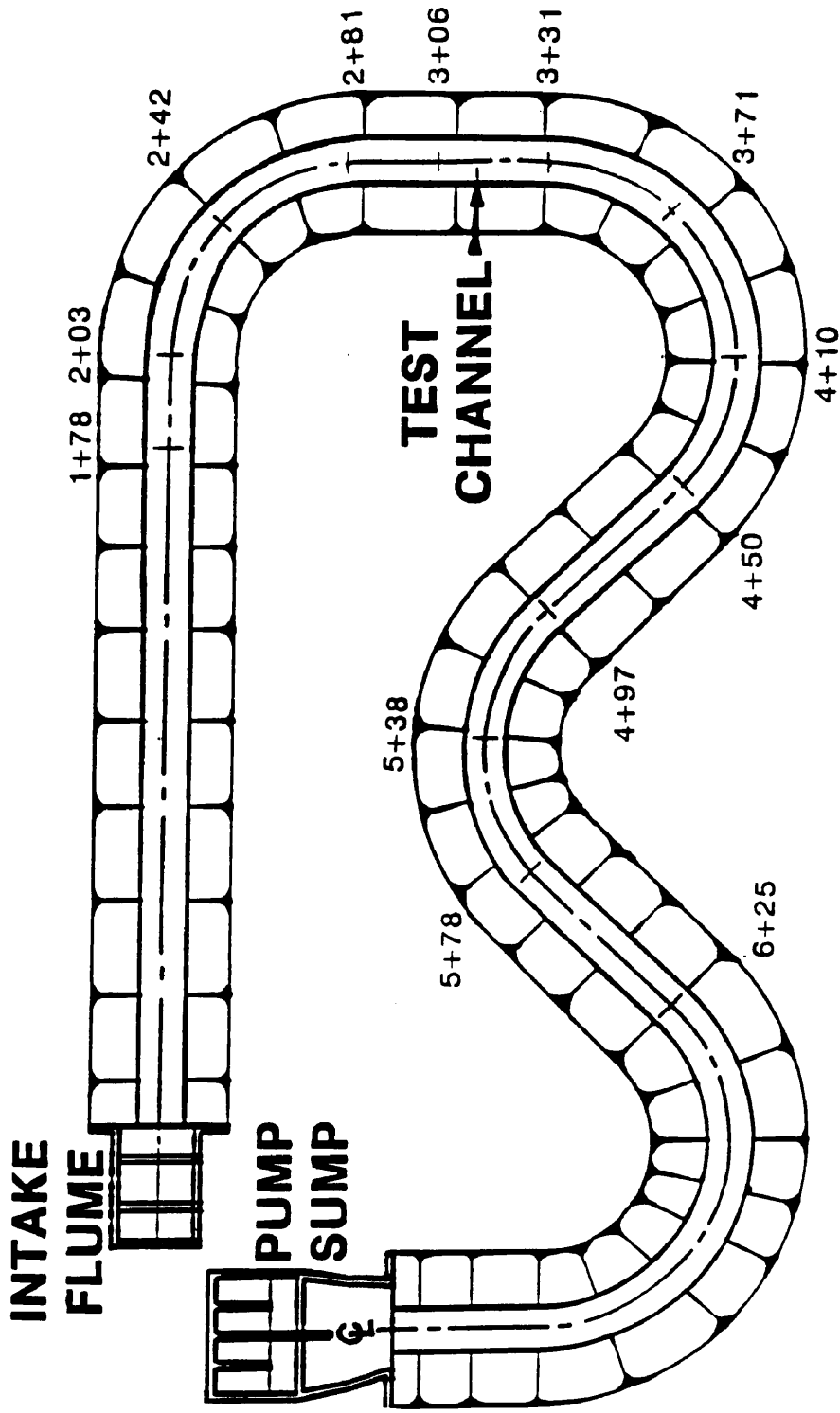


Fig. 201. John L. Grace, Jr. Riprap Test Facility Layout with Location of Cross Sections Where Prototype Data Was Collected. Flow is From Upper Left to Right.

WATER SURFACE ELEVATION = 181.537  
 BOTTOM ELEVATION = 179.12

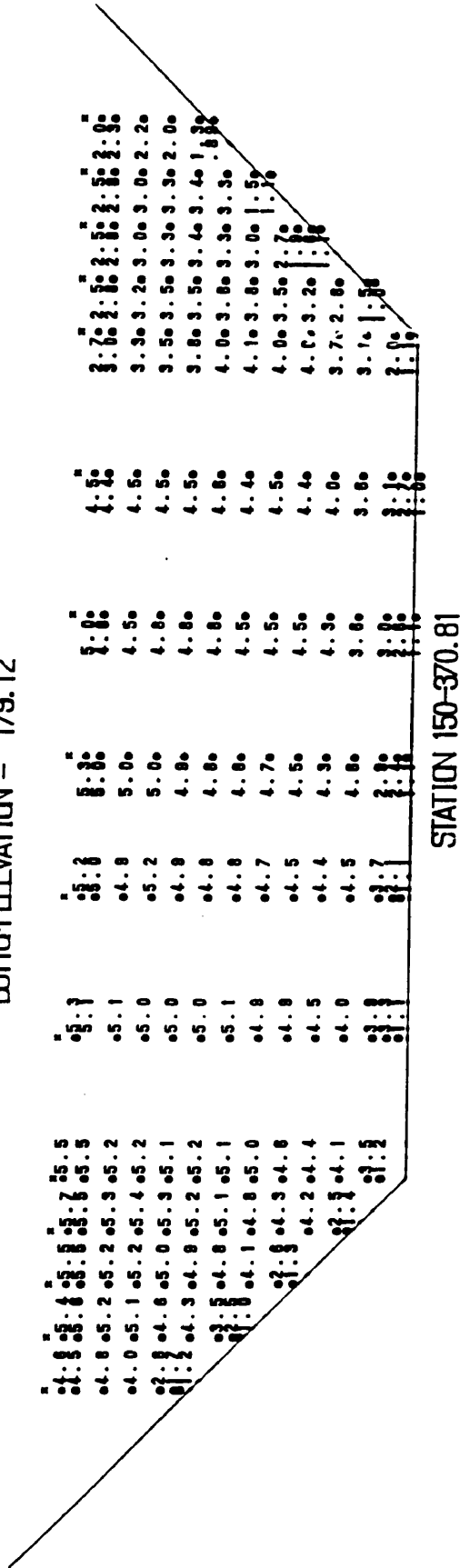


Fig. 202. John L. Grace, Jr. Riprap Test Facility Streamwise Velocity Data Collected by Maynard (1990) for Cross Section at Station 3+71 at a Flow of 150 cfs.

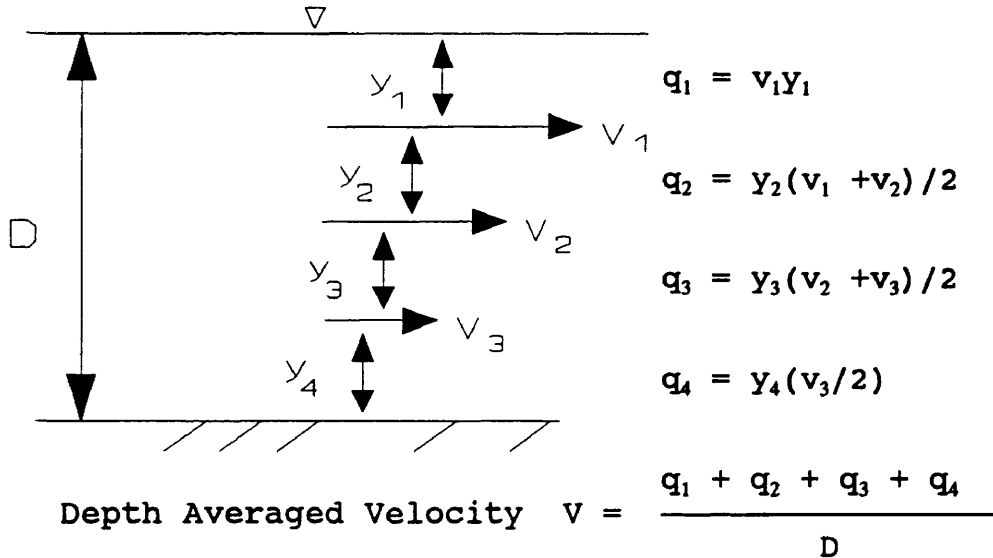
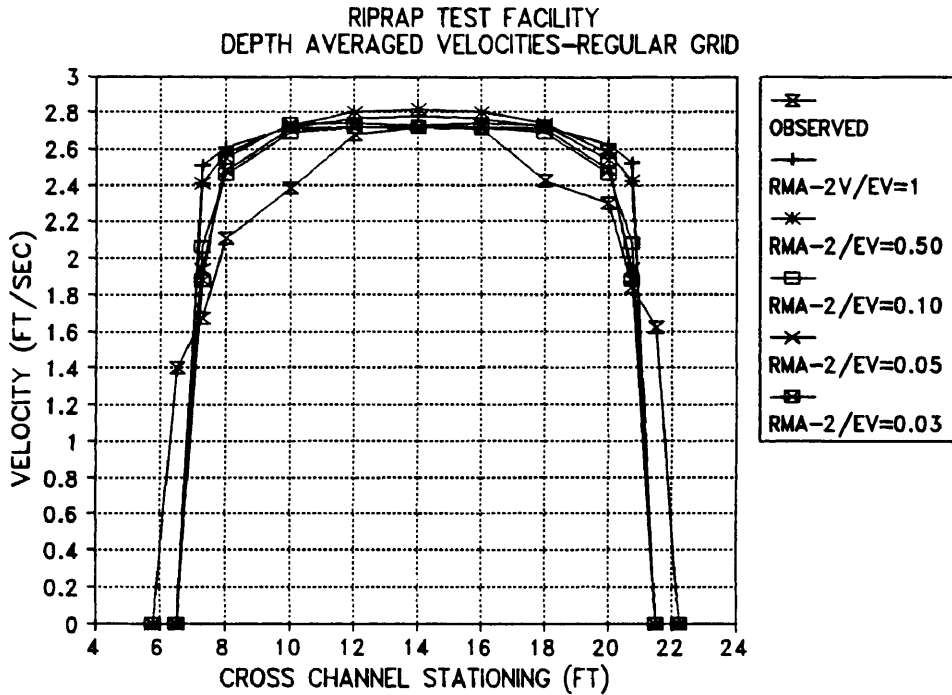


Fig. 203. Method Used by Maynard to Calculate Depth Averaged Velocity from Observed Data Points.

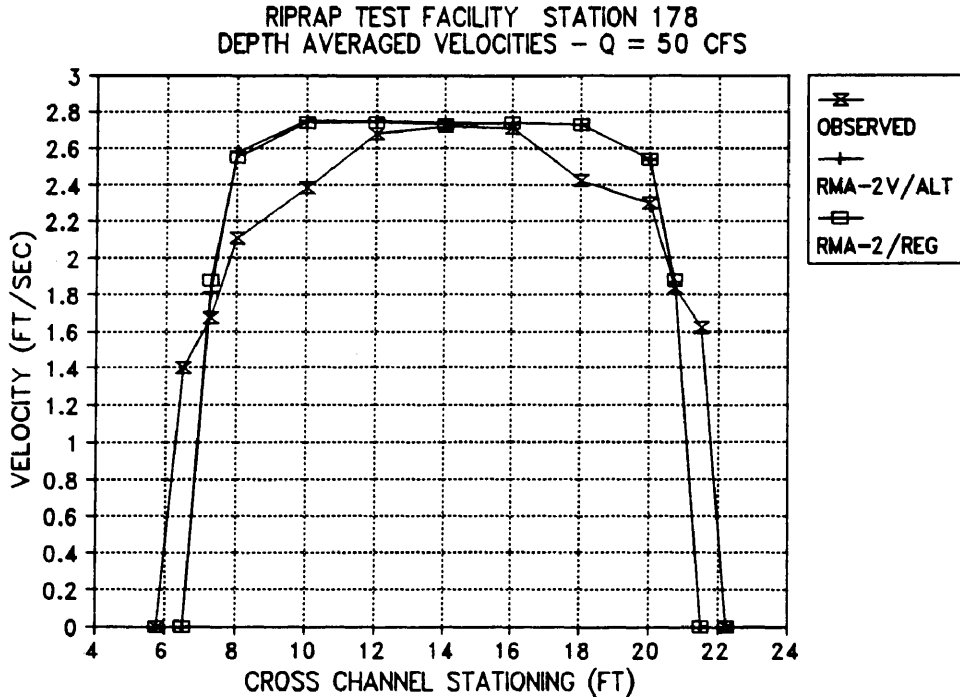
#### RMA-2V RIPRAP TEST FACILITY MODEL RESULTS

The RMA-2V model was calibrated to measured results obtained by Maynard in 1990 by adjusting the Manning's  $n$  value for the channel. Abraham used an  $n$  value of 0.027 as calculated based on the size and distribution of the channel material. Initially Abraham's value for  $n$  was used as well as his EV value of 1.0 which was higher than the value of 0.55 calculated by Vrengdenhil's formula (Equation 29). The lateral velocity distribution for this test with EV = 1.0 and an  $n$  value of 0.027 is compared with observed data at station 1+78 in Fig. 204(a) and is labeled RMA-2V/EV=1. For this test the mid-channel velocities were very near those observed but the velocities near the sides of the channel were much larger than the observed - an indication of an EV that was too high.

Since Vrengdenhil's value was significantly lower than the value used by Abraham an EV value of 0.50 was used to see if a closer match between observed and calculated data



(a) Variable EV with Regular Grid



(b) Regular and Alternating Grids at EV = 0.03

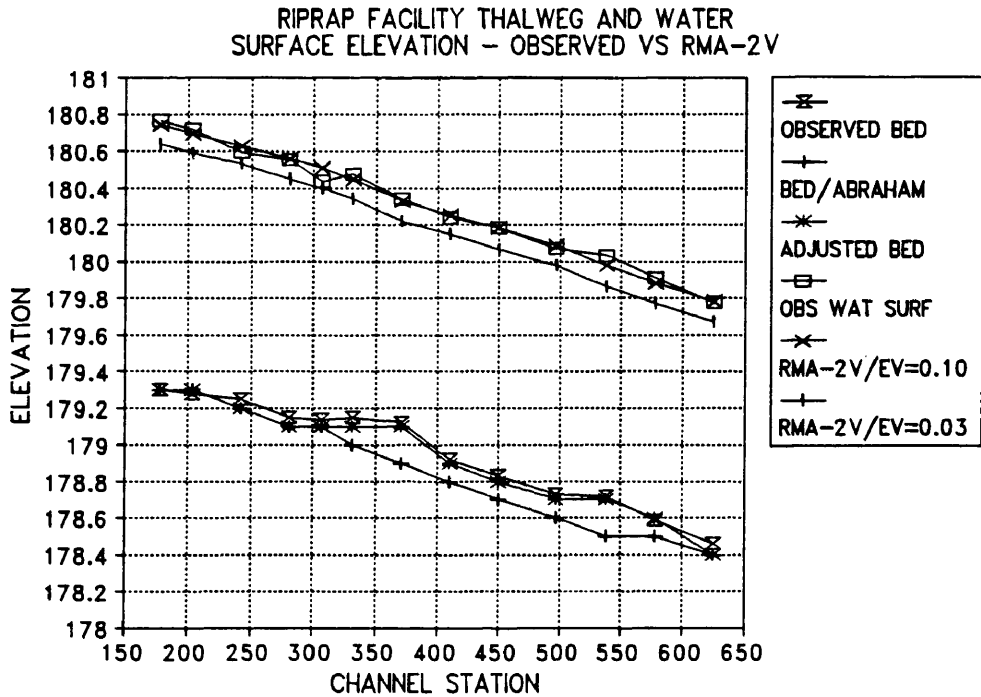
Fig. 204. RMA-2V Riprap Test Facility Lateral Velocity Distribution at Station 1+78 for Flow of 50 cfs with Observed and Calculated Data for Variable EV.

could be obtained. This resulted in the data labeled RMA-2V/EV=0.5 in Fig. 204(a). This produced a slightly improved match between the calculated and observed data. As a result of this test the model was set to automatically continue lowering EV until the model became unstable and aborted.

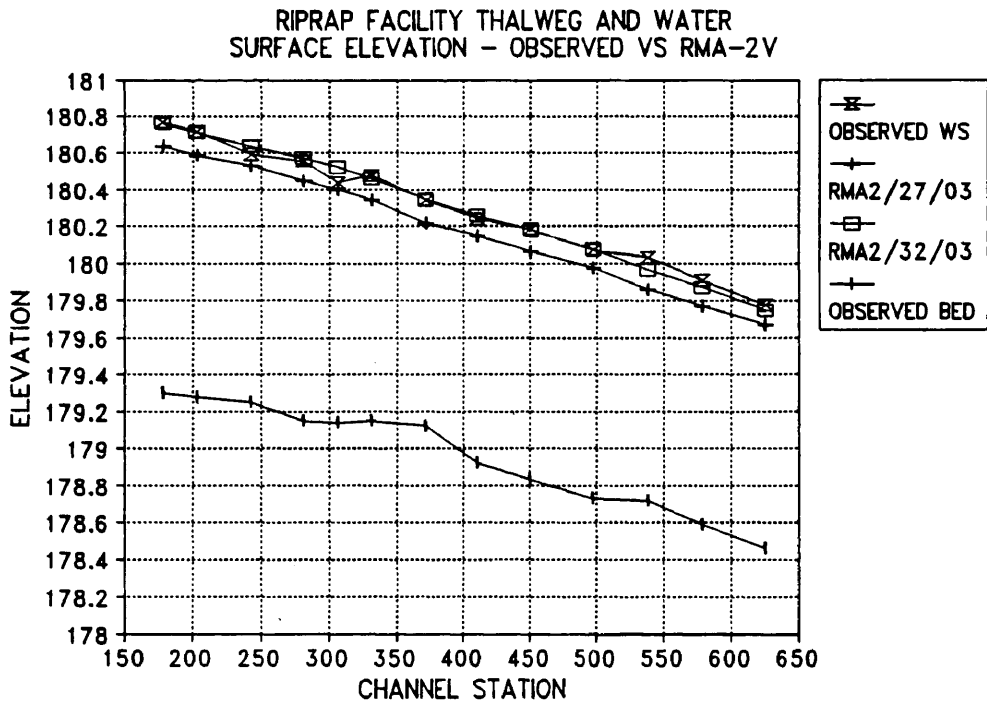
The model was stable until an EV of 0.03 was reached. Below this value the model could not converge for either the alternating or the regular grids. Lateral velocity values are also shown in Fig. 204(a) for EV values of 0.10, 0.05, and 0.03. The results showed that while the velocity in the center of the channel changed only slightly the velocity near the edges of the channel was modified significantly by the lowering of EV. At the lowest stable EV of 0.03 there is a good match between observed and calculated data with the exception of the at the toe of the channel side slopes and at the next node toward the center of the channel. The calculated velocity of 0.0 at the outside nodes where significant velocities exist in the prototype is the result of the elimination of the outer row of nodes due to drying of the elements.

The performance of the regular and alternating grids were compared at station 1+78 as shown in Fig. 204(b) for an EV of 0.03 at the 49.5 cfs flow rate. The grids perform almost identically with the exception of the area near the left outer bank where a slight difference in velocity exists at stations of 6.25 and 7.5 feet from the side of the channel. The flow values shown in figures in this section have been rounded up to 50 cfs but are actually run at 49.5 cfs.

Center line water surface elevations at stations from 1+78 to 6+25 were also used to check the model performance based on an n value of 0.027 as suggested by Abraham for EV values of 1.0 to 0.03. The water surface elevations varied significantly as EV was lowered as shown in Fig. 205(a). The bed elevations for the prototype as well as those used



(a) Variable EV with  $n = 0.027$  with Bed Elevations



(b) Variable Manning's  $n$  with  $EV = 0.03$

Fig. 205. RMA-2V Riprap Test Facility Water Surface and Bed Elevations for Variable EV and Manning's  $n$  Value for Regular Grid vs Observed Data.

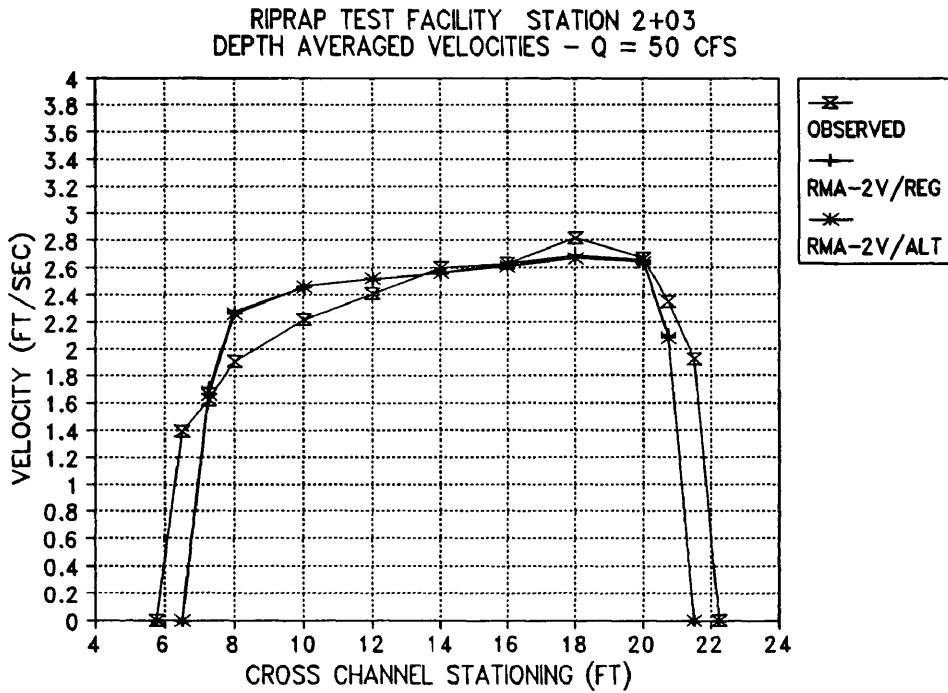


for this model and by Abraham are also shown in Fig 205(a). Abraham's bed elevations variance from the observed elevations is probably due to the grid generation routine used to produce his grid and were adjusted prior to this study.

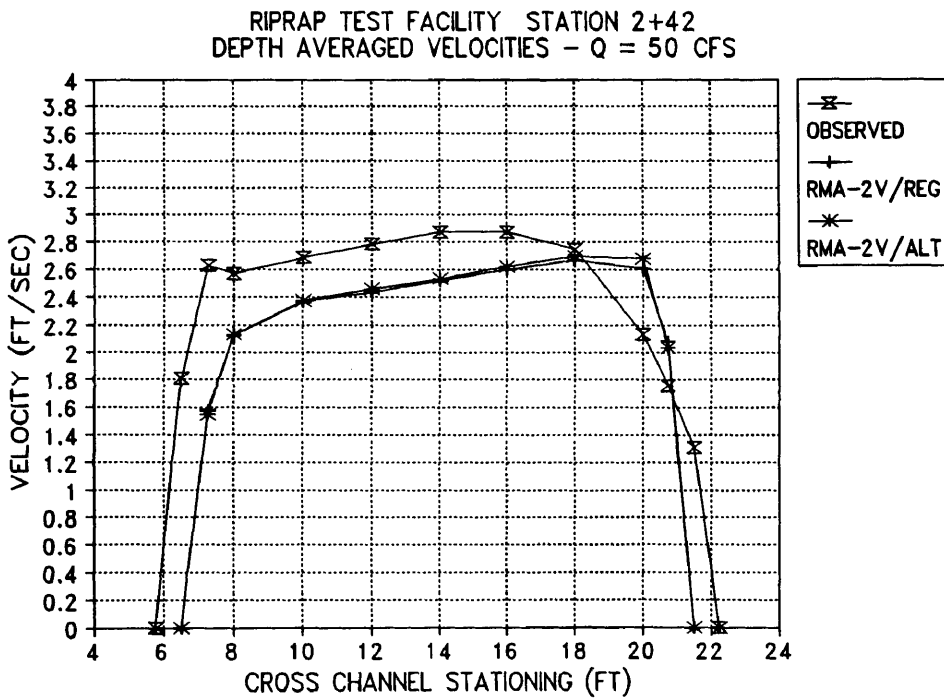
When the value of EV was reduced to 0.03 - the best match for lateral velocity distribution - the water surface elevation was significantly lower than the observed data (Labeled RMA-2V/EV=0.03 in Fig. 205(a)). The correction of this water surface problem required increasing the Manning's n value of the channel from 0.027 to 0.032. The water surface elevations for the 0.027 and 0.032 tests are shown in Fig. 205(b) as well as the observed water surface elevation. No difference in water surface elevations at the nodes selected could be noted between the alternating and regular grids for the test with EV = 0.03 and a Manning's n of 0.032.

Velocity values at all cross section where measured data was taken were next compared for the RMA-2V model. Calculated and observed values for stations 2+03, 2+42, 2+81, 3+06, 3+31, 3+71, 4+10, 4+50, 4+97, 5+38, 5+78, and 6+25 are shown in Figs. 206 to 211. In reviewing the plots it can be noted that the as the flow approaches the bend (stations 2+03, 3+31, 4+97, and 6+25) the calculated flows match the observed flow patterns very well except where the flow is still effected by an upstream bend (stations 4+97 and 6+25). Even for these cross sections the basic form of the flow pattern is obtained from the RMA-2V model but peak velocities are lower in the model than the observed values.

When the flow reaches the 45° point in the bend (stations 2+42, 3+71, and 5+38) the RMA-2V model still does a good job of producing the basic shape of the lateral velocity distribution. The calculated velocity pattern, however does tend to hold to the inside of the bend more than the observed data - a problem that is typical of two-

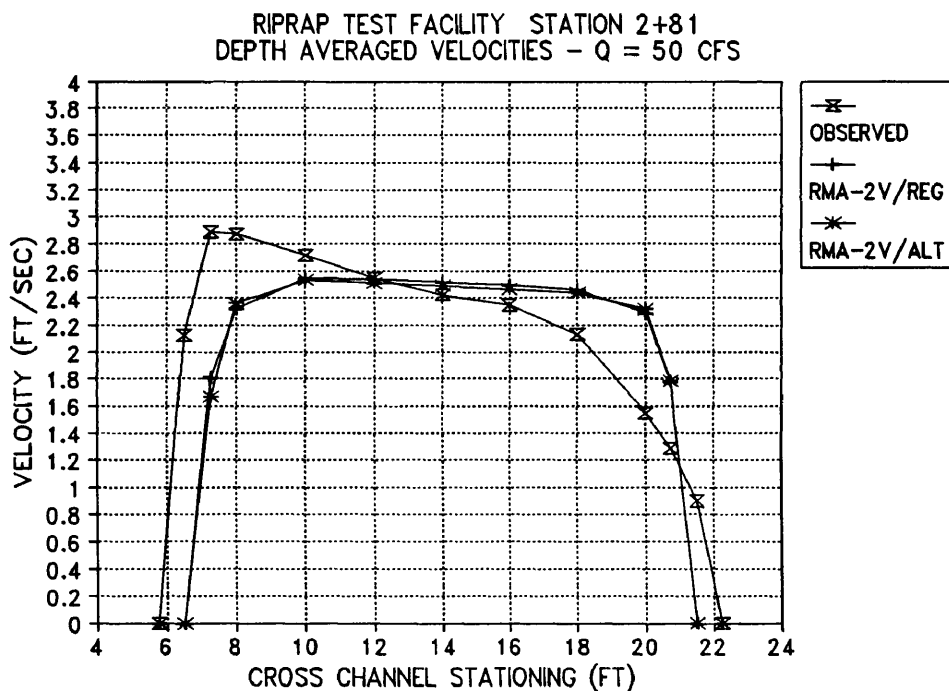


(a) Station 2+03

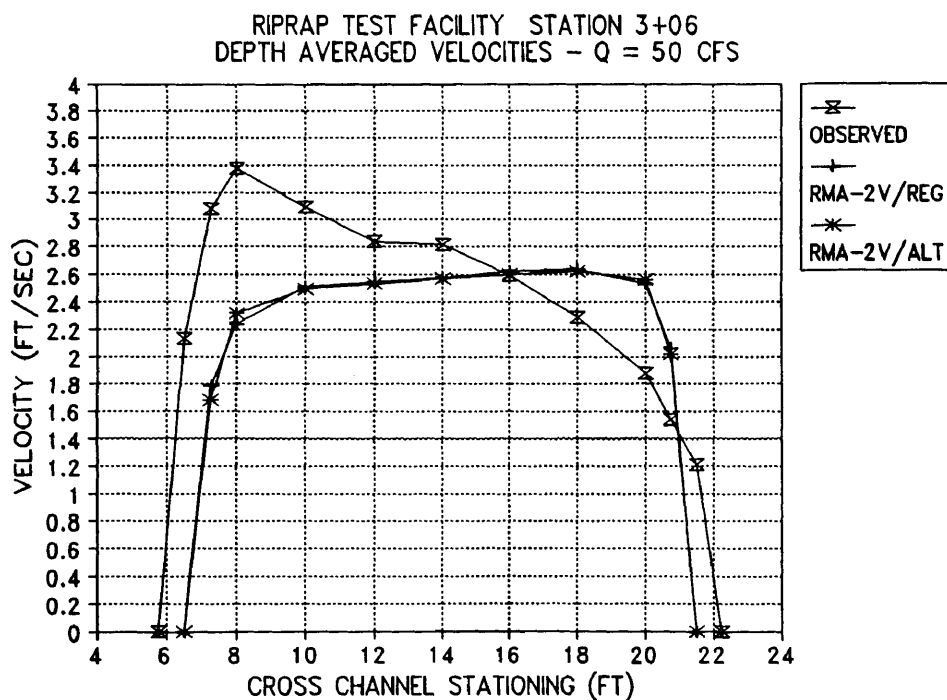


(b) Station 2+42

Fig. 206. RMA-2V Calculated Velocity vs Observed Data for Riprap Test Facility at Stations 2+03 and 2+42 with Flow of 50 cfs,  $n = 0.032$ , and  $EV = 0.03$ .

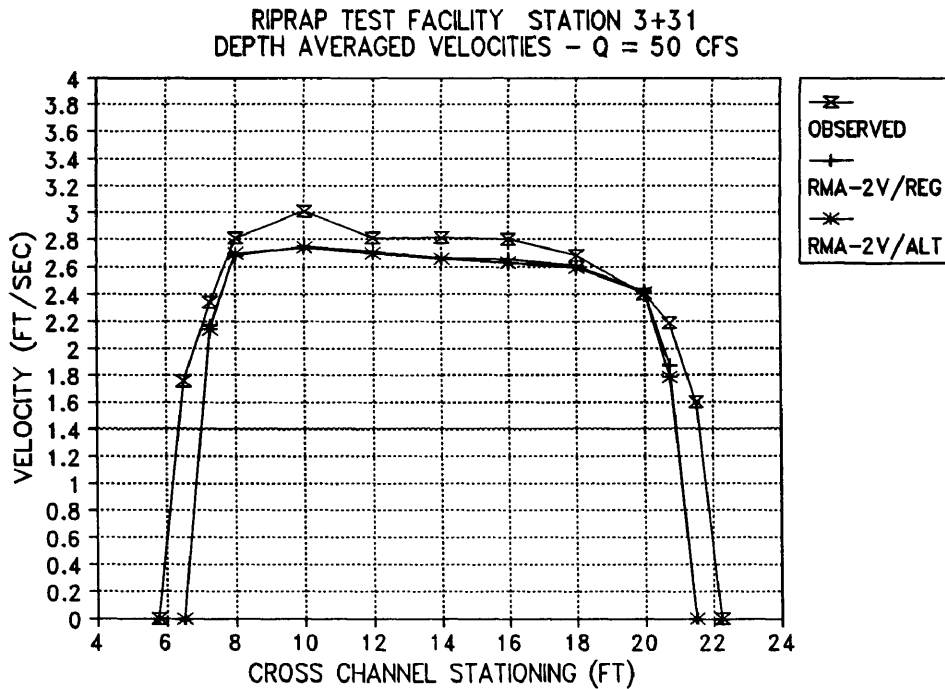


(a) Station 2+81

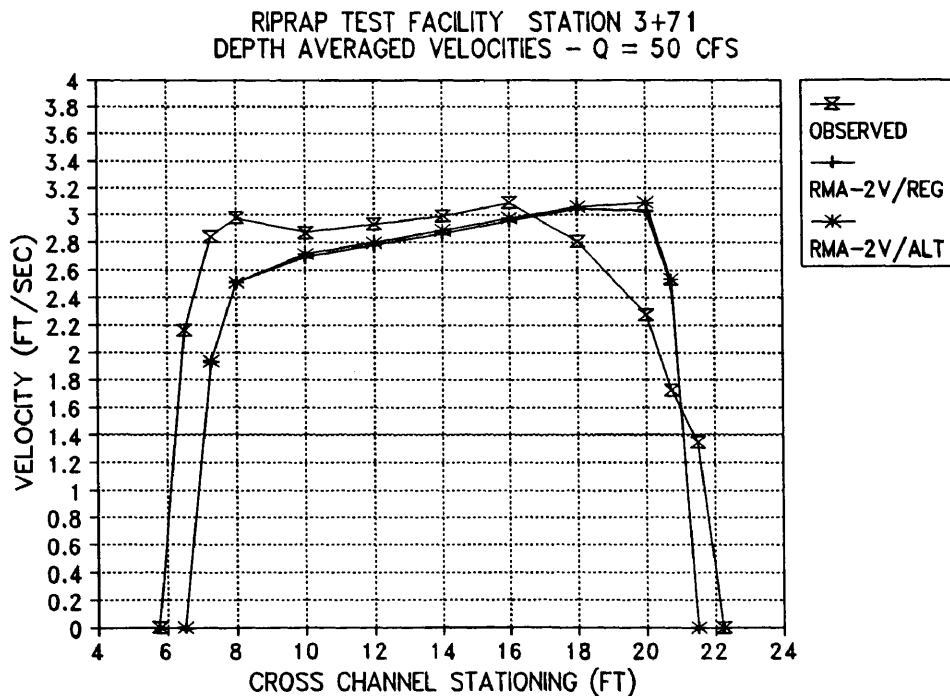


(b) Station 3+06

Fig. 207. RMA-2V Calculated Velocity vs Observed Data for Riprap Test Facility at Stations 2+81 and 3+06 with Flow of 50 cfs,  $n = 0.032$ , and  $EV = 0.03$ .

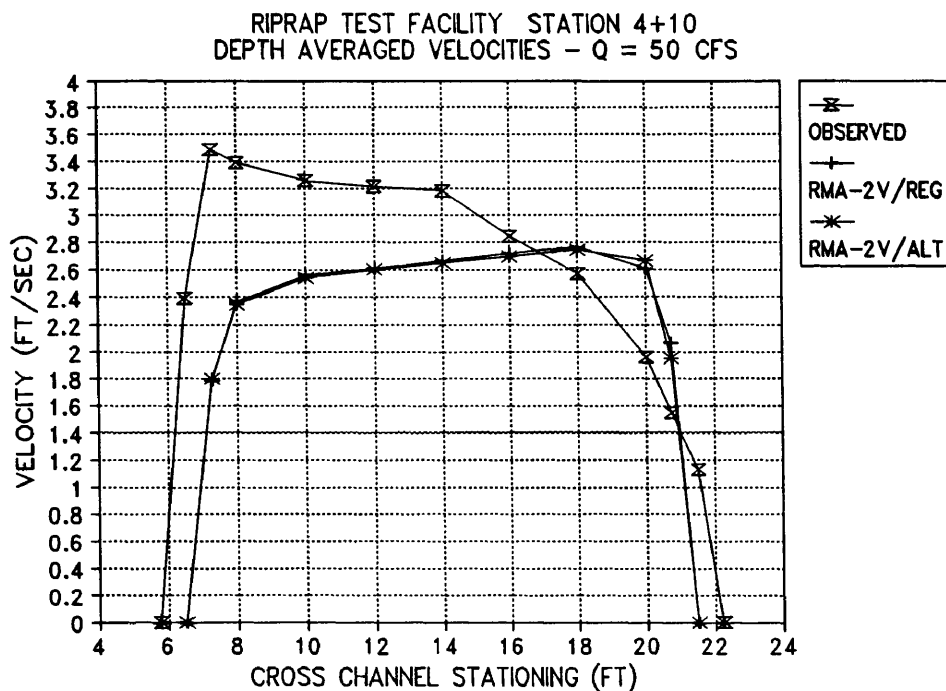


(a) Station 3+31

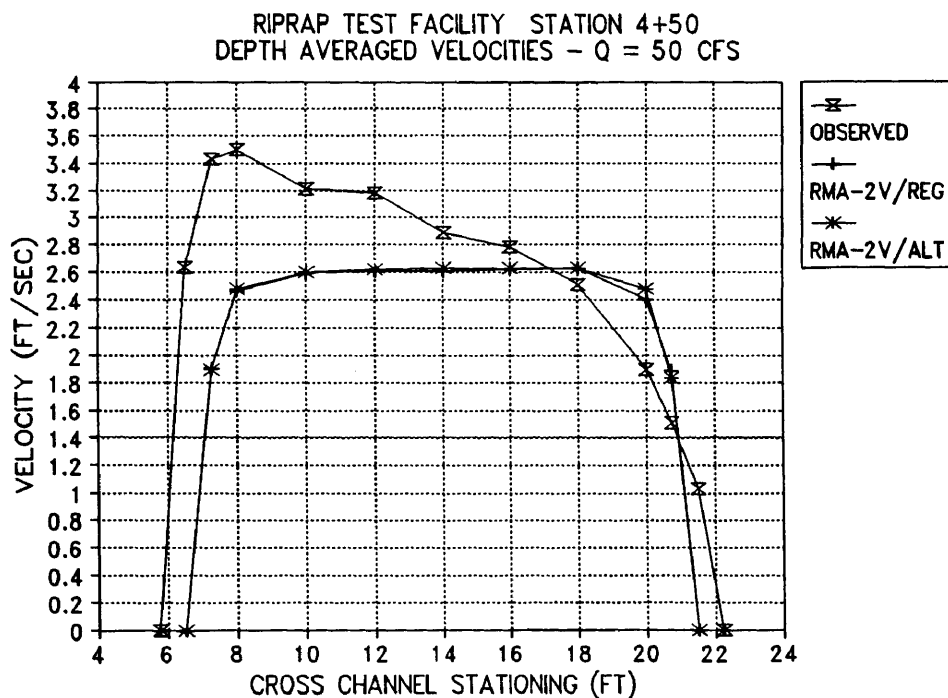


(b) Station 3+71

Fig. 208. RMA-2V Calculated Velocity vs Observed Data for Riprap Test Facility at Stations 3+31 and 3+71 with Flow of 50 cfs,  $n = 0.032$ , and  $EV = 0.03$ .

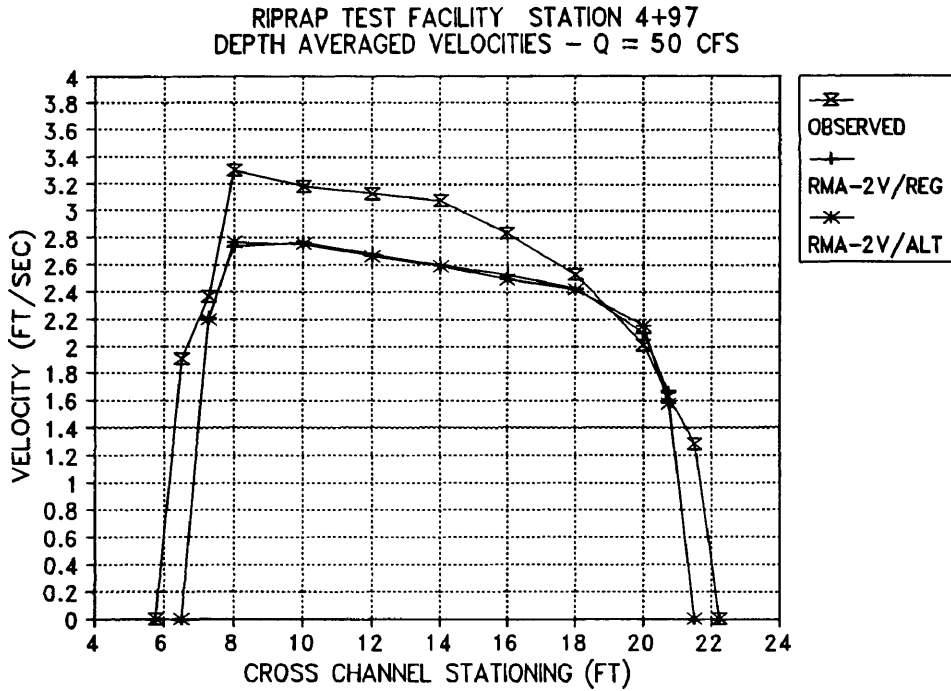


(a) Station 4+10

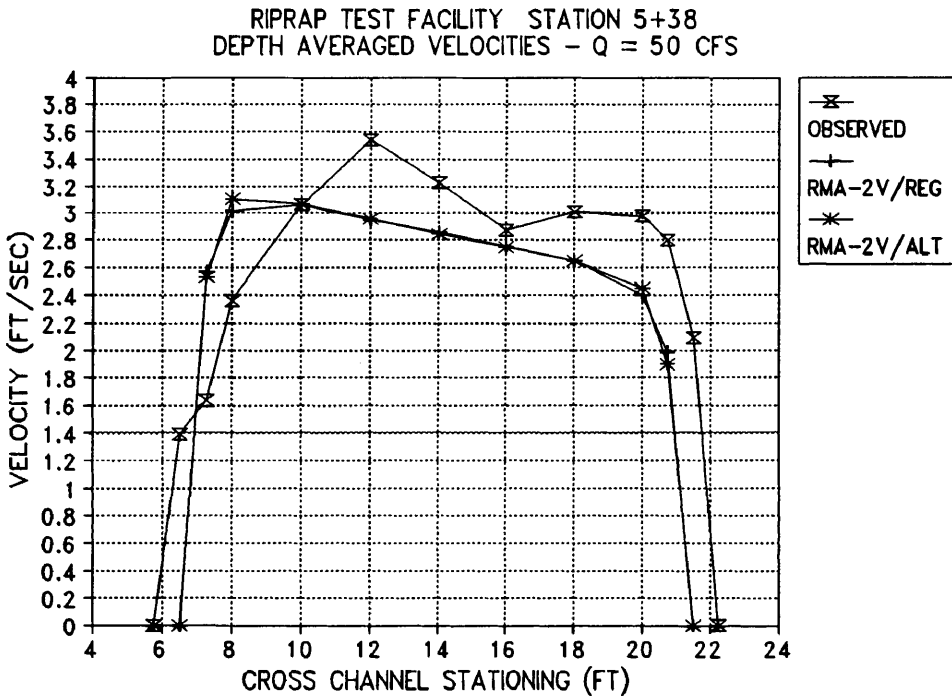


(b) Station 4+50

Fig. 209. RMA-2V Calculated Velocity vs Observed Data for Riprap Test Facility at Stations 4+10 and 4+50 with Flow of 50 cfs,  $n = 0.032$ , and  $EV = 0.03$ .

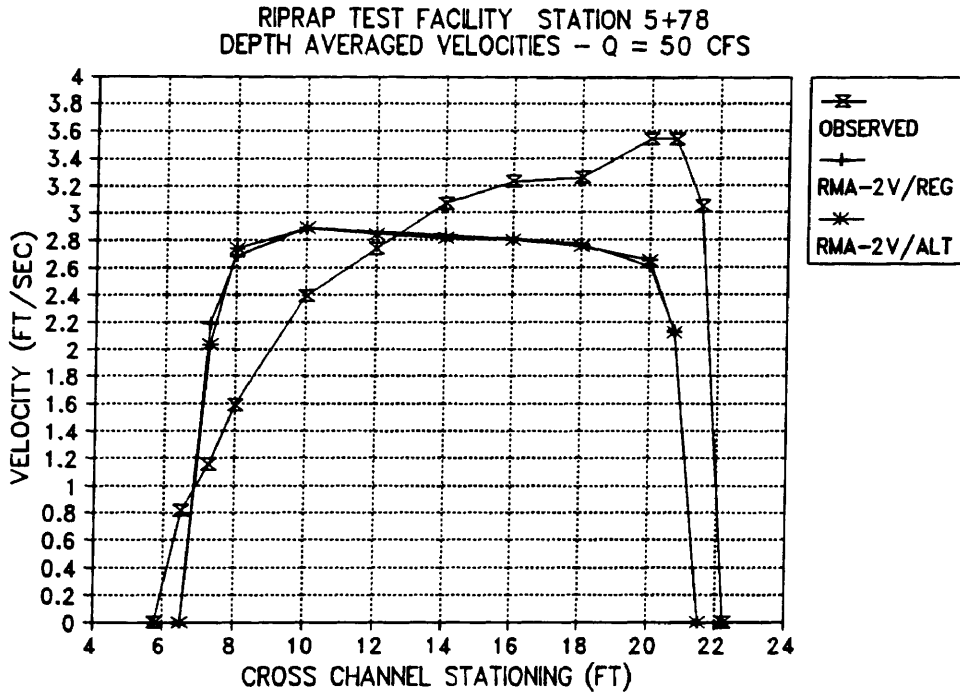


(a) Station 4+97

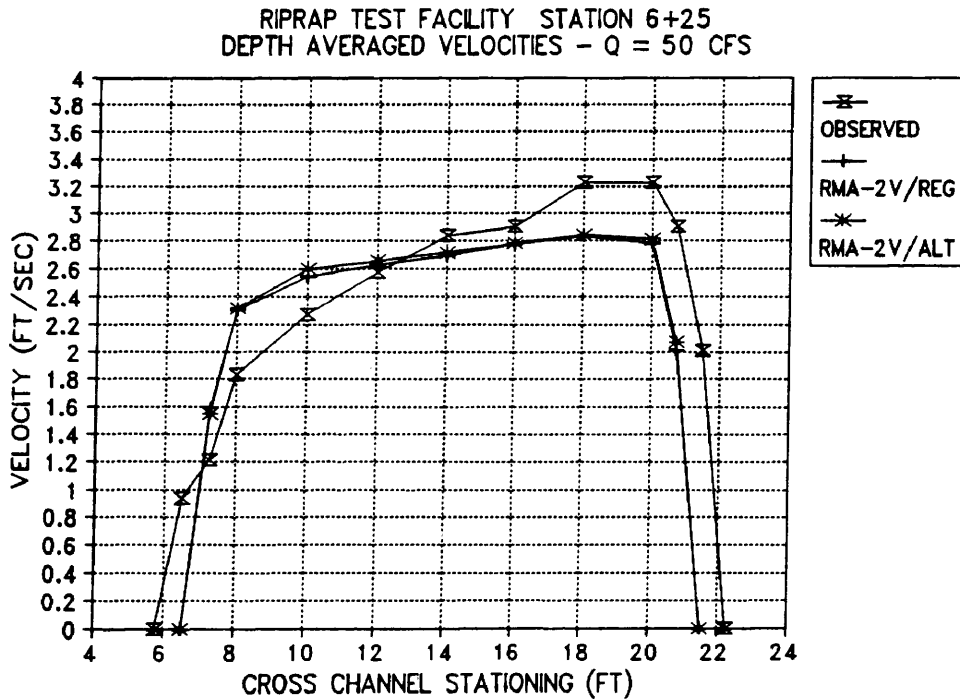


(b) Station 5+38

Fig. 210. RMA-2V Calculated Velocity vs Observed Data for Riprap Test Facility at Stations 4+97 and 5+38 with Flow of 50 cfs,  $n = 0.032$ , and  $EV = 0.03$ .



(a) Station 5+78



(b) Station 6+25

Fig. 211. RMA-2V Calculated Velocity vs Observed Data for Riprap Test Facility at Stations 5+78 and 6+25 with Flow of 50 cfs,  $n = 0.032$ , and  $EV = 0.03$ .

dimensional models. An attempt is currently underway to incorporate a bendway corrector developed at the Waterways Experiment Station by Dr. Robert S. Bernard (1992) which shows promise in allowing the flow to shift to the outside of the bend as a result of secondary currents.

As the flow continues around the bend to the 90° position (stations 2+81, 4+10, and 5+78) the flow in the RMA-2V model resumes a nearly uniform flow for the 90° while the flow in the prototype moves to the outside of the bend. For the 135° bends the RMA-2V model has the peak velocities on the inside of the bend while the observed values are on the opposite side of the channel from the calculated values - the RMA-2V model being clearly in error.

Continuity was calculated for each row of corner nodes in the model and the values for both the regular and alternating grids are shown in Fig. 212. The two grids

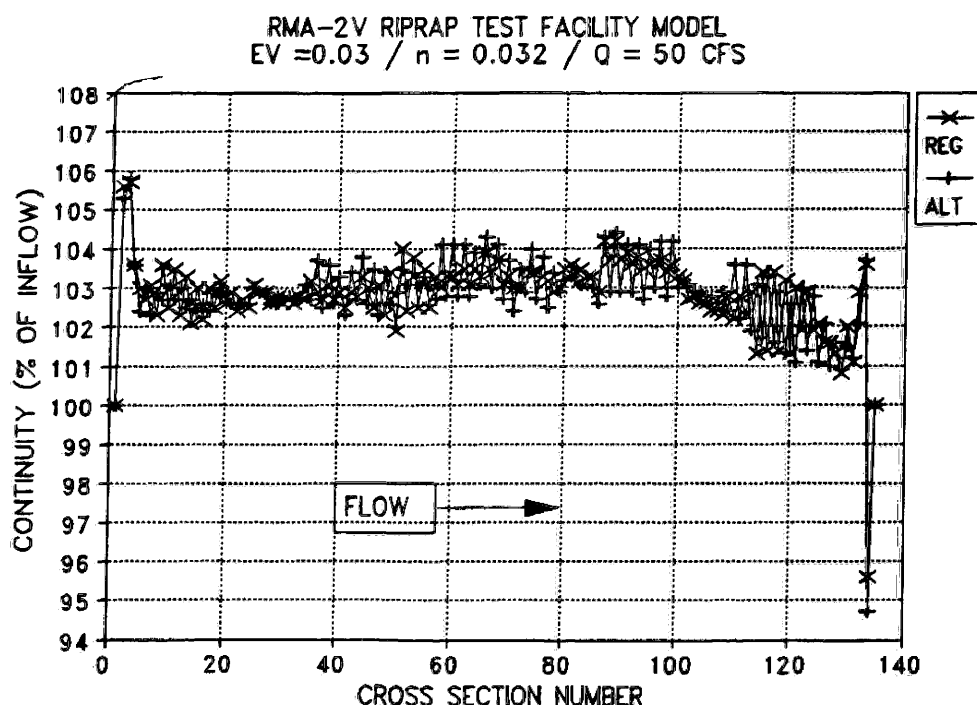


Fig. 212. RMA-2V Riprap Test Facility Model Continuity at Each Corner Node Row for Regular and Alternating Grids with EV = 0.03, Manning's  $n = 0.032$ , and Flow = 50 cfs.



performed similarly with some differences in continuity values at specific cross sections. The continuity drift in the model is at least in part due to the lack of parallel flow into the model. It can be noted that at all cross sections where flow is not parallel to the boundaries (sections 1, 2, 3, 132, 133, 134, and 135) the continuity values differ by significant amounts from the rest of the cross section values. If the inflow headbay had been constructed similar to the tailbay and allowed water to flow uniformly into and out of the model the continuity drift noted in Fig. 212 probably would have been avoided.

## 2DDI RIPRAP TEST FACILITY MODEL RESULTS

The 2DDI grids for the riprap test facility were identical linear versions of those used for the RMA-2V model. The boundary condition file for the riprap test facility model was modified in accordance with guidelines given in the program's User's Manual.

According to guidance in the manual the value for  $\tau$  was set to 0.020 - slightly higher than the estimated maximum of 0.0167. The maximum time step for the fully non-linear model was calculated to be 0.4 seconds. Since the time step was so short the length of simulation was shortened to 0.25 days with a 0.1 day ramp length.

The non-linear model was run initially with a head of 0.02 ft. The actual head difference from the riprap test facility for a flow rate of 50 cfs is 1.79 ft. The model could not be made to converge for this test although the addition of lateral diffusion did appear to stabilize the model and allow the model to run for a longer time prior to aborting.

The non-linear model aborted due to instabilities at the model inflow. This appears to be a typical failure pattern for the non-linear model when velocities at the

boundary become significant and no channel obstructions are present.

Since the fully non-linear model could not be made stable by any adjustment of EV or time step for the 0.02 ft head the linear version of the model was then run. As a result of previous tests it was already apparent that the linear model would not reproduce the variation of currents from one side of the channel to the other as would be necessary to reproduce the observed currents. This model was also in obvious violation of the finite amplitude assumption as the change water surface elevation at the lower end of the model was larger than the depth from the water surface to the channel bottom when the ramp up process was complete. In spite of these facts the model was run in the linear model to see if the model would converge.

The model was run with identically the same boundary conditions except the model head was increased to 1.6 feet - near the observed value of 1.79 feet. At this value the model would again not converge but did run to the completion of the simulation at 0.25 days. Vector plots were made at the end of the simulation (6.0 hours) and at the end of the ramp (2.5 hours) and shown very nearly identical behavior. The vector plot for the model at 2.5 hours into the simulation is shown in Fig. 213. The problems with model stability apparently occurred early in the model run and appeared to be amazingly constant in magnitude for the remainder of the simulation.

In an attempt to make the model reproduce some type of useable results for the riprap facility test, the head on the NON-LINEAR model was increased to 1.79 feet. This run was again unstable and aborted shortly after the flow rate reached about 2.2 cfs or 4.4% of the desired flow. The two dimensional velocity vectors were plotted for this run with EV = 0.001 and are shown in Fig. 214. The total velocity values for nodes on the inflow boundary are plotted with

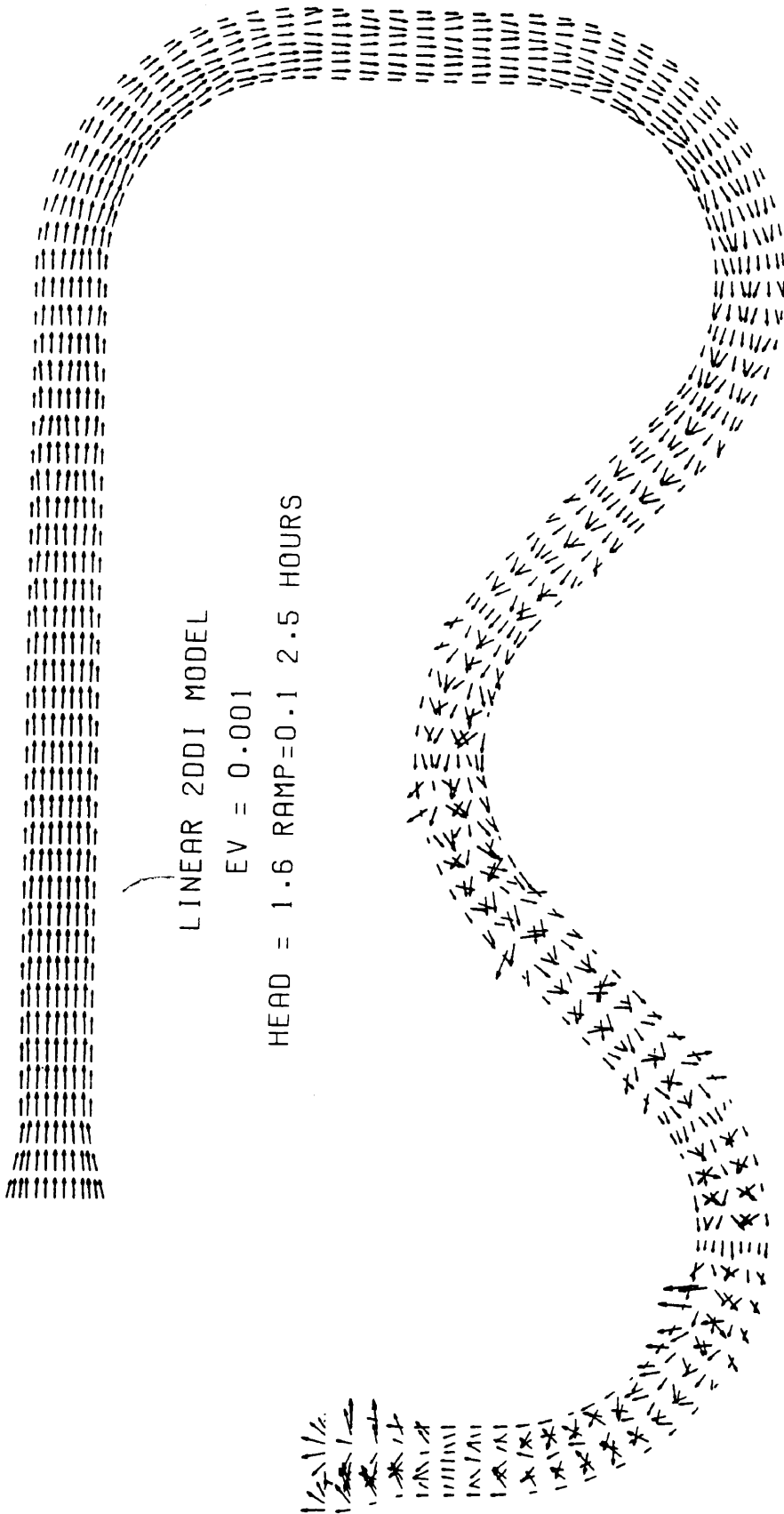


Fig. 213. Linear 2DDI Riprap Test Facility Model Vector Plot Results with Head = 1.6 Ft, EV = 0.001, Ramp = 0.1 Day, Time Step = 1.0 Second, and Time = 2.5 Hours.

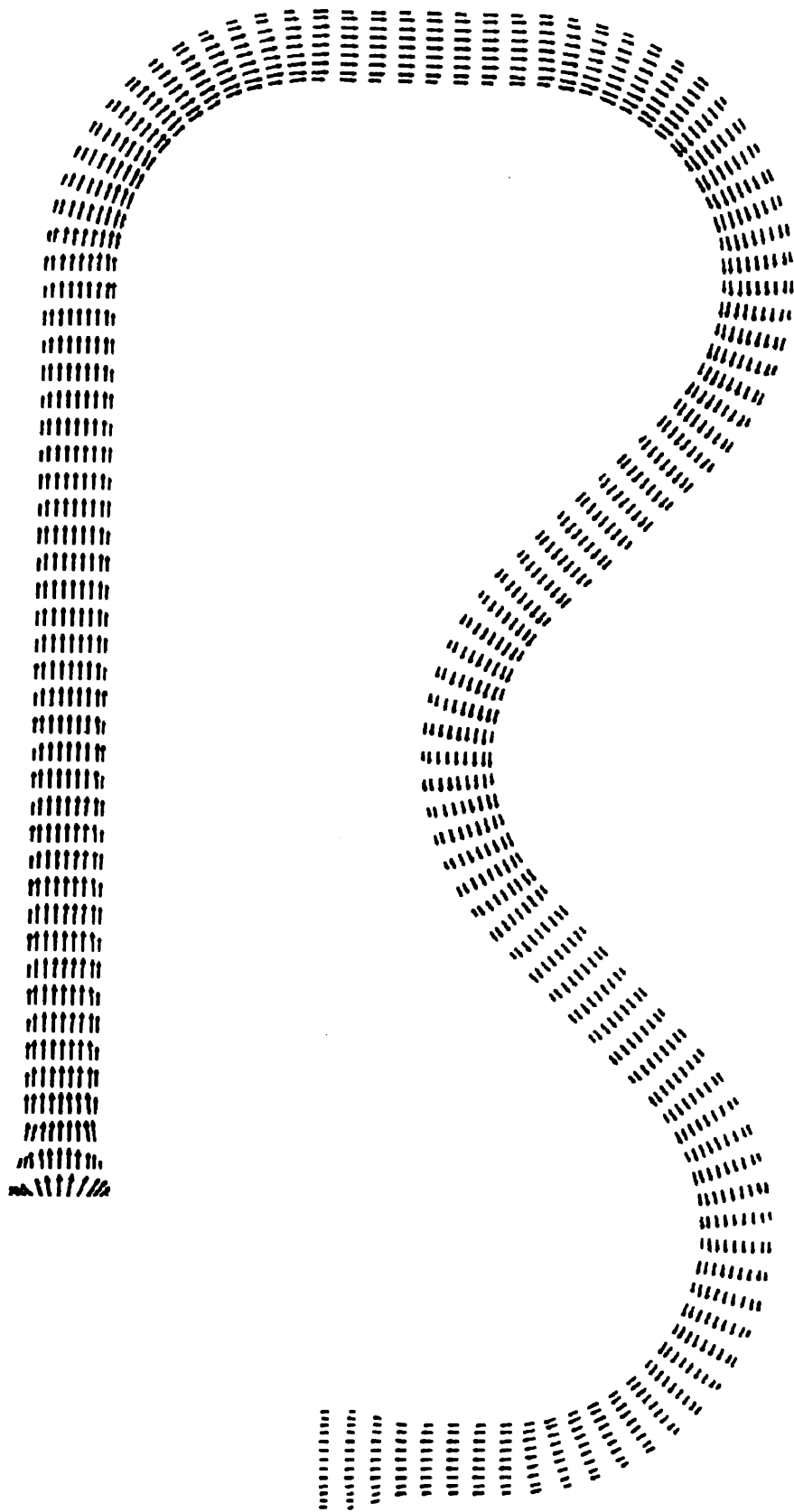


Fig. 214. Fully Non-linear 2DDI Velocity Vector Plot for Riprap Test Facility Model with Head = 1.79 Ft,  $EV = 0.0$ , 0.1 Day Ramp, and 0.4 Second Time Step at Time = 250 Seconds.

respect to time for the 13 nodes on the inflow boundary in Fig. 215. It can be noted that the velocity at the inflow boundary begins to increase normally but soon becomes unstable. This instability is in both direction and magnitude.

Since no converged results could be obtained from the 2DDI model for this test, results were extracted from the NON-LINEAR output just prior to the development of major instabilities in the calculated results. This was done for the non-linear test with a 0.02 ft head since the model had reached the end of the time ramp and flows were relatively stable in the channel. These values were then made dimensionless by dividing the depth averaged velocity calculated by the 2DDI model at each node by the average channel velocity for that section. This was also done for the observed data and the RMA-2V data in order to have a

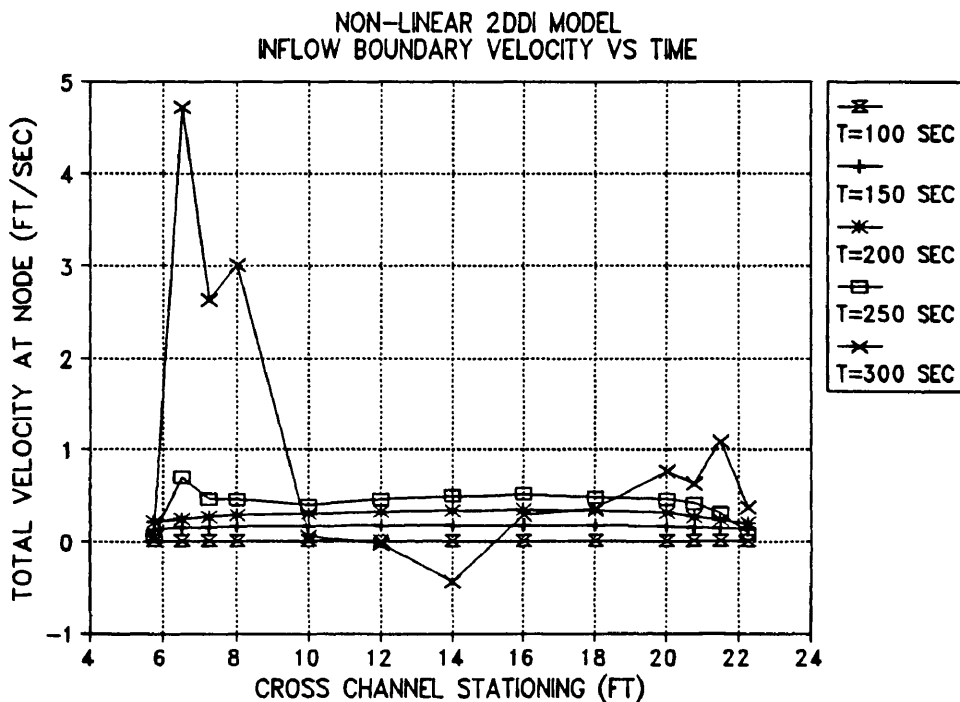


Fig. 215. Fully Non-linear 2DDI Riprap Test Facility Model Nodal Velocity Values for Inflow Boundary vs Time for Head = 1.79 Ft, EV = 0.001, Ramp = 0.1, and Time Step = 0.4 Seconds.

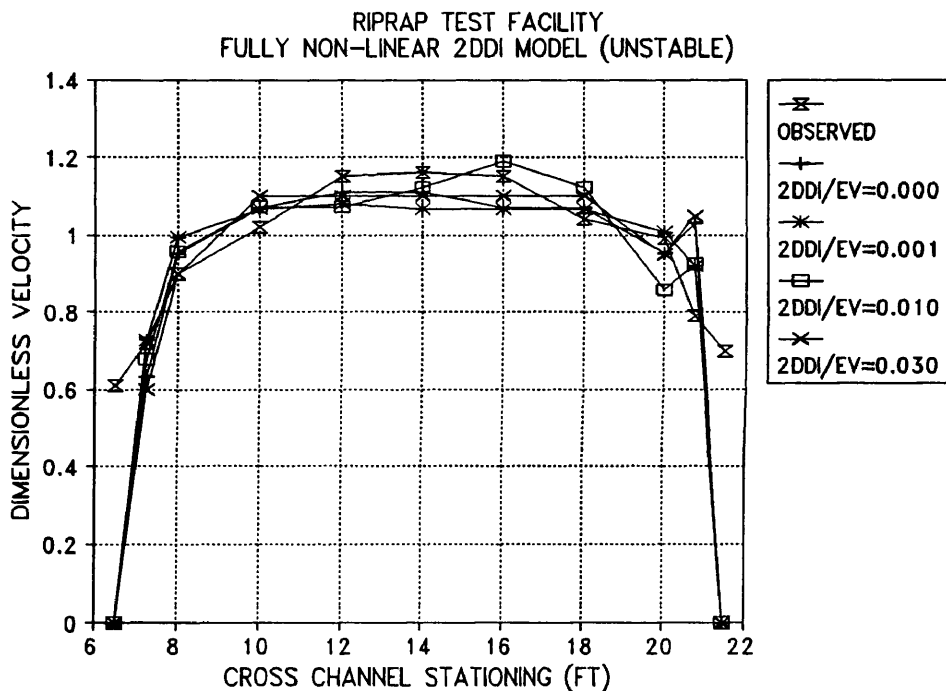
basic for comparison of the 2DDI model for this test. IN THE FOLLOWING DISCUSSION IT MUST BE REMEMBERED THAT THE MODEL WOULD NOT CONVERGE TO A FINAL SOLUTION FOR ANY OF THE ATTEMPTED VALUES AND VALUES SHOWN ARE FROM THE PERIOD WHEN THE MODEL WAS FULLY RAMPED UP BUT THE FULL HEAD WAS ONLY 0.02 FEET and flow was still increasing in the model.

The dimensionless velocity results for several runs of the NON-LINEAR 2DDI model with differing values of EV are shown in Fig. 216(a) and the run selected as the "best" is shown in Fig. 216(b) and compared with observed data and RMA-2V calculated values. The run with an EV of 0.001 was selected as best as it seemed to best match the observed data. Higher values of EV produced an extra "hump" on the right side of the main channel and were thought to be moving toward instability.

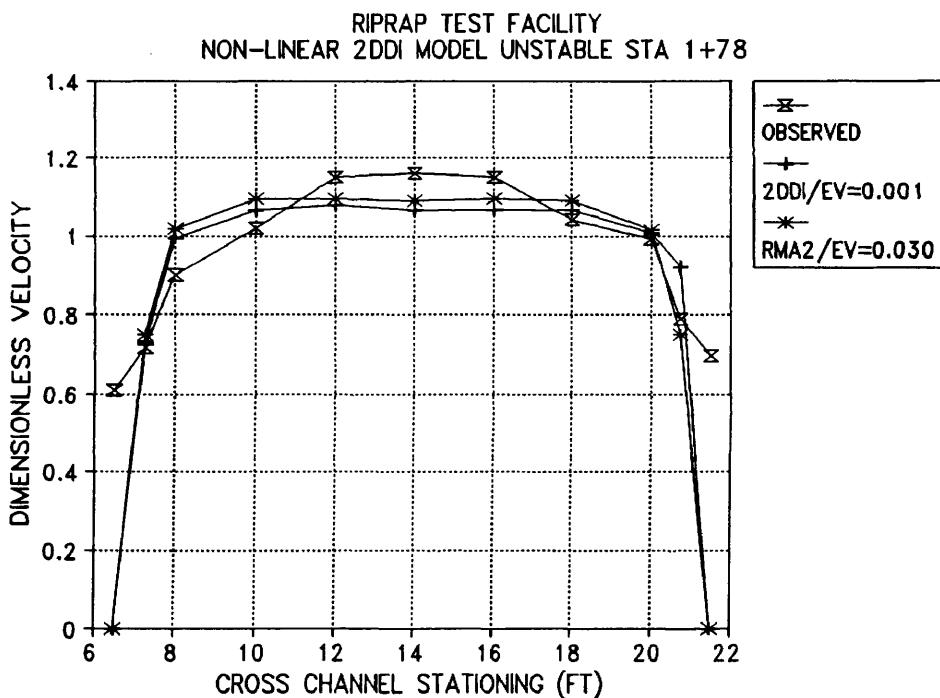
It can be seen that there is little difference between the RMA-2V results and those obtained from the 2DDI model when the results are linearized to removed the differences in model flows. Again it must be noted that prototype and RMA-2V flows are about 23 times as high as those in the 2DDI model.

The dimensionless nodal velocity values were also plotted for the remaining cross sections with measured values and are shown in Figs. 217 to 222. At all locations the differences between the RMA-2V model and the 2DDI model are slight but follow the same trends as discussed earlier in the RMA-2V results section - the models predict fairly closely to the proper velocity distributions until about the 45° point of the bend and predict maximum velocities on the wrong side of the channel for the remainder of the bend.

Continuity for the 2DDI model at the same time step at which velocity was plotted for the dimensionless plots above is shown in Fig. 223. Continuity seems rather good given the fact that the model is about to become unstable but oscillations on the order of  $\pm 2\%$  are seen at various

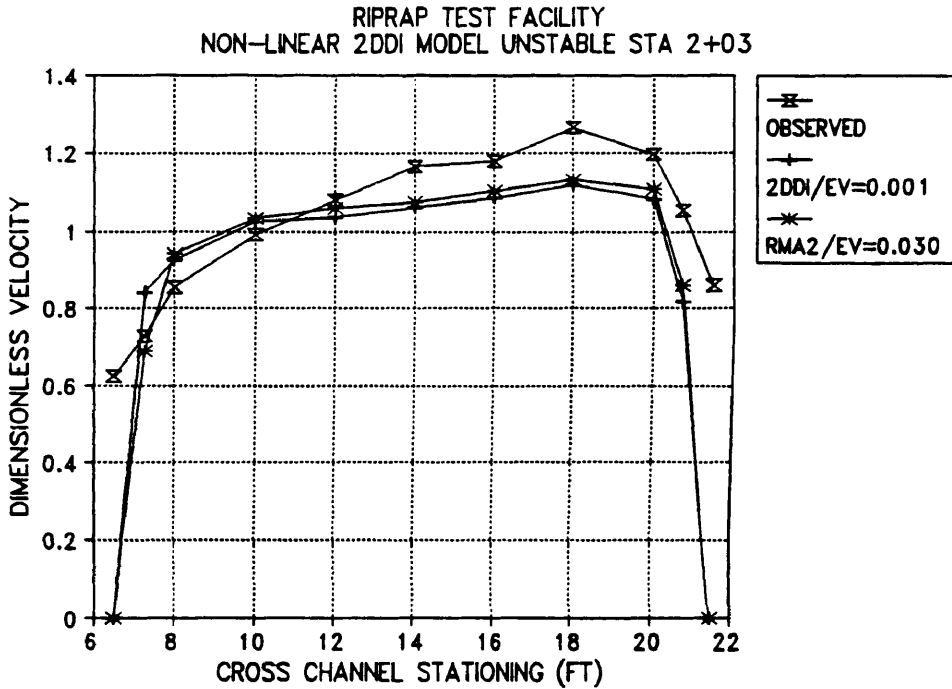


(a) Varying EV

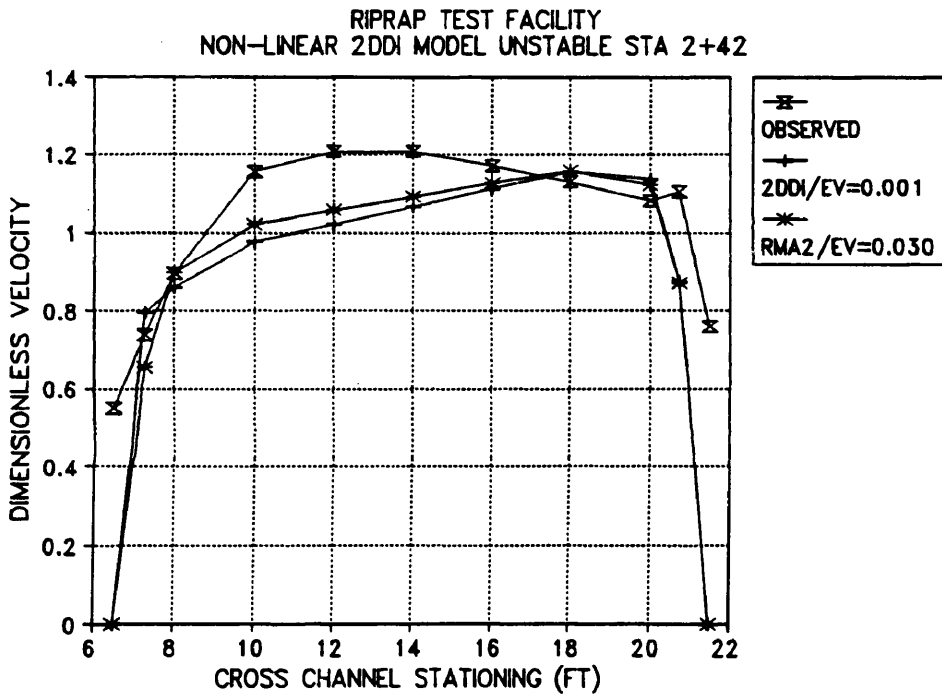


(b) 2DDI with EV = 0.001 vs RMA-2V and Observed Data

Fig. 216. Non-linear 2DDI Riprap Test Facility Dimensionless Lateral Velocity Distribution at Station 1+78 for (a) Varying EV and (b) for EV = 0.001 Compared with RMA-2V and Observed Data.



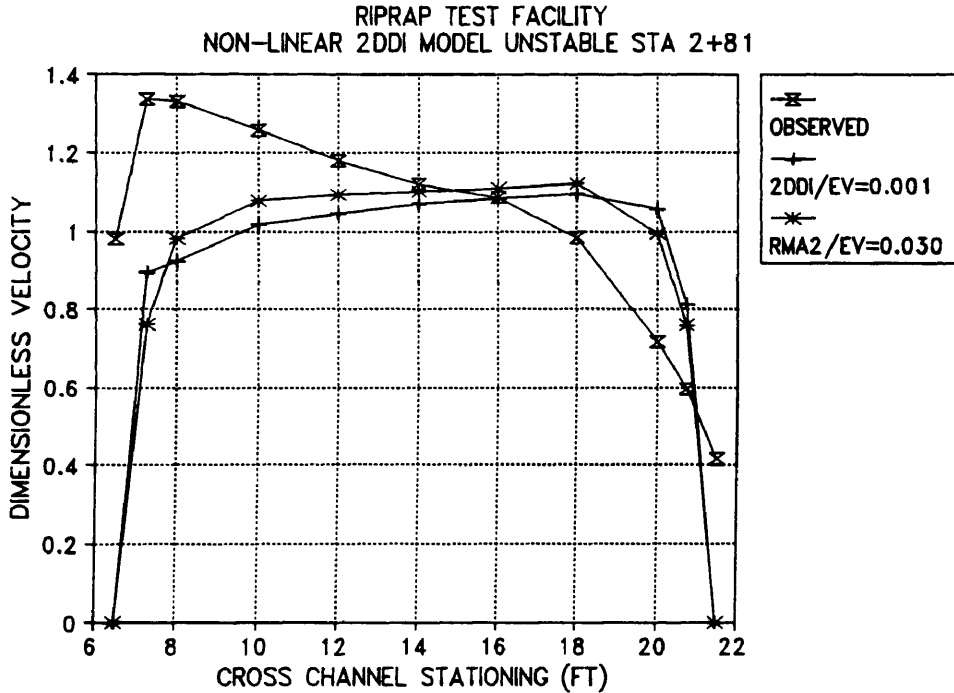
(a) Station 2+03



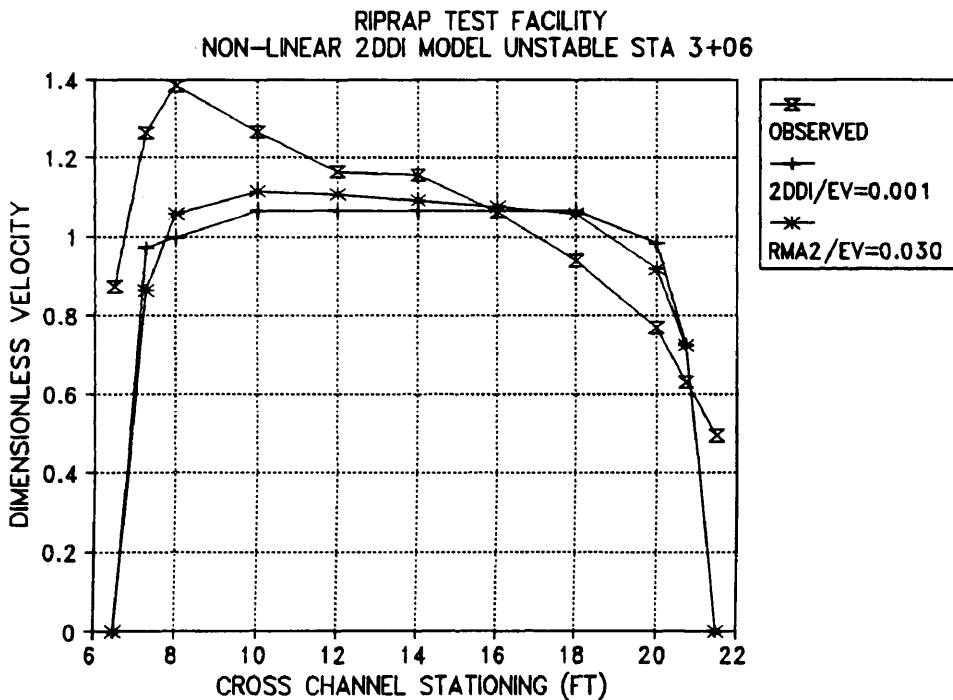
(b) Station 2+42

Fig. 217. Non-linear 2DDI Dimensionless Velocity vs Observed Data for Riprap Test Facility at Stations 2+03 and 2+42 with Flow of 2.2 cfs, EV = 0.001, 0.4 Second Time Step, and 0.1 Day Ramp.



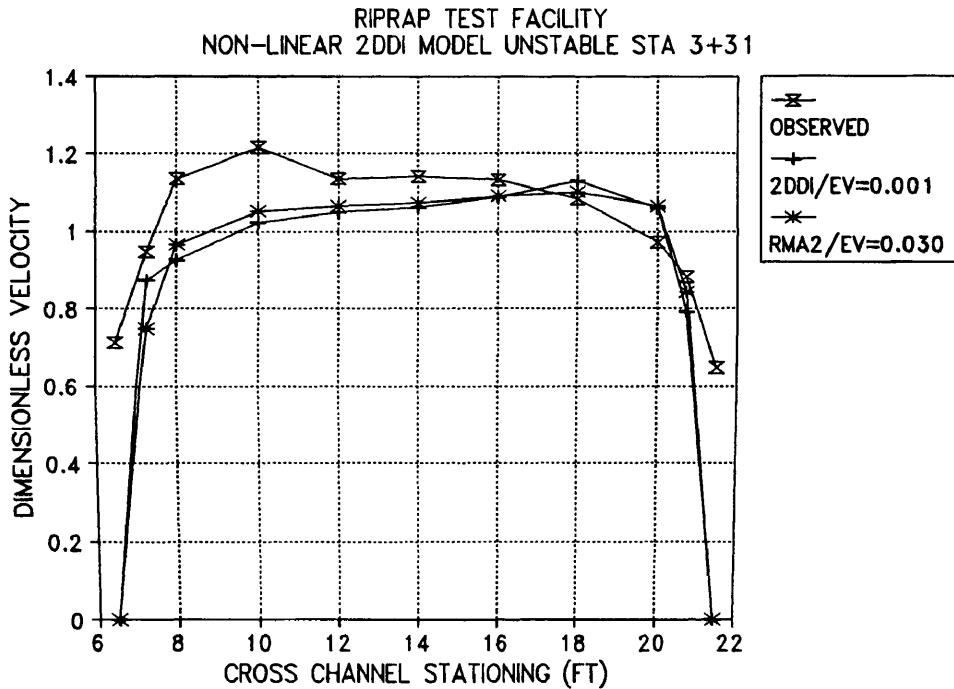


(a) Station 2+81

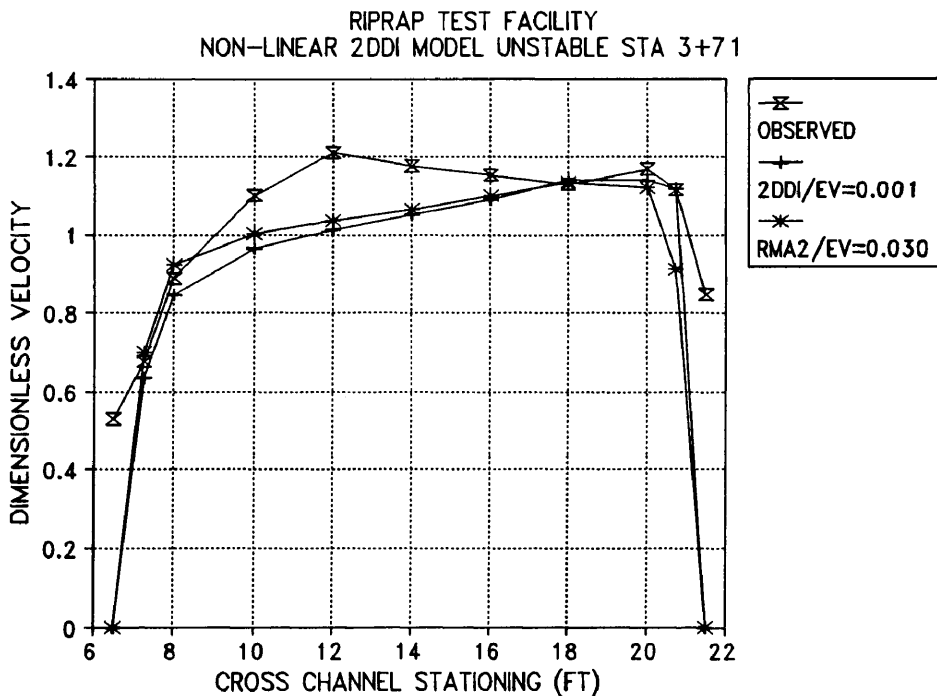


(b) Station 3+06

Fig. 218. Non-linear 2DDI Dimensionless Lateral Velocity vs Observed and RMA-2V Data for Riprap Test Facility at Stations 2+81 and 3+06 with Flow of 2.2 cfs, EV = 0.001, 0.4 Second Time Step, and 0.1 Day Ramp.

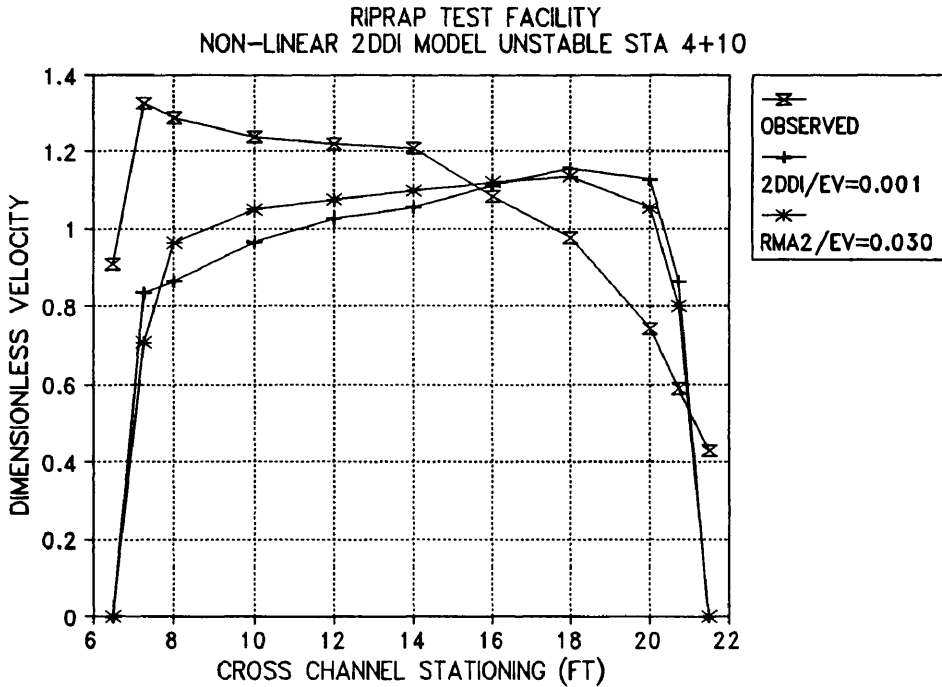


(a) Station 3+31

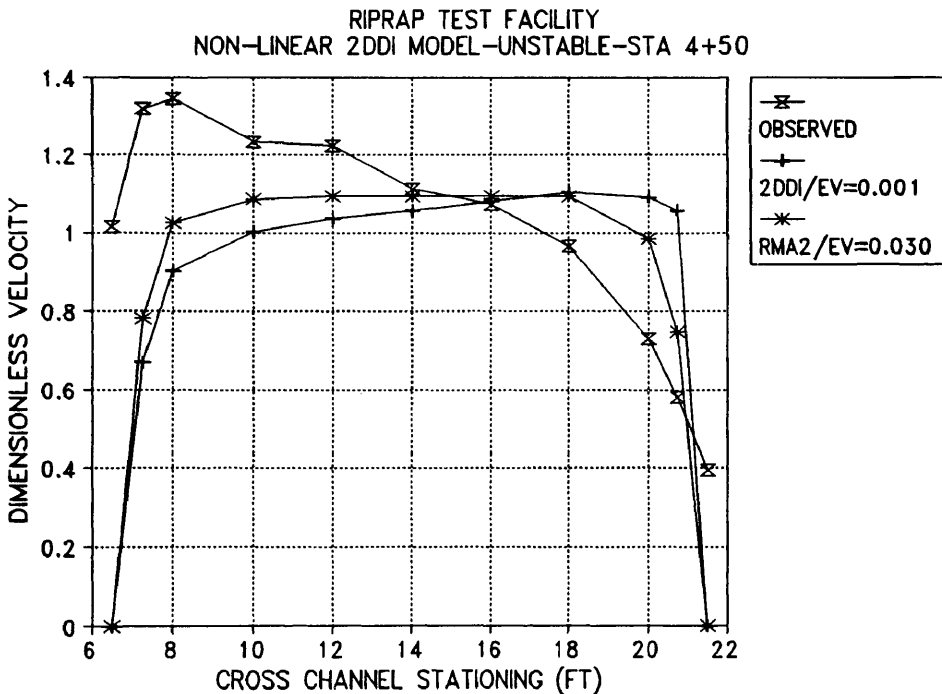


(b) Station 3+71

Fig. 219. Non-linear 2DDI Dimensionless Lateral Velocity vs Observed and RMA-2V Data for Riprap Test Facility at Stations 3+31 and 3+71 with Flow of 2.2 cfs, EV = 0.001, 0.4 Second Time Step, and 0.1 Day Ramp.

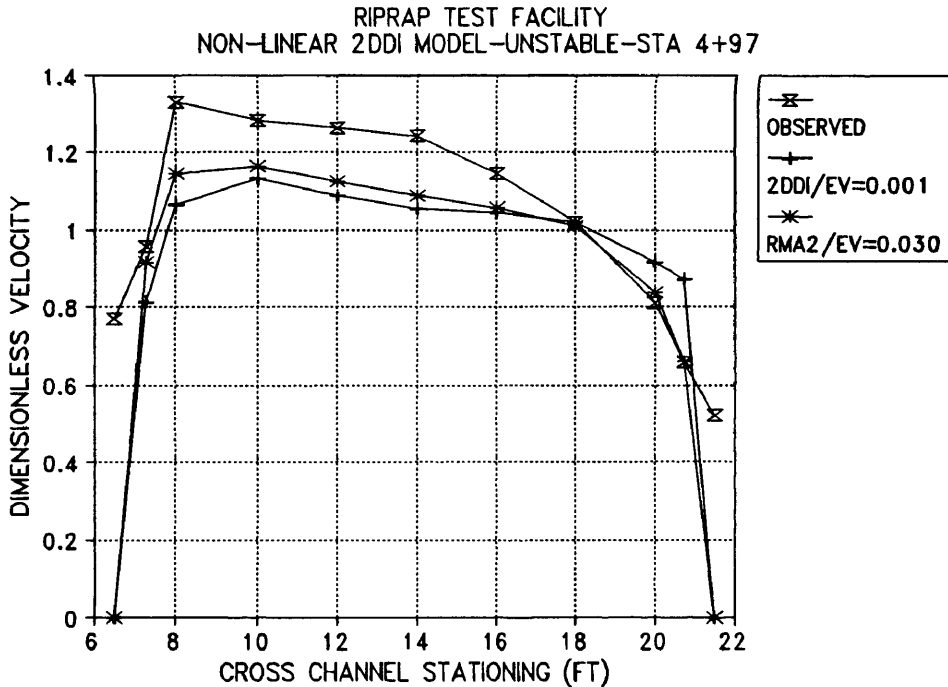


(a) Station 4+10

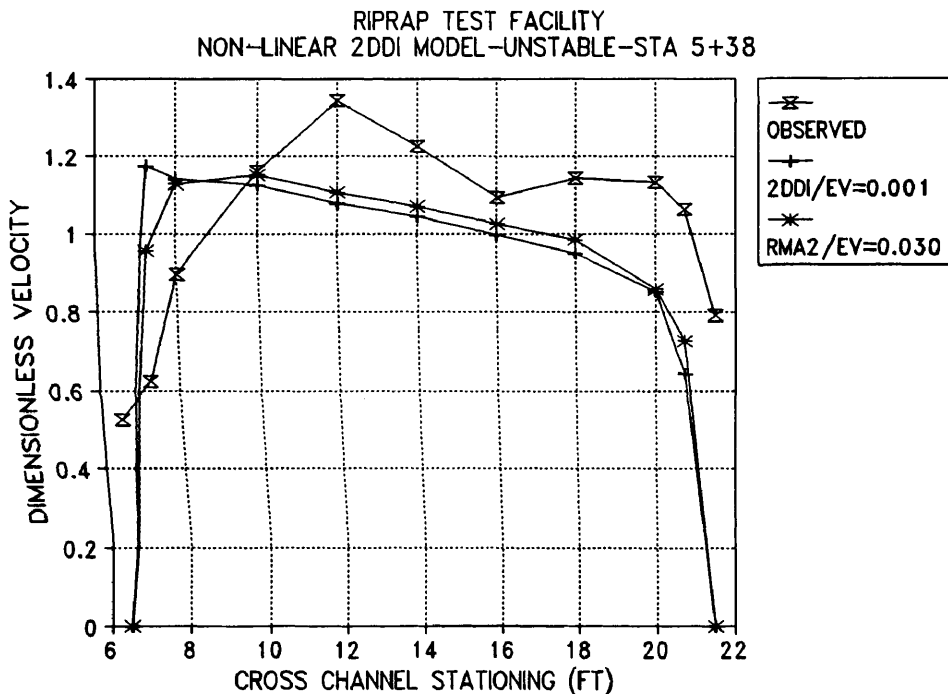


(b) Station 4+50

Fig. 220. Non-linear 2DDI Dimensionless Lateral Velocity vs Observed and RMA-2V Data for Riprap Test Facility at Stations 4+10 and 4+50 with Flow of 2.2 cfs, EV = 0.001, 0.4 Second Time Step, and 0.1 Day Ramp.

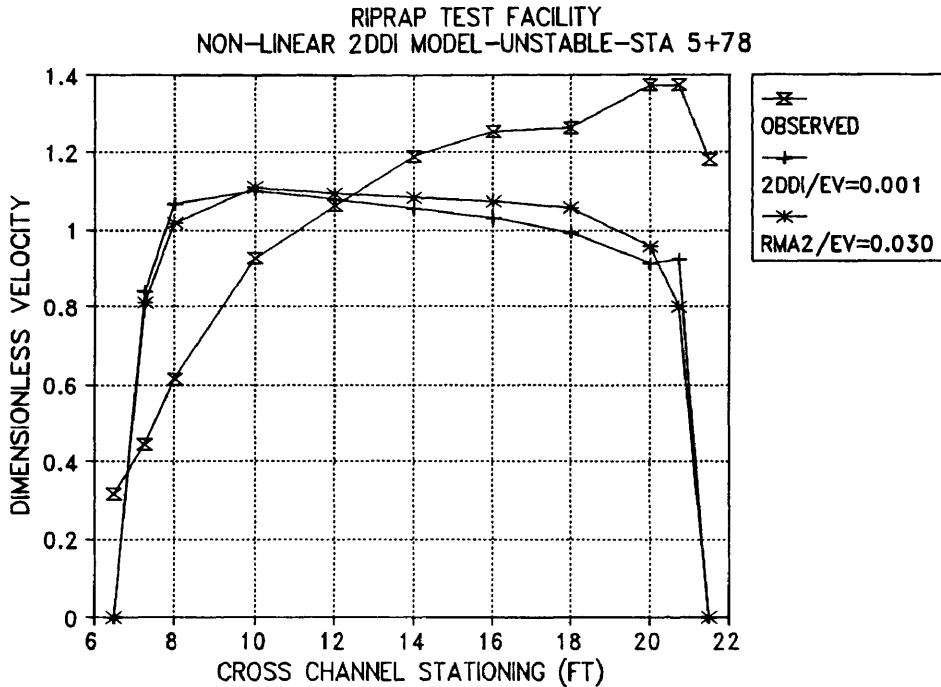


(a) Station 4+97

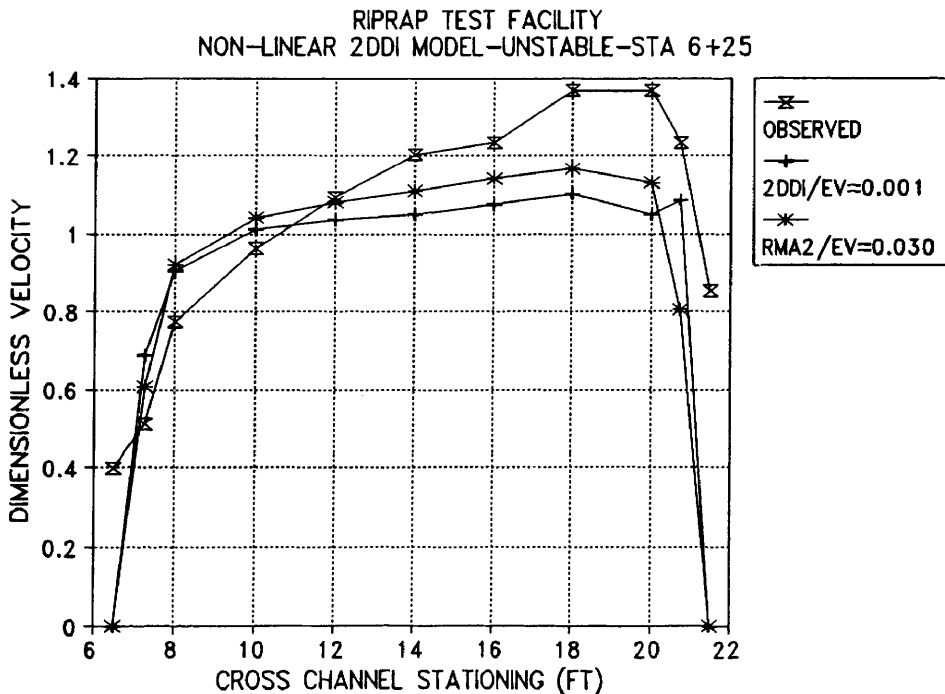


(b) Station 5+38

Fig. 221. Non-linear 2DDI Dimensionless Lateral Velocity vs Observed and RMA-2V Data for Riprap Test Facility at Stations 4+97 and 5+38 with Flow of 2.2 cfs, EV = 0.001, 0.4 Second Time Step, and 0.1 Day Ramp.



(a) Station 5+78



(b) Station 6+25

Fig. 222. Non-linear 2DDI Dimensionless Lateral Velocity vs Observed and RMA-2V Data for Riprap Test Facility at Stations 5+78 and 6+25 with Flow of 2.2 cfs, EV = 0.001, 0.4 Second Time Step, and 0.1 Day Ramp.

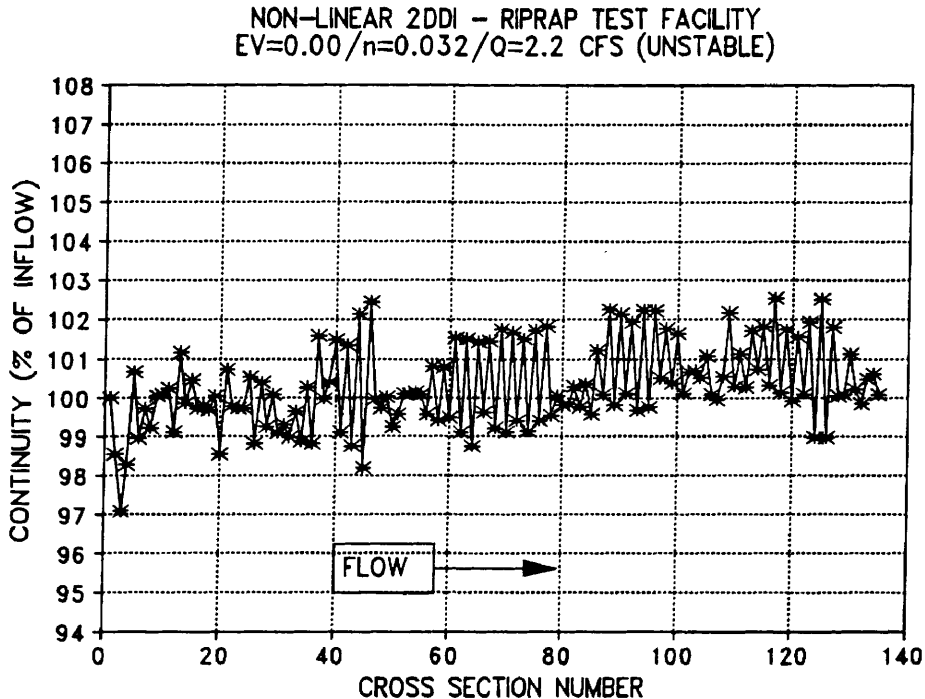


Fig. 223. Non-linear 2DDI Riprap Test Facility Model Continuity vs Location Down Channel for Flow of 2.2 cfs with Head = 0.02 ft, EV = 0.001, Ramp = 0.1 and Time Step = 0.4 Seconds.

locations in the channel.

When compared with the RMA-2V results the 2DDI model is showing oscillations nearly twice as large as the RMA-2V model at a flow rate of just over 4% of the flow in the RMA-2V model. The continuity drift in the RMA-2V model is probably due to the geometry at the inflow boundary.

From this test it appears that the 2DDI model could produce results comparable with those produced by the RMA-2V model if the 2DDI model could be stabilized such that it could operate in an environment where significant velocities are present.

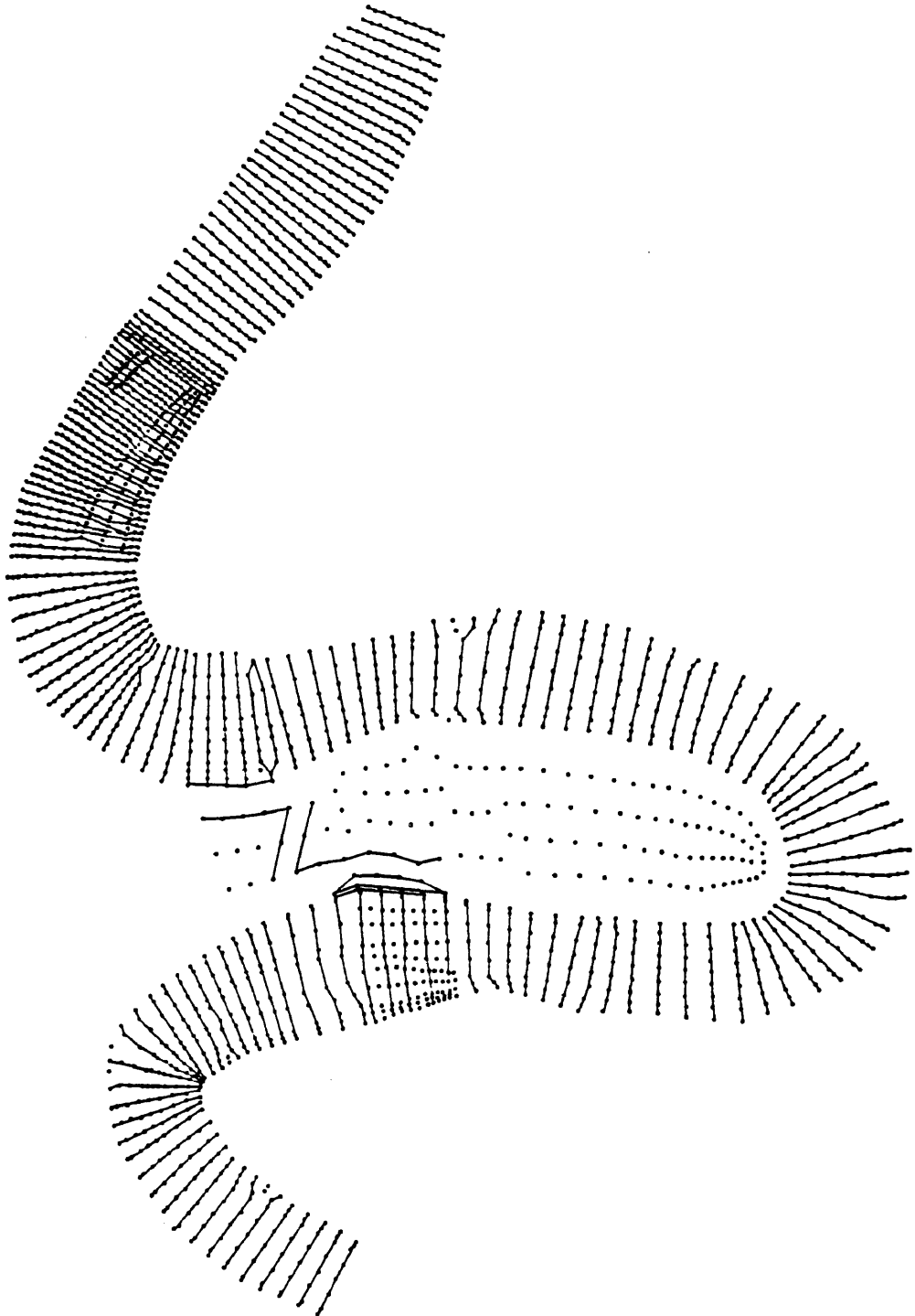
## THE MISSISSIPPI RIVER REDEYE CROSSING MODEL

The RMA-2V Redeye Crossing model was previously developed for a hydrodynamics and sedimentation study conducted at the Waterways Experiment Station. The grid consisted of quadrilateral and triangular elements. Since the 2DDI model was not able to handle quadrilaterals and the test was designed to use identical grids, the grid was converted to all triangular elements as was shown in Fig. 11.

Since the 2DDI model could not handle the addition and removal of elements due to wetting and drying of nodes it was necessary to operate the model with either the grid all wet or with the dry portions of the grid removed from the model. The selected alternative was to operate the model at a high flow rate where nearly all of the elements were covered with water. Those elements that were not wet at the selected flow rate were removed from the grid. Otherwise the geometry (bed elevation, etc) was identical to that used in the original Redeye Crossing Sedimentation Study. (Raphelt, Trawle, Pokrefke, and Nickles, 1992)

Continuity lines were specified for almost all rows of corner nodes as shown in Fig. 224 but some nodes were not included on continuity lines since including them would repeat nearly all of the continuity line immediately upstream or downstream from the nodes in question. Some lines of nodes were also ignored on the point where a flow cutoff occurs at high stages. Several continuity lines were included for this area but continuity was not calculated for nodes that were away from the direct flow path. Four rows of nodes were also neglected in areas of high resolution near dikes in the lower portion of the model.

The RMA-2V model included an inflow boundary condition at the upstream end of the model and a head boundary at the downstream end of the model. The model was originally



REDEYE CROSSING CONTINUITY LINES

1 inch = 7087.43

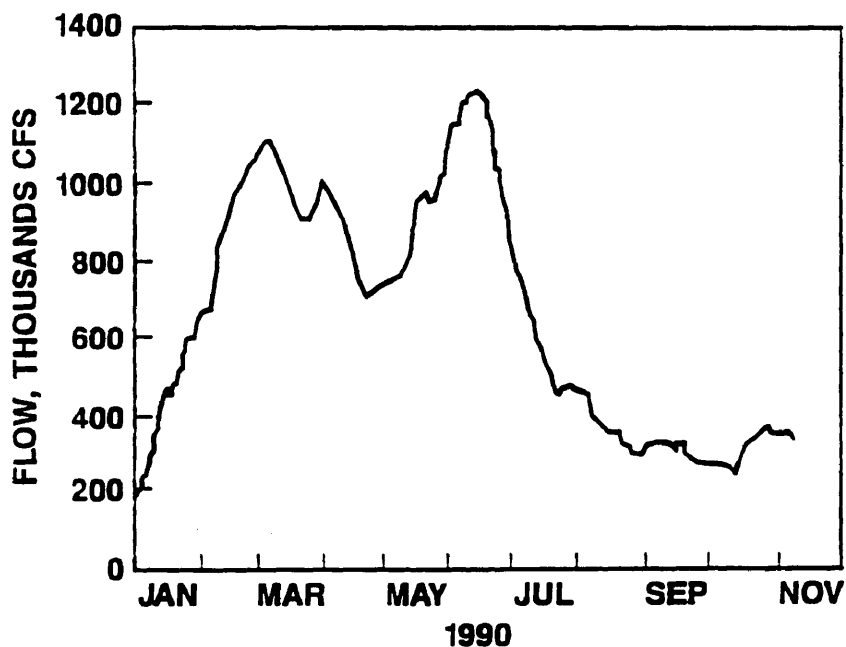
Fig. 224. Continuity Lines used in Redeye Crossing Test Model Showing Corner Nodes not Included on Continuity Lines. Scale is 1" Equals 7,087 Feet.



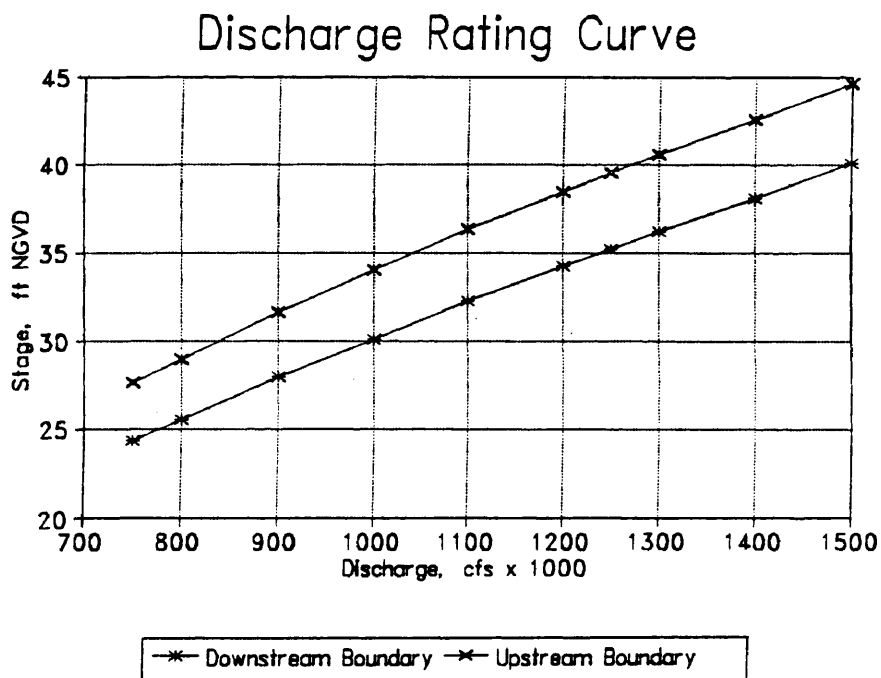
calibrated to observed values and values calculated from a calibrated HEC-6 model (HEC 1991, Raphael, Trawle, Pokrefke, and Nickles 1992).

The flow selected was a high flow from the observed 1990 hydrograph shown in Fig. 225(a). The flow was near the peak of the second major event - about June 15th when the flow in the river was approximately 1,200,000 cfs. The stage for this event was approximately +38.2 feet National Geodetic Vertical Datum (NGVD) at the Baton Rouge gauge and such that nearly all of the grid elements were wet. The stage was also sufficiently high that flow occurred across the point near the center of the grid. The stage discharge curves for the upstream and downstream model boundaries are shown in Fig. 225(b).

The original model included eight differing element types which defined the various Manning's  $n$  values and EV values used in the model. In order to reduce element types to a manageable number for display purposes, the number of element types was reduced to five by combining like areas in the model. These five element types were used in the grid to define overbank areas, dikes, main channel, point bar area, and the area where flow occurs over the point. The locations of these areas are shown in Fig. 226. The Manning's  $n$  values and EV values used for these areas are shown in Table 2. It can be noted that differing values for EV were used for the channel than were used in the other element types. This was done to increase model stability in shallow overbank and point bar areas and at dikes where rapid changes in bed elevation occurred. In light of tests previously described in this work the EV values for the dikes probably should have been lowered to reduce oscillations on the dikes rather than increased to stabilize the model. If EV values were to be increased it should have been done upstream and downstream of the dikes as indicated in the preceding section on submerged bump tests.



(a) 1990 Observed Hydrograph



(b) Stage Discharge Curves for Model Inlet and Outlet

Fig. 225. Observed Hydrograph of Mississippi River at Baton Rouge, Louisiana for Jan 1 through Nov 10, 1990 and Stage Discharge Curves for Redeye Crossing Model Inlet and Outlet.

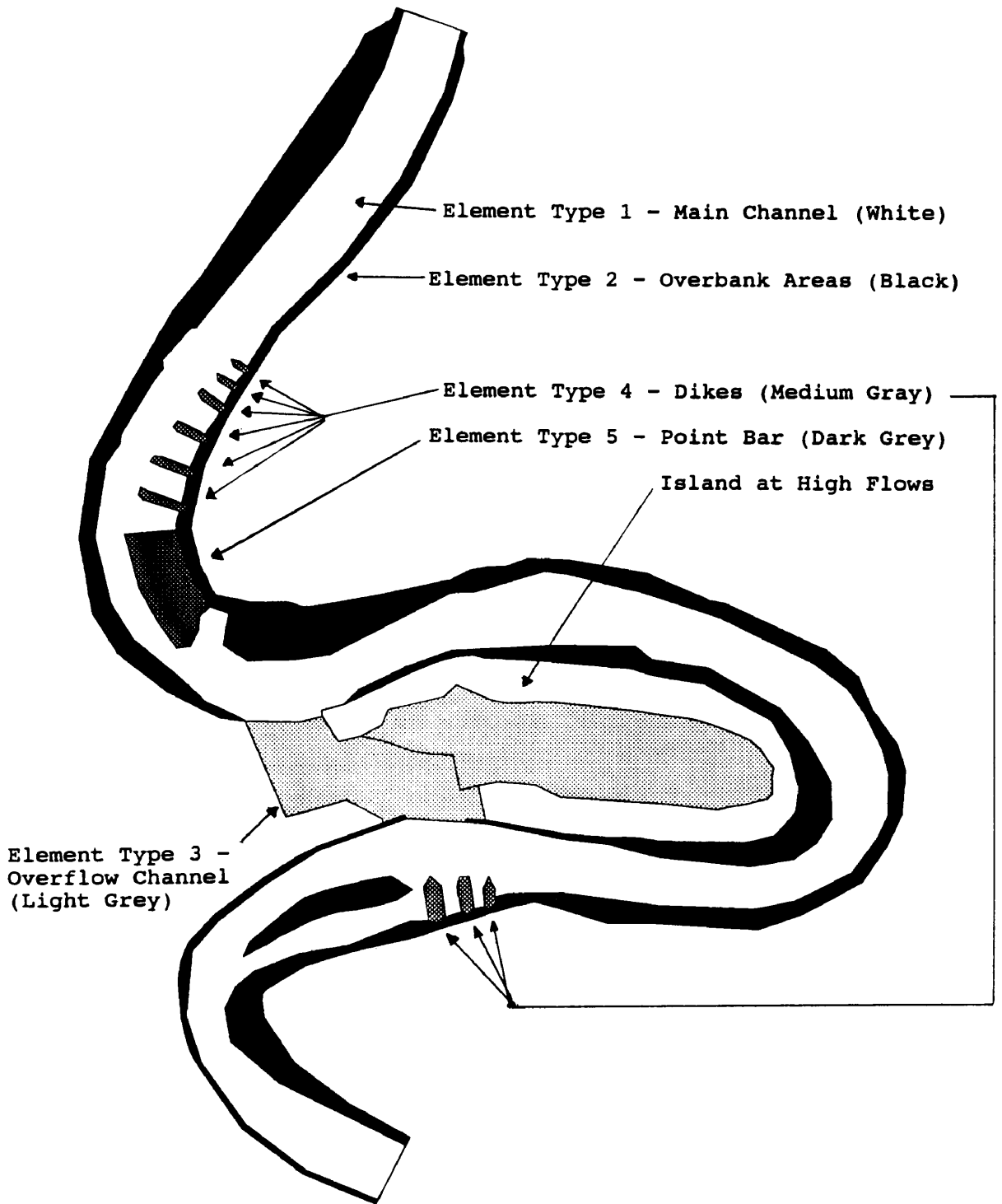


Fig. 226. Element Types and Locations Used in Redeye Crossing Mississippi River Model.

Table 2. Manning's n Values for Various Element Material Types and EV Values Used in Early RMA-2V Redeye Crossing Mississippi Model to Match Observed Conditions.

TYPE	DESCRIPTION	EV <sub>xx</sub>	EV <sub>xy</sub>	EV <sub>yx</sub>	EV <sub>yy</sub>	n Value
1	River Channel	80	80	80	80	0.016
2	Overbanks	100	100	100	100	0.060
3	Overflow Channel	100	100	100	100	0.080
4	Dikes	100	100	100	100	0.100
5	Point Bar	100	100	100	100	0.080

The Manning's n value used on the dikes was calibrated using a submerged weir calculation until the proper flow was observed over the dikes based on the calculated water surface elevation upstream and downstream of the dikes.

#### RMA-2V REDEYE CROSSING MODEL RESULTS

The RMA-2V model was set up to run as described above with a flow of 1.2 million cfs and a downstream water surface elevation equivalent to 34.2 ft NGVD in the prototype (Fig. 225(b)). The RMA-2V model cannot operate with negative elevations - i.e. elevations below sea level - and since much of the river channel was below sea level, 200 feet were added to the elevation data. The original data was from the low water reference plane which was referenced at about +3 ft NGVD. This interprets to adding about 197 feet to the RMA-2V grid datum based on NGVD to keep all values above sea level. This means that 34.2 feet NGVD is about 231.2 feet in the RMA-2V model. The bed elevations used in the RMA-2V model are shown in Fig. 227 and the river crossings known as Redeye Crossing and Medora Crossing are labeled on the figure. Flow in the model is from the top of the figure to the bottom.

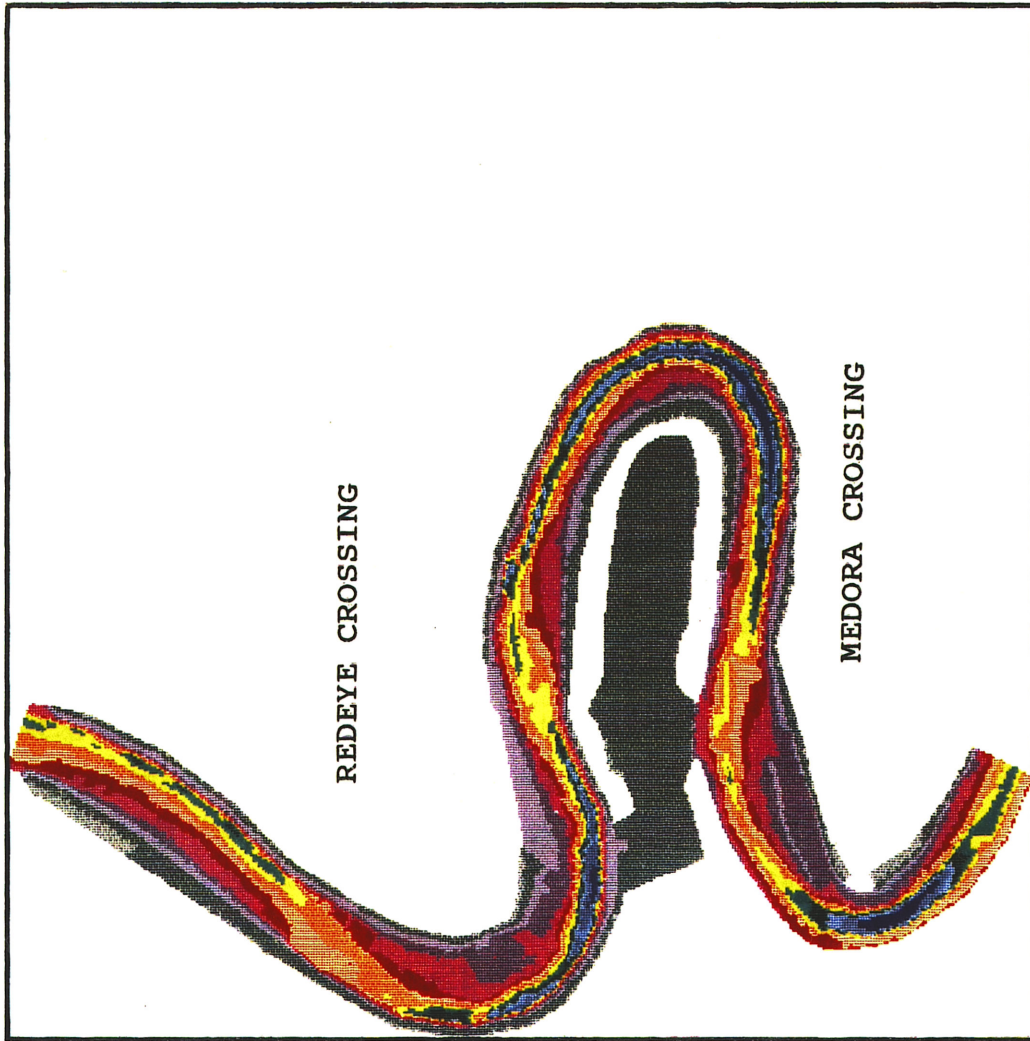
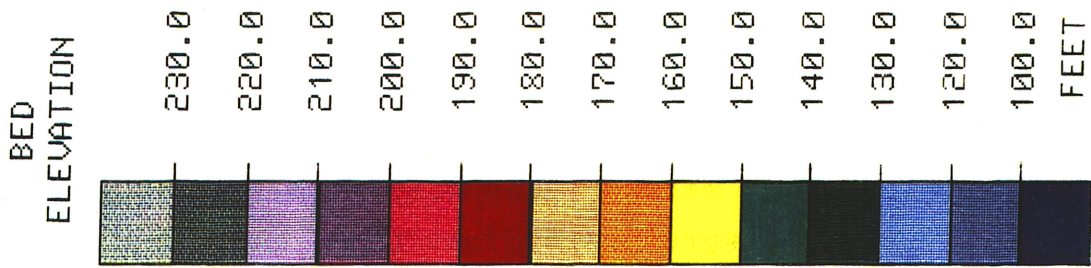


Fig. 227. Redeye Crossing Bed Elevations as Adjusted for RMA-2V Model. Actual Bed Elevations are 197 Feet Lower Than Shown.

The RMA-2V model was started with an initial elevation of 234.0 feet and an EV of 500. The values for EV and downstream water surface elevation were then gradually lowered until the EV values in Table 2 were obtained with a downstream water surface elevation of 231.2 feet. The vector plot for this test is shown in Fig. 228. Only the corner node values are plotted to improve plot clarity and the plot has been rotated clockwise about  $40^\circ$  to keep the plot and associated vectors as large as possible. All of the following vector plots have also been rotated by approximately the same amount.

In these results several problem areas are noticeable. The most serious is along the outside of the last bend in the model (below Medora Crossing). At this location several vectors are pointing almost directly upstream and are not part of an eddy or other physical occurrence. These vectors are the result of model instability as are similar vectors where flow separates from the main channel to flow across the meander point and at  $180^\circ$  bend to the far right side of the figure. Similar problems also exist at several other locations in the figure.

Due to the number of unstable vectors the value of EV for the channel was increased from 80 to 100 and the model was again run. The results for this test are shown in Fig. 229. This plot again shows instabilities at the same locations but the magnitude of the instabilities is substantially reduced. The other areas of the model look well converged and appear have converged to a good solution. Even though the solution could be improved these results were deemed acceptable for the purposes of this research.

The depth plot in Fig. 230 shows graphically the large variation in flow depths between overbank and main channel areas - a variation of more than 130 feet. The velocity plot in Fig. 231 shows more graphically how flow moves across the meander point and shifts from side to side in the

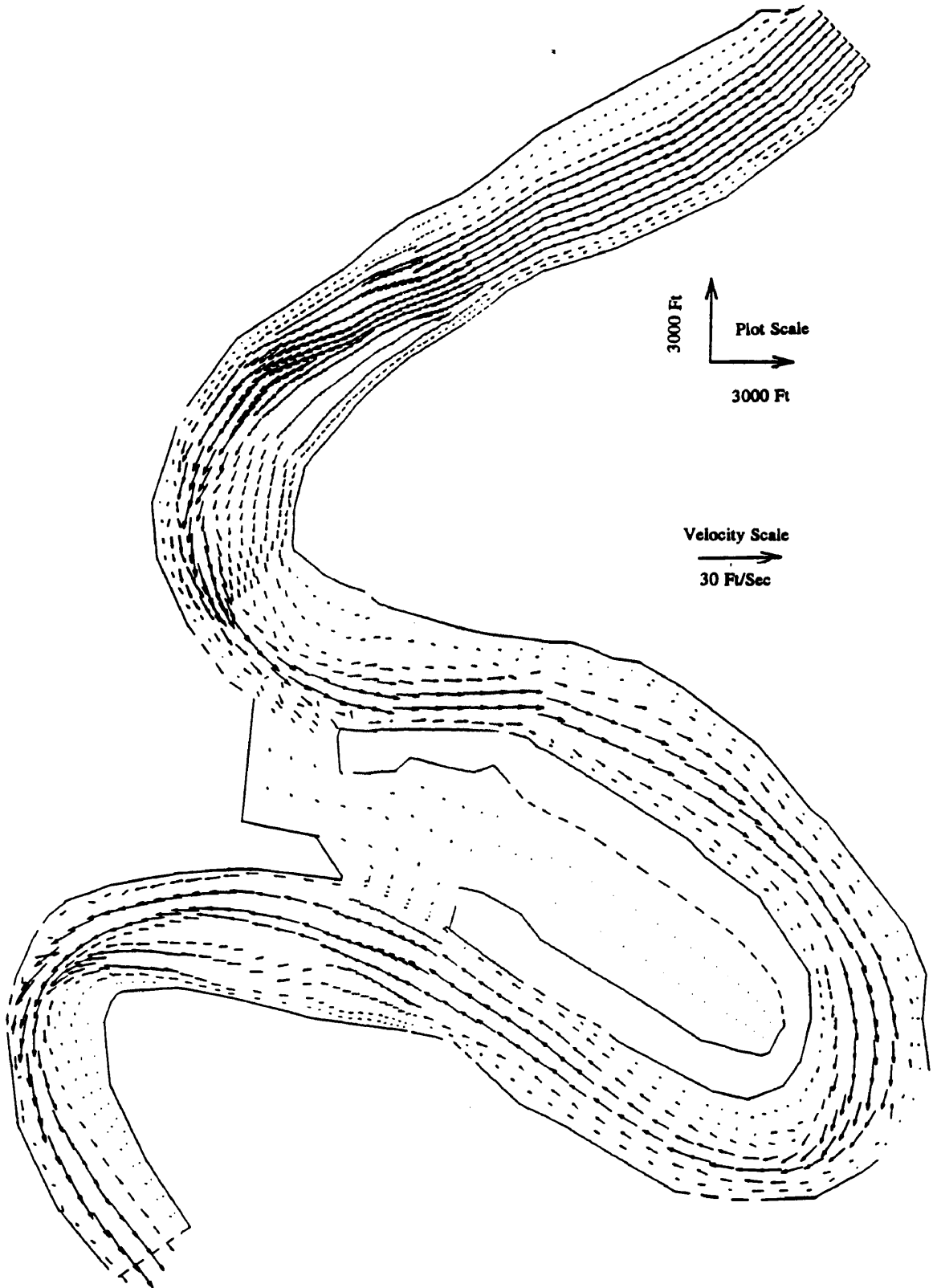


Fig. 228. RMA-2V Velocity Vector Plot for Redeye Crossing with EV = 80 in Main Channel and 100 in All Other Areas for Flow Rate of 1,200,000 cfs.

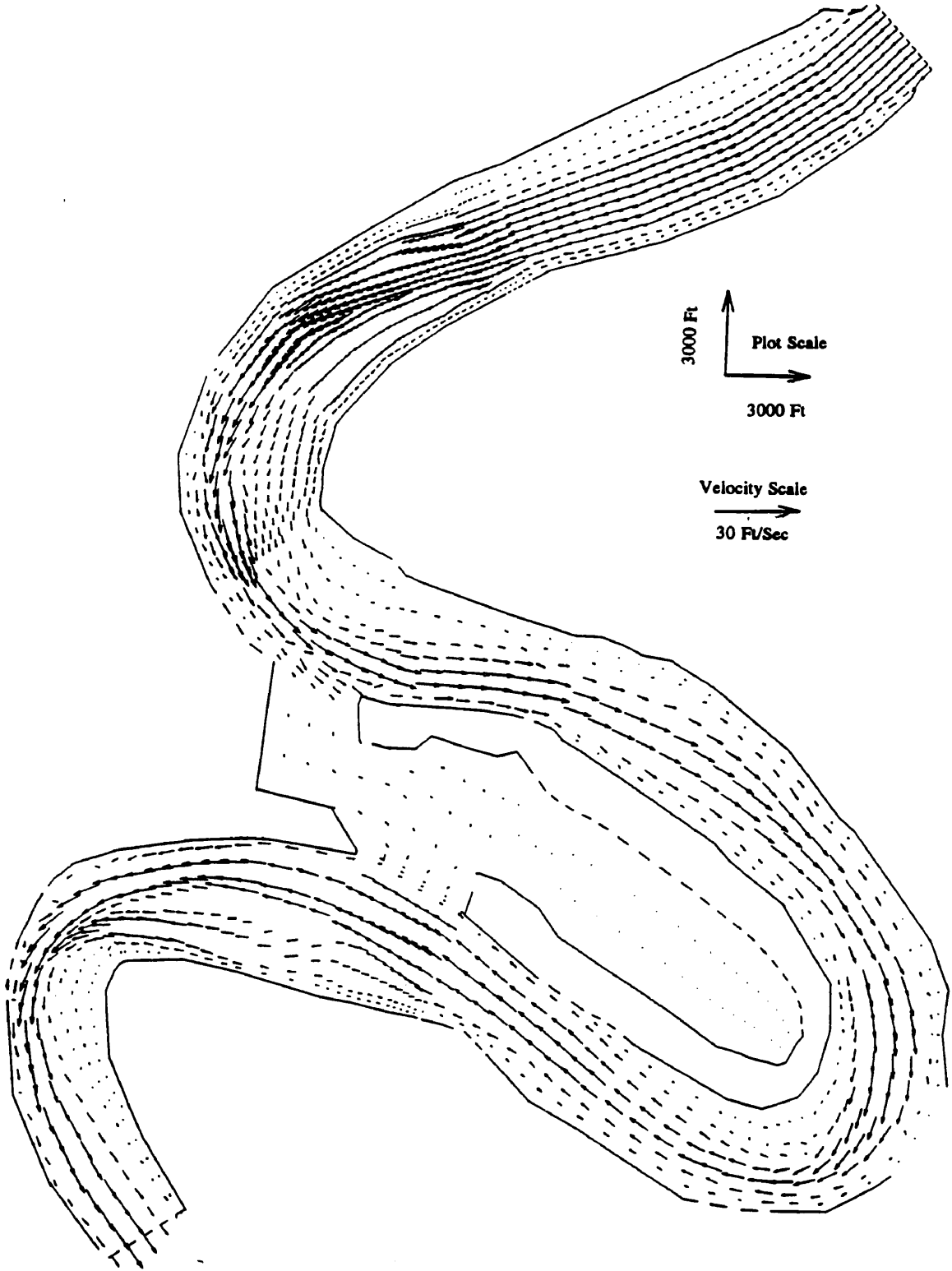


Fig. 229. RMA-2V Velocity Vector Plot for Redeye Crossing Model with  $EV = 100$  at All Locations in Model for Flow of 1,200,000 cfs.



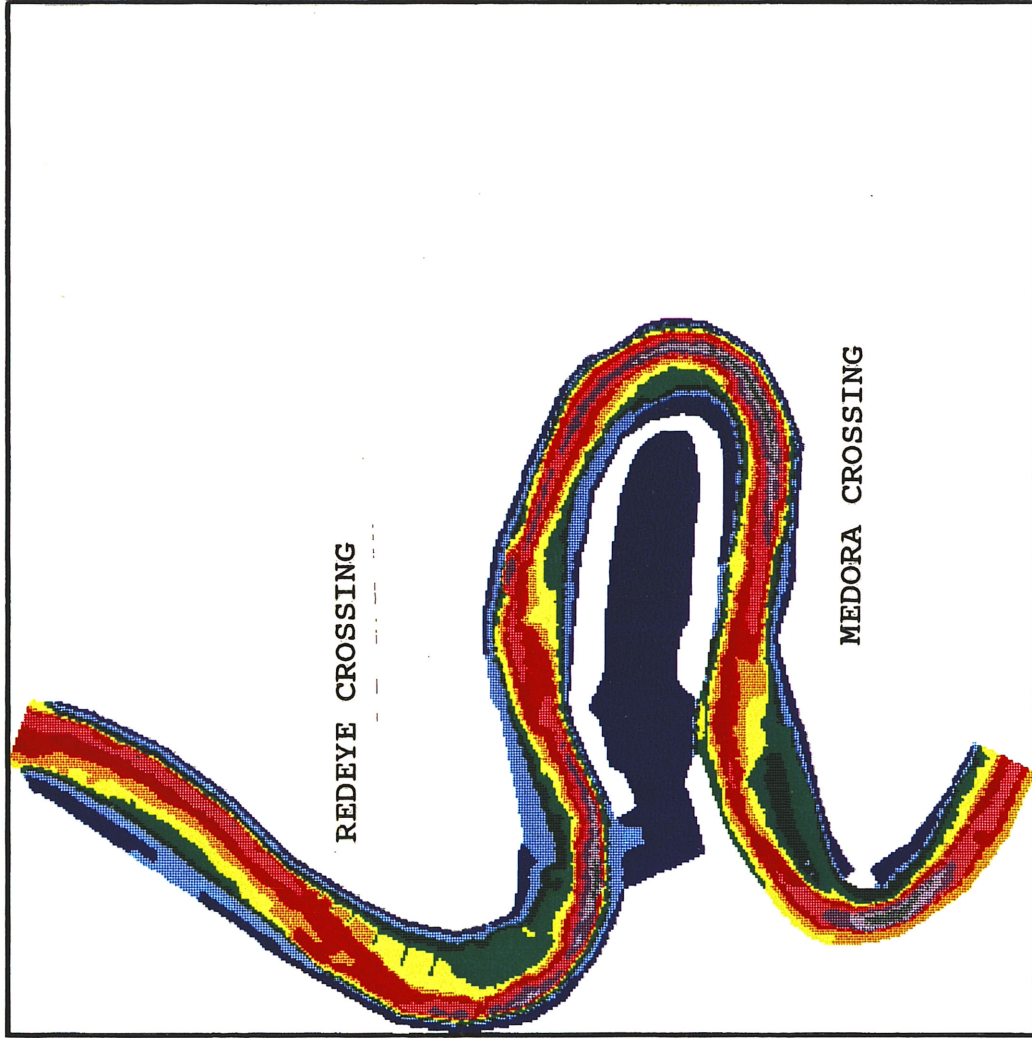
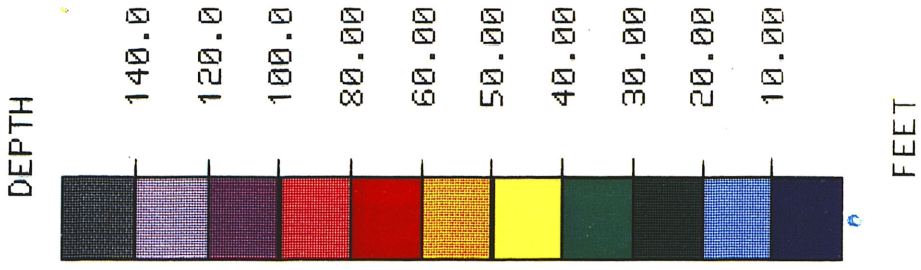


Fig. 230. RMA-2V Calculated Depth of Flow for Redeye Crossing Model with EV = 100 at All Locations for Flow of 1,200,000 cfs.

MAGNITUDE OF  
VELOCITY

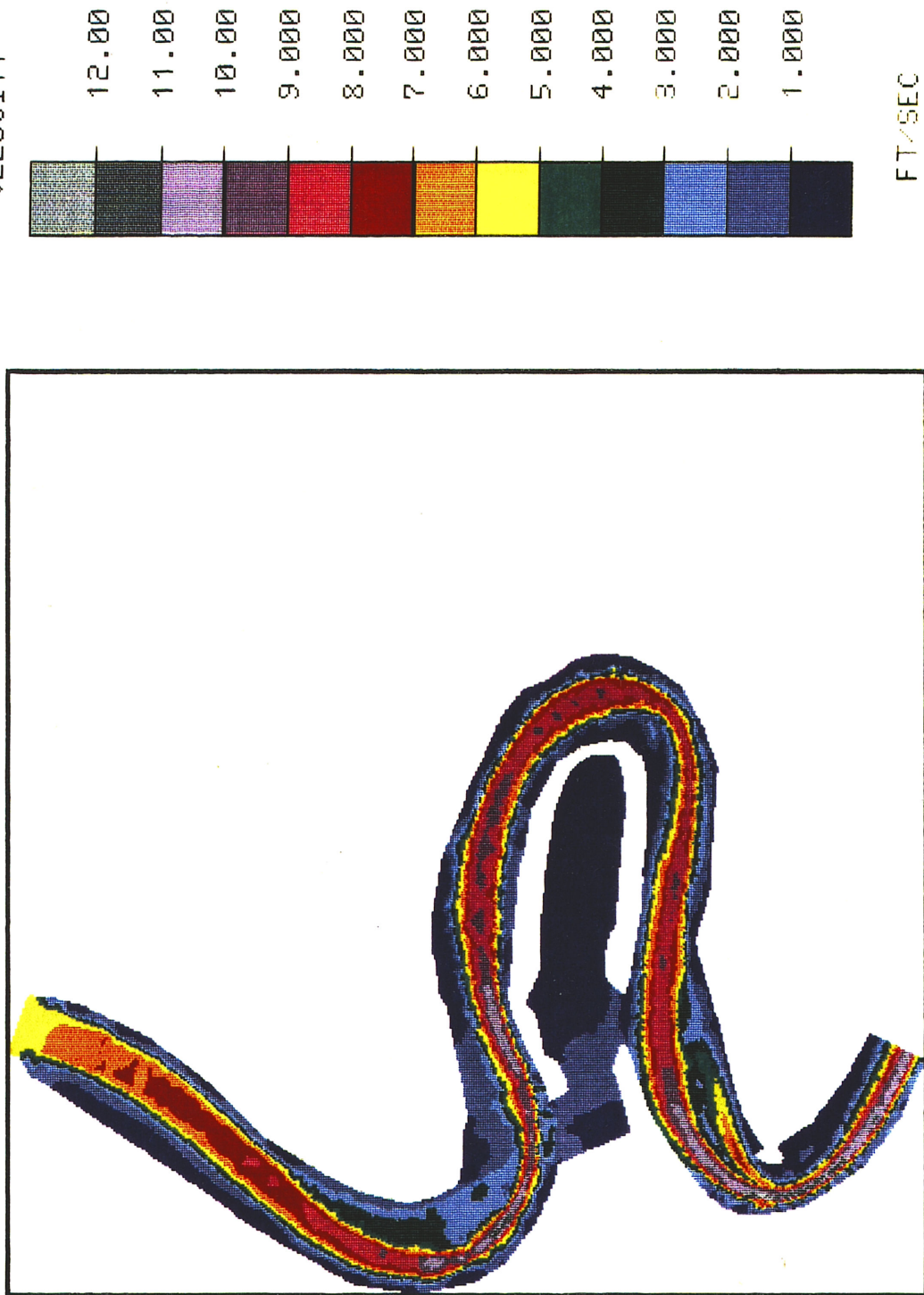


Fig. 231. RMA-2V Total Velocity for Redeye Crossing Model with EV = 80 in River Channel and 100 on Remainder of Model.

main river channel between river bends. The currents move from side to side in the model channel due to the effects of the model geometry (i.e. bed elevation) which is sufficient to overcome most of the RMA-2V model's tendency to keep currents on the inside of the bend. It was, however, also necessary to increase the hydraulic roughness on the point bar (element type 5 in Fig. 226) to move the currents to the outside of the first bend in the model in order to reproduce observed flow patterns.

Noticeable in Figs. 230 and 231 is also an area at the inside of the last curve in the model that has gone dry in the model as indicated by the irregular white area. This area is shallow but should be wet in the model and may be dry due to oscillations in the solution in this area.

Model Continuity for the model cross sections from Fig. 224 is shown in Fig. 232. Cross sections are numbered from

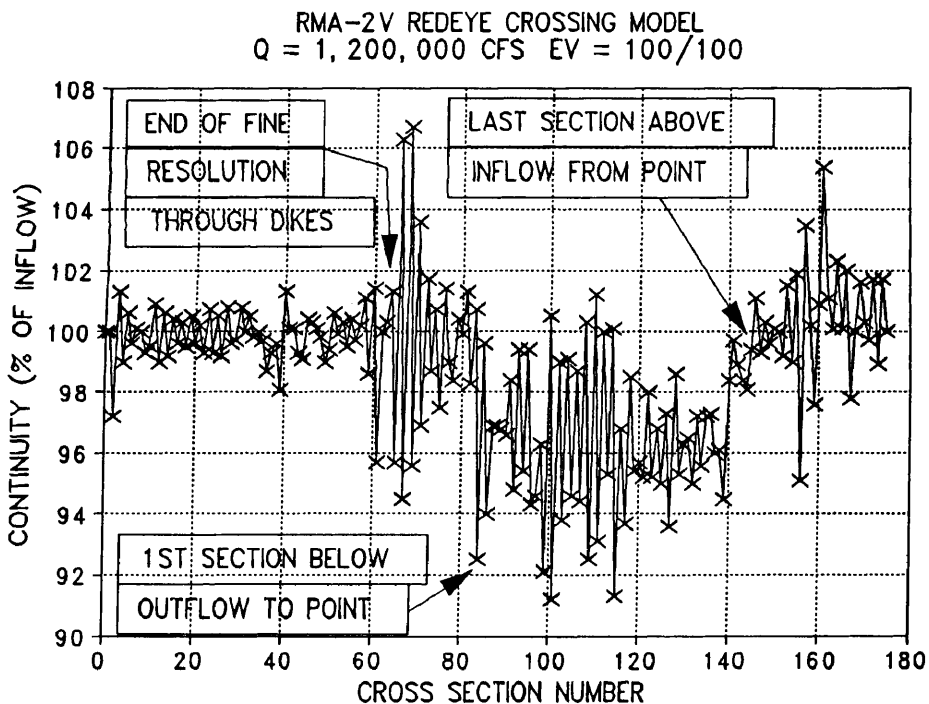


Fig. 232. RMA-2V Redeye Crossing Model Continuity for  $Q = 1,200,000$  cfs with  $EV = 100$  at All Locations. Flow Over Point Accounts for About 3.15% of Total Flow.

the inlet at the top of the figure to the outlet at the bottom. The RMA-2V model predicted that about 3% of the flow would pass across the point. If this amount of flow is added to the model continuity for the channel around the point (cross sections 84 to 124) the total flow is very close to 100%. The physical model of the area at this flow rate predicted that about 4% of the 1,200,000 cfs flow would pass over the point.

Several sets of serious oscillations appear in the continuity results. The most serious oscillations are about  $\pm 6\%$  and appear to be a result of the sudden increase in element size at the lower end of the Redeye Crossing dike field (See Fig. 11). This change in element size is in excess of the 50% rule and indicates the importance of gradually varying element size to reduce oscillations and errors in the solution.

The dikes can be seen in Figs. 230 and 226 and the continuity results show very good continuity as flow moves through the dike area. This is probably a result of the limited flow area effected by the dikes.

The oscillations in the channel around the point (between cross sections 84 and 144) may be due to inadequate resolution in the channel through the sharp bend or due to problems caused by bank irregularities. The oscillations near cross section 160 are probably due to sharp corners formed when elements went dry on the inside of the last model bend.

This solution - while not perfect - appears to be adequate for determining the hydrodynamics of the flows in this section of the Mississippi River. Further refinements were made in the original study prior to supplying data to the sediment model which is very sensitive to the hydrodynamic instabilities discussed above.

## 2DDI REDEYE CROSSING MODEL RESULTS

The Redeye Crossing test grid used for the 2DDI model tests is exactly the same as that used in the RMA-2V tests with the exception of the elimination of the midside nodes and the renumbering of nodes to eliminate unused node numbers.

The nodal elevations used in the RMA-2V model were lowered by 240 feet to place all elevations below sea level. The downstream elevation boundary condition was also lowered by an identical amount to maintain comparable flow conditions. The value for the upstream boundary condition (head specification) was taken from the plot in Fig. 225(b) and adjusted to the model datum since the 2DDI model did not accept flow boundary conditions. Initial water surface elevation in the model was at sea level - equivalent to 240 feet in the RMA-2V model and lowered to desired elevations with the ramp feature in an attempt to avoid instabilities during model start up.

The time step for the model was set by utilizing an option to show Courant Number values in the grid editor XMGREDIT developed by the Center for Coastal and Land-Margin Research (1991). An acceptable time step value was determined to be 2.0 seconds which kept the maximum Courant Number in the grid at less than or equal to 1.0 - well under the model's upper limit of 1.5. The model was run, however with a time step of 1.0 seconds to be certain that the Courant criteria was not a stability constraint in the Redeye Crossing model.

The maximum value of  $\tau$  was determined to be about 0.006 while the minimum is on the order of 0.00006 - a range of 2 orders of magnitude. The initial value for  $\tau_0$  used for initial testing was 0.007 - consistent with a maximum  $\tau$  value of 0.006. The simulation was set to run 2.0 days with a 1.0 day ramp length.

When the non-linear model was run with these values terminal instability (maximum velocity > 100 ft/sec) occurred at about 10,700 seconds into the simulation. The velocity vector results from the model at a time of  $T = 10,000$  is shown in Fig. 233. It can be seen that the model has become unstable at the inflow boundary - a problem that has been common to most tests using the non-linear form in this study. The rest of the solution looks well converged and shows only very minor instabilities. It must be noted that the model flow rate is very low, however and velocities are on the order of 2 feet per second as compared to 8 to 10 feet per second in the RMA-2V model. A color plot of velocity in the 2DDI solution is shown in Fig. 234. It can again be noted that the velocity is very low in comparison to the RMA-2V solution. The instability at the inflow boundary shows up dramatically.

Next the value for  $\tau_0$  was reduced to 0.003 to see if any difference in the solution could be noted. After close examination no difference in model stability or results could be determined. This would indicate that the value for  $\tau_0$  was in the proper range for a "good" solution.

Since the non-linear model would not converge, the linear model was run and produced the vector results shown in Fig. 235 after a simulation of 2 days with 3 second time steps. The flow patterns for this solution are not as smooth as those noticed for any of the previous solutions - whether the non-linear 2DDI or RMA-2V solutions. While no vectors are pointed upstream the flow pattern makes numerous abrupt changes in direction and magnitude and does not represent a solution that is at all similar to the non-linear solutions previously presented for either model.

One of the main reasons for the dissimilarity was the fact that the model had not stabilized even after 57,600 time steps. Longer time steps were attempted but the model was unstable when time steps were lengthened even to 30

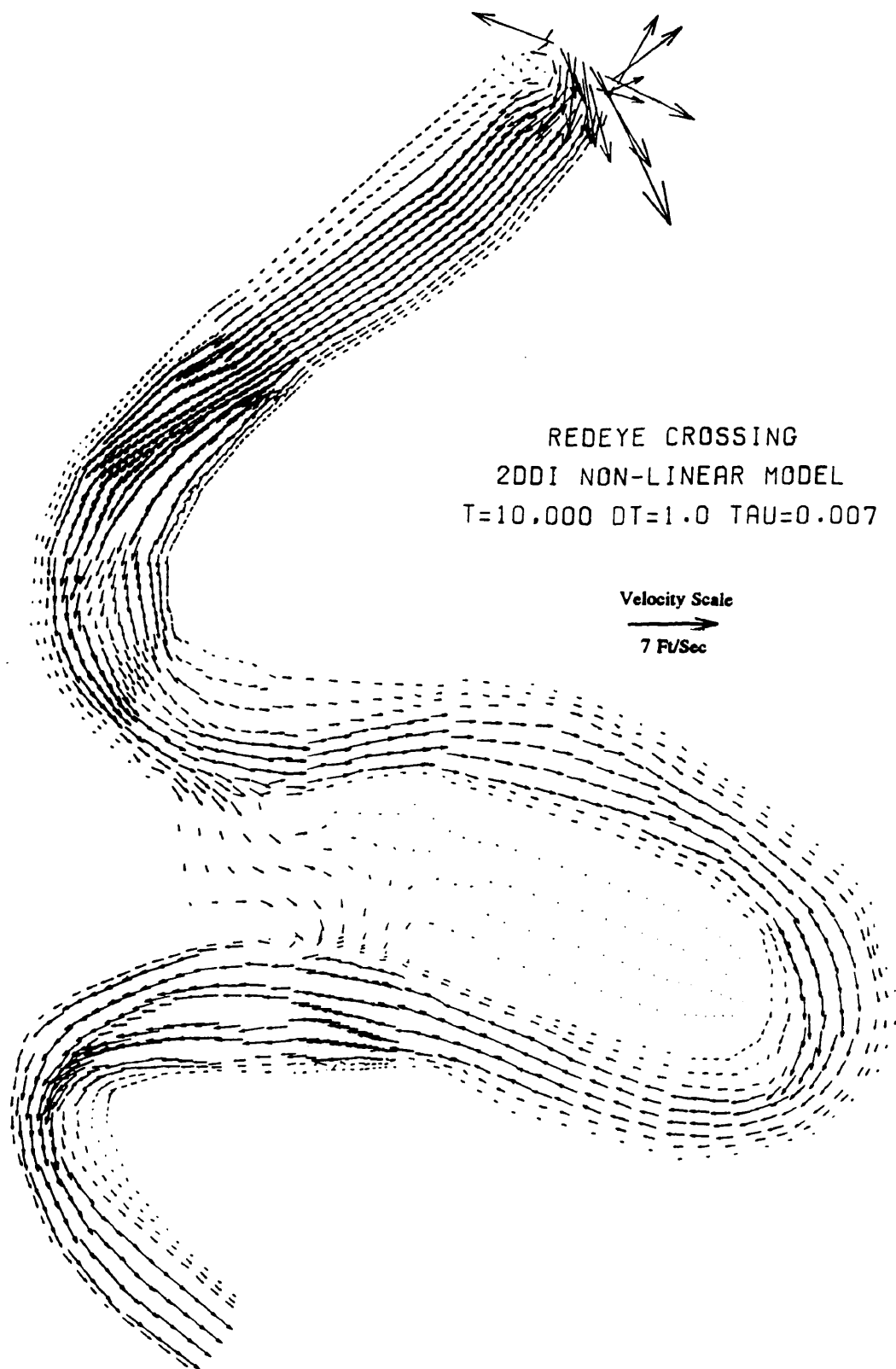
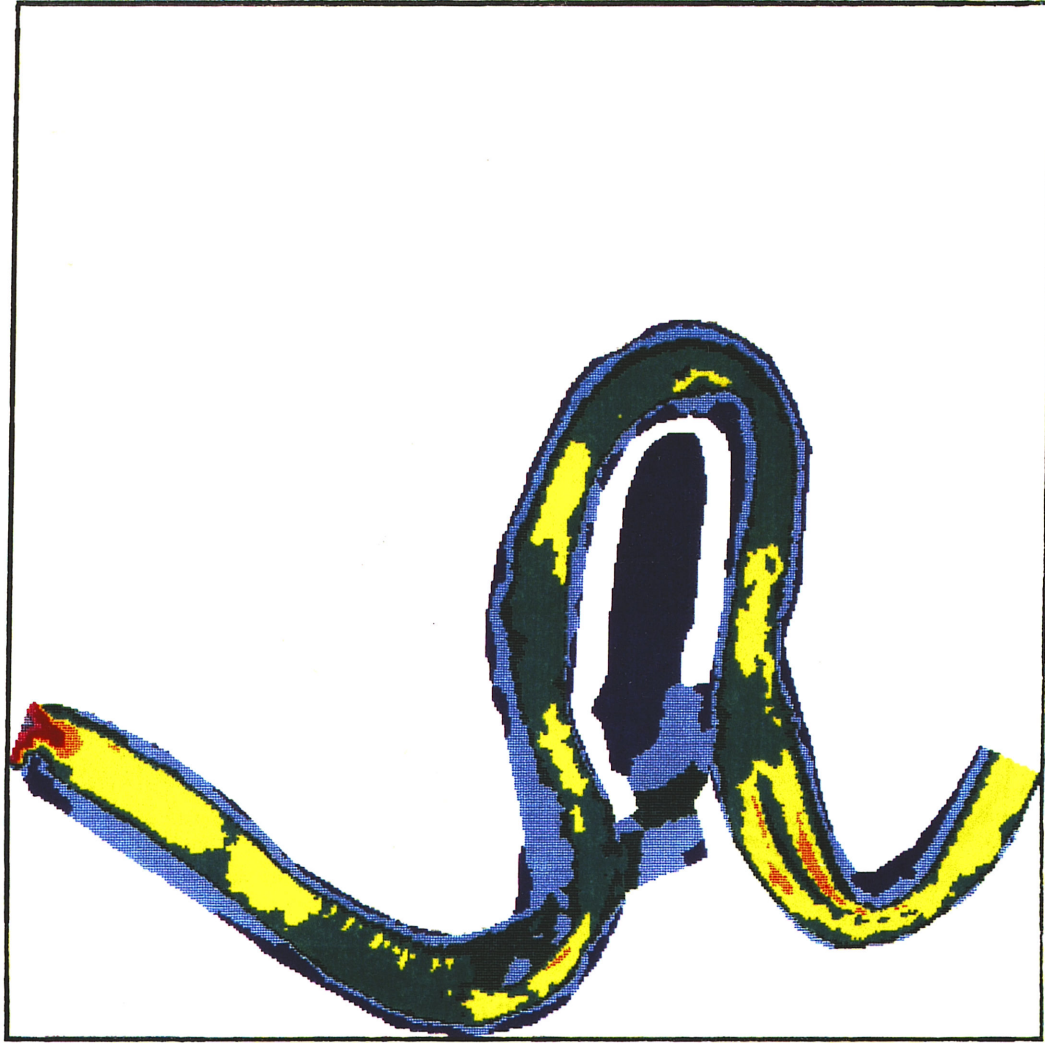
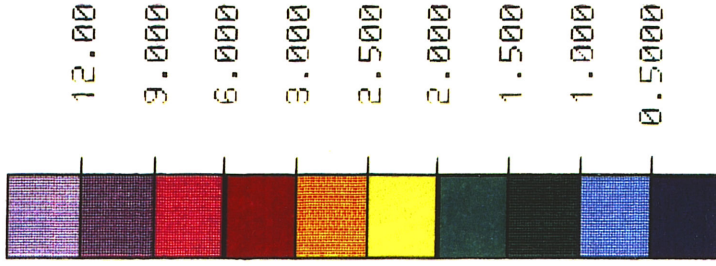


Fig. 233. Fully Non-linear 2DDI Velocity Vector Results for Redeye Crossing Model. Velocities are less than 20% of RMA-2V Values Due to Non-convergence of 2DDI Model.

REDEYE CROSSING



MAGNITUDE OF  
VELOCITY



FEET

Fig. 234. Non-linear 2DDI Redeye Crossing Model Velocity Plot Showing Low Velocities in Solution Just Prior to Terminal Instability (Velocity > 100 ft/sec).



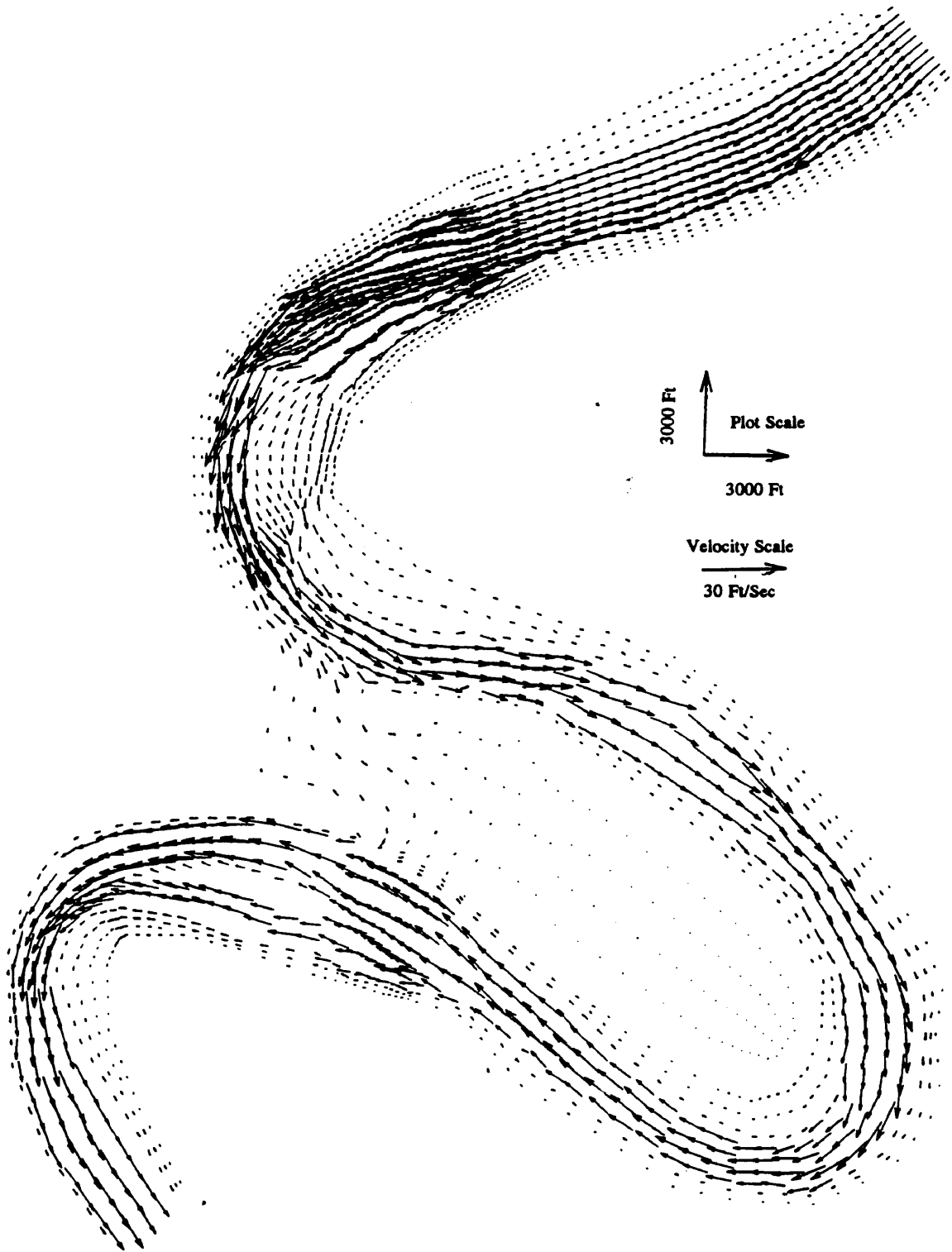


Fig. 235. Linear 2DDI Velocity Vector Results for Redeye Crossing Model After 2 Day Simulation with 3 Second Time Steps.

seconds. It is possible that the model could be made stable in the linear mode, however, given the poor results from the previous test cases it was felt that the linear model did not justify the additional effort. The linear model is clearly not applicable to river applications due to the non-linear terms that have been neglected and the finite amplitude assumption.

Continuity was calculated for both the linear model and the non-linear model but since neither had converged to a stable solution the results were not plotted. The continuity results showed primarily the water surface waves that were still moving back and forth through the Redeye Crossing Model and any continuity oscillations in the solution did not show up due to the magnitude of the surface waves.

Simulation Speed for Redeye Crossing Model. The Redeye Crossing model for the 2DDI model consisted of 2,226 nodes and 4,025 elements. For the RMA-2V model the model also included 6,251 corner nodes in addition to the 2,226 corner nodes.

Computer usage for the 2DDI model was 435.125 seconds of cpu time on a Cray Y-MP which works out to be 132.4 time steps per second. At 3 second time steps this works out to one second of model time per 397 seconds of real or prototype time.

Since all of the tests described in this work were steady state solutions to river problems, a dynamic run was made using the RMA-2V model for the Redeye Crossing Grid. The time step used in the dynamic mode was 6 hours - the same time step as used in a dynamic portion of the study conducted by Raphelt, Trawle, Pokrefke, and Nickles (1992).

The steady state RMA-2V effort required a total of 259.94 seconds including model set up, model initialization, and solution time for 22 iterations. This equates to 11.6

seconds of Cray Y-MP cpu time per iteration. Normally a time step is given a maximum of 3 iterations to converge.

The dynamic effort conducted as a part of this research was based on 2 time steps of 6 hours each. The model was set to take up to 5 iterations per time step if needed. The RMA-2V model required 361.17 seconds of cpu time to complete this simulation or a net cpu time of 101.23 seconds for 9 iterations (9 iterations beyond the steady state simulation).

This indicates that after the RMA-2V model has arrived at the initial solution and starts time stepping, approximately 11.24 seconds are required per iteration for a grid of this size. This amounts to 33.74 seconds per time step assuming 3 iterations per time step. This is 3.1% less than the time taken in the steady state model which included model set up and initialization. Often the RMA-2V model will converge in less than 3 time steps in which case the model will not iterate again but will move to the next time step.

Based on 33.74 seconds of cpu time per six hour time step the RMA-2V model can model dynamic simulations at a ratio of 640 seconds of real (prototype) time per second of cpu time. This is 1.6 times faster than the 2DDI model for the Redeye Crossing grid. If the time step in the 2DDI model is shortened to keep the Courant Number less than 1.0 the ratio is even more in favor of the RMA-2V model with the RMA-2V model being 2.4 times faster as the 2DDI model.

## CONCLUSIONS

The purpose of this research was to determine the applicability of the newer wave equation formulation of the shallow water equations to applications in the two-dimensional modeling of rivers and to compare the two test models RMA-2V and 2DDI. The 2DDI model was the newer wave equation formulation and research with the 2DDI model was delayed while model development continued. The RMA-2V model represented the older "primitive" formulation - a term coined by the wave equation modelers to differentiate between the two formulations.

The RMA-2V model was able to converge to a satisfactory solution for all test cases with some manipulation of the turbulent exchange coefficients (EV, eddy viscosity) and/or by increasing resolution. The 2DDI model in its fully non-linear form did not converge to a satisfactory solution for any of the test cases used in this research. Some may argue that the model was not designed to address problems of this nature but was designed to address ocean problems - an area where it apparently performs very well (See Westerink, et al 1992, Westerink, Leuttich, and Scheffner 1992, Leuttich, Westerink, and Scheffner 1991, etc). This argument was not made at the beginning of this research and if made at all is a result of efforts such as this to evaluate and use the model in other types of applications.

The linear version of the 2DDI model was able to converge to the desired steady state solutions for the simple test cases by time stepping to an acceptable steady state solution. The lack of the non-linear terms which are neglected in the linear version of the model makes it unacceptable in the modeling of river flow where many of the prototypes have eddies, separation zones, and areas where high velocities are adjacent to low velocities - all of

which create extremely non-linear flow patterns which are cannot be modeled with the linear model.

With this introduction we can now make specific conclusions about each of the models, using information obtained from the series of tests conducted.

#### CONCLUSIONS REGARDING RMA-2V

Grid Orientation. The RMA-2V model is sensitive to grid orientation which can cause serious differences in calculated solutions below changes in bed elevations or changes in channel width. The use of grids similar to those identified herein as regular and "C" grids can skew flows to one side of a channel or at the very least cause extremely non-uniform water surfaces and velocities downstream from the flow disturbance. The alternating and rectangular grids carried oscillations much farther downstream than the regular and "C" grids but spurious lateral variations in the channel were minimized.

Sudden Depth Reductions. The RMA-2V model appears to be sensitive to the rate at which the depth of flow is reduced due to increases in bed elevation. For total depth reductions of 50% (bottom slope  $\leq 1:10$ ) or less, resolving the local grid such that there is no more than a 20% reduction in depth per element will keep continuity oscillations under 5% and reductions of 10% per element or less of the total depth will keep continuity oscillations to less than approximately 2%.

When total depth change is on the order of 75% (bottom slope = 1:6.67) a depth change of 20% per element results in about a 10% continuity oscillation but this may be due to the violation of the mild slope assumption (bottom slope must be  $\leq 1:10$ ). Further research could be done to determine if the difference between the 50% depth reduction

tests and the 75% depth reduction tests were due to the total amount of the reduction or the bottom slope.

Sudden Depth Increases. The RMA-2V model is extremely sensitive to sudden increases in depth when the model grid is not well resolved. For the single resolution case where depth was approximately doubled in one element length (slope = 1:10) the continuity oscillations exceeded 100% for the case with the turbulent exchange coefficients (EV or eddy viscosity) set to 5. With EV set to 500 - the highest value tested - the maximum continuity deviation was still about 12%.

When the grid resolution was increased such that there was a 10% or less increase in depth per element, the maximum continuity deviation could be reduced to less than 3% for all tested values of EV.

When the bed slope was such that the mild slope assumption was violated (slope > 1:10) the continuity oscillations became extremely serious. Only at a resolution such that flow depth was increasing at less than 38% of the upstream depth per element did continuity oscillations become acceptable at values of EV commonly used for this type problem (25 to 125). For a 30% depth increase (slope = 1:5), all continuity maximum deviations were less than about 1% as long as the depth increase was 15% or less per element.

Submerged Bumps. The test case for submerged bumps produced better than expected results given the number and size of oscillations produced in the two preceding tests. It appears that the symmetry of the bump tends to create a damping effect where the oscillations created by the upstream face of the bump are damped by the oscillations formed by the downstream face.

The use of increased eddy viscosity (EV) to reduce continuity oscillations at the bump was counter productive and increases in EV tended to increase the peak oscillation at the bump crest. Increased EV did, however tend to reduce the duration and magnitude of the oscillations downstream of the bump. This would indicate that the best approach may be to use very low EV values on the bump and normal or slightly higher values upstream and downstream to damp any continuity oscillations that carry away from the bump faces.

When resolution was increased to 8 elements on the bumps in the mild slope range (slope  $\leq 1:10$ ) maximum continuity deviations were very nearly 0.0% - i.e. very nearly no oscillations at all.

Sudden Width Reductions. The width reduction tests indicated that channel width reductions should be resolved such that no more than about a 7.5% channel width reduction occurs per element if maximum continuity deviations are to be less than 5% of the model inflow.

The tests showed dramatically that the resolution at a sudden width reduction should be increased equally in both directions - i.e. streamwise and laterally. For unequally increased resolution tests the maximum continuity deviations were much higher than for comparable tests where both resolutions were increased equally. In some cases the increasing of resolution actually increased the maximum continuity oscillations.

Sudden Width Expansions. The sudden expansion tests resulted in very low values for maximum continuity deviations and the resulting oscillations for the most part damped out very rapidly. The maximum deviation noted for a very poorly resolved expansion (resolution = 1) was just less than 10% for the 20% expansion test.

It appears that unless a sudden expansion is modeled by at least two elements the RMA-2V model cannot adequately resolve the eddy that forms in the physical process. This results in increased oscillations downstream of the expansion as well as an increased continuity deviation at the expansion itself.

If the expansion was resolved such that no more than 2.5% of the expansion occurred per element all of the continuity deviations were less than 1% regardless of the value used for EV, the only exception being the 60% expansion where all values were less than 2%.

It should also be noted that it is important to carry the increased resolution far enough down the channel to capture the full length of the eddy formed by the expansion. If this is not done the flow patterns downstream from the expansion will be affected by the grid resolution. The result can be a calculated eddy length below the expansion that is shorter than the length of the eddy in the prototype due to the inability of the grid to adequately resolve the eddy. The net result is an eddy that is too short and cannot be lengthened to match prototype data by varying EV or other model parameters.

Bridge Abutments. When resolved such that the amount of channel reduction due to a bridge abutment or other effect is less than or equal to 2.5%, the maximum continuity deviation should be on the order of 3% or less. The only exception being the 60% reduction test where maximum deviations are on the order of 4%. When the grid is coarser than 2.5% reduction per element, maximum deviations can be on the order of 20 to 30% depending on the severity of the contraction and the amount of resolution.

The Riprap Test Facility. The RMA-2V did a very good job of modeling the riprap test facility given the propensity of



all two-dimensional models to keep flow to the inside of the channel. If this problem can be corrected, the model will do a very acceptable job of modeling in this type of application. The comparison of the calculated results to the observed results shows that the model can be tuned to give relatively accurate results for the initial 45° of a bend with the model predicting the flow on the wrong side of the channel for the remainder of the bend. A very short distance after the bend the flow distribution again matches the observed values.

Redeye Crossing. The RMA-2V model was able to model the Redeye Crossing area of the Mississippi River near Baton Rouge. The model exhibited oscillations in continuity as high as 6% and instabilities in areas where high velocities are impinging on banks with high roughness values. The highest observed oscillations were due to abrupt changes in element sizes which exceeded the 50% rule for element gradation. Another part of the problem may be due to lack of resolution on the bank areas where flow is trying to form eddies but resolution is not high enough for their formation in the model. The resulting solution did produce the major flow patterns as observed in the prototype.

In areas where velocity is changing directions very rapidly or areas of high velocity gradients the model shows symptoms of instabilities. Most of these problems can be either solved or reduced to insignificance given the proper grid resolution without the necessity to resort to extreme changes in the values of EV as used in differing areas of the grid.

Eddy Viscosity, Lateral Diffusion, or Turbulent Exchange Coefficients (EV). The effect of eddy viscosity, lateral diffusion, or turbulent exchange coefficients in the RMA-2V model is indeed to produce model stability and damp water

surface and velocity oscillations. The model will not converge to a solution without this type of damping.

The effect of increasing EV on the model is normally to increase damping of the oscillations with the exception of the submerged bump test. For this test increasing EV produced larger peak oscillations at the bump crest but reduced oscillations in the channel downstream of the bump. There is probably a lower limit to this phenomenon which may not be much below an EV of 5 - the lowest value used in these tests.

The most visible effect of EV in the simple test cases was the damping of oscillations downstream of the sudden change in flow characteristics. In the riprap facility the effect of EV on the lateral velocity distribution was shown to be significant and must be considered when selecting a value of EV. EV should be selected in the model such that the lateral distribution of velocity in the model is matched to the prototype and resolution should be used to reduce or eliminate continuity oscillation problems.

#### General Conclusions About Applicability to River Modeling.

The RMA-2V model is extremely applicable to river modeling and has been successfully used for 13 years. Current plans to update the model will assist in the wider use of the model in river modeling by shifting flows to the outside of bends and making the model more stable.

This research has indicated that the RMA-2V model is not perfect and could use improvement in terms of stability for the types of problems discussed. More importantly this research has shown that the RMA-2V model can be tuned such that it can successfully provide solutions to two-dimensional river problems and keep problems with continuity oscillations and deviations to values that are within acceptable limits.

## CONCLUSIONS REGARDING ADCIRC-2DDI

The non-linear 2DDI model was not stable for any of the test cases used in this research. The obvious conclusion is that the non-linear 2DDI model is not, in its present form, applicable to river flow problems. If the fully non-linear model can be stabilized for riverine problems the model could be used in river applications where dynamic simulations with short time steps are desired due to its extremely fast time stepping capabilities. However due to the extremely short time steps required by the model it may not be any faster than the RMA-2V model for long term simulations since the RMA-2V model can take much longer time steps and remain stable.

For the Redeye Crossing model the time simulation in the RMA-2V model using 6 hour time steps was 1.6 times as fast as the 2DDI model which required time steps of 3 seconds or less to remain stable. For steady state analysis the RMA-2V model will continue to outperform the 2DDI model due to the large number of time steps required to arrive at an acceptable steady state solution in a river environment.

The Simple Test Cases. The linear 2DDI model produced oscillations in the simple test cases similar to those produced in the RMA-2V model. The oscillation patterns were very similar to those produced in the RMA-2V model but the RMA-2V model out performed the linear 2DDI model in terms of maximum continuity deviations for the sudden depth reduction case, high resolution cases of the sudden depth increase case, and the submerged bump test. RMA-2V matched the 2DDI model for the sudden width expansion test while the linear 2DDI model outperformed the RMA-2V model in sudden width reductions and abutment reductions.

The linear 2DDI model was also shown to be sensitive to grid orientation. The resulting grid induced differences

were much less severe than those found in the RMA-2V model but caused significant continuity drift for the "C" grid . For the alternating and regular grids the grid induced problems occurred only at the channel inlet, outlet and at the change in channel geometry. These problems were seriously exacerbated by the use of high amounts lateral diffusion (EV) in the model. With lateral diffusion turned off the variations were relatively minor.

In terms of flow patterns the linear 2DDI model could not model eddies which form behind the channel expansions and abutment reductions. This is extremely serious of itself and eliminates the linear model from consideration for river modeling.

The linear model also could not accurately model the water surface elevations of the test cases when the velocity head had a significant impact on the water surface elevation. When the calculated water surface elevations were adjusted for the velocity head the values were very accurate but the external adjustment of water surface elevation results to account for velocity head in general applications is not feasible.

The Riprap Test Facility. The 2DDI model would not converge to an acceptable stable solution in either form for this problem. When the linear 2DDI model was used on the riprap test facility the model was not stable. This was most likely due to the violation of the finite amplitude assumption where the change in the water surface from sea level or an elevation of 0.0 was ignored. The change in water surface elevation at the downstream end of this model was over 50% of the original model depth - obviously too much to be neglected.

The non-linear model also would not converge for this test case. When the model results were take prior to the model blowing up, the non-linear model predicted lateral

velocity distributions approximately the same as those obtained by RMA-2V and suffered from the same problems discussed above for the RMA-2V model - i.e. the placement of velocities on the wrong side of the channel after the 45° point in the bend. It must be remembered that the non-linear model was not fully converged and the velocities from RMA-2V and those observed in the riprap test facility had to be made dimensionless for comparison.

Redeye Crossing Model. The 2DDI model did not converge either in the linear or non-linear form for the Redeye Crossing Model. The non-linear model did show some promise in this application if it could be made stable. The model aborted, however due to instabilities at the model inflow boundary. This type of instability has been noted throughout this testing. This type of problem seems to indicate a bug in the way the non-linear model incorporates a flow boundary condition into the solution matrix. The code was checked for bugs and none were detected, however a bug is still suspected. Efforts in the early part of this research to include a flow boundary condition resulted in no improvement in model stability and was abandoned when newer versions of the code were supplied for testing. The model developers, however, are currently pursuing the installation of a flux or flow boundary condition.

A large amount of effort was not spent with the linear model in the Redeye Crossing application since the linear form of the model was previously shown to be not applicable to river applications with significant velocity heads. The linear form of the model was run for a 2 day simulation with 3 second time steps. At the end of the simulation the model still had not converged to a stable solution but if the model had been run for a longer period of time it may have converged to a steady state solution. Attempt to run at longer time steps resulted in the linear model blowing up.

General Conclusions Regarding 2DDI Applicability to River Modeling. The 2DDI model has been presented - even touted - as being extremely fast, extremely stable, lacking in numerical over damping, and accurate. This test has indicated that while the model is extremely fast on a time step basis, the model is not any faster than the RMA-2V model due to the very short time steps required to meet the Courant Number criteria to keep the 2DDI model stable.

The model was extremely unstable in the fully non-linear form for all applications tested during this research and as such the accuracy and effect of no numerical damping could not be observed. It appears that while the model does an excellent job of tracking surface waves in the solution the modeling of significant velocity fields is currently not within its capabilities.

In application to river flows the non-linear model is extremely unstable and while fast for a single time step, leaves much to be desired when steady state conditions are modeled.

In short the model has some promise if the non-linear form can be stabilized. If the non-linear form cannot be stabilized, the model is not applicable to river applications in any form. The model appears to do extremely well at tracking surface waves but breaks down when velocities are imposed on the entire body of water being modeled.

## REFERENCES

- Abraham, David Daniel (1991). "Analysis and Verification of a Three-Dimensional Hydrodynamic Numerical Model", Thesis Presented to Texas A&M University, College Station, TX in Partial Fulfillment of the Requirements for the Degree of Master of Science.
- Ahmed, C.H. (1987). *Fluid Mechanics*, Engineering Press, San Jose, CA.
- Baker, A. J., Manhardt, P.D., and Johnson, B. H. (1987). "Methods for Reducing Computational Costs of Typical Finite Element Unsteady Hydrodynamic Models". *Miscellaneous Paper HL-87-5*, U.S. Army Waterways Experiment Station, Vicksburg, MS.
- Berger, R.C. (1990). Personal Communication, U.S. Army Waterways Experiment Station, Vicksburg, MS.
- Bernard, Robert S. (1992). Personal Communication, U.S. Army Waterways Experiment Station, Vicksburg, MS.
- Brebbia, C. A., and Partridge, P.W. (1976a). "Finite Element Models for Circulation Studies", *Mathematical Models for Environmental Problems: International Conference Proceedings, Southampton, U.K.*, John Wiley, New York, NY, 141-160.
- Brebbia, C. A., and Partridge, P.W. (1976b). "Finite Element Simulation of Water Circulation in the North Sea", *Applied Mathematical Modeling*, 1(2), 101-107.
- Center for Coastal and Land-Margin Research (1991). "ACE/gredit user's manual; Software for semi-automatic generation of two-dimensional finite element grids, Version xml.0 of August 1991" (draft). *Software Documentation Series SDS2, 91-2*, Oregon Graduate Institute of Science and Technology, Beaverton, OR 97006.
- Comes, Bradley, M., Copeland, Ronald, R., and Thomas, William A. (1989). "Report 5, Sedimentation in Lock Approaches, Red River Waterway, John H. Overton Lock and Dam", *Technical Report HL-89-16*, U.S. Army Waterways Experiment Station, Vicksburg, MS.
- Conner, J.J., and Wang, J.D. (1974). "Finite Element Modeling of hydrodynamic Circulation", *Numerical Methods in Fluid Dynamics*, Pentech Press, London, 135-140.

- Dronkers, J.J. (1964). *Tidal Computations in Rivers and Coastal Waters*, North Holland, Amsterdam.
- Froehlich, David C. (1989). "FESWMS-2DH Finite Element Surface-Water Modeling System: Two-Dimensional Flow in a Horizontal Plane, Users Manual". Publication No. FHWA-RD-177, Federal Highway Administration, McLean, VA.
- Gray, W.G. (1980). "Do Finite Element Models Simulate Surface Flow?", *Finite Elements in Water Resources, 3rd, Proceedings*, University of Mississippi, University, MS, 1.122-1.136.
- Gray, W.G. (1982). "Some Inadequacies of Finite Element Models as Simulators of Two-Dimensional Circulation", *Advances in Water Resources*, 5(Sep), 171-177.
- Gray, W.G, and Kinnmark, I.P.E. (1986). "Evolution of Two-Dimensional FE Wave Equation Models", *Finite Elements in Water Resources, Computational Mechanics Publications*, London, 29-47.
- Gray, William G., and Lynch, Daniel R. (1977). "Time-Stepping Schemes for Finite Element Tidal Model Computations", *Advances in Water Resources*, Vol. 1 No. 2, 83-95.
- Grotkop, G. (1973). "Finite Element Analysis of Long-Period Water Waves", *Computer Methods in Applied Mechanics and Engineering*, 2, 147-157.
- Harrington, R.A., Kouwen, Nicholas, and Farquhar, G.J. (1978). "Behavior of a Hydrodynamic Finite Element Model", *Finite Elements in Water Resources: International Conference 2d, London, Proceedings*, Pentech Press, London, 2.43-2.61.
- HEC (1990). "HEC-2 Water Surface Profiles, User's Manual", Hydrologic Engineering Center, U.S. Army Corps of Engineers, Davis, CA.
- HEC (1991). "HEC-6 Scour and Deposition in Rivers and Reservoirs User's Manual", Hydrologic Engineering Center, U.S. Army Corps of Engineers, Davis, CA.
- Hirsch, C. and Warzee, G. (1979). "An Orthogonal Finite Element Method for Transonic Flow Calculations", *International Conference on Numerical Methods in Fluid Dynamics, 6th, Tbilisi, U.S.S.R., Proceedings*, Springer-Verlag, Berlin, 350-359.



- Hood, P., and Taylor, C. (1974). "Navier-Stokes Equations using Mixed Interpolation", *Finite Element Methods in Flow Problems: International Symposium, Swansea, U.K., 1974, Proceedings*, UAH Press, Huntsville, AL, 121-132.
- Jones, Norman L. (1990). *NGRID 1.0 USER'S MANUAL*, Norman L. Jones, Provo, UT.
- Kawahara, Mutsuto, Nakazawa, Shohei, Ohmori, Shunsuke, and Hasegawa, Ken'ichi (1978). "Tsunami wave propagation analysis by the finite element method", *Finite Elements in Water Resources: International Conference, Proceedings*, Pentech Press, London, 2.131-2.150.
- King, I.P., Norton, W.R., and Orlob, G.T. (1973). *A Finite Element Solution for Two-Dimensional Density Stratified Flow*, Water Resources Engineers, Walnut Creek, CA.
- King, I.P., and Norton, W.R. (1978). "Recent Application of RMA's Finite Element Models for Two Dimensional Hydrodynamics and Water Quality", *Finite Elements in Water Resources Proceedings of the Second International Conference on Finite Elements in Water Resources, Imperial College, London*, Pentech Press, London, 2.81-2.100.
- Kinnmark, I.P.E., and Gray, W.G. (1984). "An Implicit Wave Equation Model for the Shallow Water Equations", *Finite Elements in Water Resources: Proceedings of the 5th International Conference, Burlington, VT*, Springer-Verlag, Berlin, 533-543.
- Kinnmark, I.P.E. (1986). *The Shallow Water Wave Equations: Formulation, Analysis and Application, Lecture Notes in Engineering, XXV*, Springer-Verlag, New York, NY.
- Kinnmark, I.P.E., and Gray, W.G. (1986). "A Wave Equation Formulation of River Flow", *Finite Elements in Water Resources, Lisboa, Portugal*, Springer-Verlag, Berlin, 599-605.
- Lapidus, Leon, and Pinder, George F. (1982). *Numerical Solution of Partial Differential Equations in Science and Engineering*, John Wiley & Sons, New York, NY.
- Lee, Jonathan K., and Froehlich, David C. (1986). "Review of Literature on the Finite Element Solution of the Equations of two-Dimensional Surface-Water

Flow in the Horizontal Plane", *USGS Circular 1009*, USGS, Denver, CO.

Li, Wen-Hsiung, and Lam, Sau-Hai (1976). *Principles of Fluid Mechanics*, Addison-Wesley Publishing Co., Reading, MA.

Luetlich, R.A., Jr, Westerink, J.J., and Scheffner, Norman W. (1991). "ADCIRC: An Advanced Three-Dimensional Circulation Model for Shelves, Coasts, and Estuaries. Report 1: Theory and Methodology of ADCIRC-2DDI and ADCIRC-3DL", Department of the Army, U.S. Army Corps of Engineers, Washington, D.C.

Lynch, D.R., and Gray, W.G. (1979). "A Wave Equation Model for Finite Element Tidal computations", *Computers and Fluids*, 7(30), 207-228.

Lynch, D.R. (1983). "Progress in Hydrodynamic Modeling", *Reviews of Geophysics and Space Physics*, 21(3), 741-754.

Lynch, D.R., and Gray, W.G. (1988). "On the Well Posedness of Some Wave Formulations of the Shallow Water Equations", *Advances in Water Resources*, 11, 84-91.

Maynard, Steve T. (1990). Personal Communication, U.S. Army Waterways Experiment Station, Vicksburg, MS.

Norton, W.R., King, I.P., and Orlob, G.T. (1973). "A Finite Element Model for Lower Granite Reservoir, Vol. 3, Appendix F", *Water Quality Report, Lower Granite Lock and Dam, Snake River, Washington - Idaho*, U.S. Army Corps of Engineer District, Walla Walla, WA.

Norton, W.R., and King, I.P. (1977). *Operating Instructions for Computer Program RMA-2*, Resource Management Associates, Lafayette, CA.

Platzman, G.W. (1981a). "Some Response Characteristics of Finite Element Tidal Models", *Journal of Computational Physics*, 40, 36-63.

Platzman, G.W. (1981b). "Normal Modes of the World Ocean. Part I. Design of a Finite Element Barotropic Model". *Journal of Physical Oceanography*, 8(3), 323-343.

Pritchards, I.D.W. (1971). "Two Dimensional Models", *Estuarine Modelling: An Assessment*, NTIS

Publication PB206-807, Chapter 11-12, Water Quality Office, Environmental Protection Agency. Washington, D.C.

- Raphelt, N.R., Trawle, M.J., Pokrefke, T.J. and Nickles, C.R. (1992). "Redeye Crossing Reach Lower Mississippi River", Report 1, Sediment Investigation, U.S. Army Waterways Experiment Station, Vicksburg, MS. (In Preparation).
- Richards, D.R. (1990). "Flow Separation Around a Solitary Dike: Eddy viscosity and Mesh Considerations", *Hydraulic Engineering Proceedings of the 1990 National Conference*, ASCE, New York, NY, 867-872
- Richards, David Reed (1992). "Numerical Simulation of Training Structure Influenced Flows", Presented to the University of Texas at Austin, TX in Partial Fulfillment of the Requirements for the Degree of Master of Science.
- Segerlind, Larry J. (1987), *Applied Finite Element Analysis*, John Wiley and Sons, New York, NY.
- Tanaka, Toyoki, Ono, Yoshio, and Ishise, Toshikazu (1980). "The Open Boundary Problems in Ocean Dynamics by Finite Elements", *Finite Elements in Water Resources, Proceeding of the Third International Conference on Finite Elements in Water Resources*. University of Mississippi, Oxford, MS, 5.47-5.63.
- Taylor, C., and Davis, J. (1975). "Tidal and Long Wave Propagation-a Finite Element Approach", *Computers and Fluids*, 3, 125-148.
- Thomas, William A., McAnally, William H., Jr., and Letter, Joseph V. (1990). "Appendix F: User Instructions for RMA-2V, A Two-Dimensional Model for Free-Surface Flows", Draft, *Generalized Computer Program System For Open-Channel Flow and Sedimentation*, U.S. Army Waterways Experiment Station, Vicksburg, MS.
- Thomas, William A. (1992). Personal Communication. U.S. Army Waterways Experiment Station, Vicksburg, MS.
- Vrengdenhil, C.B. (1973). *Secondary Flow Computations*, Publication No. 114, Delft Hydraulics Laboratory, Delft, The Netherlands.
- Walters, Roy A., and Cheng, Ralph T. (1980). "Accuracy of an Estuarine Hydrodynamic Model Using Smooth

Elements", *Water Resources Research*, 16(1), 187-195.

- Walters, Roy A. (1983). "Numerically Induced Oscillations in Finite Element Approximations to the Shallow Water Equations", *International Journal for Numerical Methods in Fluids*, 3, 591-604.
- Wang, J.D., and Conner, J.J. (1975). *Mathematical Modeling of Near Coastal Circulation*, Report 200, Massachusetts Institute of Technology, Department of Civil Engineering, Cambridge, MA.
- Westerink, Johannes (1990). Personal Communication and Class Notes, University of Notre Dame, Notre Dame, IN.
- Westerink, J.J., Wu, J.K., and Luettich, R.A. (1990). "Normal Flow Boundary Conditions Force the Severe Spurious Modes in Finite Element Solutions to the Shallow Water Equations", *International Journal for Numerical Methods in Engineering*, In Publication.
- Westerink, J.J., Luettich, R.A., Jr., and Scheffner, Norman W. (1992). "ADCIRC: An Advanced Three Dimensional Circulation Model for Shelves, Coasts, and Estuaries. Report 2: Users Manual for ADCIRC-2DDI", Department of the Army, U.S. Army Corps of Engineers, Washington, D.C.
- Westerink, J.J., Luettich, R.A., Jr., Blain, C.A., and Scheffner, Norman, W. (1992). "ADCIRC: An Advanced Three Dimensional Circulation Model for Shelves, Coasts, and Estuaries. Report 2: Users Manual for ADCIRC-2DDI", Department of the Army, U.S. Army Corps of Engineers, Washington, D.C.
- Westerink, Johannes (1992). Personal Communication, University of Notre Dame, Notre Dame, IN.

## VITA

Gary Eugene Freeman is currently pursuing a Doctor of Philosophy Degree in Civil Engineering at Texas A&M University. He received a Associate of Arts Degree in Engineering from The College of Southern Idaho in May of 1973, a Bachelor of Science Degree from Utah State University in June of 1978 in Agricultural and Irrigation Engineering, and a Master of Science Degree in Irrigation Engineering in June of 1983. He has worked as a research assistant for the University of Idaho at the Kimberly Research and Extension Center and operated an irrigation equipment sales and installation business in addition to operating a family farming/ranching business. Since that time he has worked for two years in the Timbuktou Region of Mali in West Africa as an agricultural/irrigation engineer and served as a consultant on international development projects. Currently he is a Research Hydraulic Engineer in the Hydraulics Laboratory of the U.S. Army Waterways Experiment Station in Vicksburg, Mississippi. He has been active in the American Society of Civil Engineers, the American Society of Agricultural Engineers, and the U.S. Committee on Irrigation and Drainage. He is a member of the Sigma Gamma Chi Fraternity and a member of Tau Beta Pi. Upon Graduation he plans to continue work in hydraulics and irrigation related engineering. His permanent mailing address is:

1473 So. 680 E.  
Orem, UT 84058